Hydraulic Road Binder (HRB) and Its Use for Subgrade Stabilization in Ontario, Canada

by

Shenglin Wang

A thesis

presented to the University of Waterloo

in fulfillment of the

thesis requirement for the degree of

Doctor of Philosophy

in

Civil Engineering

Waterloo, Ontario, Canada, 2019

EXAMINING COMMITTEE MEMBERSHIP

The following served on the Examining Committee for this thesis. The decision of the Examining Committee is by majority vote.

External Examiner	**Dr. Alireza Bayat** Civil and Environmental Engineering, University of Alberta
Supervisor	**Dr. Hassan Baaj** Civil and Environmental Engineering, University of Waterloo
Internal Member	**Dr. Susan Tighe** Civil and Environmental Engineering, University of Waterloo
Internal Member	**Dr. Shunde Yin** Civil and Environmental Engineering, University of Waterloo
Internal-external Member	**Dr. Maurice B. Dusseault** Earth and Environmental Sciences, University of Waterloo

AUTHOR'S DECLARATION

I hereby declare that I am the sole author of this thesis. This is a true copy of the thesis, including any required final revisions, as accepted by my examiners.

I understand that my thesis may be made electronically available to the public.

STATEMENT OF CONTRIBUTIONS

Shenglin Wang was the sole author for Chapters 1 (Introduction), 2 (Literature Review), 3 (Research Methodology and Materials), and 7 (Conclusions and Recommendations). These chapters were written under the supervision of Professor Hassan Baaj.

In addition, this thesis consists in part of three co-authored manuscripts which were written for publications. For these papers, the literature review, test design and conducting, data analysis and manuscript drafting were solely performed by myself. These papers were written under the supervision of Professor Hassan Baaj. In addition, the papers received comments from other co-authors.

- **Chapter 4**

  S. Wang, H. Baaj*, "Impact of Supplementary Cementitious Materials on the Hydration and Strength Properties of Hydraulic Road Binders", Submitted to *Construction and Building Materials* on December 2nd, 2019. Under review.

- **Chapter 5**

  S. Wang, H. Baaj*, T. Smith, S. Zupko, "Improvement of Clayey and Organic Subgrade Materials with Cement and Hydraulic Road Binder (HRB)", Submitted to *Road Materials and Pavement Design*, Submission ID: RMPD-19-03-25. Accepted for revision.

- **Chapter 6**

  S. Wang*, H. Baaj, S. Zupko, and T. Smith, "Field and lab assessment for cement-stabilized subgrade in Chatham, Ontario." Conference paper of the *Transportation Association of Canada*, Saskatoon, SK, (2018).

ABSTRACT

The term “subgrade” refers to the in-situ material composed of natural soil located underneath the pavement structural layers. The quality of natural subgrade is highly influenced by soil type, moisture content, and organic content. Furthermore, the failure of subgrade soils may lead to severe pavement distresses including rutting, potholes, and cracking. In order to enhance the subgrade engineering properties, a variety of stabilization methods have been developed. One of the most popular and cost-effective methods is in-situ subgrade soil stabilization using hydraulic binders.

In-field soil modification and stabilization frequently use Portland cement as the chemical additive. Such method significantly enhances the engineering characteristics of soils in terms of plasticity, strength, stiffness, and durability. Despite the advantages, the chemical mixing also brings some disadvantages including rapid setting, drying shrinkage cracking, and higher cost. Recently, Supplementary Cementitious Materials (SCMs) made of by-products and industrial secondary materials (e.g. granulated blast furnace slag, cement kiln dust and fly ash) have been studied extensively to reduce the use of cement. Hydraulic Road Binder (HRB) is a European specified material designed for treatment of road bases, subbases as well as earthworks. HRB contains both cement clinker and a substantial amount of SCMs. Therefore, the use of HRBs has the potential to be more cost-effective and environmentally friendly than Portland cement. However, the research and application of HRB is new in Canada.

The study started with an investigation of cement and different formulated HRBs in the form of paste and mix (mortar). Then, selected HRBs were used to evaluate their impacts on the chemical and physical properties of three local subgrade soils. In addition, a field application of weak subgrade stabilization using cement was introduced. Lastly, a study aiming to predict the long-term pavement performance was conducted in order to simulate the impact of stabilized subgrade in pavement design. The research findings are summarized as follows:

- HRBs were found to reduce the setting time, reduce the speed of hydration, and the hydration temperature compared to Portland cement. The hydration products in hydrated HRBs and Portland cements were generally the same, but their contents were different. In addition, a reduction of drying shrinkage was observed in HRB mortars especially in those containing substantial SCMs. Regarding the strength, several HRB mortars had equivalent strength as cement mortars after 28 days of curing. Furthermore, a linear correlation was found between the compressive strength and flexible strength. Statistical analysis further revealed that the strength of HRB mix highly correlated to the content of GU, GUL, and GGBFS.
- All the three subgrade soils (named Dresden, Blenheim, and Niagara) were fine-grained soils with substantial silt- and clay- sized particles. Ignition test indicated that all the three soils include high content of organic matters. In particular, Niagara soil with high plasticity, high organic material content had lower strength and modulus compared to the other two soils. Using the stabilizers, the soil's pH values increased to around 12 and above. In addition, significant improvement had been observed in stabilized soils in terms of strength, durability, and resilient modulus. Nevertheless, the clay particles and organic matters inhibited the treatment. Increase of stabilizer content further promoted improvement. In particular, HRB-4LS had the best stabilization effect followed by GU, HRB-4LF, and HRB-3S. On the other hand, HRB-2S and HRB-3C treated soils had lower strength and modulus values. Finally, statistical analysis indicated that soil's UCS values correlated with binder strength, binder content, curing, and untreated soil's strength.
- Field testing indicated that the workability and conditions of subgrade were significantly improved by hydraulic binder. Moreover, the modulus of subgrade surface further increased with curing time. After one year of service, the conditions of roads were good in most test sections. Furthermore, long-term pavement performance

prediction (LTPP) revealed the feasibility of using cement and HRB stabilized subgrade to reduce the thickness of subbase layer. In terms of international roughness index and subgrade deformation, pavements constructed with HRB stabilized subgrade materials had equivalent performance as cement treated one over their design life.

To summarize, this study focused on evaluating the used of Hydraulic Road Binders formulated in Canada for pavement subgrade stabilization. The research showed that HRB mortars have similar or slightly better strength compared to Portland cement alone with sufficient curing time. Moreover, The HRB improved subgrade soils were shown to perform adequately using several HRB types. In addition, the use of HRB-stabilized subgrade in pavement structure would improve the LTPP of pavement. Therefore, the use of HRB in the subgrade stabilization could be a promising solution in pavement construction due to its equivalent performance and with the potential environmental and cost advantages.

ACKNOWLEDGEMENT

I would like to sincerely appreciate my PhD supervisor Professor Hassan Baaj for his guidance and help during my PhD program. Your humor, honesty, trust, and encouragement always make me progress. I would also like to acknowledge my PhD committee members, Professor Susan Tighe, Professor Shunde Yin, and Professor Maurice Dusseault from University of Waterloo; as well as, Professor Alireza Bayat from University of Alberta.

I would like to appreciate many other people who dedicated a lot to me during the past few years. Namely:

- Technical staff in Civil and Environmental Engineering Department: Anne M. Allen, Douglas Hirst, Mark Merlau, Richard Morrison, and Peter Volcic.
- Lafarge Canada Inc. for project collaboration and materials supply, especially Steve Zupko.
- Tim Smith who used to work for Lafarge, for his technical guidance and constructive comments.
- Lafarge Innovation and Training Centre, especially Abdurahman Lotfy and Shahid Quraishi.
- Stabilization Canada Inc., especially Sal Melillo for helping me with soil sampling and field work.
- All of my friends, colleagues, and co-op students at CPATT who spent their time helping me during the program, especially Adam Schneider, Andy Zhong, Eskedil Abebaw Melese, Taher Baghaee Moghadam, Hawraa Kadhim, Haya Almutairi, Rob Marko Aurilio, Ali Qabur, Dandi Zhao, Yashar Azimi Alamdary, Sina Varamini, Drew Dutton, Dan Pickel, Donghui Lu, Victoria Yang, Changjiang Kou, Ting Cao, Shi Dong, Frank Liu, Frank Ni, Wei Li, Julia Ju, Luke Zhao, Kamal Hossain, Peter Mikhailenko,

and Pezhouhan Tavassoti-Kheiry. There are a lot of others whose names are not listed here, but I want to thank them for making my time in Waterloo as like living in home.

I am grateful to have my parents, Xiao Wang and Xueying Chen, who gave me life, unconditional love, education, and support.

Last but not least, I would like to say a big thank you to my wife Xiaoyuan, you always give me love, trust, support, and encouragement. We together build a family here in Canada. I have the great fortune of having you in my life!

DEDICATION

To My Dear Children!

TABLE OF CONTENTS

LIST OF FIGURES

LIST OF TABLES

LIST OF ABBREVIATIONS

AASHTO	American Association of State Highway and Transportation Officials
ASTM	American Society for Testing and Materials
C-A-H	Calcium Aluminate Hydrates
C-S-H	Calcium Silicate Hydrates
CEC	Cation Exchange Capacity
CSA	Canadian Standard Association
CKD	Cement Kiln Dust
CPATT	Centre for Pavement and Transportation Technology
(E)SEM	(Environmental) Scanning Electron Microscopy
EDS	Energy Dispersive Spectroscopy
GU	General Use Cement
GUL	General Use Portland-Limestone Cement
GGBFS	Ground Granulated Blast-Furnace Slag
HRB	Hydraulic Road Binder
HBM	Hydraulically Bound Mixture
IRI	International Roughness Index
LVR	Low-Volume Road
LTPP	The Long-Term Pavement Performance
MEPDG	Mechanistic-Empirical Pavement Design Guide
M_r	Resilient Modulus
OPC	Ordinary Portland Cement
PCA	Portland Cement Association
SCM	Supplementary Cementitious Materials
SOM	Soil Organic Matter
SSA	Surface Specific Area
TAC	Transportation Association of Canada
UCS	Unconfined Compressive Strength
XRD	X-Ray Diffraction

CHAPTER 1 INTRODUCTION

1.1 Background

Canada has a vast land area covering approximately 10 million km^2. In addition, it has a high-capacity transport system spanning vast distances between urban areas, agricultural districts and natural resource mining sites. Canada's transportation system is composed of more than 1.4 million km of public road (TAC, 2014). Among all the roads in Canada, over 75% of the total length of roadways resides in four provinces: Ontario, Québec, Saskatchewan, and Alberta (Transport Canada, 2017). Furthermore, the transportation industry contributes approximately 4.6% to the Canadian **G**ross **D**omestic **P**roduct (**GDP**) (Transport Canada, 2017). As approximately 90% of the total goods and services are transported using Canadian roads, these roads must be safe, efficient and durable. According to Canada's Road Safety Strategy 2025, effective construction and management for road infrastructure is one of the key factors to reduce injuries and vehicular fatalities (CCMTA, 2016).

The typical constructed pavement structure in Canada consists of several layers, including surface, base, and subbase. The term "**subgrade**" usually refers to the in-situ material composed of natural soil and is located underneath all the pavement layers (Pavement Interactive, 2019). Subgrade exists in all pavement types: flexible, rigid, composite, and gravel roads. The distribution of traffic loading in a typical pavement structure is demonstrated in Figure 1-1. As it is presented, traffic loading is distributed through the pavement layers, and it is reduced when transferred to the subgrade. Meanwhile, the distribution and reduction are highly depended on the pavement type and thickness. On the other hand, the quality of natural subgrade is highly influenced by soil type, geological information, and climate conditions (MTO, 2013). A weak subgrade soil, high water table, or insufficient pavement thickness may lead to a subgrade failure, which can cause severe pavement distresses including rutting, potholes, and frost heaving. Since the conditions of subgrade can greatly influence the behavior and serviceability of pavement; therefore, the strength and bearing capacity of

subgrade are crucial inputs for the pavement structural design.

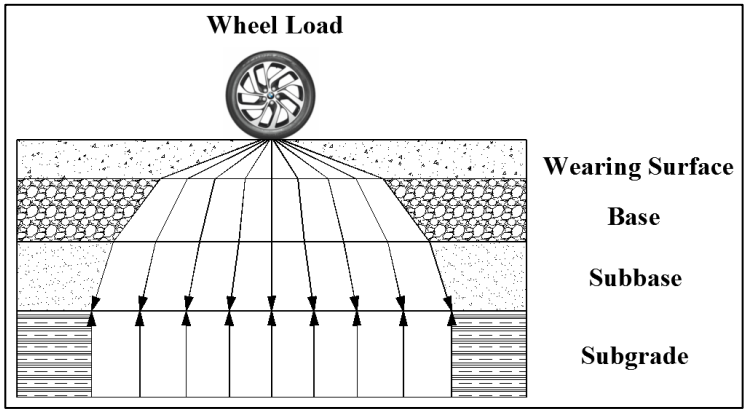

Figure 1-1 Typical load distribution in pavement structural layers

In some cases where a poor subgrade is inevitable, **subgrade stabilization** is recognized as an effective method. There are various stabilization techniques adopted to improve the strength in weak subgrade, to provide drainage in pavement, as well as to distribute the load. One of the most cost-effective methods is in-field mixing of soil and hydraulic binder. The hydrated mix functions as a permanent bound layer spreading loading over natural subgrade. The typical treatment depth of subgrade stabilization is 200 mm to 300 mm. The cost efficiency is therefore achieved when the stabilized layer reduces the required thickness for a granular base or subbase layer and the need for quarried aggregates. Such design has been frequently found in new pavement constructions (Wang *et al.,* 2018).

Historically, cement and lime are the most common materials that used for soil improvement. Past experience had indicated that cement is more suitable for soils with low plasticity (plasticity index<10), whereas lime is recommended for soils with higher plasticity. However, some literature (Prusinski and Bhattacharja, 1999; Petry and Little, 2002) argued that cement is still suitable for soils with plasticity index as high as 50, especially in the aspect of strength improvement.

Nowadays, Portland cement is the most frequently used binder for subgrade soil stabilization in Canada. However, the cement stabilization also brings some engineering disadvantages such

as rapid setting, drying shrinkage cracking, and excessive sulfate content (George, 1968). Consequently, **S**upplementary **C**ementitious **M**aterials (**SCMs**) have been studied extensively as alternatives for cement due to their lower cost and environmental advantages. SCMs are made of by-products and industrial secondary materials. The typical SCMs used include fly ash, industrial kiln dusts, and furnace slags.

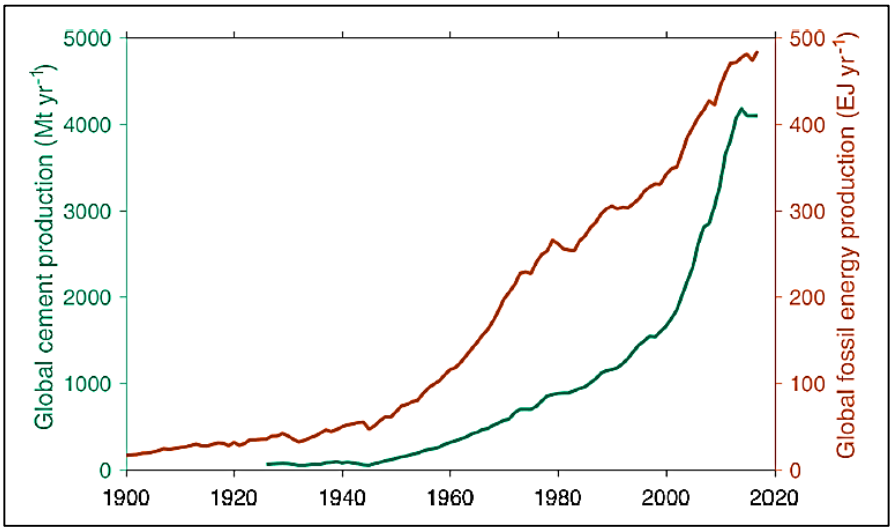

Figure 1-2 Global cement and fossil energy production from 1900 to 2017 (Andrew, 2018)

From an environmental perspective, **G**eneral **U**se (**GU**) cement or ordinary Portland cement production contributes to approximately 5%-8% of total man-made global carbon emissions (Schöler *et al.,* 2015). Moreover, since the late 1950's, annual man-made global carbon emissions have been increasing sharply (shown in Figure 1-2). The raw material supply, transporting and manufacturing for cement consumes a substantial amount of energy and gives rise to substantial greenhouse gas emissions (*e.g.* CO_2). The cradle-to-gate estimates of embodied CO_2 energy for different construction materials are summarized in Table 1-1. Data is taken from UK, USA, and Canada. It is evident that, as by-products and industrial secondary materials, SCMs and blended cements require less energy for manufacturing and material transport. Use of SCMs therefore leads to a significant reduction of carbon footprint. If HRB treatment could provide equivalent performance as cement treatment with similar stabilizer content, then it could be considered as a "green solution" for pavement construction and

rehabilitation.

Table 1-1 Embodied CO_2 of blended cement (UKQA 2010, CAC 2016, PCA 2016)

Blended cement type	SCM constituent	Embodied CO_2 kg/tonne		
		UK	USA	Canada
Portland cement (GU)	--	913	1040	940
Portland limestone cement	Limestone 6%~20%	859~745		855
Portland fly ash cement	Fly ash 6%~35%	859~615		
Portland slag cement	GGBFS 21%~35%	743~639		
Fly ash		4		
Ground granulated blast-furnace slag (GGBFS)		67	147	147

Hydraulic **R**oad **B**inder (**HRB**) is termed in European standard (EN 13282 1&2) as "*a factory manufactured stabilizer for treatment of road bases, subbases as well as earthworks*". The use of HRBs for pavement stabilization has been widely conducted in European countries including France, Germany, UK, Czech Republic, and Poland. The main difference between HRB and Portland cement is that HRB usually contains a high content and large variety of SCMs. The use of HRBs in bound pavement mixes have the potential of providing similar engineering properties as cement treatment (Melese *et al.,* 2019). In addition to cement, SCM treated pavement materials were also documented to have a mild and prolonged gaining of strength, but with less potential of drying shrinkage cracking (Adaska and Luhr, 2004). However, based on different resources, SCMs often have diverse properties. This significantly affects the performance of HRBs and HRB-treated pavement materials. Therefore, one of major challenges of using HRB for subgrade soil stabilization in Canada is to find suitable SCMs that can formulate local HRBs.

To achieve this goal, this research started with a laboratory characterization of cement and different formulated HRBs. Then, selected HRBs types were used for the treatment of three local subgrade soils. Performance testing were conducted for HRB-soil mixtures. Lastly, the feasibility of using stabilized subgrade in pavement design was further analyzed.

The thesis work was conducted under supervision of professor Hassan Baaj in University of

Waterloo. In addition, the research involved collaborations between **C**entre for **P**avement **A**nd **T**ransportation **T**echnology (**CPATT**) and Lafarge Canada Inc. Some laboratory tests were performed by author at Lafarge's **I**nnovation and **T**raining **C**entre (**ITC**).

1.2 Problem Statement

It has been over 80 years since the first soil-cement construction project was carried out in South Carolina, United States (Das, 2015). Since the late 1960s, literature has indicated both advantages and disadvantages in cement-treated pavement layers; as well as, the need for using alternatives to mitigate the engineering and environmental drawbacks. Past experiences also indicated that Portland cement, when used for field practice, had a short setting time. In some cases, the cement-treated pavement materials started to harden before the final compaction. This resulted in insufficient compaction which gave rise to low density and strength. HRB was therefore developed in Europe to have a slower setting but equivalent stabilization effect to replace the use of cement.

The current experience of HRBs in Europe cannot ensure the successful implementation in Canada without the appropriate research and design. Consequently, several aspects were considered in this study regarding the properties of local SCMs and subgrade soil types.

Before being incorporated as a subgrade soil stabilizer, the HRB binder itself should be studied and formulated locally. The reason is that, due to different sources, the properties of SCMs and their formulated HRBs will be highly variable. It is also indicated that some SCM types require a certain amount of activator (usually cement and lime) to initiate hydration. This calls for the experimental study and statistical analysis which will help to understand the role of each local SCM type and their contribution to the strength and other engineering properties.

The next challenge is then to validate the feasibility of using HRB for the treatment of local subgrade soils. The reduction of cement clinker in HRB could lead to the change of the properties of hydraulically bound mixtures. Different soil types will also significantly affect the treatment outcome. Performance testing for HRB-treated soils and cement treated soils

are therefore needed for the selection of proper HRB type. Furthermore, statistical analysis is also required to investigate the significant factors which affect treatment. These factors may be related to soil's organic content, plasticity index, pH value, and binder type.

1.3 Research Hypothesis

The research was conducted based on the following hypotheses:

1. HRBs containing SCMs have slower setting and less shrinkage potential compared to cement. In addition, they release less heat during hydration.
2. Some SCMs have strong self-hydration ability. Therefore, HRBs containing both cement and SCMs could reach equivalent strength levels compared to cement.
3. The engineering properties of subgrade soils could be significantly improved through the treatment with cement and HRBs in terms of strength, modulus and durability.
4. The formulation of HRB and the binder content will significantly affect the engineering properties of treated soils.
5. The field conditions of subgrade could be significantly improved when stabilized with cement and HRBs.
6. Pavements having HRB improved subgrade incorporated have the potential to behave well in the long-term.

1.4 Thesis Objectives and Contributions

The global objective of this research is to introduce HRB to Canada, to formulate HRBs using local manufactured cement and SCMs, and to investigate the engineering properties of HRB stabilized subgrade soils. Furthermore, the long-term performance is also conducted to predict the behavior of HRB stabilized roads. In particular, the research objectives are:

1. Validating the adoption of local SCMs in reducing the hydration heat, shrinkage potential and slowing down the setting of HRBs. Investigating the strength of

different HRBs and their strength development. In addition, discussing the role of each SCM type and their contribution. Furthermore, characterizing HRBs based on performance testing.

2. Investigating the performance of HRB-treated real subgrade soils at different HRB types and binder contents. Analyzing the strength development of HRB improved subgrade soils. Finding the relationships between treated soil's strength and untreated soil's geotechnical information as well as stabilizer's properties. In addition, discussing the relationships between different parameters of treated soils.
3. Monitoring the subgrade stiffness, and the in-field condition of stabilized subgrade. Analyzing the effect of stabilized subgrade in pavement design.

Several contributions are made based on the study. Detailed contributions in each chapter are summarized below in Figure 1-3:

In particular, the results of the study are summarized in several co-authored publications:

Chapter 4

S. Wang, H. Baaj*, "Impact of Supplementary Cementitious Materials on the Hydration and Strength Properties of Hydraulic Road Binders", Submitted to *Construction and Building Materials* on December 2nd, 2019. Under review.

Chapter 5

S. Wang, H. Baaj*, T. Smith, S. Zupko, "Improvement of Clayey and Organic Subgrade Materials with Cement and Hydraulic Road Binder (HRB)", Submitted to *Road Materials and Pavement Design*, Submission ID: RMPD-19-03-25. Accepted for revision.

Chapter 6

S. Wang*, H. Baaj, S. Zupko, and T. Smith, "Field and lab assessment for cement-stabilized subgrade in Chatham, Ontario." Conference paper of the *Transportation Association of Canada*, Saskatoon, SK, (2018).

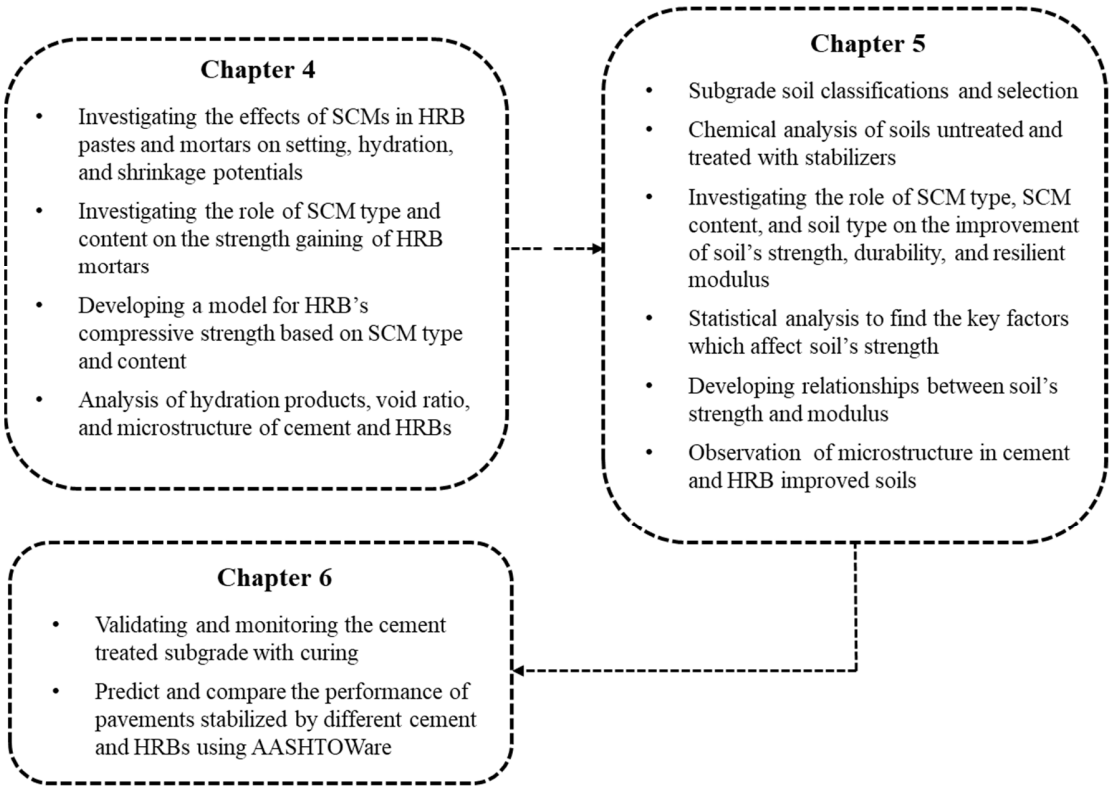

Figure 1-3 Flow chart illustrating the thesis contributions

1.5 Thesis Scope and Organization

The thesis contains 7 chapters. The contents of each chapter are introduced as follows:

Chapter 1: ***Introduction.***

This chapter provides a general introduction, the problem statement, an illustration of the scope and contributions of this research project.

Chapter 2: ***Literature Review.***

This chapter presents a bibliographical study on hydraulic binders, subgrade and subgrade soils, and the use of hydraulic binders for subgrade soil improvement.

Chapter 3: ***Research Methodology and Materials.***

This chapter illustrates the flow and organization of laboratory tests. The basic information of cement and SCMs used for HRB formulation is also presented. In

addition, it introduces the procedure of soil sampling and specimen preparation.

Chapter 4: ***Investigation of Hydraulic Road Binder.***

This chapter illustrates the characterizations of cement and HRBs in the form of paste and mortar. Portland cement is used as the control binder. Results of performance testing are presented and analyzed.

Chapter 5: ***Investigation of Subgrade Soil and Hydraulic Road Binder Improved Subgrade Soil.***

Soil investigation and classifications are first introduced. Then, it presents performance testing for the chemical and physical properties of treated subgrade soils. Test data is analyzed to compare the stabilization effects of different hydraulic binders.

Chapter 6: ***In-Field Subgrade Stabilization and Its Impact on Pavement Structure.***

This chapter introduces a field subgrade stabilization using cement. The field data is also presented. Moreover, this chapter introduces a prediction of long-term pavement performance using AASHTOWare.

Chapter 7: ***Conclusions and Recommendations.***

This chapter summarizes the significant results and findings from previous chapters. It also provides recommendations for HRB and HRB-soil mixing. Potential research problems are also discussed.

CHAPTER 2 LITERATURE REVIEW

2.1 Hydraulic Binders

Hydraulic binders are additives composed of complex chemical ingredients and have the ability to react and harden when mixed with water. When it is mixed with water and aggregates, chemical bonding is created between aggregates and soil particles. Such hydraulically bound mixtures then have significantly improved strength and durability. The most important examples of hydraulic binders are cement, lime, different types of ashes, blast furnace slag, and kiln dust. Because of the different compositions of hydraulic binders, there are always significant variations of engineering characteristics in hydraulically bound mixtures.

2.1.1 Portland Cement

Portland cement was initially developed and patented by an English manufacturer Joseph Aspdin in 1824 (Pavement Interactive, 2019). The common raw materials used for manufacturing cement are limestone, clay, silica sand and other minor ingredients (Pavement Interactive, 2019). These materials are heated at high temperature (1400 to 1600°C) to form a rock-like substance commonly called “clinker”. The clinker is then cooled and ground into a fine powder. Ordinary Portland cement is formed by blending clinker powder with 5% to 8% of gypsum and fillers (PCA website; Pavement Interactive, 2019).

The most commonly used cement in North America is Ordinary Portland Cement (OPC) or General Use Cement (GU). It has been used as binders for infrastructure constructions for decades. The major oxide phases in hydrated cement are tricalcium silicate (C_3S[1]), dicaulcium silicate (C_2S), tricalcium aluminate (C_3A), as well as tetracalcium aluminoferrite (C_4AF) (Prusinski and Bhattacharja 1999). Among them, C_3S constitutes between 50% and 80% of

[1] In cement notation, C means CaO, S means SiO_2, A means Al_2O_3, and F means Fe_2O_3, these conventions will be frequently adopted hereafter.

Portland cement by mass and is the dominant strength development element in the cement (Scrivener *et al*., 2015). The hydration products after cement hydration are calcium silicate hydrate (C–S–H), calcium hydroxide ($Ca(OH)_2$, CH), and ettringite (Scrivener *et al*., 2015).

2.1.2 Supplementary Cementitious Materials and Their Use in Blended Cementitious Systems

Supplementary **C**ementitious **M**aterials (**SCMs**) or Supplementary Cementing Materials are materials other than cement that have hydraulic and pozzolanic reactions. With the help of hydration properties, some SCMs make considerable contributions in strength development. SCMs are widely used in conjunction with cement to initiate and promote hydration process. The engineering benefits of using SCMs in blended cement include increasing workability, improved resistance to sulfates, mitigation of alkali silica reaction, and the decrease of permeability (Lothenbach *et al.,* 2011).

Figure 2-1 by Lothenbach (2011) shows the general chemical components of SCMs and Portland cement. Due to manufacturing process, SCMs, especially fly ash and pozzolan, contain high percentages of fine silicate fumes and have a large surface area. Such properties could give rise to reactivity and pozzolanic reactions. In contrast, SCMs have less reactive CaO content than in Portland cement. Slag, on the other hand, has a more balanced proportion of CaO and SiO_2. In addition, fly ash and natural pozzolans contain a small percentage of Al_2O_3. The hydration products of these SCMs may include more calcium aluminate hydrates.

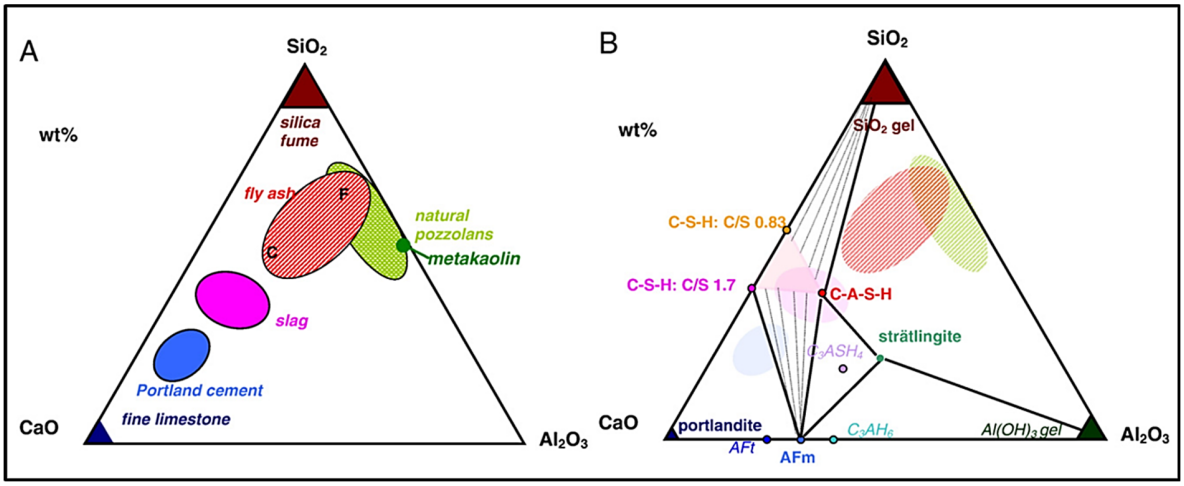

Figure 2-1 Ternary diagram of SCMs, and their hydrated phases (Lothenbach *et al.*, 2011)

Recent studies mainly focused on mechanical or durability aspects of one specific fly ash or slag (Lothenbach *et al.,* 2011). On the other hand, only few researches addressed the comparisons between different components and their roles in blended cements and their bound mixtures. Papadakis *et al.,* (2002) proposed a fundamental estimation for the efficiency factors of SCMs in blended cement. In addition, various strength models have been proposed for concrete and mortars considering the SCM content, water-to-binder ratio, and binder types. Nevertheless, the knowledge about the role of each SCM in the overall blended systems, their impact on hydration, and the strength development is still insufficient (Lothenbach *et al.,* 2011).

Ground Granulated Blast Furnace Slag (GGBFS)

Ground **G**ranulated **B**last **F**urnace **S**lag (**GGBFS**), commonly called slag cement, is a recovered industrial by-product from the iron and steel industry (Slag Cement Association). GGBFS are composed of a mixture of iron oxide, magnesium oxide, and silicon dioxide. In order to produce GGBFS, molten slag is first obtained from a blast furnace. It is then rapidly chilled to become glassy, non-metallic slag granules (Slag Cement Association). The granules are further dried and ground to be incorporated into the cement. Slag has been used extensively for concrete and road construction for over a century (Slag Cement Association). Research papers published from the 1990s have demonstrated that when blended properly with cement,

slag can achieve benefits such as better concrete workability, higher strength, lighter weight, and better controlled hardening processes (Cheng and Yan, 2011). Slag, when blended with 50% of cement, will extend the initial setting time from approximately 175 min to over 250 min. Moreover, a blended system containing 50% cement, 30% slag, and 20% fly ash was found to further increase the initial setting to approximately 350 min (Slag Cement Association). The extension of setting could reduce the rate of heat flow, decrease the internal temperature of hydraulic concrete, and also reduce the potential of shrinkage cracks due to rapid hydration and drying.

Fly Ash

Fly ash is a fine-grained by-product from coal combustion, and is mainly a composite of metal oxides including silicon dioxide (SiO_2), aluminum oxide (Al_2O_3), iron oxide (Fe_2O_3), and calcium oxide (CaO) (Trivedi *et al.,* 2013).

Based on its self-cementing abilities, fly ash used for soil stabilization is generally classified as two major categories: Class C type and Class F type. Between the two, Class C fly ash has higher content of calcium oxide (CaO) resulting in a stronger self-cementing property. In contrast, Class F fly ash contains a substantial content of natural pozzolanic materials, and it includes a relatively lower amount (less than 7%) of calcium oxide (CaO), as it is presented in Figure 2-1. The other components frequently found in fly ash are aluminum oxide (Al_2O_3), silicon dioxide (SiO_2), and iron oxide (Fe_2O_3). In Europe, fly ash is classified as Calcareous fly ash, and Siliceous fly ash, similar to Class C and F, respectively.

Cement Kiln Dust (CKD)

Cement kiln dust (CKD) is the by-product of Portland cement manufacturing (Little and Nair 2009). CKD generally contains about 30%-40% calcium compounds (CaO, $CaCO_3$, and $CaSO_4$) and about 20%-25% pozzolanic materials (AASHTO 2008). With such “free lime” present, most CKDs have hydration properties similar to Portland cement and lime. When it is mixed with water, they will generate a strong alkaline environment and promote cementitious

reactions (Peethamparan, 2008). However, as a kind of by-product, some CKDs contain a large proportion of loss of ignition (LOI) content as high as over 30%, which in turn, may result in a low hydration property.

2.1.3 Hydraulic Road Binder

"A hydraulic road binder is a factory produced hydraulic binder, supplied ready for use, having properties specifically suitable for treatment of materials for bases, subbases and capping layers as well as earthworks, in road, railway, airport and other types of infrastructures." --- EN 13282

The term hydraulic road binder (HRB) is from European Standard (EN 13282-1& EN 13282-2). A hydraulic road binder consists of a powder-formed binder manufactured from a blend of different chemical components. As the name implies, the mechanisms of HRB treatment is by hydration with water. They have been used for decades in road projects in some European countries such as France, UK, and Germany. As mentioned before, the purpose of HRB development is to slow down setting and reduce the usage of cement clinker.

HRBs are composed of multiple materials. HRBs can be formulated by one, two, or multiple SCMs and by-products based on local materials availability (Buczyński and Lech, 2015). Portland cement clinker is blended into HRB to activate hydration and to improve strength. The most common SCM constituents standardized in HRB include granulated blast-furnace slag, kiln dusts, natural pozzolan, by-product ashes (*e.g.*, fly ash, wastepaper sludge ash, fluidized bed combustion ash), burnt shale and limestone fillers (EN 13282). HRBs are classified and graded in specifications based on their hardening time and mortar compressive strength.

In North America, the standard ASTM C595 specifies cement and blended cements with different types of SCMs. There are some overlaps between HRBs and blended cements classified in ASTM C595 and CSA-A3001. Table 2-1 below presents comparisons of composition, specifications and conformity between HRBs and blended cement introduced in

ASTM C595 and CSA-A3001.

In particular, HRBs are classified into rapid hardening and normal hardening based on their cement clinker content and setting time. HRBs with more than 20% clinker content and less than 150 minutes of initial setting time are classified as rapid hardening HRB in EN 13282-1. On the other hand, EN 13292-2 standardizes HRBs having initial setting times more than 150 minutes.

In addition, EN 13282-1 presented a wide range of 7-day mortar compressive strength (CS) (5 MPa~16 MPa) and 28-day compressive strength (12.5 MPa~32.5 MPa) for rapid hardening HRB. For normal hardening HRB, there is no required compressive strength at 7-day and 28-day, however it specifies a range of 5-52.5 MPa at the age of 56 days. Based on their strength, they are graded from E2 to E4 in rapid hardening, N1 to N4 in normal hardening HRBs. Meanwhile, ASTM C150 and Canadian Standard (CAN/CSA-A3001-13) has minimum requirement of 20 MPa (7-day) and 26.5 MPa (28-day) respectively for general use (GU) cement.

It should be noted the current use of blended cement in Canada is not significant. According to Statistics Canada (Government of Canada website), the production of Portland cement was the most dominantly produced cement in the last 12 years. In contrast, the other types of cement only accounted for a small percentage, see Figure 2-2. In the US, SCMs are usually added to concrete while mixing rather than blending with clinker (Juenger and Siddique, 2015). However, use of a manufactured HRB in pavement construction could save the cost of transport of different materials. In addition, it can be more convenient for quality control.

Table 2-1 Composition, specifications and conformity for HRB (EN 13282), ASTM C595 and CSA-A3001 specified blended cement

		EN 13282-1 HRB Rapid Hardening	EN 13282-2 HRB Normal Hardening	ASTM C595 IL, IP, IS(<70%), IT(S<70%)	ASTM C595 IS(S>70%), IT(S>70%)	CAN/CSA-A3001 Blended hydraulic cement
Main Constituents		Clinker (K), slag (S), natural pozzolana (P) & burnt ones (Q), fly ashes (V & W with LOI ≤ 9%), burnt shales (T) and limestone fillers (L & LL)		Slag (S), natural pozzolana (P), limestone (L)		Slag (S), fly ash, natural pozzolana (P), limestone (L), silica fume
		hydrated calcium lime (CL-S) and natural hydraulic lime (NHL)	CL-S and NHL, Ashes (Va), calcium ashes (Wa), BOF slag (Sb)			
Clinker Content		≥ 20%	No requirement	≥ 30%	≤ 30%	
Minor Additional Constituents		≤ 10% in weight				
		-	To be declared if > 5%			
Calcium Sulfate		Gypsum, semi-hydrate, natural or synthetic anhydrite				
Additives		≤ 1% dry mater (or content + function must be noticed if > 1%)				
Specifications	**Initial Setting Time**	E ≥ 90 min; RS (rapid setting) ≤ 90min	≥ 150 min	⩾ 45 min	⩾ 45 min	Minimum: 45 to 90 min; Maximum: 250 to 480 min
	Soundness	E ≤ 10mm; RS ≤ 30 mm	≤ 30mm			
	CS 7-day	E2 ≥ 5MPa; E3 ≥ 10MPa; E4 and E4-RS ≥ 16MPa	No requirement	⩾ 13 MPa	No requirement	⩾ 8.5 to 20 MPa
	CS 28-day	12.5≤E2≤32.5 MPa; 22.5≤ E3≤42.5 MPa; 32.5≤ E4≤ 52.5 MPa and E4-RS≥32.5 MPa	No requirement	⩾ 20 MPa	⩾ 5 MPa	⩾ 25.0 to 26.5 MPa
	CS 56-day	No requirement	5≤N1≤22.5 MPa; 12.5≤N2≤32.5 MPa; 22.5≤N3≤42.5 MPa and 32.5≤N4≤52.5 MPa	⩾ 25 MPa	⩾ 11 MPa	No requirement
	SO_3	≤ 4%		≤ 3%	≤ 4%	≤ 3%

Nowadays, most cement sold in Europe is blended cement consists of Portland cement clinker and SCMs (Scrivener *et al.,* 2015). In the author's point of view, analyzing the HRB as a blended system is important for understanding the role and effect of each SCM type. Moreover, such research also helps to determine the optimum SCM percentage in local HRB manufacturing.

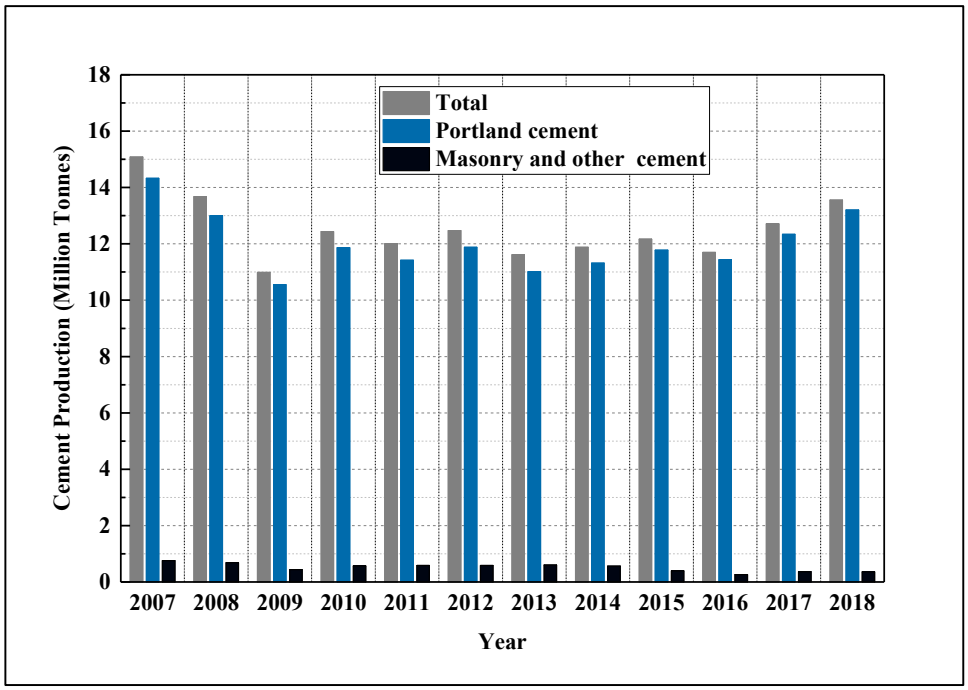

Figure 2-2 Recent cement production in Canada

2.2 Subgrade in Pavement Structure

Subgrade is the part of the roadbed which lies underneath the constructed pavement. Figure 1-1 in the previous chapter illustrates the location of subgrade, and the load distribution in pavement. The subgrade itself is not usually considered to undertake significant traffic loading compared to other pavement layers. However, the bearing capacity and stiffness of subgrade soil are fundamental factors which influence the thickness of pavements (AASHTO, 1993).

Subgrade can be composed of natural soil, or compacted soil to meet bearing capacity requirements (Thom 2003). Subgrade supports the pavement section and undertakes the distributed load from upper layers. A strong natural subgrade provides reliable stiffness and support that will reduce the requirement of pavement thickness. Moreover, the long-term pavement performance depends considerably on the durability of underlying subgrade. The

deformation of subgrade may cause pavement failure such as severe rutting, wheelpath depressions, and cracking (Pavement Interactive, 2019). The impact may be exacerbated under climate conditions, including frequent precipitation, salt corrosion, and seasonal freezing and thawing.

In AASHTO 1993 pavement design, the resilient modulus (M_r) is used to describe the stiffness of subgrade soil, furthermore, M_r is used to determine the thickness of flexible pavement. The M_r value is defined as the ratio of cyclic stress divided by the resilient strain under a rapidly cyclic load (TAC, 2014). The cyclic loading simulates the rapid traffics loading spreads on the top of subgrade. AASHTO T307 introduces the laboratory method for measuring the subgrade soil's M_r value. The test is conducted in a tri-axial loading cell. Such modulus can also be estimated in field by a non-destructive stiffness testing, usually by a Falling Weight Deflectometer (FWD) (ASTM D5858). Since the modulus of roadbed changes significantly over the year due to moisture and thermal effects, the effective M_r value is therefore calculated based on the modulus obtained in different months or seasons. Detailed calculation of the effective M_r can be found in AASHTO 1993 pavement design method and TAC guide (2014).

2.3 Pavement Distress Due to Failure of Subgrade

Soil type, moisture, temperature, and excessive loading are four important factors which may lead to subgrade deterioration and failure. In particular, heavy and prolonged rainfall increases the moisture content of subgrade soil, causing soil to become saturated. Therefore, the fine soil particles are flocculate in water, the cohesion between soil particles are significantly reduced, thus it decreases the bearing capacity and stiffness. Fine soils such as silt and clay are sensitive to wetting and drying cycles. In some cases, the CBR value and compressive strength may drop by 90% when saturated (Petry and Little, 2002; Halsted, 2011). Thermal impact is another crucial impact for subgrade soil. The strength and modulus of subgrade soils become higher in winter due to freezing, however they decrease significantly during thawing period. Detailed descriptions of each factor related to the deterioration of subgrade are introduced in the following sections.

2.4 Subgrade Soils

Subgrade soils are the soils that are naturally present in the construction area. The property of

natural subgrade soils significantly varies with depth, moisture, geological mapping, and particle size. There are various types of subgrade soils in Ontario, some of them are difficult soils with low strength and bearing capacity, making them unsuitable for pavement construction.

The typical subgrade soils observed in Ontario includes organic sand, silty sand, organic clayey silt and clay. Table 2-2 below introduces the default values used in Mechanistic-Empirical Pavement Design for subgrade properties.

Table 2-2 Ontario subgrade moduli for various classifications of soils (Data from TAC Guide 2014)

Brief Description	MTO classification	Drainage	Susceptible to frost action	M_r (MPa) Good	M_r (MPa) Fair	M_r (MPa) Poor
Rock, rock fill, shattered rock, boulders/cobbles	Boulders/ cobbles	Excellent	None	90	80	70
Well graded gravels and sands suitable as granular borrow	GW, SW	Excellent	Negligible	80	70	50
Poorly graded gravels and sands	GP, SP	Excellent to fair	Negligible to slight	70	50	35
Silty gravels and sands	GM, SM	Fair to semi-impervious	Slight to moderate	50	35	30
Clayey gravels and sands	GC, SC	Practically impervious	Negligible to slight	40	30	25
Silts and sandy silts	ML, MI	Typically, poor	Severe	30	25	18
Low plasticity clays and compressible silts	CL, MH	Practically impervious	Slight to severe	35	20	15
Medium to high plasticity clays	CI, CH	Semi-impervious to impervious	Negligible to severe	30	20	15

All the data in Table 2-2 is obtained from TAC pavement design guide (2014). Soil types mentioned in the table are based on AASHTO and MTO soil classification guide.

Not only has the design guide implied the reduction of subgrade behavior based on soil type; literature have also indicate that, subgrade soils can be problematic when prone to swelling, decreased strength, cracking, or excessive deformation (Petry and Little, 2002). Such

characteristics are often caused by their particle size distribution, clay minerals, and organic contents. Moreover, based on national soil survey reports (Government of Canada), clay and clayey soils containing organic contents are frequently observed in some areas in Ontario, Canada.

The following parts introduce the typical properties of local subgrade soils: clayey and organic.

Clayey soil and clay

Whether a soil particle is clay, sand, or gravel is based on the particle size and mineral content. Soil particles are classified based on their sizes (Das, 2015):

- Gravel particle: fraction passing 76.2 mm sieve and retained on the No. 4 (4.75 mm) sieve.
- Sand particle: fraction passing the No. 4 (4.75 mm) sieve and retained on No. 200 (0.075 mm) sieve.
- Silt and clay (fine soil) particle: fraction passing No. 200 (0.075 mm) sieve.

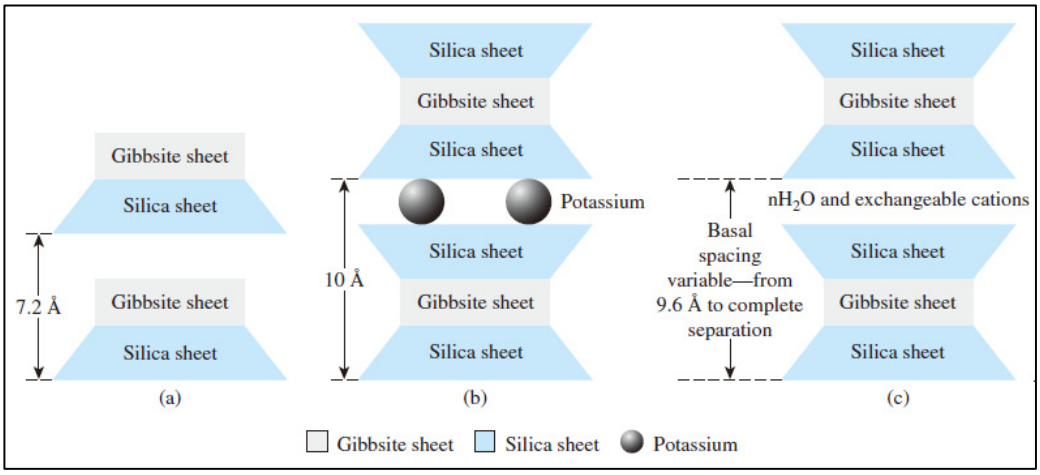

Figure 2-3 Structure of (a) kaolinite; (b) illite; (c) montmorillonite (Å = 10-10 m) (from Das, 2015)

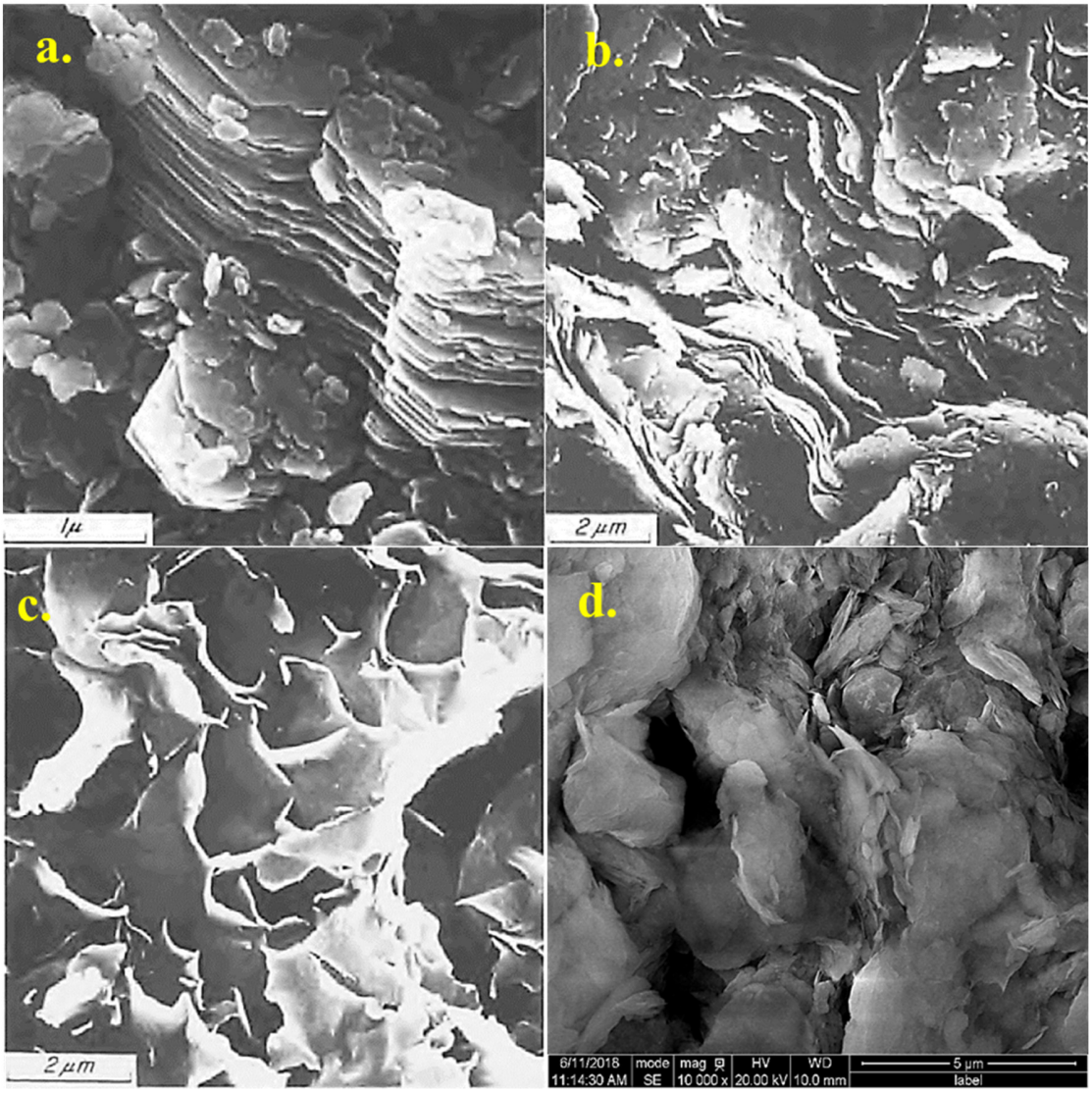

Figure 2-4 Microstructure of (a) kaolinite; (b) illite; (c) montmorillonite (Terzaghi *et al.*, 1996), and (d) clay soil from Niagara, Ontario

The terminology "clayey" is applied for the fine-grained soils which behave plastically. Typical clayey soils have a plasticity index of 11 or more (Das, 2015). Clay and clayey soils, due to their fine particle size, usually have high **S**urface **S**pecific **A**rea (**SSA**) and therefore lead to high **C**ation **E**xchange **C**apacity (**CEC**) and attract more water molecules (Petry and Little, 2002). Clay particles can have high SSA of approximately 800 m^2/g, thus enabling the largest amount of water attraction between structural layers.

The three primary clay minerals are kaolinite, illite, and montmorillonite. Their mineral

structures are shown in Figure 2-3, and SEM micrographs are presented in Figure 2-3. One can observe from the figures that the voids between kaolinite minerals are narrower than the other two with the particles contacting in a face-to-face pattern. The illite mineral has bigger crystal size with particles contacting in face-to-face and face-to-edge patterns. The montmorillonite layers are bounded together by weak van der Waal's forces. (Das, 2015). The undisturbed montmorillonite minerals contacts substantially in face-to-edges forms.

Moreover, a porous structure with more voids is observed in the montmorillonite micrograph from Figure 2-4 (c). The significant water attraction ability will lead to a thicker double-water layer and a larger plasticity index (PI). Consequently, they have engineering disadvantages including low strength, plastic deformation and drying shrinkage potential. A clay specimen obtained from Niagara, Ontario is presented in Figure 2-4 (d), the microstructure of clay exhibits similar patterns compared to illite and montmorillonite.

Organic soil

Organic soils have a wet appearance with a darker color and visual organic fibers. The major compositions of **S**oil **O**rganic **M**atter (**SOM**) in natural subgrade consists of plants, roots, animal tissues, microorganisms, and other colloidal organic substances (Harris *et al.,* 2009). In practical road construction, the top 10-15 cm of unsuitable soil is removed. Deeper removal of soil and backfilling may cause higher construction cost and time. However, in some areas, ground soils may still contain a considerable amount of organic matter. Figure 2-5 shows the condition of a subgrade soil after top soil removal in a local construction. The land was originally used for agricultural purposes. Therefore, there is still a considerable amount of organic fibers that remains visible from the pictures.

The main chemical elements in SOM generally includes carbon (C), nitrogen (N), sulfur (S), and phosphorus (P) (Terzaghi *et al.,* 1996). In particular, 60~80 % of SOM is made of soil humus or humic materials (Harris *et al.,* 2009). Humus is significantly responsible for the cation exchange capacity (CEC) of soil organic matters (Brady and Weil, 1996). Because of high CEC ability, soil organics will consume a considerable amount of cations such as Ca^{2+}, Mg^{2+}, and Al^{3+} from chemical stabilizers, thus affects the stabilization.

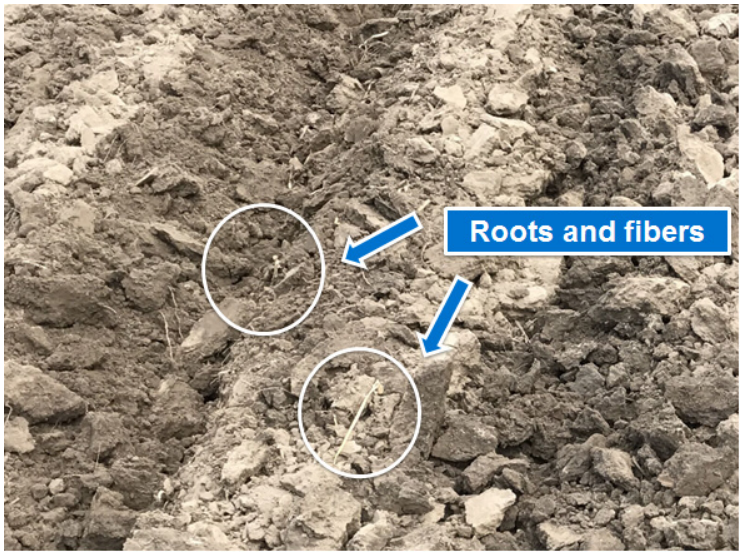

Figure 2-5 Subgrade soil containing organic material

Soils can be both clayey and organic. Soil humus was tested to produce a low pH (<9) cement treated soil using West Québec City clays (Tremblay *et al.,* 2002). That literature also indicated that, the low pH of the clayey-organic specimens significantly affected the hydration and long-term pozzolanic reactions, which in turn, inhibited strength development (Tremblay *et al.* 2002). Accordingly, the Portland Cement Association (PCA 1992) commonly recommends an increased cement ratio for organic soil stabilization to ensure the soil-cement durability and strength.

There are several methods to measure the organic content in soils. However, the most successful method has not yet been established due to the complexity and composition of soil organic matter (SOM) (Harris *et al.,* 2009). ASTM D2974 and its similar tests are frequently introduced in Canada and US to determine SOM by loss-on-ignition (LOI) method. The method compares the weight difference between oven dried soil (110°C) and furnace ignited soil (440°C). The weight loss due to ignition is considered as the weight of SOM. However, it should also be noted that during the ignition process, some crystallized water may also be broken down. As a result, the LOI method could exaggerate the actual organic content.

2.5 Climate Effects on Subgrade Soils

2.5.1 Effects of Wetting and Drying

Soils, especially fine-grained soils for instance clay and silt are sensitive to moisture change.

Once they are dry and hard, and the next moment they can be wet and soft (Petry and Little, 2002). This range of moisture sensitivity properties is due to two main reasons: first, the high moisture content of silt and clay; second, the high potential of capillary action attributed by the particle and void size. The figure below shows the damaged road due to precipitation and wheelpath loading.

Figure 2-6 Damaged road due to rainfall and loading effects (Picture was taken in Niagara, 2017)

As it was introduced before, moisture is highly attracted to clay particles. With the increase of moisture content, the soil's double-water layer becomes thicker leading to increasing particle distances. As a result, the soil's volume has been changed as swelling occurs. Rapid drying leads to evaporation of soil bulk and shrinkage. As a result of cyclic wetting and drying, the void ratio in a soil mass could be changed causing volumetric change. Such phenomenon will further decrease the bearing capacity and strength. The typical geotechnical hazards caused by moisture effects in subgrade soils include lack of strength, self-weight collapse, and volumetric swelling. Therefore, AASHTO and PCA guidelines for soils stabilizations require a soaking period before strength testing.

2.5.2 Effects of Freezing and Thawing

Canada is one of the coldest countries in the world with vast areas experiencing seasonal frost and permafrost freezing. In seasonal freezing and thawing areas, low temperature in winter causes freezing of moisture in subgrade soils, whereas spring thawing results in decrease of subgrade strength and capacity. It should also be noted that in the last 100 years, the global

mean near surface air temperature has increased by 0.74°C (Pachauri and Reisinger, 2008). Global warming causes the freezing and thawing cycles more frequent and drastic.

The freezing of gravity water and double-layer water in soil form ice lenses and causes moisture and salt migration towards the freezing front (Akagawa *et al.*, 1991; White *et al.*, 1999). With sufficient moisture supply, the ice lens grows continually and causes frost heave in the subgrade. During periods of rising temperatures, the ice thaws, but leaves voids in the subgrade structure. This repeated freeze-thaw action changes void ratio distribution and soil particles aggregation, thus weakening the engineering properties of subgrade (Viklander, 1998; Rempel *et al.,* 2007).

After the cyclic freezing and thawing, engineering properties of subgrade soil such as compacted density, strength, stiffness, and hydraulic conductivity are significantly affected, even if the soil has been well compacted (Rempel *et al.,* 2007; Qi *et al.,* 2008). When the traffic loads transferred from above pavement layers, cracking and rutting can occur in pavement structure.

Public Works Canada (1992) suggested utilizing the typical bearing strength reduction of natural subgrade soils in spring compared to fall for airport pavement facilities design. It is indicated from the report that soils with higher liquid limit (over 50) and high clay particles could have 45% to 50% reduction of strength due to freeze-thaw cycles.

Another important question is the depth of which will the pavement structure and the subgrade be affected. The term frost penetration, also known as frost depth or freezing depth, is usually used to demonstrate the depth of frozen groundwater in pavement at winter. Field investigations conducted during the late 1960s and 1970s indicated that the average depth of frost penetration (in meters) underneath paved highways in Southern Ontario ranges between 1.0~1.8 meters and could be up to 3.0 meters in Northern Ontario. A typical flexural pavement in Ontario could be design as 100 mm of asphalt surface, 150 mm of coarse base, and 450 mm of granular subbase. The total pavement thickness is less than 1.0 meter. Therefore, most high-volume and low-volume roads have their subgrade exposed to cyclic freezing and thawing cycles.

2.6 Subgrade Stabilization

2.6.1 Subgrade Stabilization Techniques

Soil stabilization is one of several ground improvement methods which have both scientific and artistic achievements. Throughout the long history of stabilization, various methods were developed including infill straw blended with soil for additional strength by the ancient Roman Empire; the use of rice paste as an additive to enhance soil compaction properties in ancient China; and the use of elephants for earth dams compaction in South Asian civilizations (Bahar *et al.,* 2004; Chen and Lin, 2009; Hejazi *et al.,* 2012; Gnanendran *et al.,* 2015; Jefferson *et al.,* 2015). Modern subgrade improvement technologies include surface soil-stabilizer mixing, deep vibratory compaction, soil replacement and backfill, deformation control of soft ground with high tensile geosynthetics, offshore foundation stabilization and anchoring, high pressure chemical grouting and intelligent dynamic compaction (Jefferson *et al.,* 2015). Those methods introduced previously can be used exclusively or combined for better soil improvement. Although there are various subgrade stabilization methods, the scope of this thesis is only to study the chemical stabilization method using hydraulic binders.

The general mechanism of chemical stabilization is to increase bonding between soil particles, thus increasing the load bearing capacity. The stabilized subgrade will also have controlled moisture content in wet conditions. Moreover, plasticity of soil are permanently reduced (Jefferson *et al.,* 2015).

In pavement engineering, stabilized subgrade becomes an additional layer separating the natural subgrade soil and pavement structure. With a high stiffness, stabilized soils can also be considered as an extra bound layer in the pavement. As a result, a thinner pavement is required. This achieves a more cost-effective and environmentally friendly solution. The bound subgrade layer has the potential to function as an additional subbase layer to spread the load evenly on the subgrade, to provide thermal insulation for the subgrade, and to prevent migration of fine particles from the natural subgrade to the base and surface layer (CTAA, 2018).

2.6.2 Subgrade Soil Stabilization Using Hydraulic Stabilizers

Among all the stabilization methods, soils mixed hydraulic stabilizers has the advantage of easy construction, low cost, and shallow excavation depth. The basic principle is to use hydraulic materials to mix with soil and water and to create a hydraulically bound mixture. During such process, the moisture sensitivity and engineering properties of subgrade soils are permanently improved.

Cement and lime have been used in subgrade construction for a long time as the most traditional stabilizers. Currently they are still commonly used. In recently years, emphasis on environmental considerations has led to more frequent utilization of liquid slurry instead of powders (Kowalski, 2007). The stabilizer powders are pre-mixed with water to form liquid slurry before applying to the ground. Slurry utilization not only reduces the occurrence of chemical dust during the spreading and mixing process, but it also gives more accurate and more uniform blending effects (Kowalski, 2007). Nevertheless, it will also bring drawbacks such as excessive moisture and high cost due to slurry transportation.

2.6.3 Mechanisms and Current Laboratory Mix Design Considerations of Subgrade Soil Improvement Using Cement

Before it is applied to the field construction, a mix design of cement-soil mixtures should be performed in lab. Nowadays, there are mix design guidelines and criteria established for cement treatment of subgrade soils. The type of cement considered in the current guidelines is GU cement.

Chemical products of cement hydration include crystalline **C**alcium **S**ilicate **H**ydrates (**C-S-H**), **C**alcium **A**luminate **H**ydrates (**C-A-H**), $Ca(OH)_2$ (**CH**) and Ettringite (Wang, 2015). The cementitious hydration reactions which provide early strength for soil matrix are presented below (Prusinski and Bhattacharja, 1999):

Equation 2-1

$$2C_3S + 6H \rightarrow C-S-H + 3Ca(OH)_2$$

Equation 2-2

$$2C_2S + 4H \rightarrow C-S-H + Ca(OH)_2$$

Where H means H_2O. On the other hand, it should be noted that the composition for C-S-H is quite variable, the dash between C-S-H means that there is no unique ratio between SiO_2 and CaO. During the process of cation exchange (Figure 2-7 left), higher ordered ion cations (Al^{3+}, Ca^{2+}, and Mg^{2+}) from stabilizers replace the current lower order ion cations (Ka^{+} and Na^{+}) in soil double layer. Consequently, the thickness of double layer can be decreased, so that the space between soil particles and soil plasticity will be reduced.

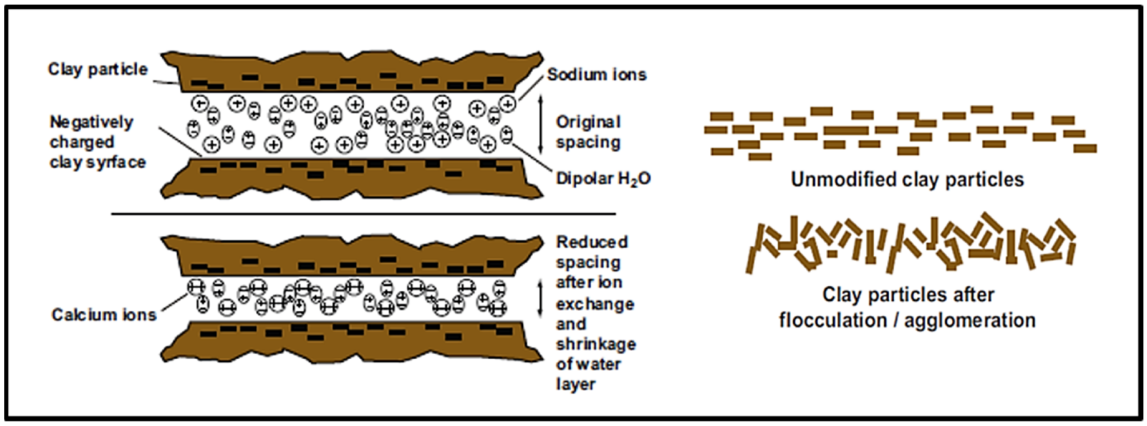

Figure 2-7 Cation exchange (left), and particles flocculation/agglomeration (right) (Halsted, 2011)

Soil flocculation (Figure 2-7 right) changes the soil matrix from a natural deposited flat, face-to-face structure to a more randomly configured edge-to-face orientation (Prusinski and Bhattacharja 1999). On the other hand, soil agglomeration is the formation of larger lumps which helps the flocculation process and improve the soil texture, therefore, reducing the number of fine-grained particles (i.e. silt and clay) (Kowalski, 2007).

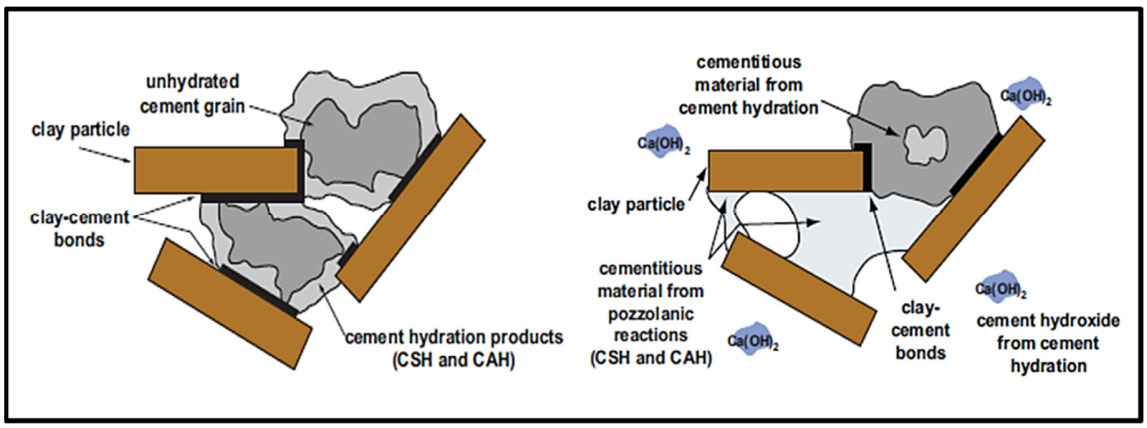

Figure 2-8 Cementitious hydration (left) and pozzolanic reactions (right) (Halsted, 2011)

Pozzolanic reaction (Figure 2-8) is a secondary process after cementitious hydrations that may take months or years to occur causing late-stage strength increase as well as plasticity reduction (Al-Rawas *et al.,* 2005; Halsted, 2011). The pozzolanic reactions exist in soil-cement and other cementitious stabilizers (cement kiln dust, slag cement) soil systems. In order to maintain a consistent reaction, the stabilized soil should be controlled in a high pH environment (around 12). Basic reactions are shown as follows (Prusinski and Bhattacharja, 1999):

Equation 2-3

$$Ca(OH)_2 + SiO_2 \rightarrow C-S-H$$

Equation 2-4

$$Ca(OH)_2 + Al_2O_3 \rightarrow C-A-H$$

The goals for soil mix design are to find proper stabilizers and adequate dosage for soil improvement. The basic considerations for soil-cement mix design are Atterberg limits, compaction property, strength, and durability (freezing and thawing cycles, and wetting and drying cycles) (Little and Nair, 2009).

PCA (1992) and AASHTO (2008) suggested a range of cement content based on material's soil type. The guidelines also introduce the criteria of soaked unconfined compressive strength (UCS) and their durability (freezing and thawing cycles and wetting and drying cycles). Table 2-3 presents the current mix design considerations and the criteria for soil-cement.

Table 2-3 Cement content suggested by PCA and AASHTO for soil stabilization, with recommendations of strength and durability requirement

AASHTO Soil Groups	Usual Range in Cement Requirement (%)		Minimum Soaked UCS (MPa)		Maximum Durability weight loss (%)
	By Volume	By Weight	7 Days	28 Days	
A-1-a	5~7	3~5	2.06	2.76	14
A-1-b	7~9	5~8	2.06	2.76	14
A-2	7~10	5~9	2.06	2.76	14
A-3	8~12	7~11	2.06	2.76	14
A-4	8~12	7~12	1.72	2.07	10
A-5	8~12	8~13	1.72	2.07	10
A-6	10~14	9~15	1.38	1.72	7
A-7	10~14	10~16	1.38	1.72	7

There is another method of subgrade soil treatment, called **soil modification**. If cement is only used to reduce the subgrade soil's plasticity, to improve the workability and bearing capacity, the content of cement can be significantly reduced. This technique is referred to as **C**ement **M**odified **S**oil (**CMS**). The objective of the CMS layer is to add an additional layer between pavement structure and weak subgrade soil. The cement content for such treatment typically varies from 2% to 5% by dry weight of soil (Halsted *et al.,* 2008). A soaked UCS of between 0.2 MPa to 0.4 MPa is usually recommended, or an enhancement of 0.4 MPa compared to the soil before treatment (Jones *et al.,* 2010). Table 2-4 below summarizes the difference between cement stabilized soil and cement modified soil.

Table 2-4 Comparisons between cement stabilized soil and cement modified soil

	Cement stabilized soils	**Cement modified soils**
Cement ratio by weight	3% to 11% for A-1 to A-3 8% to 16% for A-4 to A-7	2% to 5%
Recommended UCS	≥1.38 MPa (7-days)	0.2 MPa to 0.4 MPa for fine-grained soils
Durability test limit	7% to 14% (less than)	N/A
Application layer	Base, subbase	Subbase, stabilized subgrade

As it is shown in Table 2-4, cement stabilized soil or soil-cement is considered to function as a base or subbase layer and undertake significant traffic loading. On the other hand, cement modified soil is used to improve the bearing capacity of subgrade soil. Alternatively, the stabilized subgrade with improved stiffness can also be considered to function as a subbase and reduce the thickness of granular subbase layer.

Nowadays, CMS is more widely used in subgrade soil treatment especially for fine-grained subgrade soils. Such method reduces the use of cement and reduce the cost by using existing materials. For low-volume road constructions, especially when granular materials are not easy to obtain, cement treated soils with 6% or more by weight are also used. Such treated layer functions as a base layer lies above a natural subgrade. 50 to 100 mm of granular materials is paved above the treated layer for protection and drainage. With light and low-volume traffic, such gravel road provides satisfied performance. Chapter 6 introduces a case with such design.

2.6.4 Mechanisms and Current Laboratory Mix Design Considerations of Subgrade Soil Improvement Using Supplementary Cementitious Materials (SCMs)

Ground Granulated Blast Furnace Slag (GGBFS)

GGBFS has been extensively used for soil improvement, solely, or in conjunction with other hydraulic binders. Like other by-products and industrial secondary materials, slags have various engineering properties due to the slag source and manufacturing technique. Overall, the hydration and pozzolanic reactions are highly dependent on the content of free lime and calcium aluminates, whereas the improvement of particle packing depends on the calcium silicates content (Manso *et al.,* 2013).

Poh *et al.* (2006) suggests that at sufficient binder contents of slag (15%–20%) and after a prolonged curing period, soil strength can be improved distinctly. Yadu and Tripathi (2013) evaluated slag stabilized soft clay with the slag content ranging from 3% to 12%. Results indicated that the optimum amount of GGBFS for such soils was determined as 9%, and the UCS of stabilized soft soil was found to be more than 25% higher than raw soil. Substantial improvements also had been observed for both the unsoaked and soaked CBR values. Apart from strength increase, slag modified soil also has the benefit of reducing the expansion of clay due to moisture. Higgins (2005) indicated that the combination of 4% to 5% slag with 1% to 2% lime together significantly reduce the linear expansion of clay to be lower than 2%, such results are shown in Figure 2-9.

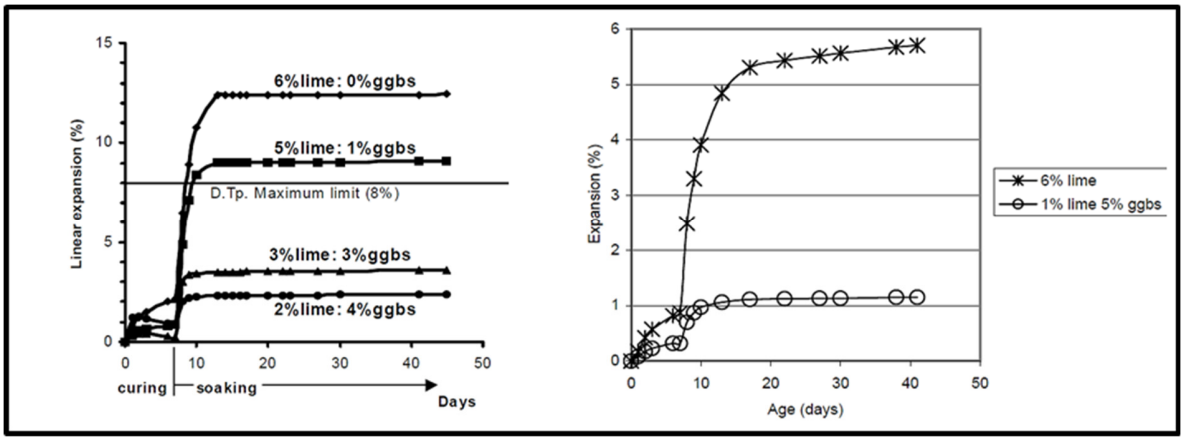

Figure 2-9 Suppression of swelling by GGBS treated Kaolinite (left) and Lower Oxford Clay (right) (Higgins, 2005)

In general, the presence of the slag reduces the soil's plasticity and enhances its moisture control ability. It also contributes to the continuous improvement of soil's compressive strength and durability (Manso *et al.,* 2013). Since slag itself does not have a strong self-cementing ability, a dosage of an activator (*e.g.,* lime and cement) is usually needed to improve the stabilizing effect (Cheng and Yan, 2011).

Fly ash

Fly ash-based soil stabilization mechanisms consist of hydraulic reactions and pozzolanic reactions. The mechanical properties such as UCS, M_r, and CBR value are considerably enhanced when using proper mix design (Kolias *et al.,* 2005). Fly ash addition reduces CEC properties and swelling characteristics (Nalbantoğlu, 2004); moreover, with an increasing amount of fly ash, soil expansion is minimized, and cohesion is increased continuously. However, compared to cement, fly ash treated soil will have a lower compressive strength and a milder strength development process.

As for mix design, moisture density relationship, compressive strength and durability tests are generally considered for determining the optimum fly ash content. Typical fly ash additions applied in lab are between 10-40%. However, like slag, the different fly ashes have various degrees of improvement effects due to their source, type, and chemical components. The differences between different fly ash types could be more distinct than different slag types, as shown in Figure 2-10.

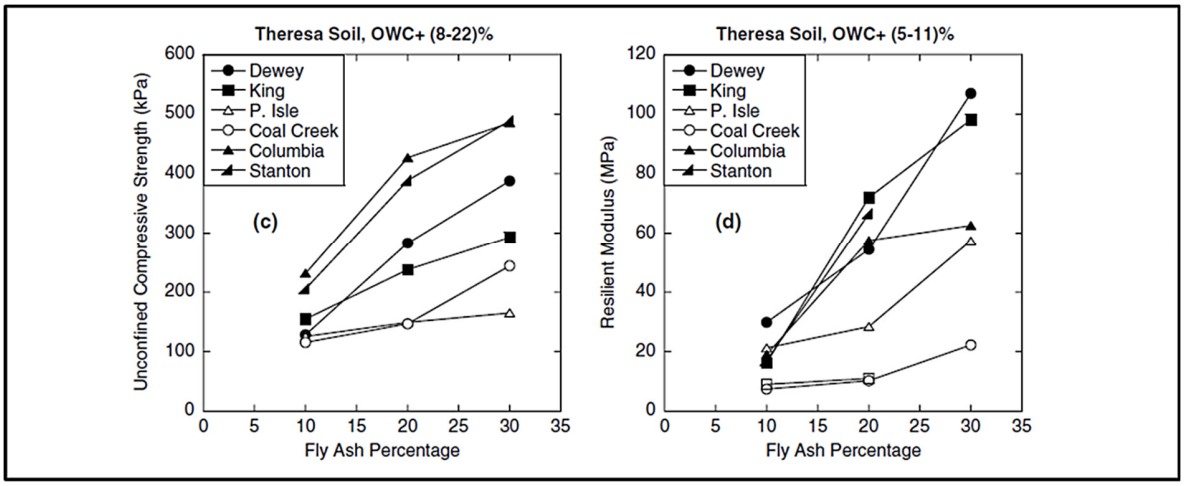

Figure 2-10 Effects of various fly ash types on the UCS and M_r of fine-grained soil (Tastan *et al.,* 2011)

Additionally, an activator, such as Portland cement or hydrated lime, is often required for Class F fly ash stabilizing, to initiate the hardening process (Kolias, 2005). Literature illustrates that the typical cement-fly ash ratio ranges from 1:3-1:4 whereas the lime-fly ash ratio should be 1:2 for better performance (Little and Nair, 2009).

Cement Kiln Dust (CKD)

CKD has been found to have promising effects in improving the unconfined compressive strength (UCS), freeze-thaw cycles resistance, and reducing the plasticity index (Miller and Azad, 2000). Moreover, CKD treatment can be more cost-effective and require less mellowing time than that of lime stabilization (Trivedi *et al.,* 2013).

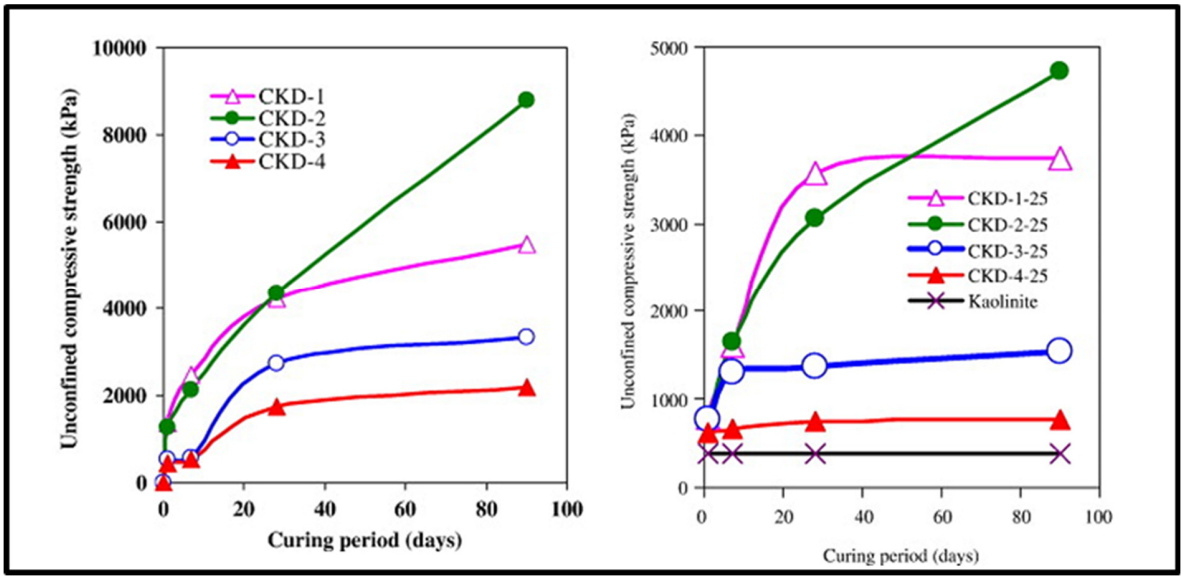

Figure 2-11 UCS of hydrated CKD paste CKD-treated Kaolinite (Peethamparan *et al.*, 2008)

However, it is also indicated that high content of loss on ignition (LOI) in CKD could result in lower percentage of free lime and other hydraulic materials. Therefore, it could cause lower strength (Adaska and Taubert, 2008). Also, as a by-product material, the oxide compositions in CKD may vary widely depending on the manufacturing process, storage, fuel nature, and equipment used during production (Little and Nair, 2009). An empirical guide suggests that in order to achieve good performance, the content of SO_3 and MgO in CKD should not exceed 3-5%, and loss on ignition (LOI) should not be greater than 8-10%. Consequently, the chemical composition of the candidate CKD should be determined before usage. Figure 2-11 presented UCS of 4 different hydrated CKD pastes (water content 31%) (left), and UCS of 25%

CKD-treated Kaolinite (right) (Peethamparan *et al.,* 2008). As it was shown, the resource of CKD plays a significant role on the stabilization effects.

2.6.5 Subgrade Soil Stabilization for clayey and organic soils

Chemical Stabilization for Organic Soils

The current practice for pavement construction on a heavy organic subgrade is referred to as "cut and replace". However, if the thickness of organic soil layer is too high. It could still be practical and economical to chemically treat the subgrade soil (Tastan, 2011). Again, hydraulic binders such as cement, lime, and fly ash have been widely considered for organic soils treatment.

Clare and Sherwood (1954) evaluated the 7-day UCS value of 10% cement-treated organic soil. Based on the strength, they classified the organic soil by three categories: inactive, active, and very active. Research conducted by Université Laval (Tremblay, 2002) introduced 10% cement treatment for marine clay and fluvioglacial silt from Québec City, Canada. Results illustrated that with much lower pH value (less than 9), hydration and pozzolanic reactions were significantly affected such that almost no strength growth was noted.

Lime, on the other hand, can be used to maintain a strong alkaline environment (pH value over 12) and provide more calcium that can be consumed for exchange by SOM (Eades *et al.,* 1962). Moreover, lime hydration product (*e.g.*, CSH gel) will give rise to the strength development and will improve the soil inner textures (Harris *et al.,* 2009). Overall, the pH value and the SO_4^{2-} concentration are two crucial criteria for lime-based stabilization.

Other cementitious materials, for example, fly ash, slag, and anhydrous calcium sulfate, $CaSO_4$, have also been found to achieve higher UCS strength of organic soils (Hebib and Farrell, 1999; Tastan *et al.,* 2011). Those organic soils, when stabilized with cement and SCMs, had a significant improvement of strength and resilient modulus. However, with increasing organic matter content, an exponential decrease of resilient modulus was also observed.

Overall, soil organic matters had a negative effect on cement and lime treatment. With sufficient amount of stabilizer and the addition of slag, gypsum, and fly ash, stabilization effects could be improved (Chen and Wang, 2006). Nevertheless, there is still need for research on chemical reactions and soil-stabilizers interactions on chemically treated organic-rich soils

(Hampton and Edil, 1998).

Chemical Stabilization for Clayey Soils

The objective of clay stabilization is to control volume change characteristics, modify plasticity and substantially enhance strength, thus improving workability. Successful experience in chemical stabilization of clays had been documented since the 1950s. Previous literature focused on the ion exchange process in clay, the mellowing period for lime treated soil, and the hydraulic and pozzolanic products generated during stabilization (Rosenqvist, 1959; Mitchell and Hooper, 1961). The hydration products fill the tiny voids between soil particles, also lead clay particles to flocculate into larger lumps (Nalbantoğlu, 2004, Wang *et al.,* 2016). Therefore, the plasticity of soil will be reduced which in turn reduces the expansive potential, and enhances the workability of the clay.

Current stabilizers used for clay subgrade stabilization are generally divided by three major groups (Petry and Little, 2002): traditional stabilizers (*e.g.*, hydrated lime, Portland cement, and fly ash); by-product stabilizers (*e.g.*, kiln dusts from cement and lime manufacture, rice husk ash (RHA) and wastepaper sludge ash (WSA)), as well as nontraditional stabilizers (*e.g.*, enzymes, sulfonated oils, high molecular weight polymer, *etc.*). The former two categories of stabilizers mainly rely on mechanisms of calcium exchange, hydraulic reactions, and pozzolanic reactions while the third category is based on a range of various mechanisms. The use of by-product stabilizers has the benefits of energy savings and reducing CO_2 emissions. Also, they act in a role resembling traditional additives and help the stabilized soil having mild strength gains and long-term durability enhancements (Segui *et al.,* 2012; Manso *et al.,* 2013).

As long as hydraulic binders are mixed with clay, a series of hydration processes will take place rapidly. Mellowing of the clay and stabilizers before mixing has been recognized as an effective method, especially for lime and other calcium-based stabilization. Additionally, proper curing is important for stabilized clay, especially for hydraulically treated mixtures. During the curing time, traffic is prohibited on the subgrade, and the surface should be kept damp.

Figure 2-12 shows comparisons between cement stabilized clay subgrade and the natural subgrade. The project in the figure was conducted for a low-volume road in Chatham, southern Ontario. Soils that have been stabilized and cured will give a higher stiffness and a smoother

surface (shown in the figure). The stabilized soil will also be more resistance to moisture and thermal change. Once the stabilized subgrade been sealed and capped with gravel or hot mix asphalt (HMA), the drastic vibration of moisture in the subgrade will be prevented and the long-term performance of pavement will be significantly improved.

Figure 2-12 Comparison between natural and stabilized clay subgrade (Pictures were taken in Chatham-Kent, 2017).

2.7 Hydraulic Road Binder (HRB) and Its Current Application for Subgrade Soil Stabilization

Hydraulic road binders were initially developed from 1975 to 1985 in France (Sétra 2008). HRB was first developed to reduce the use of cement by incorporating slag and pulverized fuel ashes. Moreover, blends of hydraulic binders set slower than cement while providing longer working times and mitigated the effects of sulfates (Little and Nair, 2009). In the 1990s, an important milestone was established when HRB was introduced in French standard "*NF P 15-108 'Hydraulic Binders – HRBs – Composition, specifications and conformity criteria*" (Abdo *et al.* 2013). From the late 1990s to the present, the use of hydraulic road binder and hydraulically bound mixtures has been widely used in European road construction (Buczyński and Lech, 2015). Nowadays, HRBs have been particularly designed for various performance objectives including treatment of regional soils, pavement reclamation and recycling (Abdo *et al.,* 2013; Saussaye *et al.,* 2013; Melese *et al.,* 2019).

Subsequent research on HRB and HRB applications for pavement reclamation and soil stabilizations has been conducted in Poland, France, United Kingdom, and other European countries. HRB has also been recognized in developing countries: Rapid Hardening HRB

developed by Kenya's Savannah Cement is expected to achieve 30% saving of construction cost due to a lower retail rate than ordinary cement (Savannah Cement, 2014).

Although there are extensive researches focusing on soil stabilization using slag and fly ash, very few studies have considered the multi-mixed SCM as an integral binder-hydraulic binder. In the author's point of view, HRB refers to a pre-mixed binder with considerations of local material's properties, strength grade, and components formulation studies. Table 2-6 summarizes the recent researches on the use of hydraulic road binders for pavement materials stabilization.

As it is indicated from Table 2-6, HRB-treated soils, with proper design, could have improved performance. However, since HRBs are usually composed of local materials, their physical properties and compositions will vary significantly. It was also indicated that some lower strength graded HRBs may not be suitable for certain soil types, especially for those containing high amounts of clay (Ćwiąkała *et al.,* 2012). Due to the variety of HRB properties, HRBs are usually adopted based on a considerable amount of experience in local road construction (Sétra, 2008). Additionally, supplemental laboratory testing of HRB mortar and HRB-soil should be performed to provide proper HRB formulation and HRB content for field application. A recent study performed by Melese *et al*. (2019) indicated that manufactured HRBs could significantly improve the strength and modulus of full-depth reclaimed material to meet restrict strength and durability requirement. It was also indicated that strength was significant improved even from early curing age (7 days).

Since a considerable percentage of HRB is still composed of cement clinker, the hydration properties and strength development characteristic could be similar to that of Portland cement. With the substantial experience of cement treatment, it will be an interesting idea to compare the stabilization between HRB and cement treatment at the same test criteria. In this study, different types of local soils from Ontario, Canada are selected, and these soils are treated with formulated HRBs containing different SCMs. Portland cement is used as a control for the evaluation of these laboratory-blended HRB types.

Table 2-5 Selected literature on the use of hydraulic binders for soil stabilization

Researcher	HRB composition	Stabilizer content	Soil type	Highlights
Sétra and CFTR (2008)	Not specified			Presented some mix design criteria and guidelines for hydraulic binder and/or lime treated soil for road base in France.
Ćwiąkała *et al.* (2012)	3MPa class HRB: 90% Brown coal fly ash, 10% cement 9MPa class HRB: 80% Brown coal fly ash, 20% cement	2% to 10% of HRB	7 types of soils including sand and clay	3MPa class HRB is not suitable for two types of soils with heavy clay; both HRBs increased compressive strength of non-cohesive soils significantly.
Segui *et al.* (2012)	Wastepaper sludge ash (WSA)			WSA has a greater Blaine value, but its particles are very porous. Lime and metallic aluminium in WSA could be responsible for swelling.
Saussaye *et al.* (2013)	64% to 79% Clinker + 21% to 35% limestone; 35±10% Clinker + 64±10% limestone	1% CaO + 6% cement; 1% CaO + 6% HRB	Silty, sandy, and gravel	The soils performance is improved by the presence of chloride, (e.g. NaCl), but chloride ions should not exceed $10g \cdot kg^{-1}$. Sulfate content higher than $10g \cdot kg^{-1}$ could lead to decrease of indirect tensile strength; while $1g \cdot kg^{-1}$ will affect the development of mechanical strength.
Buczyński and Lech (2015)	Fluidized bed combustion ash (PF), cement kiln dust (CKD) and Portland cement		Fine aggregate	100% Portland cement mortar has the highest compressive strength while the second strongest binder was a combination of 50% PF and 50% cement.
Rica *et al.* (2016)	Clinker 35%, and limestone 65%	6% HRB and 1% Quicklime	Silt	Sodium and potassium sulfates induce swelling on HRB-treated soils, reducing the tensile strength. Chloride, phosphate and nitrate salts do not produce volumetric stability failures, but the indirect tensile strength can be reduced.
Melese *et al*. (2019)	Rapid hardening	2% to 6% HRB	Reclaimed pavement material	HRB-treated full-depth reclaimed materials have equivalent performance as cement treated ones.

2.8 Summary of Literature Review

This chapter first introduced the properties of hydraulic binders, the subgrade soil and the deterioration, the types and effects of problematic soils in local condition. It then presented the property of cement and cementitious materials, and their application in subgrade soil stabilizations. The chapter also introduced the current HRB types and their applications. Based on the discussion in the chapter, a summary can be addressed as follows:

- Subgrade soils can be problematic when they have the property of swelling, failure, cracking, or undergo an excessive settlement. Such characteristics may be attributable to their particle size distribution, clay mineral content, and organic content. The organic material and clay particles in soil could inhibit the cement hydration and decrease the strength.
- The stabilization mechanisms for cement include cementitious hydration, cation exchange, particle flocculation/agglomeration, and pozzolanic reactions. PCA and AASHTO recommend a high requirement of cement content to achieve strength and durability criteria. On the other hand, the current cement-soil modification guidelines do not have a restrict criteria of durability and recommend much less cement content. However, a cement ratio between 6% and 10% is also used for the modification of a weak subgrade soil or for the stabilization in a low-volume road.
- The moisture and thermal effects in Ontario are severe such that the pavement and subgrade conditions can be significantly affected. The durability of the improved subgrade soils, therefore, needs to be conducted.
- Supplementary cementitious materials (SCMs) help to build strength in blended cements by hydraulic and pozzolanic reactions. SCMs are widely used in conjunction with Portland cement to provide multiple advantages. The use of blended cement or HRB is insignificant in Canada thus more research could be conducted.
- Hydraulic road binder (HRB) has the potential to be used for pavement materials stabilizations. However, its formulation, binder characterizations and stabilization effects need to be investigated before field application.

CHAPTER 3 RESEARCH METHODOLOGY AND MATERIALS

3.1 Introduction

This chapter introduces the detailed research plan for 3 research Parts: investigation of hydraulic road binder, investigation of hydraulic road binder improved subgrade soils, in-field subgrade stabilization and its impact on pavement structure. Materials sampling and basic information is also introduced in this chapter.

In order to achieve the research goals, a research plan was developed and its overview is shown in Figure 3-1.

The research activities include three research parts:

- **Research Part I**. Laboratory testing for different formulated HRBs. Tests for paste included setting time, hydration heat, and XRD. Tests for mortars included mortar flow, drying shrinkage, compressive strength, flexural strength, and ESEM. An image processing technology was applied to characterize the voids in mortars. A strength model considering percentages of cement and SCMs were therefore developed based on the lab results.
- **Research Part II.** Laboratory testing and investigation of cement and HRB-treated subgrade soils. Tests started with soil characterizations and classifications. Afterwards, the effects of soil type, binder type and binder content on the properties of improved soils were analyzed. Laboratory tests included chemical analysis, strength, modulus, durability, microstructure observation. The author further analyzed the key factors which influence soil's strength.
- **Research Part III.** Field subgrade constructions with cement were conducted and the stiffness was monitored along with curing time. Combined with lab testing results, the potential of stabilized subgrade soils with HRBs are further evaluated using AASHTOWare.

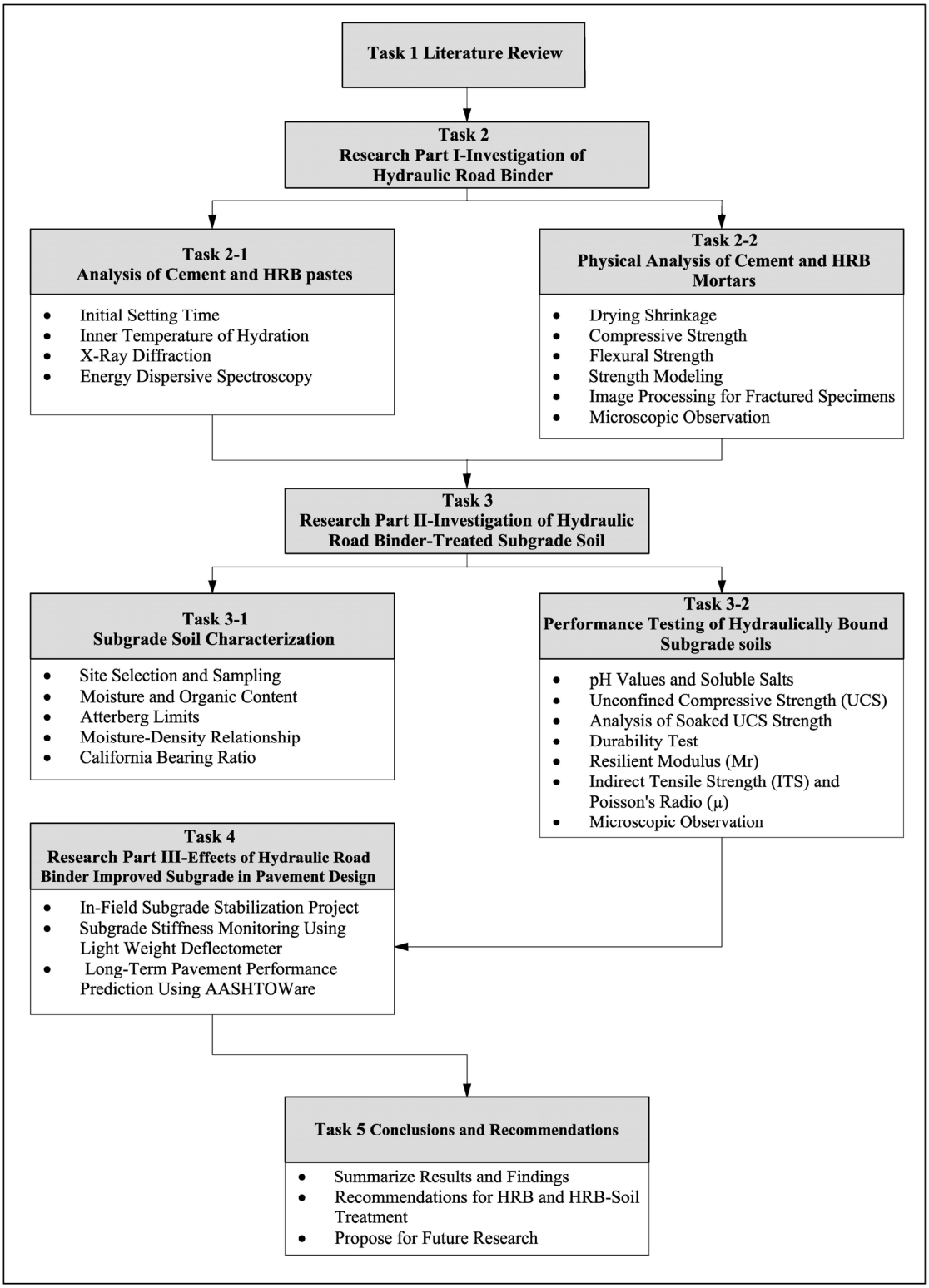

Figure 3-1 Overview of research activities and tasks

Laboratory tests were conducted according to standards of American Society for Testing and Materials (ASTM), Ministry of Ontario (MTO) standard, and American Association of State Highway and Transportation Officials (AASHTO). Some modifications of test procedures were made based on research purpose and were illustrated separately in Chapter 4 and Chapter 5. General concept, test plan, and test set up are shown and presented in the following chapters.

3.2 Research Part I- Investigation of Hydraulic Road Binder

3.2.1 Materials

Portland Cement

The cement and all the other SCMs used in the research were kindly supplied by Lafarge Canada Inc. from plant in Bath, Ontario. Two types of cement were used in the study: **G**eneral **U**se (**GU**) cement and **G**eneral **U**se **L**imestone (**GUL**) cement.

Ordinary Portland Cement (OPC), or General Use (GU) cement is a powder-formed binder consists of approximately 92% by weight of cement clinker, 5% gypsum, and 3% limestone.

General Use Limestone (GUL) cement is produced by intergrinding approximately 83% Portland cement clinker with 12% limestone powder and 5% gypsum. It is defined as Type IL cement in ASTM C595 that with up to 15% limestone ($CaCO_3$) is permitted in blended systems. The limestone powder has the effects of increasing the specific surface area, promoting the reactions, and reducing the permeability and porosity.

Supplementary Cementitious Materials

SCMs used in the research include ground granulated blast-furnace slag (GGBFS), fly ash (type F), and cement and kiln dust (CKD). GGBFS and CKD were supplied from mill plants in Ontario. On the other hand, the resource of fly ash is from Sundance Power Plant in Edmonton, Alberta. Table 3-1 summarizes the chemical components of GU cement, GUL cement, GGBFS, fly ash and CKD. Data was conducted by suppliers using rapid X-Ray scanning method. Moreover, the specific gravity of each powder was conducted by author according to ASTM C188.

Table 3-1 Chemical compositions of cement and SCMs used in the study

Chemical Compositions	GU	GUL	GGBFS	Fly ash	CKD
Calcium Oxide (CaO) (%)	62.2	60.8	37.1	9.3	42.6
Silicon Dioxide (SiO_2) (%)	19.6	18.6	38.5	57.2	13.9
Aluminum Oxide (Al_2O_3) (%)	5.0	4.8	10.7	23.5	3.5
Magnesium oxide (MgO) (%)	2.5	2.4	12.2	1.0	1.8
Iron Oxide (Fe_2O_3) (%)	3.3	3.1	0.4	3.5	1.8
Sulphur Trioxide (SO_3) (%)	3.9	3.9	1.2	0.2	2.5
Loss of Ignition (%)	2.3	4.9	0.6	0.8	31.4
Blaine Fineness (m^2/kg)	383	508	515	560	--
Specific Gravity	3.3	3.2	2.9	2.0	2.8
Phase Compositions					
Tricalcium Silicate (C_3S) (%)	55				
Dicaulcium Silicate (C_2S) (%)	15				
Tricalcium Aluminate (C_3A) (%)	8				
Tetracalcium Aluminoferrite (C_4AF) (%)	10				

As it is shown from the table, the GU cement has highest content of CaO, accounting for 62.2%. The second most significant content in GU and GUL is SiO_2, ranging from 18.6% to 19.6% in both types of cement. As for the phase composition, tricalcium silicate (C_3S) or alite makes up more than half of the total binder weight. C_3S is documented to contribute to the dominant strength development during cement hydration (Scrivener *et al.,* 2015). Other considerable phases include dicaulcium silicate (C_2S) (15%), tricalcium aluminate (C_3A) (8%), and tetracalcium aluminoferrite (C_4AF) (10%). These three phases together attribute to early hydration and long-term strength development in hydraulic bound mixtures. Meanwhile, GUL cement has slightly lower CaO content than GU with which also exceed 60%. It is also observed that GUL has larger value of Blaine Fineness than GU, indicating that GUL has finer particle sizes and larger specific surface area. Same phenomenon is shown in GGBFS and fly ash.

On the other hand, GGBFS and fly ash have much less CaO content but considerable amounts of SiO_2 and Al_2O_3. Such results coincide with the trends in Figure 2-1 and information from literature. Additionally, cement has higher specific gravity than SCMs. The fly ash has the lowest specific gravity compared to that of 3.3 of general use cement. That means the HRBs and blended cements with substantial SCMs will significantly reduce the weight.

Standard Graded Sand (Ottawa Sand)

Standard graded sand, or called Ottawa sand, was used for making mortar. The sand was composed of quartz mineral with a standard gravity of 2.65. The gradation of the graded sand meets the requirement of ASTM C778. The detailed gradation is tested and presented in Table 3-2 below.

Table 3-2 Gradation of graded sand

Particle Size (μm)	Percent Passing (%)
600	98
425	74
300	28
150	2

3.2.2 Sample Preparation for HRBs Investigation

Investigation was conducted on cement and HRB pastes and mortars respectively. Hydration properties were investigated on cement and HRB pastes. Pastes were made by mixing cement and HRB powders with water. The water-to-binder ratio $(w/b)_{paste}$ for each paste was set to be 0.385. Such value was determined by normal consistency test conducted on GU cement paste.

In addition, cement and HRB mortars were made by mixing binders, water with standard sand. The sand is composed of natural silica with specific gravity of 2.65. The sand was specifically graded with according to ASTM C778. One part by weight of binder was mixed with 2.75 part by weight of sand. Moreover, the water-to-binder ratio $(w/b)_{mortar}$ was determined to be 0.5 for drying shrinkage beams. But $(w/b)_{mortar}$ for mortar specimens prepared for strength testing was determined separately based on flow test of each mortar (ASTM C1437).

Pastes and mortars were molded in different shapes based on testing. The paste and mortar were cured in humidity chamber for 24 hours, then they were demolded from the molds and soaked in tap water for curing.

Figure 3-2 shows the sample preparation for paste and mortar samples. The figure also presents the curing chamber located in structures lab, University of Waterloo.

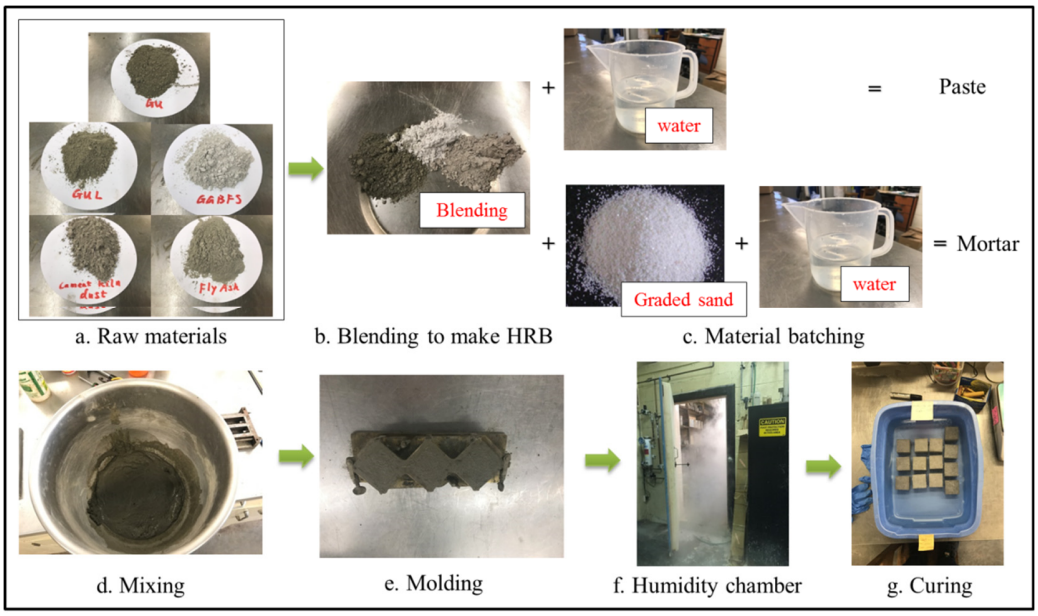

Figure 3-2 Mortar and paste preparation

The designations of HRBs and their composition follow the rules presented in the Table 3-3. The same designation is used for both HRB pastes and mortars containing the same HRB type.

Table 3-3 Designation and formulations of cement and HRBs

Name	GU (%)	GUL (%)	GGBFS (%)	Fly ash (%)	CKD (%)	Clinker Content (%)
GU	100	0	0	0	0	92
GUL	0	100	0	0	0	83
HRB-1S	20	0	80	0	0	18
HRB-1C	20	0	0	0	80	18
HRB-1LS	0	20	80	0	0	17
HRB-1F	20	0	0	80	0	18
HRB-2LS	50	0	0	0	50	41
HRB-2S	50	0	0	50	0	46
HRB-2C	65	0	35	0	0	46
HRB-2F	65	0	0	0	35	46
HRB-3S	65	0	0	35	0	60
HRB-3C	0	80	20	0	0	60
HRB-3F	0	80	0	0	20	60
HRB-4LS	0	80	0	20	0	66
HRB-4LC	0	80	0	0	20	66
HRB-4LF	0	80	0	20	0	66

It should be noted that other HRB formulations were produced for compressive strength testing. The relevant information is detailed in Section 4.2.2. Among all the HRB types, HRB-1 series (HRB-1S, HRB-1C, HRB-1L, and HRB-1F) have the low cement content accounting for around 20%. HRB-2 series have medium clinker content of around 50%, while HRB-3 series have slightly higher ratio of cement than HRB-2 series (around 65%). On the other hand, HRB-4L series are blended by 80% GUL and SCMs. Additionally, the types of SCMs included in the HRBs can be realized from the designations. For example, "S" stands for GGBFS, "F" stands for fly ash, and "C" stands for cement kiln dust. Each HRB composed of either GU or GUL cement. If the there is "L" in the name of HRB, it means that such HRB contains limestone powders.

Figure 3-3 summarizes the actual cement clinker content in different HRB types. Here, cement clinker is assumed to compose 92% of total GU cement. It is also assumed that GUL contains GU cement and 12±1.5% by weight of limestone. It is indicated from the figure that HRBs significantly reduce the cement clinker content compared to GU and GUL.

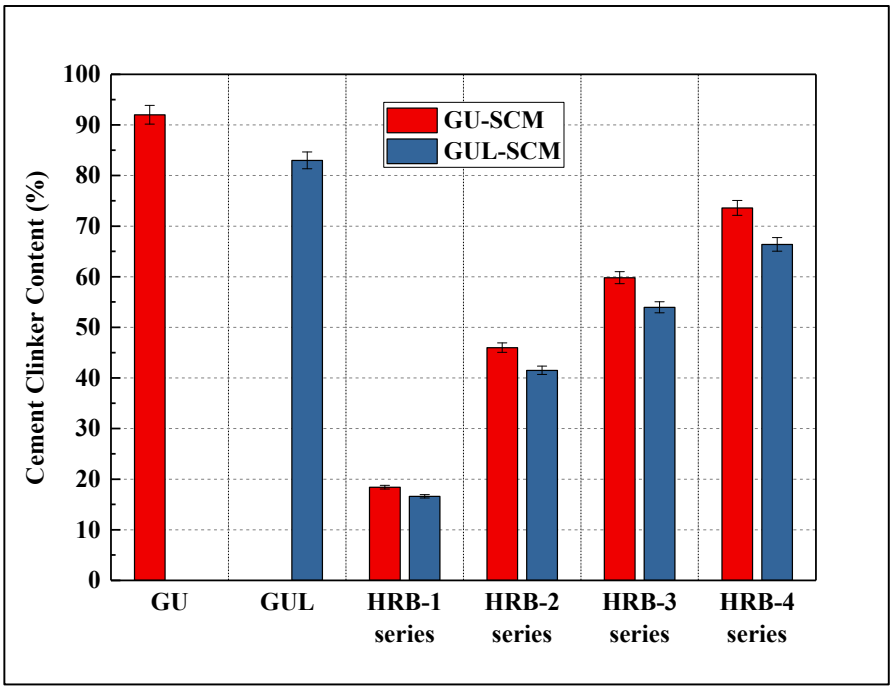

Figure 3-3 Approximate cement clinker in cement and other hydraulic binders

Several representative formulated HRBs with different SCMs were investigated through X-Ray diffraction test and Energy Dispersive Spectroscopy test to identify the hydration component and their contents. They were also scanned to observe their microstructure and morphology characters. Next, selected HRBs were mixed with soil and form hydraulic bound mixtures.

3.2.3 Testing for HRB Binder Investigation

Table 3-4 presents the content and description for each test.

Table 3-4 Tests used for investigation and formulation of HRBs

	Test name and standard	Description
Tests for paste	Initial setting time (ASTM C187)	Measuring the initial setting time of cement and HRB pastes. Analyzing the impact of each SCM type on the effect of delay of setting time.
	Inner temperature monitoring during hydration	Investigating the hydration kinetics of cement and HRB pastes. Comparing the heat release, temperature rise and time spot of peak temperature occurrence.
	X-ray diffraction	Characterization of hydration products after 56 days of curing. Investigation the role of cement and SCMs in hydration.
	Energy dispersive spectroscopy	Investigating different elements existing in hydrated pastes. Characterizing the amorphous hydration products.
Tests for mortar	Drying shrinkage (ASTM C596)	Investigating the shrinkage of hydraulically bound mortars due to drying along with time. Analyzing the effects of SCMs on controlling and shrinkage potentials.
	Compressive strength (ASTM C109)	Characterizations of cement and HRB mortars. Analyzing the role of each SCM type on the strength development. Tests were conducted on 7 days, 28 days, and 56 days respectively. Developing a strength model based on SCM type, content and water-to-binder ratio, and curing times.
	Flexural strength (ASTM C348)	Analyzing the role of each SCM type on flexural strength. Finding correlations between flexural strength and compressive strength.
	Image processing	Characterization the pore distribution, surface porosity of mortar specimens.
	Environmental scanning electron microscope (ESEM)	Observing the morphology, and hydration products of cement and HRB mortars.

3.3 Research Part II- Investigation of Hydraulic Road Binder Treated Subgrade Soils

3.3.1 Subgrade Soil Sampling

Subgrade soils were collected from several construction sites located in Southern Ontario, Canada. Three typical subgrade soils with different organic contents and clay contents were sampled. They were named after their sampling locations: Dresden, Blenheim, and Niagara respectively. The sampling locations are presented in Figure 3-4, image was screenshot from Google Map 2019. Among them, Dresden and Blenheim soils were collected from municipality of Chatham-Kent, while the Niagara soil was sampled from the region of Niagara Falls. The air temperature and precipitations of sampling locations are shown in the Figures 3-5 and 3-6. Data was observed from Government of Canada website.

Figure 3-4 Sampling locations in Southern Ontario. (Screenshot from Google Map 2019)

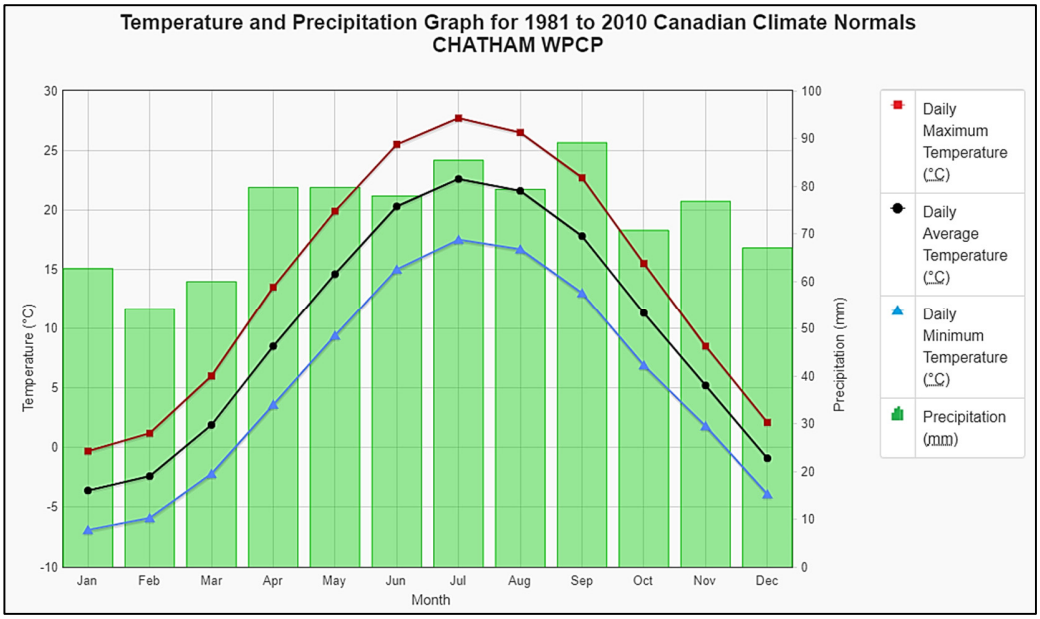

Figure 3-5 Air temperature and precipitations in Chatham-Kent (Figure captured from Government of Canada)

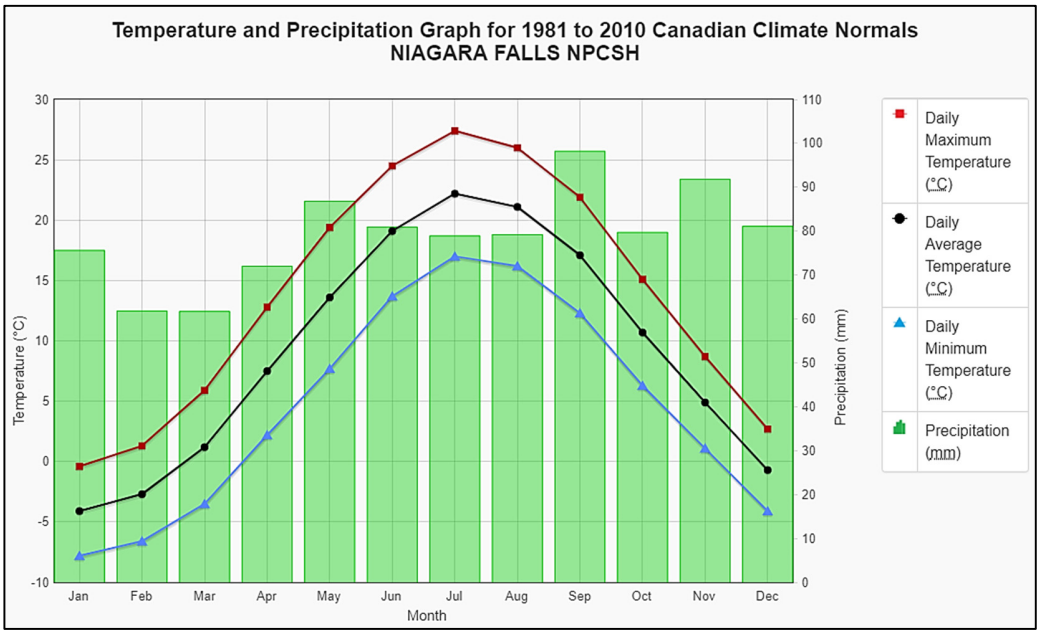

Figure 3-6 Air temperature and precipitations in Niagara Falls (Figure captured from Government of Canada)

As it is shown from the figures, both the sampling locations experience severe freezing and

thawing cycles. The trend of air temperature in the two regions are similar. The coldest months are December, January, and February, with the daily average temperature ranging from 0°C to -5°C. On the other hand, the daily minimum temperature may drop to lower than -5°C at night in January and February. In addition, the daily maximum temperature increases sharply to a high between 25°C to 30°C at summer. Regarding the precipitation, both of the regions have high precipitations throughout the year. Highest level of precipitation occurs in September and July in Chatham-Kent. The highest precipitation happens in September, November, and May at Niagara Falls. Sampling of subgrade soils are presented in Figure 3-7.

Figure 3-7 Sampling of subgrade soils

All the subgrade soils were collected at least 100 mm below the ground surface. Specifically, Dresden soil was collected on July 2017 from a Windfarm road construction site. The soil was collected after pulverizing. Blenheim soil was sampled on December 2016 from an unconstructed site. The sampling was conducted when the ground was not frozen. On the other hand, the subgrade soil from Niagara was sampled from a full-depth reclamation project on July 2017. Niagara soil was excavated approximately 600 mm below the road surface.

3.3.2 Investigation of Cement and HRB Improved Subgrade Soils

As it is introduced before, 3 types of subgrade soils were selected to be as representative soils in order to be treated with hydraulic binders. Various cement and HRBs types are used to evaluate the effects of each SCM component, and to compare the engineering properties between cement and HRB stabilization. Soils are mixed with different percentages of hydraulic binders from low (6%) to high (10% to 12%). Laboratory works for HRB-soil treatment generally composed of the following stages:

1) **Soil characterization and classification:**
   Subgrade soil samples were characterized and classified based on their particle size distribution, plasticity index, moisture density relationship, and CBR values. These three subgrade soils represent the typical weak subgrade soils in Southern Ontario.
2) **Typical HRB selection:**
   Several HRBs were selected which have different SCM types and overall low shrinkage potentials and high strength levels in the later curing period. These HRB types were then mixed with candidate soils at different binder contents.
3) **Chemical and strength development characteristics:**
   Conducted chemical analysis, and soaked UCS test (7 day and 28 day) for typical soil types at different binder contents (6% to 12% by soil mass). Investigating the role of soil's geotechnical information and HRB's property on the properties of hydraulically bound mixtures. Conducted statistical analysis to find crucial factors which affected soil's strength; furthermore, developed strength models to predict the strength of treated soils.
4) **Further study:**
   Based on the proposed binder content from previous stage. Conduct various tests (M_r, durability, IDT, microstructure observation) for HRB improved soils at the same binder content. The relationships between different parameters were also investigated.

Table 3-5 describes the tests designed in this research Part.

Table 3-5 Tests used for investigation of cement- and HRB-treated soils

Test name and referred standard	Specimen type and production	Description
Moisture (ASTM D2216) and organic matters content (ASTM D2974)	Pulverized soils	Measuring the natural moisture content and organic matters of subgrade soils
Particle size distribution, including sieving (ASTM D6913) and Hydrometer analysis (ASTM D422)	Pulverized soils	Measuring the clay content, silt content, and sand content. Draw the particle size distribution curve.
Atterberg limits (ASTM D4318)	Fine-grained soils passing 425 μm sieve	Measuring the liquid limit, plastic limit, and plasticity index of subgrade soils. Also analyzing the effect of stabilizers on the change of soil's Atterberg limits.
Moisture-density relationship, standard proctoring test (ASTM D698)	Cylindrical specimen (100 mm in diameter and 110 mm in height)	Determining the optimum moisture content and maximum dry density for subgrade soils before and after treatment. Provide information for specimen preparation afterwards.
California bearing ratio (ASTM D1883)	Cylindrical specimen (150 mm in diameter and 150 mm in height)	Determining the laboratory CBR value of compacted subgrade soils. In addition, measuring the linear swelling of subgrade soils due to soaking.
pH values (ASTM D6276) and ion chromatography test	Pulverized soils and hydraulic binders	Investigating the effect of hydraulic binders on the chemical environment and soluble salt in subgrade soils.
Unconfined compressive test (ASTM D1633)	Cylindrical specimen (100 mm in diameter and 110 mm in height)	Investigating the role and effect of each HRB type on the strength development subgrade soils. Tests were conducted on different HRB types, binder contents, and at different curing ages. Tests were conducted at soaked and unsoaked conditions. Generate a strength model considering soil's particle size, plasticity index, and HRB type.
Durability test, including freezing and thawing cycles (ASTM D560), and wetting and drying cycles (ASTM D559)	Cylindrical specimen (100 mm in diameter and 110 mm in height)	Measuring the weight loss of improved soil samples subjected to cyclic freeze-thaw and wet-dry conditions.
Resilient modulus test (AASHTO T307)	Cylindrical specimen (100 mm in diameter and 200 mm in height)	Measuring the resilient modulus of untreated and treated subgrade soils. Find relationship between M_r and UCS.

Table 3-5 Continued

Indirect tensile strength (ASTM D6931)	Cylindrical specimen (150 mm in diameter and 85 mm in height)	Measuring the indirect tensile strength of treated subgrade soils in different curing ages. Determine the Poisson's ratio of the specimens.
Environmental scanning electron microscope (ESEM)	Pieces from UCS specimens	Observing the morphology of different subgrade soils. Investigating the effects of stabilization on the soil's microstructure.

3.3.3 Preparation for Soil Samples

Samples preparation for UCS, resilient modulus and durability consisted of five steps: drying, soil breaking and sieving, mixing, compaction, and curing. The procedure of the preparation was presented in Figure 3-9 below.

To begin with the preparation, subgrade soils were first air dried at room temperature. Afterwards, clay clods were broken into small pieces by hammer and screened. A sieving test was conducted to observe the percentage of soils passing the 4.75 mm (No. 4) sieve.

Air dried subgrade soils were used for pH values and ion chromatography test. On the other hand, soils for strength and modulus testing were oven dried at a temperature of 110 °C until the weight became constant. Standard proctoring test was conducted for soil and improved soils to determine the optimum moisture content (OMC) and its corresponding maximum dry density (MDD). During specimen preparation, the dry soil was mixed with cement and HRB binder at first, then, a certain amount of water was added in. A mixer was used to mix the water, binder, and soil homogeneously together.

Compaction was conducted in the same effort as standard proctor test, and compacted specimens were back checked to have their moisture contents within ± 1% of the OMC and their dry densities above 95% of the corresponding maximum dry densities (MDD). Specimens prepared for different tests may have different sizes but with the same moisture content and dry density.

In particular, specimen size for UCS and durability tests were approximately 100 mm for diameter and 116 mm in height. On the other hand, the resilient modulus testing sample has the diameter of 100 mm but the height to be around 200 mm. On the other hand, specimens

prepared for indirect tensile strength are compacted by a gyratory compactor. There are converting factors for specimens with different heights. The calculation and determination of the factors are introduced in Section 5.6.

For the subgrade soils re-compacted according to their OMC and MDD, we call them **remolded** or **re-compacted** soil, since their property will be different from their original state in field. The term will be substantially used in the later text.

Figure 3-8 Soil Sample Preparation

Prepared samples were cured in a controlled humidity (100%) and temperature (20°C) curing chamber for certain period (7 days, 28 days, and 56 days) before testing. Specimens were transferred from the chamber and before they were immediately tested.

3.4 Research Part III- In-field Subgrade Stabilization and Its Impact on Pavement Structure

In this research part, a field project of cement improved subgrade was introduced. There were several low-volume road sections constructed on July 2017. The road included a cement-treated subgrade functioning as a base. Afterwards, gravels were paved on the top of stabilized subgrade for protection and drainage. Light weight deflectometer (LWD) test was

conducted in field to monitor the subgrade stiffness before treatment, after stabilization, 3 days after stabilization, and 7 days after stabilization. The road conditions of the low volume roads were also monitored along with the service time.

In addition, 20 years filed performance prediction for a flexural pavement was conducted using MEPDG model. For the prediction, the HRB-treated subgrade material was designed to replace 50% of the subbase thickness. Meanwhile, surface layer, base layer and natural subgrade layer were considered to be the same for different designs. The prediction concerned the differences of pavement deformation and **I**nternational **R**oughness **I**ndex (**IRI**). Results helped to analyze the potential and feasibility of using HRB-treated subgrades in pavement design.

CHAPTER 4 INVESTIGATION OF HYDRAULIC ROAD BINDER

This chapter introduces the physical and chemical properties of different formulated hydraulic road binders. The formulations and designations of each binder have already illustrated in the Table 3-3. This chapter addresses the various engineering behaviors and hydration properties of the cement and HRB in paste and mortar form. Detailed test procedure and results are illustrated in the following sections.

4.1 Investigations of Cement and HRB Pastes

Tests for HRB pastes in this section include the initial setting time test, hydration temperature investigation, X-ray diffraction test, and energy dispersive spectroscopy test.

4.1.1 Initial Setting Time

The goal of the initial setting test is to provide information related to hardening time for different HRB and cement pastes. In a field construction, a short setting time requires that compaction to be conducted immediately after mixing while too long of a setting will delay the construction schedule. The ASTM C150 and CSA A3001 both recommend the initial setting time to be in the range from 45 minutes to 375 minutes.

The initial setting time test was conducted according to ASTM C191, "*Time of Setting of Hydraulic Cement by Vicat Needle*". The initial setting time test was performed by the author in Lafarge's ITC lab. See Figure 4-1 for the equipment used for the setting time test. During the test, the prepared paste was mixed and placed in the conical ring. The paste was then leveled and remained for 30 min without being disturbed. Thereafter, a 1-mm needle was used to penetrate into the paste every 10 min until a penetration of 25 mm or less was obtained (ASTM C191). The time when the needle penetrates 25 mm in the paste was determined as the initial setting time. The test used an equipment which was able to automatically penetrate and record the time and penetration.

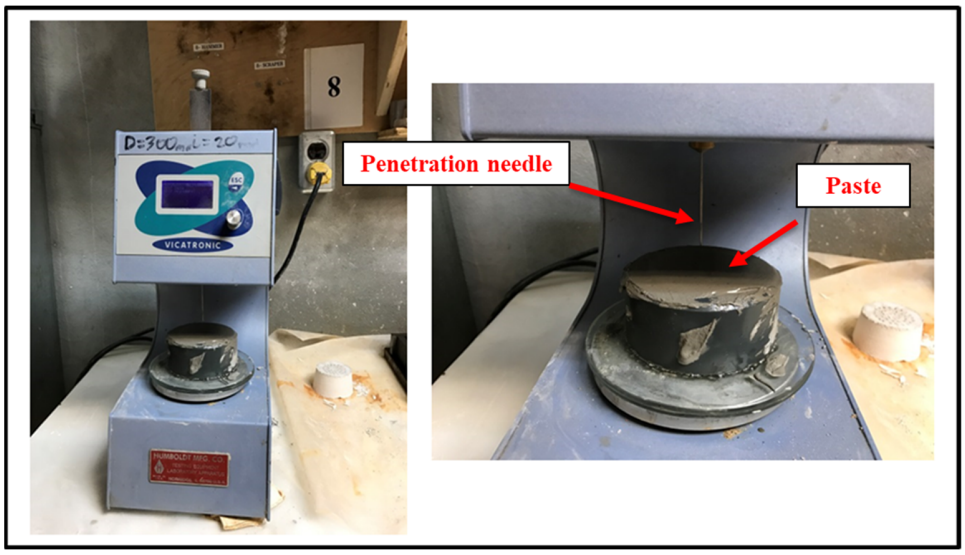

Figure 4-1 Initial setting time test

The test results are presented in Table 4-1. The initial setting time of selected HRB paste was calculated by interpolation method and was precise to 1 minute.

Table 4-1 Initial Setting Time of Cement and HRB Pastes

HRB ID	Water-to-binder Ratio	Initial Setting Time (min.)
GU	0.385	90
GUL	0.385	86
HRB-1S	0.385	232
HRB-2S	0.385	174
HRB-2C	0.385	159
HRB-2F	0.385	222
HRB-3S	0.385	153
HRB-3C	0.385	135
HRB-4LS	0.385	173
HRB-4LF	0.385	182

The GU cement had an initial setting time of 90 minutes, which is within the ASTM C150 and CSA A3001 specified time range (45 minutes to 375 minutes). The GUL cement, on the other hand, showed a slightly reduced setting time (86 minutes). Such phenomenon may be due to the effects of limestone filler which had a higher water absorption potential. The shorter setting time might also be due to the relatively small particle size and the high reactivity of GUL cement.

All HRBs had significantly longer initial setting times than GU and GUL cement. In particular, the HRB-1S, which was composed of 80% GGBFS, had the longest setting time of

232 minutes; nevertheless, it was still in the range of standard requirement. With the clinker content increasing, the HRB-2S and HRB-3S had relative shorter setting times compared to that of HRB-1S, but they were still longer than 150 minutes which allows a longer gap between material spreading and pavement compaction. It should be noted that the CKD-based HRBs (HRB-2C and HRB-3C) had longer setting time compared to other HRB types at the same cement content. This could be due to the higher content of calcium-based components (e.g. CaO). In contrast, fly ash made the setting time longer than other HRB types with the help of higher content of silica.

Overall, longer setting time was observed in HRBs compared to cement. The time of setting could be controlled by changing the cement clinker content and SCM type. In fact, the slow setting properties of HRBs would be beneficial for construction as this would increase the time window for good compaction in the field. Furthermore, slower strength development would help reducing shrinkage cracking and improve the durability of the stabilized pavement layer.

4.1.2 Early Hydration Temperature Monitoring

Cement hydration generates considerable amount of heat in concrete and pavement structures. The over heat of hydration causes formation of substantial ettringite which will lead to expansion and subsequent cracking. Moreover, the extremely high core temperature (over 70 °C) causes failure and thermal cracking resulting from temperature gradient. On the other hand, the hydration temperature in the mix varies significantly with the specimen size, binder type, and water-to-binder ratio (Scrivener *et al.,* 2015). The purpose of this test was to investigate the temperature rise and change rate between different binder types. In order to control the accuracy, the size of each sample, the environmental temperature and humidity in chamber, and the water-to-binder ratio of each mortar were kept the same. Figure 4-2 indicates the test set up. The left side of the figure shows the temperature and moisture control system, while data acquisition system is presented on the right side. The chamber used in the test was modified from a fridge and was insulated from room temperature.

Immediately after the pastes were prepared, they were put in the medal cube molds at an inner size of 50 mm × 50 mm × 50 mm and transferred into the chamber. Thereafter, temperature probes were inserted into the center of the paste. Inner temperature of each paste was then

recorded every 1 minute until 48 hours after hydration.

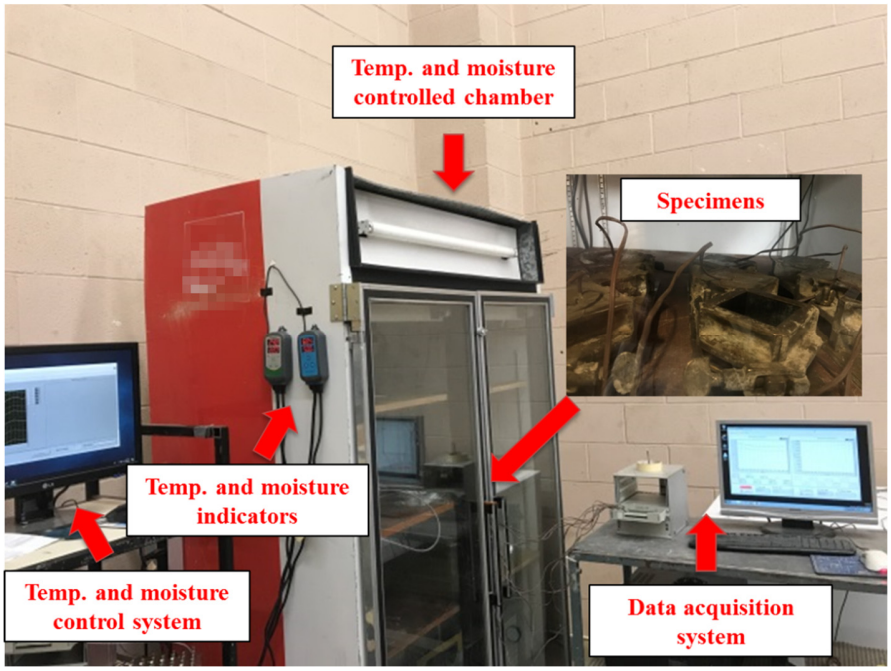

Figure 4-2 Test set up and arrangement for inner temperature detection during paste hydration

During the test, the temperature inside the chamber was controlled to be 20.0 ± 0.5 °C, and the relative humidity was kept to be above 80% to promote the process of hydration. Results of hydration temperatures for cement and HRBs are analyzed and summarized in Figure 4-3 and Figure 4-4.

Binder and water used for mixing had an initial temperature of 20 °C. There was an immediate increase of temperature just after paste mixing. Such phenomenon may be due to the sample mixing and initial reaction effects, especially, the dissolution of C_3S (alite) (Bullard *et al.,* 2011). The second stage of hydration is called slow reaction. 1 hour to 2 hours after binder mixing, the inner temperature of specimens decreased sharply to approximately 20.5 °C. Such phenomenon complies with the decrease of heat release which was introduced in Figure 4-5 (Bullard *et al.,* 2011). Moreover, the decrease rate and the lowest temperature of each paste were different. In particular, HRB-1 series and HRB-2S had a longer decrease period than GU and GUL.

During the third stage of hydration, a significantly accelerated heat flow was released due to the drastic hydration of C_3S and C_2S. Meanwhile, substantial amount of hydration products,

mainly calcium silicate hydrates (C-S-H), were generated. Morphology study from literature indicated a quick growth of C-S-H on the surface of alite and other minerals during this period. The peak point of hydration of GU often takes place on approximate 9 hours after mixing (Bullard *et al.,* 2011). Such phenomenon was also observed from the temperature change. The acceleration of heat flow brought the sharp rising of inner temperature. The inner temperature of GU and GUL paste rose from around 21 °C to over 28.5 °C in approximately 4 hours. It was also observed from the curve that GUL had slightly higher hydration temperature compared to GU at early stage. Such difference is due to the filler effect and addition nucleation contributed by SCM blending (Scrivener *et al.,* 2015; Schöler *et al.,* 2017). On the contrary, HRBs had less peak temperatures than GU and GUL. Not surprisingly, the increase of cement clinker in HRBs leaded to an increase of peak temperature during hydration. Furthermore, at the same cement content, GGBFS blended HRBs had higher temperature compared to fly ash and CKD blended HRBs.

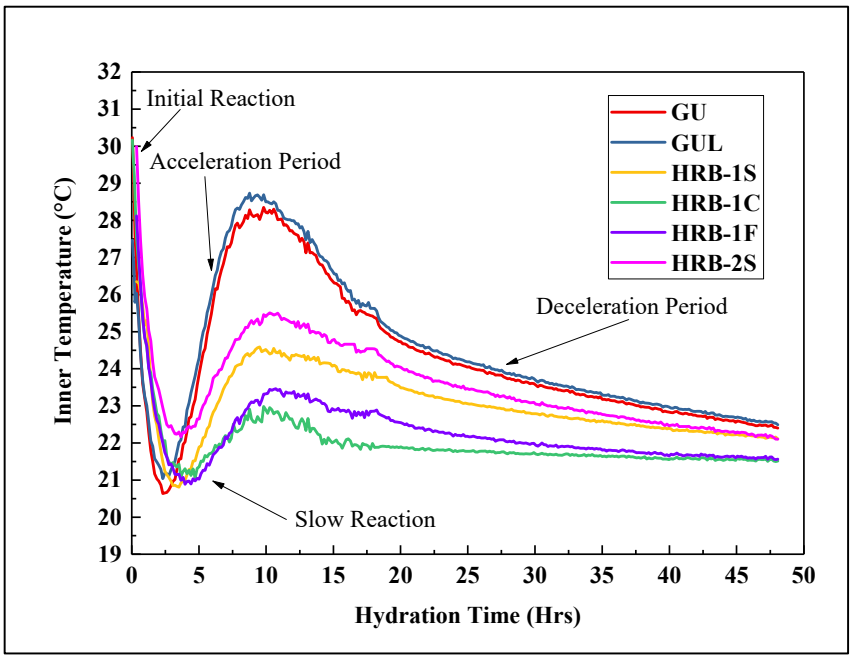

Figure 4-3 Inner temperature of cement and HRB pastes during hydration

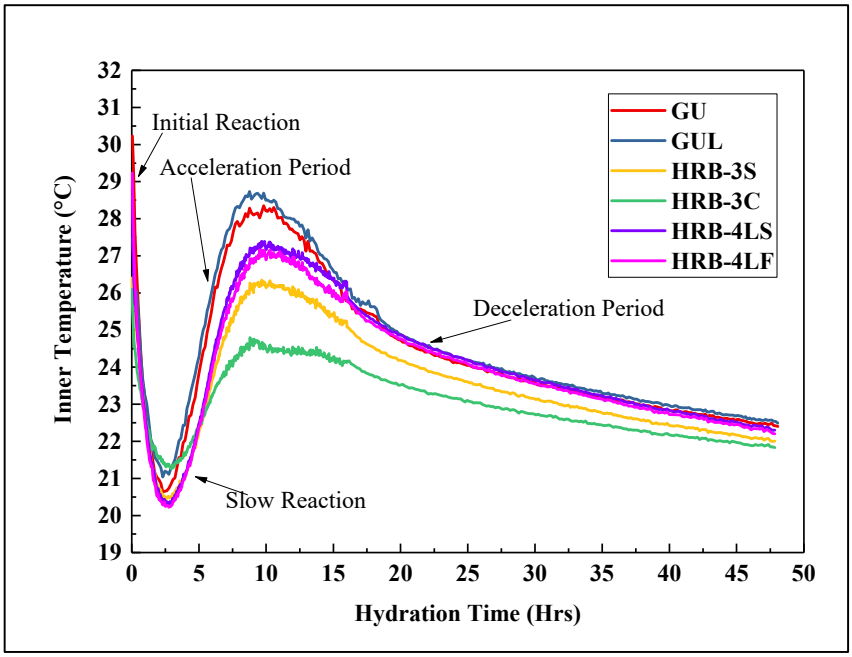

Figure 4-4 Inner temperature of cement and HRB pastes during hydration

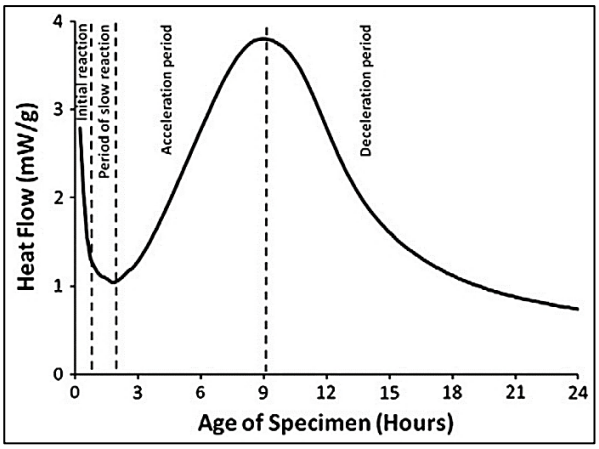

Figure 4-5 Heat release of alite (Bullard *et al.*, 2011)

The fourth stage of hydration is called deceleration period. During this period, the inner temperature of mixtures gradually decreased to the constant value. This implied that the hydration had become milder. Instead, the subsequent period of hydration and pozzolanic reactions in paste and concrete may last for over weeks and months. However, the rate of heat release was significantly reduced. It should be noted that the inner temperatures of cement and HRB pastes after 48 hours are still different, indicating a continuous reaction in

the pastes.

Furthermore, the cumulative temperature of each binder was calculated as follows in Eq. 4-1. The cumulative change of sample's inner temperature compared to chamber temperature was solely attributed by the heat release of binder hydration. Therefore, such factor indirectly revealed the differences of total heat release between various binders.

Equation 4-1

$$T_{cumulative} = \int_{t_0}^{t_t} (T_t - T_{chamber}) dt$$

where, $T_{cumulative}$ = the cumulative temperature (°C) during hydration;

t_0 = timing at the beginning of hydration, which equals to 0;

t_t = specific timing (hour);

T_t= inner temperature (°C) of specimen at t_t;

$T_{chamber}$ = chamber temperature (°C).

The trend of temperature accumulation was similar among all the binders. The temperature accumulates intensively starting from 5 hours after hydration. Such curves were similar to the cumulative heat release curves from literature (Scrivener *et al.,* 2015; Schöler *et al.,* 2017). Likewise, the GU and GUL had higher temperature accumulation than other binders from the beginning of hydration until the end of observation. HRB-4LS and HRB-4LF had slightly lower temperature accumulation compared to cement. In contrast, HRB-1F and HRB-1C accumulated less temperature as a result of lower heat release.

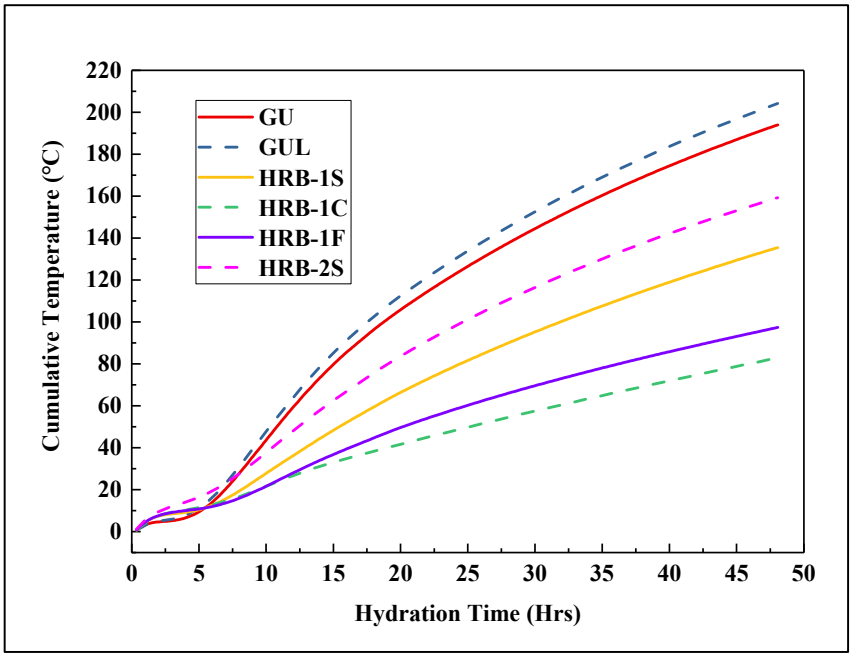

Figure 4-6 Cumulative temperature of pastes during hydration

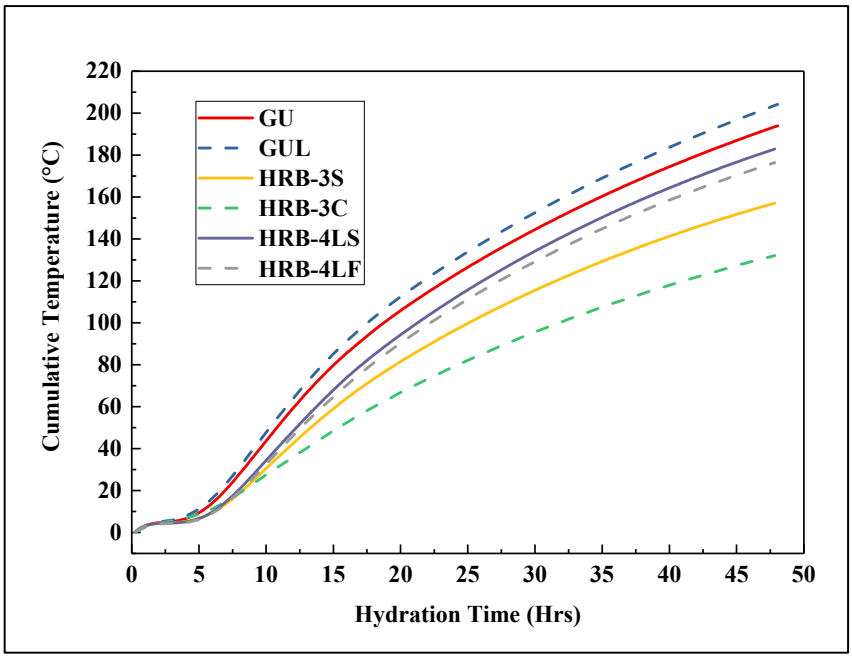

Figure 4-7 Cumulative temperature of pastes during hydration

In general, it was indicated that with the help of SCM blending, HRBs could have reduced temperature rising and peak inner temperature compared to GU and GUL. The reduction of inner temperature was affected by the cement clinker content and also by the SCM type included. In particular, fly ash and cement kiln dust released less heat compared to slag at the same binder content.

4.1.3 X-Ray Diffraction

For this study, X-Ray powder diffraction (XRD) was used to rapidly identifying the crystalline phases in hydrated pastes. The fundamental principle of an XRD is Bragg's Law ($n\lambda=2d\sin\theta$). The XRD test was conducted on the pulverized powders from cement and HRB pastes after 56 days of curing.

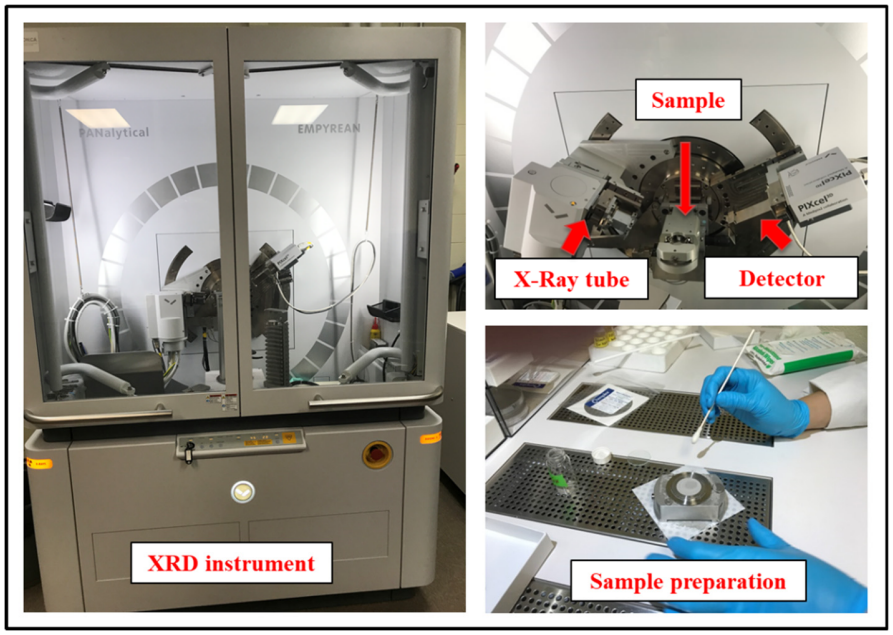

Figure 4-8 Test set up for X-ray diffraction test

During the test, X-rays were generated by the tube and directed towards the sample. After diffraction, the X-rays were then detected, processed, and calculated for the determination of the crystal. The specimen was kept circling while scanning, thus the X-rays could be directed in the powder in every orientation. Figure 4-9 and Figure 4-10 summarize the XRD patterns of each hydrated binder with the estimated hydrated products contents.

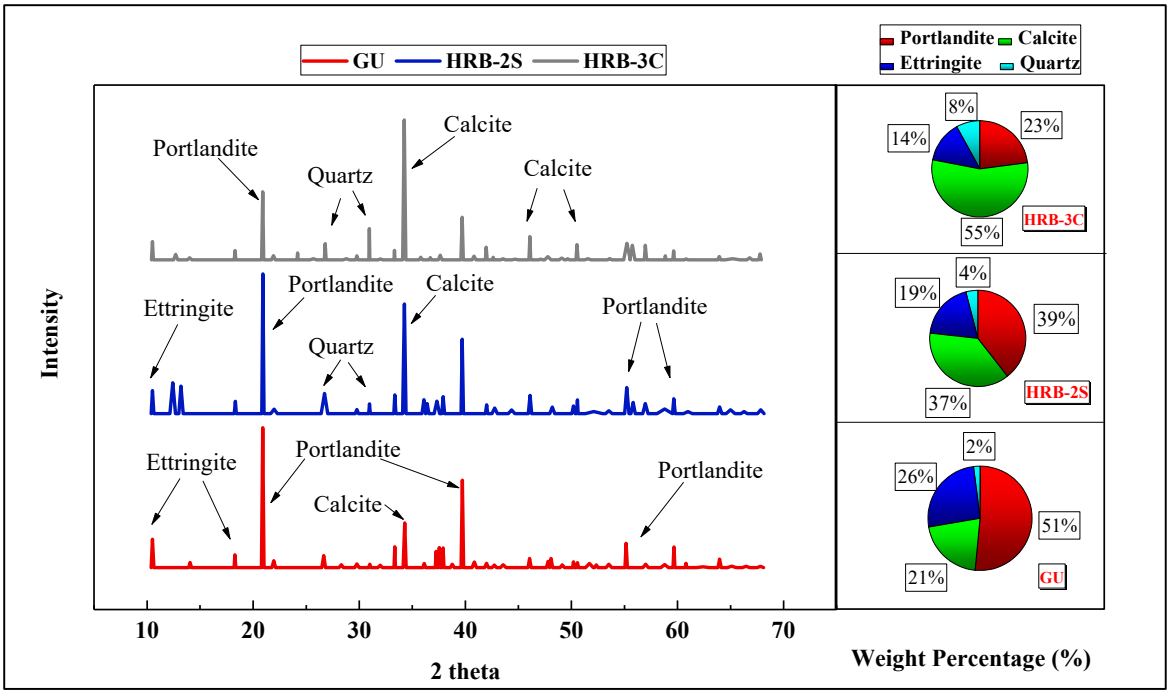

Figure 4-9 XRD patterns of GU, HRB-2S, and HRB-3C

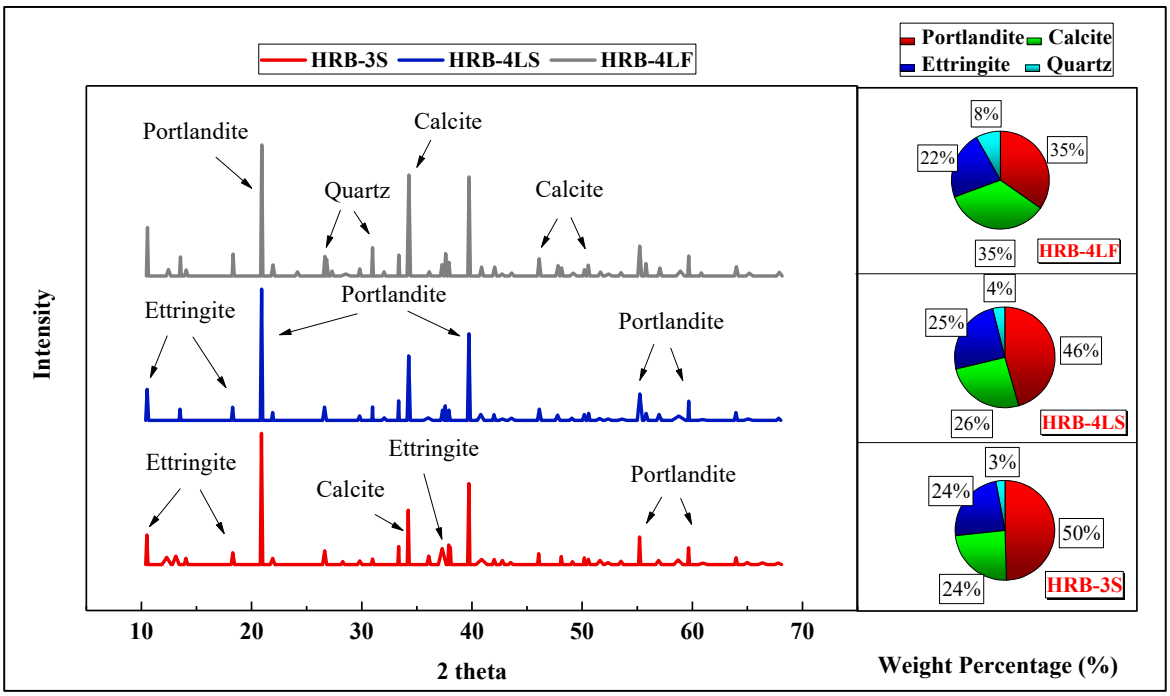

Figure 4-10 XRD patterns of HRB-3S, HRB-4LS, and HRB-4LF

The *y* axis in figures represents the intensity (or count) of electrons. On the other hand, the *x* axis "*2θ*" (2 theta) indicates the rotation angles. The overall XRD patterns of different hydrated pastes were similar, with the major peaks observed at the same angles. However, the intensities of each peak were different indicating the difference contents of the chemical compounds. Four distinct crystalline patterns are observed from XRD patterns: Portlandite ($Ca(OH)_2$, CH), Calcite ($CaCO_3$), Ettringite, and Quartz (SiO_2).

A close look of data indicates that, after 56 days of curing, the relative percentage of portlandite (52.0 %) and Ettringite (26%) produced in GU cement was larger than those in HRBs. Following cement, hydrated HRB-3S and HRB-4LS had similar portlandite ratios. On the other hand, HRB-3C and HRB-4LF had less portlandite content but more relative calcite content after hydration. They also include higher relative content of quartz. SCMs especially GGBFS and fly ash had substantial quartz and calcite included. These two minerals were introduced in literature to have the effect of slowing down the hydration and reducing the hydration heat. Their effects on controlling the drying shrinkage will be further discussed in the next section 4.1.4.

4.1.4 Energy Dispersive Spectroscopy

Energy-**D**ispersive **X**-ray **S**pectroscopy (**EDS**, or **EDXS**), is a technique frequently used to quantify the chemical elements. The procedure of sample preparation for EDS testing is the same as that used in XRD tests. The EDS is usually conducted at the same time as Scanning Electron Microscope (SEM). In order to start the test, a high-energy beam of charged electrons is focused into the specimen surface. An energy-dispersive spectrometer is equipped to collect and measure the number and energy of the emitted (Goldstein *et al*., 2017). Afterwards, the elemental and chemical composition of the specimens are measured. The equipment used for the EDS measurement in the research is presented in Figure 4-11. EDS was conducted in the equipment in the scanning instrument on the right side of the image. On the other hand, the electrons were analyzed in the EDS analysis equipment as it is shown in the figure. Test was conducted on the specimens at a round scanning area of around 150 μm in radius. The test was performed 3 times for each specimen at different scanning positions. Figures The average atomic contents of each element are summarized in Figure 4-12.

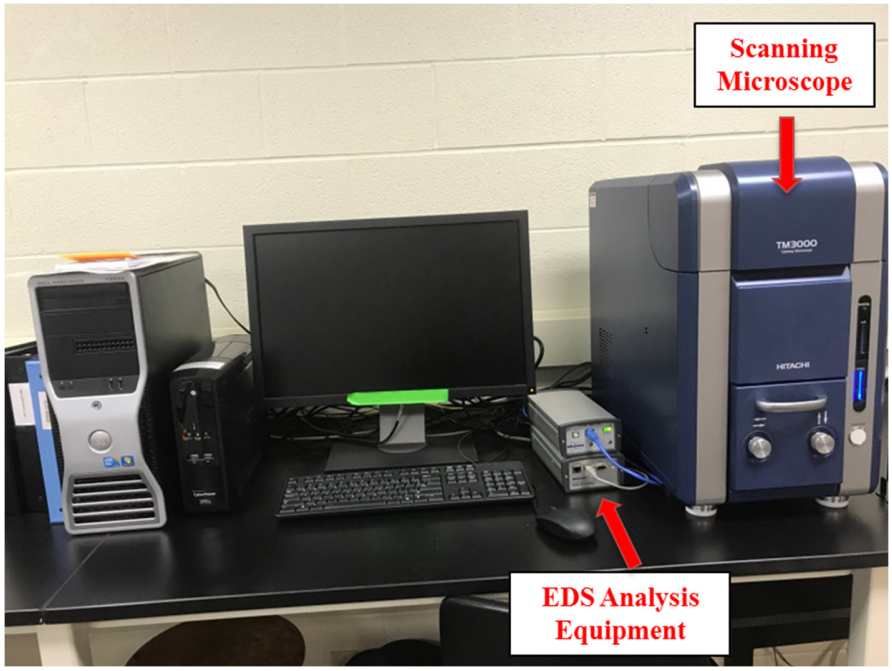

Figure 4-11 Equipment for EDS measuring

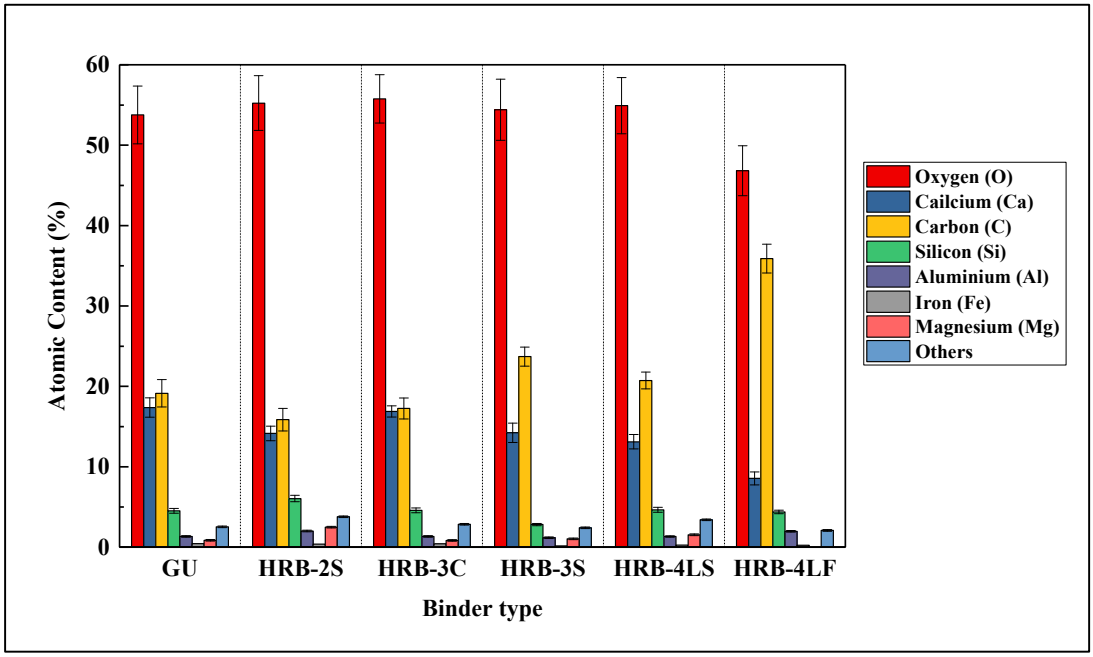

Figure 4-12 Atomic content of chemical elements

As the figure implies, the atomic content of oxygen was higher than any other elements. The majority of oxygen originated from the oxides, SiO_2 and $CaCO_3$ in binders. Another source of oxygen was the hydration between binders and CO_2 and H_2O. Among all the hydrated pastes, GU, HRB-2S, HRB-3C, and HRB-4LS had the higher oxygen content of more than 50%. The element of calcium (Ca) originated from the binder itself. Between the binders, GU cement had the most substantial amount of Ca compared to other HRBs. On the other hand, the HRB pastes had lower Ca content but more Carbon (C). C ranked the second most significant element in hydrated binders. Part of carbon was originated from hydration and pozzolanic reactions.

Figure 4-13 presents the average atomic ratios of Si/Ca and Al/Ca in hydrated HRBs and GU pastes. Calcium silicate hydrate, as the main source of strength of hydration cement, is often abbreviated as "C-S-H" (Winter, 2012). The dashes indicate that the ratio of SiO_2 to CaO is often variable. The Si/Ca ratio in C-S-H typically varies between 0.4 and 0.5 (Winter, 2012). The area of C-S-H was plotted in Fig. 10. Meanwhile, the two groups of calcium sulfoaluminate hydrates, AFm and AFt were also recognized in the figure by their Al/Ca. In addition, both the Al/Ca and Si/Ca of CH and Calcite equal to 0.

HRBs and GU have their plots falling between the lines named “CH+C-S-H” and “AFt+C-S-H”. It should be noted that the AFt here mainly indicated ettringite which has an Al/Ca ratio of 0.33. In particular, the plots of GU, HRB-3C, and HRB-4LS were closer to “CH+C-S-H”. Therefore, those types of hydraulic binders generated substantial portlandite (CH) and calcite ($CaCO_3$). This information complies with XRD results in Figure 4-9 and Figure 4-10. It was also indicated that, by adding GGBFS and fly ash, the Si/Ca and Al/Ca were increased. HRB-4LF and HRB-2S had the higher ratio of Al/Ca compared to other binders; this could generate more sulfoaluminate hydrates.

In addition, cementitious hydration and the pozzolanic reactions brought more oxygen (O) into the mixture. The increase of oxygen in different binders were different as a result of various reactivity characteristics in different binders. In general, the atomic content of O in GU and HRBs increased from 35% ~ 42% to approximately 45% ~ 57% after hydration. On the other hand, the Si/Ca ratio was not affected by hydration as it should be.

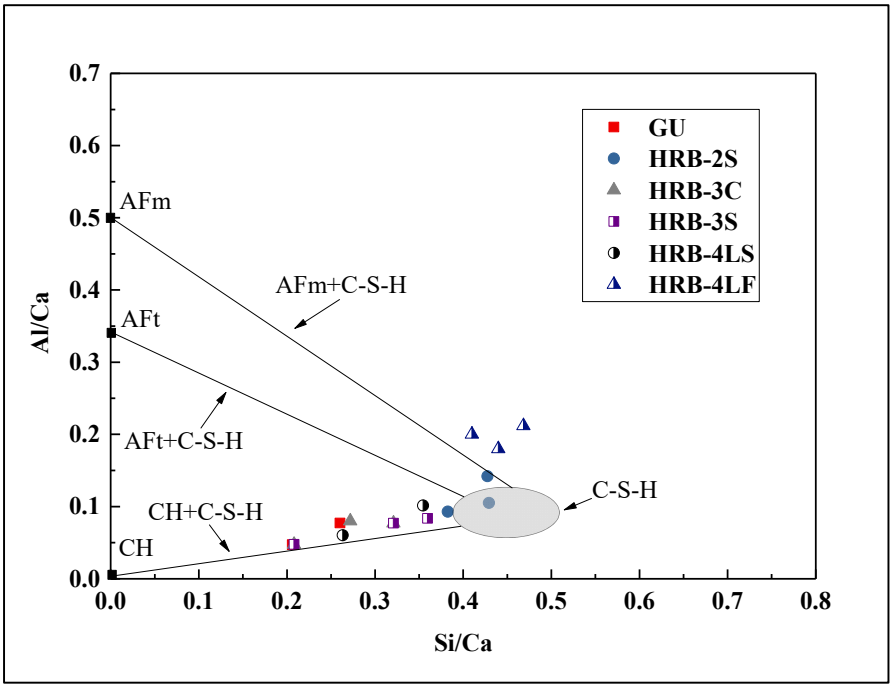

Figure 4-13 Atomic content of chemical elements

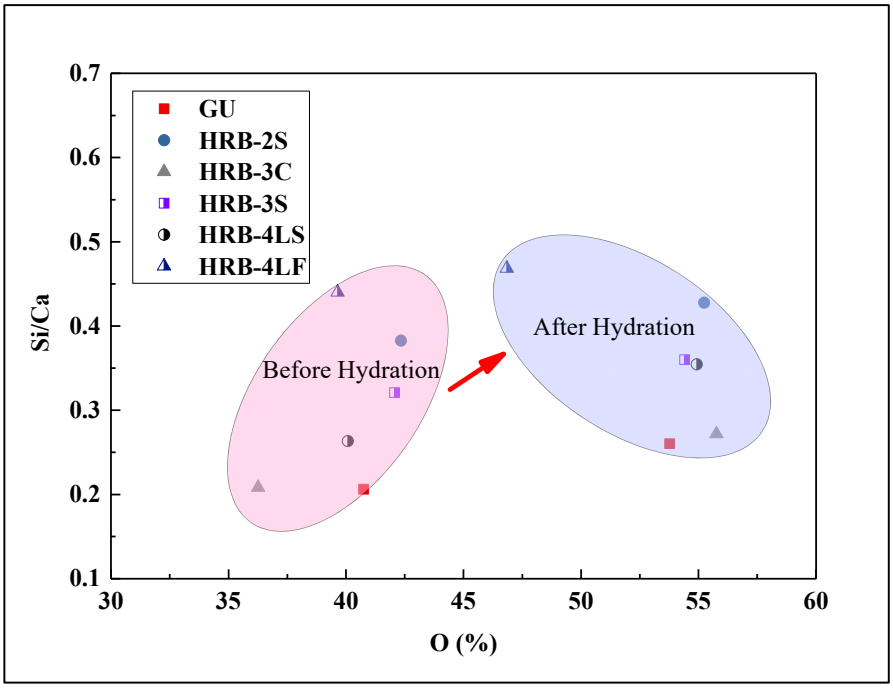

Figure 4-14 Chemical elements before and after hydration

In general, the hydrated HRBs scatters are more close to C-S-H area which indicate a potential to general more relative C-S-H compared to cement despite the fact portlandite is still present in most systems, However it is found in this study and supported by the literatures that SCM-blended systems will change the C-S-H phase with higher Si/Ca ratios. As a consequence of the change, the pore solutions in blended systems will be different from those in cement ones. And the main tendency is to slightly lower the levels of pH and the risk of long-term alkali silica reaction (Lothenbach *et al.,* 2011). However, more knowledge is needed to extend the illustration.

4.2 Physical Evaluations of Cement and HRB Mortars

Specimen preparation of cement and HRB mortars are discussed in Section 3.2.2 and 3.2.3. The fresh mixed mortars are tamped and placed in the metallic molds. After 1 day of moist curing, the specimens were demolded and cured in tap water. Shapes of mortar beams vary significantly based on different test requirements. The typical curing period for compressive and flexible strength testing is 7 days, 28 days, and 56 days.

4.2.1 Drying Shrinkage

The drying shrinkage is a crucial consideration for hydraulic cement and HRBs. The drying shrinkage caused by cement hydration is the main reason which leads to cracks in cement treated base and subbase layers. The cracks then often reflect through the surface, allowing water penetration and exacerbating deterioration (Louw and Jones, 2015). In order to measure the drying shrinkage, mortar beams were made in the size of 30 mm × 30 mm × 300 mm. Two metal pins were installed on both ends of the beam for length measurement. Prepared mortar beams were demolded at 24 hours after curing, and were soaked in lime-saturated water for 48 hours. At the age of 72 hours, the beams were removed from the water, wiped dry and immediately measured for the initial length L_0 (ASTM C596). Then the specimens were placed on a drying stage for air storage at room temperature of 20 °C. The length of the specimen was then measured at 4 days, 11 days, 18 days, 25 days, and 32 days (L_{nd}) after drying. Figure 4-15 presents the measurement of shrinkage. The drying percentage of specimen at each time was calculated according to Eq. 4-2. For each binder type, at least 4 mortar specimens were made and calculated to have the average reading.

Equation 4-2

$$Drying\ percentage = \frac{L_0 - L_{nd}}{L_0} \times 100\%$$

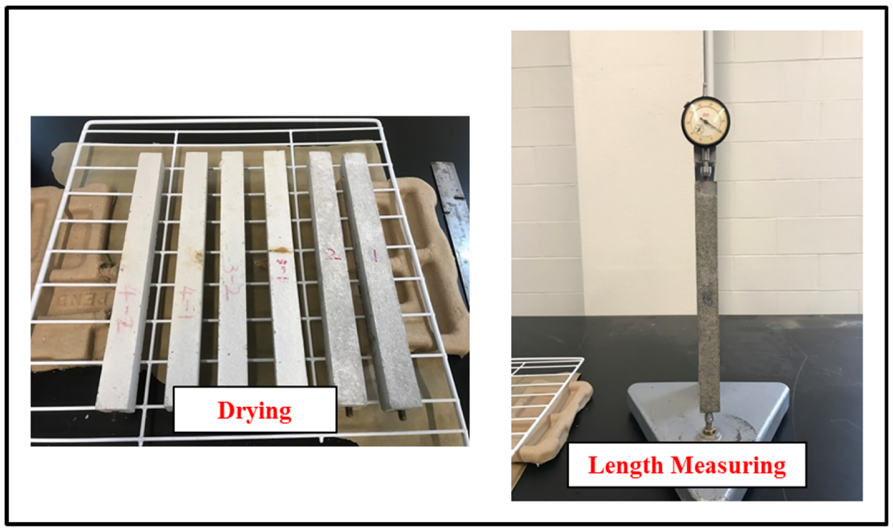

Figure 4-15 Drying shrinkage measuring

Results of the drying shrinkage are illustrated in Figure 4-16, with the error tolerance. As it was shown, drying shrinkage in mortars occurred most rapidly in the early 18 days. After 32 days of drying, the growth of shrinkage became insignificant. Among all the binder types, the drying shrinkage in GU mortar beam was more significantly and grew more rapidly than in other HRB mortars. The 32 days of drying shrinkage of GU mortar accounted for approximately 0.12%, followed by GUL mortar which has the drying shrinkage to be around 0.10%.

On the other hand, HRBs showed lower drying shrinkage which ranged from 0.04% to 0.08% after 32 days of testing. In addition, the shrinking rates of HRB mortars were milder than GU and GUL, especially in the early shrinkage period (0 to 18 days). Among them, HRB-1S had the lowest 32 days drying accounting for 0.045%, which was significantly lower than those of GU and GUL mortars. With the increase of cement clinker content, the value of drying shrinkage increased. HRB-4LS, HRB-3S, HRB-4LF, and HRB-3C mortars exhibit higher shrinkage values than HRB-1S and HRB-2S after the same drying period. Among the three types of SCMs, fly ash composed HRBs tended to have lower shrinkage potential than GGBFS and CKD composed HRBs.

In general, the 32 days drying shrinkage in HRB mortar beams was approximately 40% to 80%

lower compared to Portland cement beams. This result indicates that the HRB-treated material would have a lower drying shrinkage potential than GU-treated materials and reduce the risk of shrinkage cracking which is frequently found in cement-treated pavement layers.

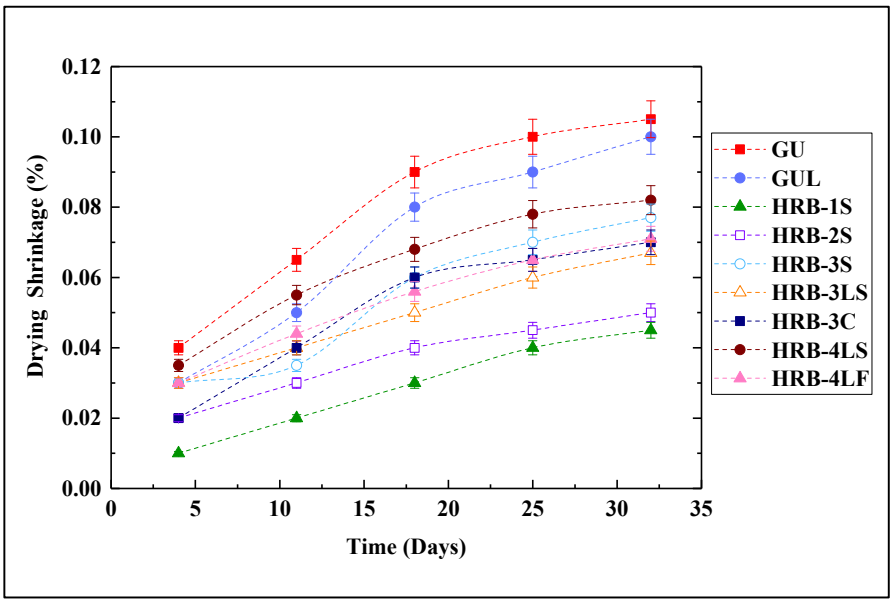

Figure 4-16 Drying shrinkage of cement and HRB mortars

4.2.2 Compressive Strength of Mortars

The compressive strength of mortar cubes is one of the most important parameters that illustrates the physical performance of hydraulic binders. And they are also one of the most crucial factors that influence the stabilization effects of HRB bound mixtures. ASTM C109, *"Standard Test Method for Compressive Strength of Hydraulic Cement Mortars"* was followed to determine compressive strength of cement and HRB mortars.

The test uses 50 mm cube specimens for testing. After the specimens were molded, they were transferred into the humidity chamber for curing of 24 hours. They were then demolded and immediately soaked in water for further curing. The storage water was replaced every week. When the specimens were ready for testing, they were removed from the water, wiped, and immediately put underneath the lead cell. Based on the standard, the cube was tested corresponding to a loading rate of 1000 N/s. The machine records the maximum load before yield failure. Figure 4-24 presents the loading cell used for compressive strength testing and the specimens after testing. Moreover, the compressive strength of cube is calculated as

follows, where f_c represents the compressive strength in MPa, P equals to the maximum load in N, and A is the area of loaded surface, which is 2500 mm^2.

Equation 4-3

$$f_c = \frac{P}{A}$$

Figure 4-17 Testing of mortar cubes (left), cubes after testing (right)

This test was replicated 3 times for each formulated specimen and an average reading is calculated with the error less than 5%. Specimens were tested on three curing times: 7 days, 28 days, and 56 days. The average compressive strength of the mortars tested on different curing periods are summarized below in Table 4-2. Results are drawn in Figures 4-18 and 4-19.

The GU cement mortar has compressive strength of 22.1 MPa at 7 days, 29.3 MPa at 28 days, and 35.7 MPa at 56 days, respectively. The values fulfilled the standard CSA A3001 which requires a minimum compressive strength of 20.0 MPa at 7 days and 26.5 MPa at 28 days. The GUL cement, meanwhile, had slightly higher strength values than GU: 23.0 MPa at 7 days, 30.1 MPa at 28 days, and 37.2 MPa at 56 days. A continuous strength increase with curing was observed from GU and GUL cement mortars.

Table 4-2 Compressive strength f_c (MPa) of cement and HRB mortar cubes

HRB Nomination	GU (%)	GUL (%)	SG (%)	FA (%)	CKD (%)	w/c	7 Days	28 Days	56 Days
GU	100	0	0	0	0	0.520	22.1	29.3	35.7
GUL	0	100	0	0	0	0.520	23.0	30.1	37.2
HRB-1S	20	0	80	0	0	0.528	8.5	19.0	22.8
HRB-1C	20	0	0	0	80	0.530	10.8	21.8	22.9
HRB-1LS	0	20	80	0	0	0.533	3.0	3.2	4.1
HRB-1F	20	0	0	80	0	0.505	4.4	5.0	6.4
HRB-1SFC	20	0	30	30	20	0.528	7.6	16.2	17.8
HRB-2SFC	50	0	20	30	10	0.528	11.4	19.3	23.6
HRB-2LS	0	50	50	0	0	0.530	11.6	23.8	31.7
HRB-2S	50	0	50	0	0	0.530	11.2	24.5	29.6
HRB-2C	50	0	0	0	50	0.535	9.5	16.9	20.2
HRB-2F	50	0	0	50	0	0.510	9.5	22.7	28.1
HRB-3S	65	0	35	0	0	0.525	16.1	26.1	35.3
HRB-3C	65	0	0	0	35	0.537	11.1	19.9	23.3
HRB-3F	65	0	0	35	0	0.510	12.0	16.8	22.6
HRB-4LS	0	80	20	0	0	0.530	18.5	28.6	38.9
HRB-4LC	0	80	0	0	20	0.535	12.8	19.8	25.2
HRB-4LF	0	80	0	20	0	0.530	16.3	22.9	30.3
HRB-SFC	0	0	60	20	20	0.520	3.8	8.6	7.5
HRB-SFC"	0	0	40	30	30	0.510	2.4	4.1	5.2

The GU cement mortar has compressive strength of 22.1 MPa at 7 days, 29.3 MPa at 28 days, and 35.7 MPa at 56 days, respectively. The values fulfilled the standard CSA A3001 which requires a minimum compressive strength of 20.0 MPa at 7 days and 26.5 MPa at 28 days. The GUL cement, meanwhile, had slightly higher strength values than GU: 23.0 MPa at 7 days, 30.1 MPa at 28 days, and 37.2 MPa at 56 days. A continuous strength increase with curing was observed from GU and GUL cement mortars.

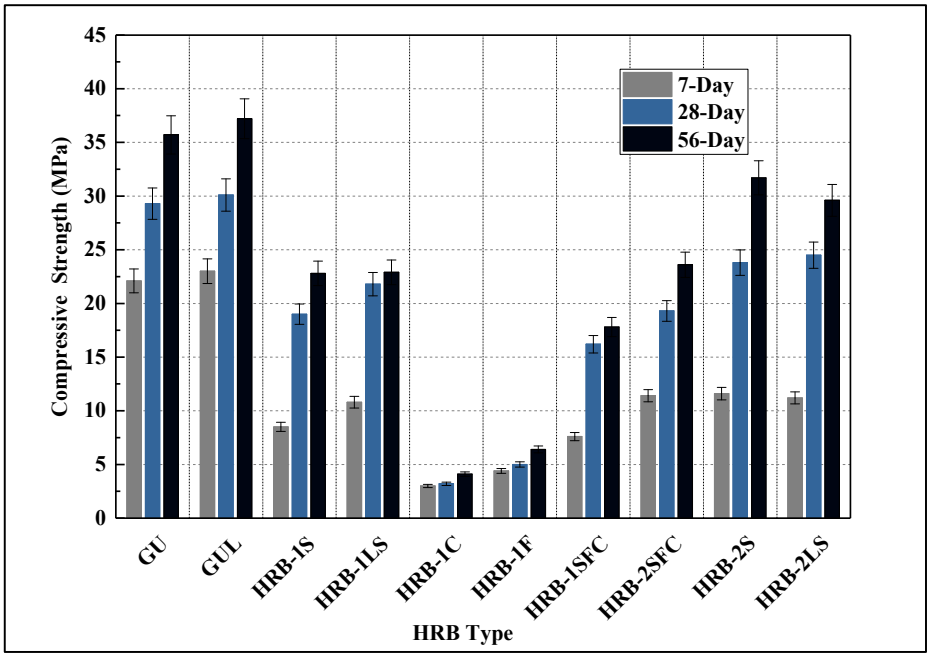

Figure 4-18 Compressive strength of HRB mortar cubes

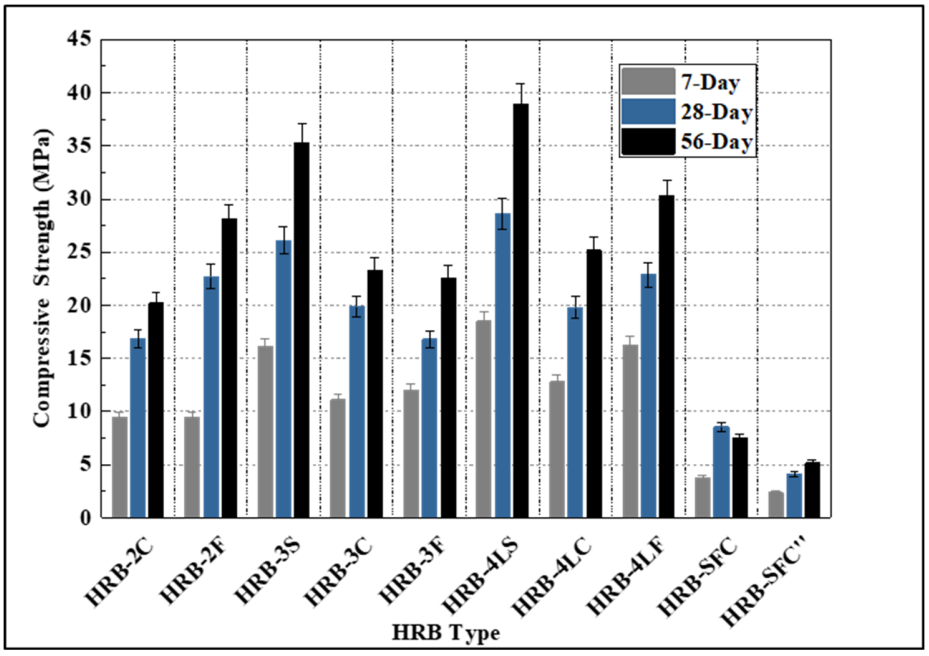

Figure 4-19 Compressive strength of HRB mortar cubes

On the other hand, HRB-1S and HRB-1LS with 80% of GGBFS blended had the compressive strength approaching approximately 38.4%-48.8% of GU at 7 days, 64.8%-73.2% at 28 days, and 63.8%-64.2 % at 56 days. However, HRB-1C and HRB-1F had compressive strength less than 7 MPa and their strength development were limited along with time. With the cement content increase in the HRB, the compressive strength increased considerably. The HRB-2C and HRB-2F had significantly improved strength values compared to HRB-1C and HRB-1F respectively. In addition, HRB-2S and HR-3S had only slightly lower compressive strength compared to GU and GUL at all curing ages. Such fact was also found from HRBs containing fly ash and CKD. The phenomenon indicated that cement is playing a significant effect of activating the hydration and hardening of SCMs. HRB-4LS, on the other hand, had similar strength compared with GU and GUL, and higher strength on 56 days, although the actual cement clinker content in HRB-4LS was lower than those in GU and GUL. The reasons may be due to the fine binder particles, better reactivity, and high cement content. It was also indicated from the results that SCMs, especially GGBFS used in this study, made a notable contribution to the strength. Meanwhile, the effect of fly ash and CKD did not provide significant effect on the strength development. Moreover, the increase of cement content from HRB-2C to HRB-4C did not lead to a significant strength increase. Lastly, HRB-SFC and HRB-SFC" which contained only SCMs without cement had similar strength values with HRB-1C and HRB-1F, and their strength development along with curing were not distinct.

Based on their strength criteria which introduced in Table 2-1, all the HRB types are characterized based on EN 13282 and are summarized in Table 4-3. It should be noted that although HRB-2S, HRB-3S, and HRB-4LS had lower compressive strength than GU and GUL at 7 days and 28 days, due to a continuous and substantial strength increase from 28 days to 56 days, the values approached or exceeded GU and GUL at age of 56 days. Nevertheless, they were still classified as E3 compared to E4 of GU and GUL. In general, HRB-2S, HRB-3S, HRB-4LS, and HRB-4LF were considered to have higher strength values than other HRB types.

Table 4-3 HRB type characterization of GU and HRBs

HRB nomination	EN 13282-1 HRB-Rapid Hardening	EN 13282-2 HRB-Normal Hardening	Classification
GU	√		E4
GUL	√		E4
HRB-1S	√		E2
HRB-1C		√	N1
HRB-1LS		√	N2
HRB-1F		√	N1
HRB-1SFC		√	N2
HRB-2SFC	√		E2
HRB-2LS	√		E2
HRB-2S	√		E3
HRB-2C	√		E2
HRB-2F	√		E2
HRB-3S	√		E3
HRB-3C	√		E2
HRB-3F	√		E2
HRB-4LS	√		E3
HRB-4LC	√		E2
HRB-4LF	√		E3
HRB-SFC		√	N1
HRB-SFC"		√	N1

In addition, the dry density (ρ_d-cube) (g/cm^3) of each specimen was calculated based on the dry weight of specimen (M_d-cube) (g) and its volume after testing (V_d-cube) (cm^3), as it is presented as follows:

Equation 4-4

$$\rho_{d-cube} = \frac{M_{d-cube}}{V_{d-cube}}$$

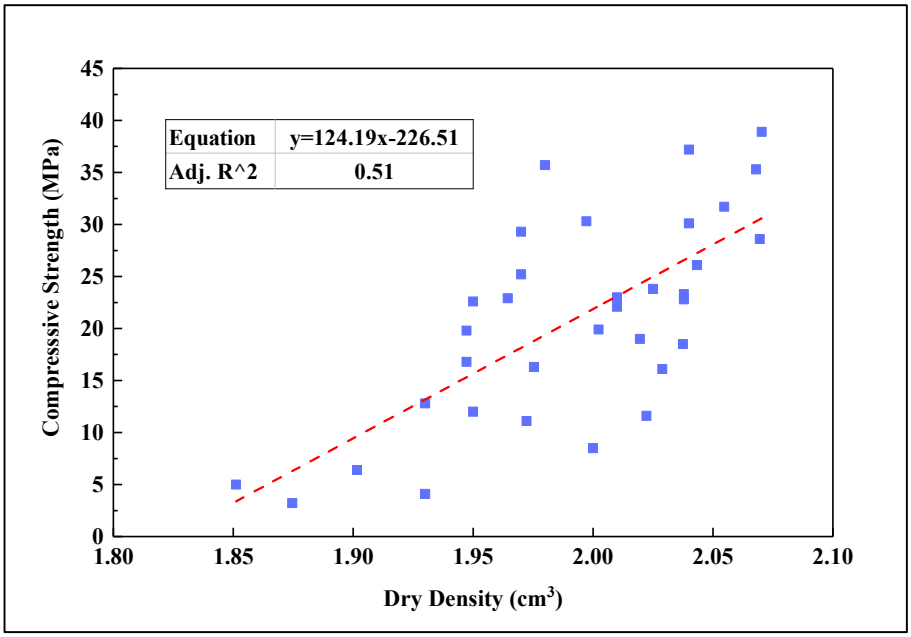

Figure 4-20 Relationship between specimen's compressive strength and dry density

There is a general positive trend between the specimen's compressive strength and its dry density, as it is shown in Figure 4-20. The larger the density, the possible higher compressive strength it will have. However, the relationship did not simply follow the linear trend. It is because material's specific density affects significantly the dry density. Another reason is that the dry density of the specimen did not increase as much as strength with curing.

4.2.3 Flexural Strength of Mortars

Flexural strength or bending strength testing of cement and HRBs mortars was then conducted. The flexural strength is an important parameter for hydraulic road binder since it presents the failure strength of beam under bending. Likewise, the bounded pavement layers frequently fail due to the bending. As a result, cracks generated at the bottom of pavement layer and propagated throughout the thickness. Standard ASTM C348, *"Flexural Strength of Hydraulic-Cement Mortars"* was followed for the testing. The mortar beams were prepared in the size of 40 mm × 40 mm × 160 mm.

The test used a center load system, the span of the supports is 120 mm. According to the standard, the beam was tested corresponding to a loading with the rate of 2640 N. The machine recorded the maximum load before failure. Figure 4-23 shows the setup for flexural strength testing and the specimens after testing. At the optimum condition, the breaking should be

parallel to the center loading and should be perpendicular to the top surface of the specimen. The result of flexural strength of mortar beam is calculated as follows, where the f_f represents the flexural strength in MPa, P equals to the maximum load in N.

Equation 4-5

$$f_f = 0.0028 \times P$$

Figure 4-21 Testing of flexural strength (left), specimen after testing (right)

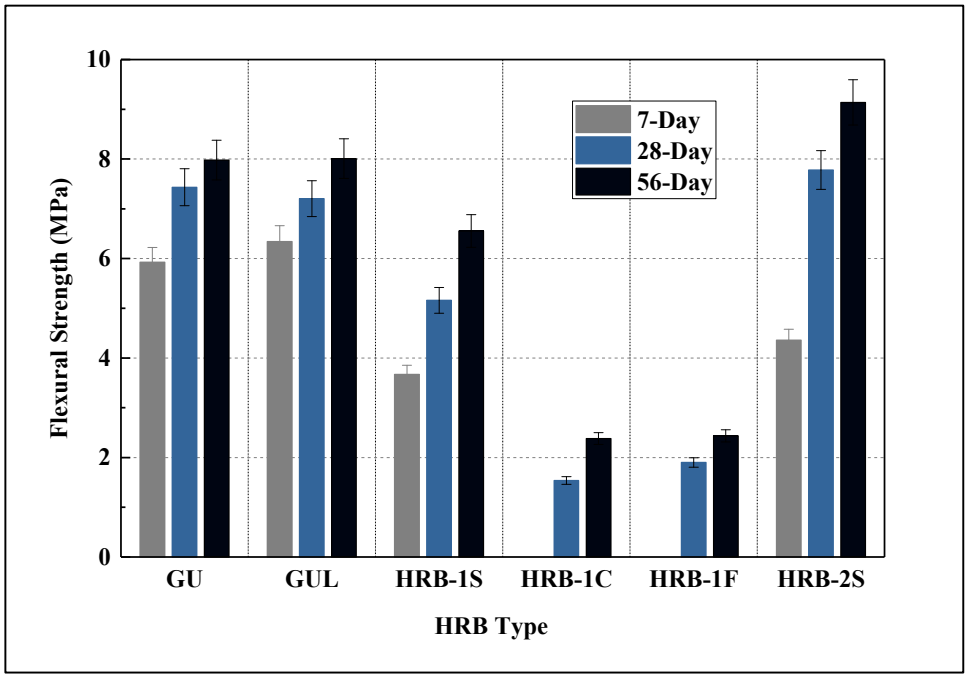

Figure 4-22 Flexural strength of cement and HRB mortars

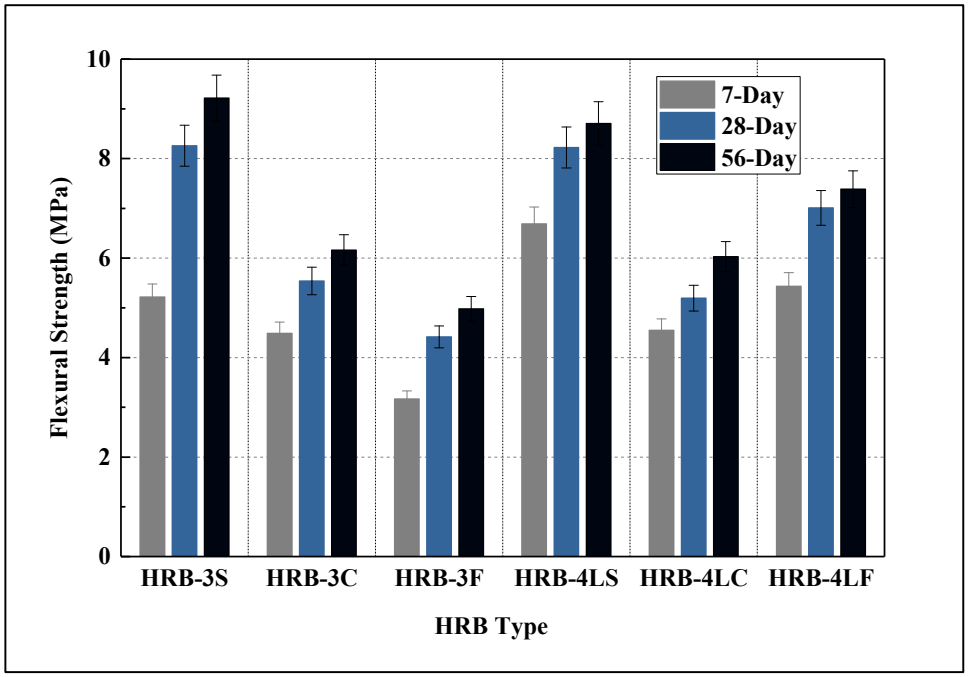

Figure 4-23 Flexural strength of cement and HRB mortars

Results of flexural strength of cement and HRB mortars are shown in Figure 4-23 and 4-24. Tests were conducted for specimens at different curing ages 7 days, 28 days, and 56 days on cement and some HRB types. GU cement had flexural strength of 5.93 MPa at 7 days. With curing, the flexural strength increased to 7.43 MPa at 28 days, and further increased to 7.98 MPa at 56 days. The GUL cement had similar strength as GU at all curing ages. On the other hand, HRBs have significant variation of strength based on their formulations. GGBFS again played an important role in strength establishment, HRB-1S had the flexural strength approximately 61.8 % of that of GU at 7 days, and the value grew to 69.5% at 28 days, and further enhanced to 82.1% at 56 days. On the other hand, HRB-1C and HRB-1F had the same cement content as HRB-1S but showed very low flexural strength values. Like compressive strength, the increase of clinker content considerably increased the flexural strength. The HRB-2S, HB-3S, and HRB-4LS containing GGBFSs all approached or exceeded the strength of GU at the age of 28 days and 56 days. Meanwhile, the HRB-4LF had enhanced strength compared to HRB-3C. But the increase of clinker in CKD blended cement did not bring distinct strength treatment. Among the three SCMs, GGBFS was still the best strength contributor. The CKD and fly ash blended HRBs could have considerable flexural strength when adequate cement content was included. The role of each chemical component on

strength development were analyzed statistically in section 4.2.4.

Same as what was done in compressive strength, The dry density (ρ_d-beam) (g/cm^3) of each specimen was calculated based on the dry weight of specimen (M_d-beam) (g) and its volume after testing (V_d-beam) (cm^3):

Equation 4-6

$$\rho_{d-beam} = \frac{M_{d-beam}}{V_{d-beam}}$$

Similar to compressive strength, the dry density (ρ_d-beam) (g/cm^3) of each specimen was calculated based on the dry weight of specimen (M_d-beam) (g) and its volume after testing (V_d-beam) (cm^3), as it is presented as in Figure 4-26. Like it is in compressive strength, only a general trend was observed between mortar's flexural strength and its dry density.

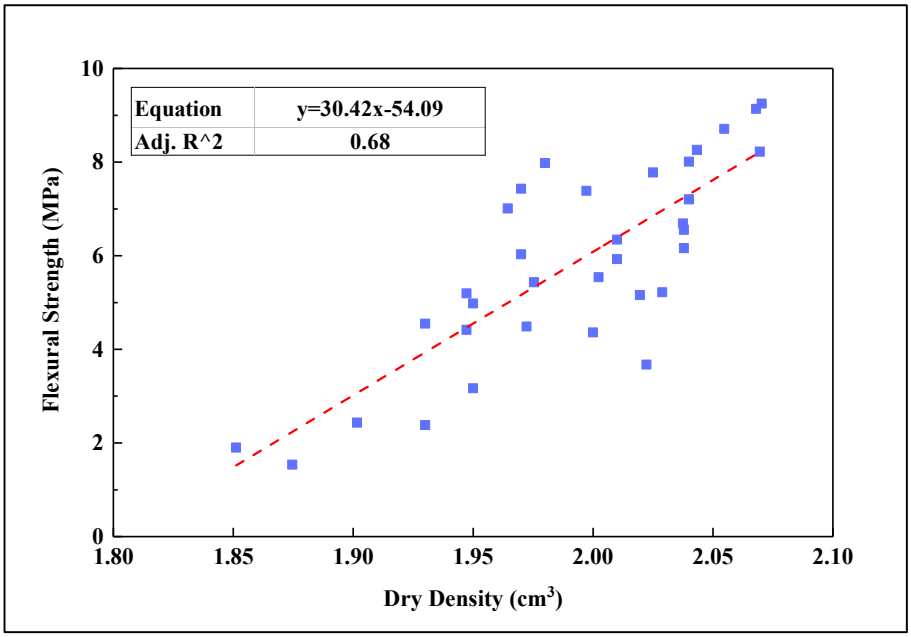

Figure 4-24 Relationships between flexural strength and dry density

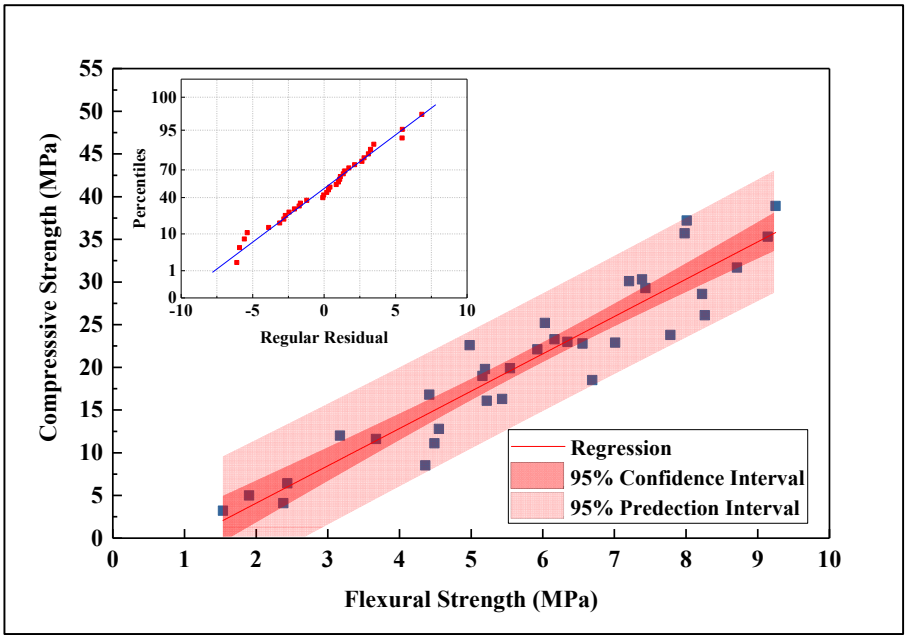

Figure 4-25 Relationships between compressive strength and flexural strength

Furthermore, Figure 4-27 presents the relationships between specimen's compressive strength and flexural strength. The regression was observed for the same formulated binder at the same curing age. The 95% confidence interval (CI) and 95% prediction interval (PI) were also drawn along with the regression. It was distinct that, a linear positive correlation exists between the two parameters, even though the failure condition of the two types of strength are different. The higher the compressive strength, the higher the flexural strength could have. And the adjusted coefficient of determination R^2 value for the linear correlation accounts for 0.88, showing a well correlation between the two parameters, regardless of binder type and curing age. In addition, the linear regression showed well prediction and confidence interval. This correlation is essentially beneficial for the estimation between the two parameters.

In particular, the proposed relationship between the two was presented as follows:

Equation 4-7

$$f_c = 4.37 \times f_f - 4.66$$

Where, f_c = compressive strength (MPa) of HRB mortar at a given curing age;

f_f = flexural strength (MPa) of HRB mortar at a given curing age.

Overall, the results of the two strength tests indicate that the SCMs (in particular GGBFS in this study) provide a considerable contribution in cementitious hydration and strength

development especially in the later curing age (after 7 days). Some HRB types containing GGBFS would have equivalent or higher strength values than GU and GUL cements in the long term. As a result, this confirms a feasibility of using HRB in lieu of cement in pavement materials treatment.

4.2.4 Effects of SCMs on HRB Strength

Different models have been studied for predicting cement and concrete's compressive strength. Among them, Neville (1995) introduced an empirical model for Portland cement concrete. Papadakis and Tsimas (2002) further developed the model, shown as follows:

Equation 4-8

$$f_c = K(\frac{1}{(w/c + kP)} - a)$$

Where *w/c* is the water to cement ratio, *K* is a parameter that varies according to cement type; *a* is a parameter representing curing time; *P* is the SCM content with factor *k* representing the efficiency of the SCM type. However, such model only considered one SCM type and its percentage. In addition, there was no comparison of the efficiency between cement and SCM.

Most recently, Buczyński and Iwański (2015, 2016) proposed a second-degree strength model for HRB bound mixtures. The HRBs were composed of cement, fly ash, and CKD. Such model considers 3 different components and their percentages. The model is shown as follows:

Equation 4-9

$$f_c = a_1x_1 + a_2x_2 + a_3x_3 + a_{1,2}x_1x_2 + a_{2,3}x_2x_3 + a_{1,3}x_1x_3$$

Where x_1, x_2, x_3 represent the percentages of cement, fly ash, and CKD, and a_1 to $a_{1,3}$ are the regression coefficients. The paper indicated that the models have general very high R^2 values (>0.90). The model not only considers the percentage of each component, but also included second-degree terms indicating the multiplied percentages of cement and each SCM. However, the polynomial did not take the water-to-binder ratio (w/b) into consideration.

In order to understand the efficiency of each chemical component, Figure 26 to Figure 30 were drawn as follows indicating the relationship between chemical content in HRB and the HRB's strength. As the results implied, the increase of cement ratio in HRB formulation

enhanced the mortar strength. Such treatment was more distinct when the cement changed from 20% to 50%. Moreover, increase of cement from 65% and forward enhanced the mean strength value; however, the overall strength values did not increase significantly. Curing is an important factor for strength development, especially in HRBs with cement ratios higher than 50%. The effect of cement in both strength tests were similar.

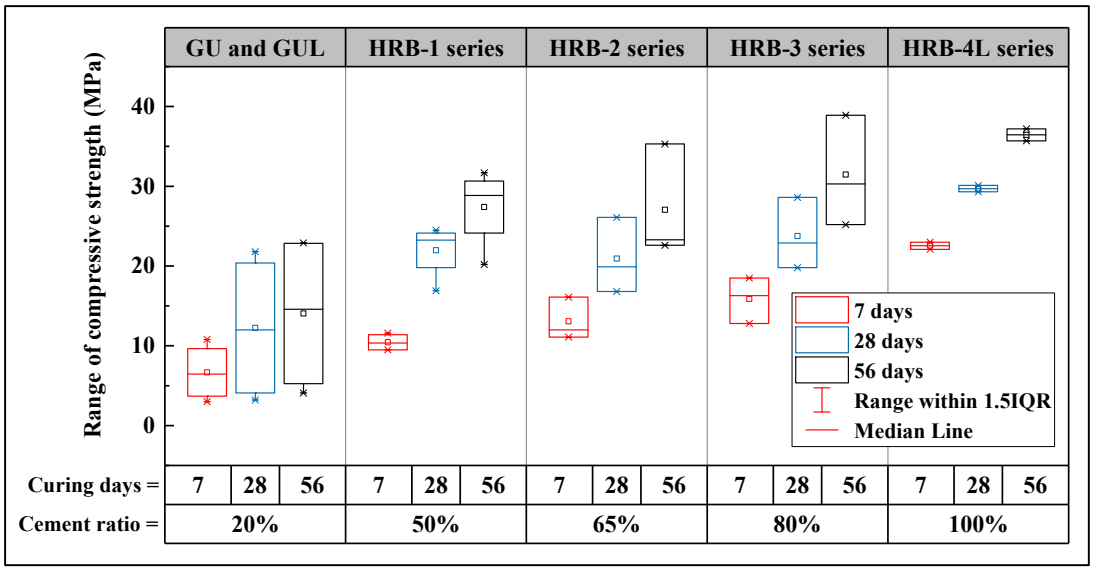

Figure 4-26 Relationship between cement content and compressive strength

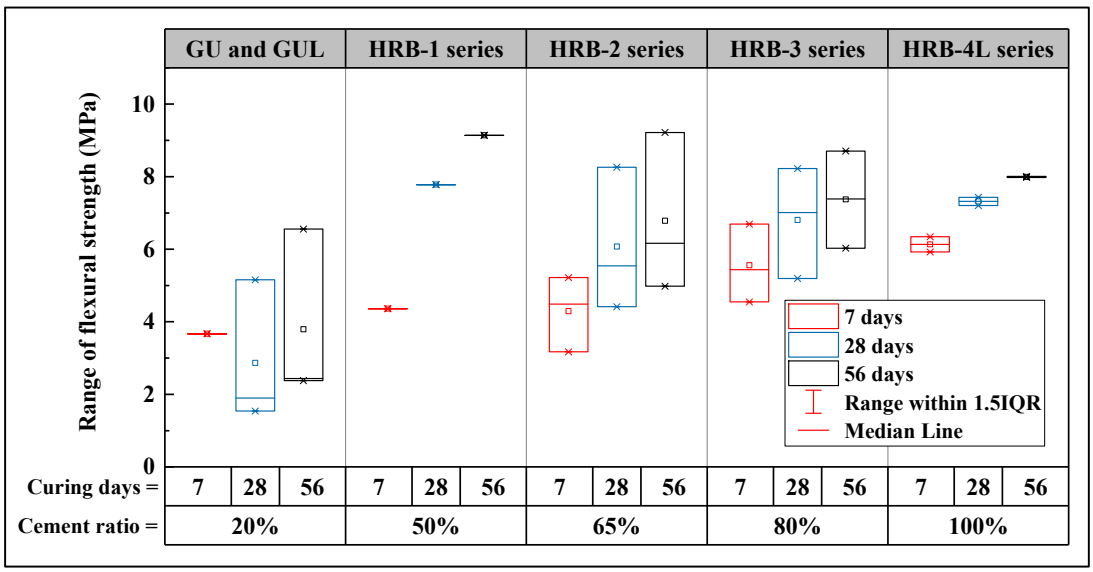

Figure 4-27 Relationship between cement content and flexural strength

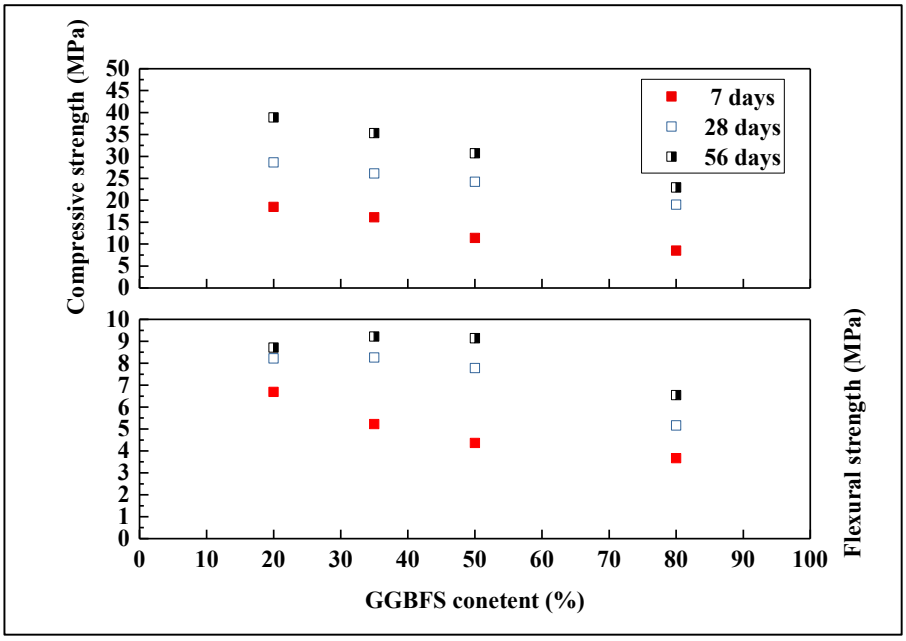

Figure 4-28 Relationship between GGBFS content and strength

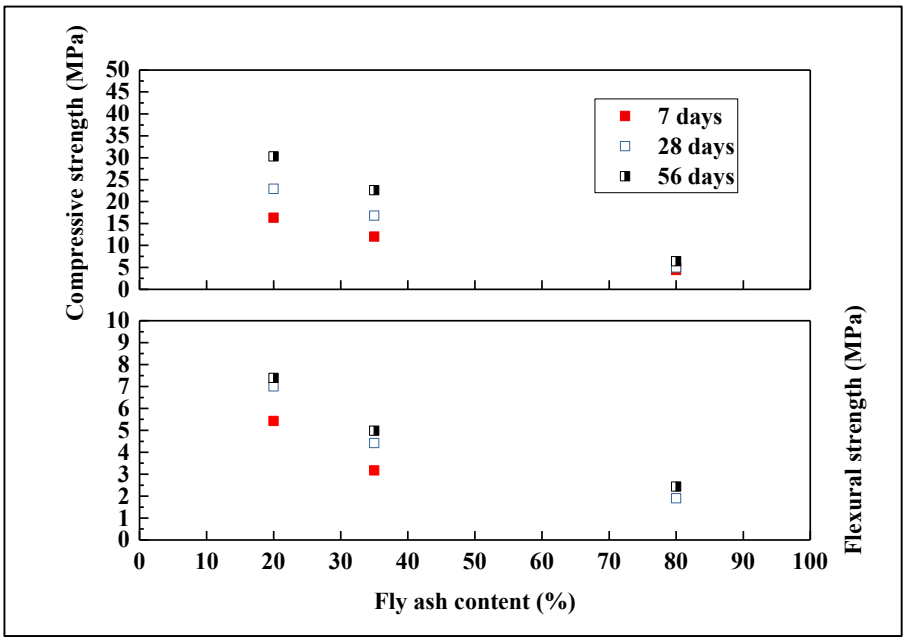

Figure 4-29 Relationship between fly ash content and strength

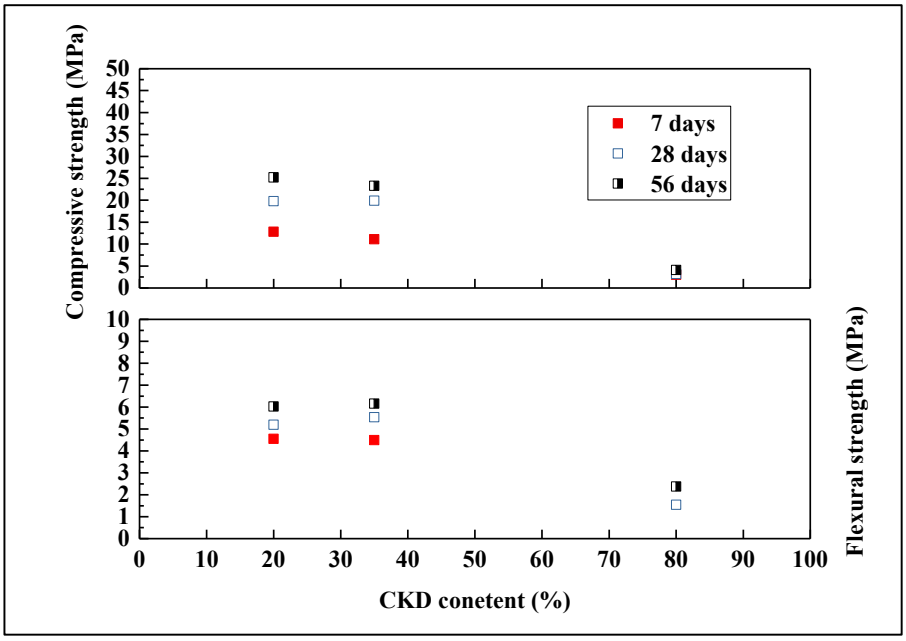

Figure 4-30 Relationship between CKD content and strength

On the other hand, the increase of SCMs amount decreased the overall strength values, especially when their content exceeded 35% to 50% in formulated HRBs. Nevertheless, strength of HRBs maintained the same level when the ratio of GGBFS and CKD increased from 20% to 35%.

Based on the literature review and the trend shown in the figures. Eq. 4-10 and 4-11 were proposed for the strength modeling. Table 4-4 presents all the input parameters used for regression analysis.

Equation 4-10

$$f_c = \frac{1}{w/b}[(K_{GU} \times P_{GU}) + (K_{GUL} \times P_{GUL}) + (K_{BFS} \times P_{BFS}) + (K_{FA} \times P_{FA}) + (K_{CKD} \times P_{CKD})]$$

Equation 4-11

$$f_f = \frac{1}{w/b}[(K'_{GU} \times P_{GU}) + (K'_{GUL} \times P_{GUL}) + (K'_{BFS} \times P_{BFS}) + (K'_{FA} \times P_{FA}) + (K'_{CKD} \times P_{CKD})]$$

Where, *w/b* = water-to-binder ratio of each specimen;

P_{GU}, P_{GUL}, P_{BFS}, P_{FA}, P_{CKD} = percentage of each component;

K_{GU}, K_{GUL}, K_{BFS}, K_{FA}, K_{CKD} = efficiency factors of each component.

Table 4-4 Input parameters for strength regression model

HRB Nomination	P_{GU}	P_{GUL}	P_{BFS}	P_{FA}	P_{CKD}	w/b
GU	1.00	0.00	0.00	0.00	0.00	0.520
GUL	0.00	1.00	0.00	0.00	0.00	0.520
HRB-1S	0.20	0.00	0.80	0.00	0.00	0.528
HRB-1LS	0.00	0.20	0.80	0.00	0.00	0.533
HRB-1C	0.20	0.00	0.00	0.00	0.80	0.530
HRB-1F	0.20	0.00	0.00	0.80	0.00	0.505
HRB-1SFC	0.20	0.00	0.30	0.30	0.20	0.528
HRB-2SFC	0.50	0.00	0.20	0.30	0.10	0.528
HRB-2S	0.50	0.00	0.50	0.00	0.00	0.530
HRB-2LS	0.00	0.50	0.50	0.00	0.00	0.530
HRB-2C	0.50	0.00	0.00	0.00	0.50	0.535
HRB-2F	0.50	0.00	0.00	0.50	0.00	0.510
HRB-3S	0.65	0.00	0.35	0.00	0.00	0.525
HRB-3C	0.65	0.00	0.00	0.00	0.35	0.537
HRB-3F	0.65	0.00	0.00	0.35	0.00	0.510
HRB-4LS	0.00	0.80	0.20	0.00	0.00	0.530
HRB-4LC	0.00	0.80	0.00	0.00	0.20	0.535
HRB-4LF	0.00	0.80	0.00	0.20	0.00	0.530
HRB-SFC	0.00	0.00	0.60	0.20	0.20	0.520
HRB-SFC"	0.00	0.00	0.40	0.30	0.30	0.510

The sum of the P should be 1. For example, HRB-1S had the P_{GU} of 0.2 and P_{BFS} of 0.8, and the other coefficients P_{FA} and P_{CKD} accounted for 0. On the other hand, coefficients K values are regression results which indicated the efficiencies in strength, the higher the K, the higher contribution of such component in the specified curing age.

The results of strength regression were shown in Table 4-5. GUL had slightly higher efficiency factors than GU at 7 days, but after 28days, GU had the highest efficient factor. Other than GU and GUL, GGBFS had the highest efficient factors. And its factors grew considerably along with curing time from 7 days to 28 days. The factor of GGBFS K_{BFS} for compressive strength started at 3.46 at 7 days, making up 32.7% of K_{GU} at the same curing age. However, it increased sharply to 9.44 at the time of 28 days, and it further grew up to 10.61 at 56 days, making up 50.6% of K_{GU} at 56 days. Same trend was also observed in results of flexural strength.

Table 4-5 Regression results for strength

Efficiency factors	Compressive strength					Flexural strength				
	K_{GU}	K_{GUL}	K_{BFS}	K_{FA}	K_{CKD}	K_{GU}'	K_{GUL}'	K_{BFS}'	K_{FA}'	K_{CKD}'
Factor for 7 days	10.57	10.74	3.46	0.01	-0.88	3.15	3.47	1.79	-0.19	0.02
P-value	0.00	0.00	0.00	0.99	0.30	0.00	0.00	0.00	0.64	0.95
Adjusted R^2	0.92					0.84				
Factor for 28 days	16.29	15.42	9.44	0.50	-1.19	4.26	4.09	3.21	-0.01	-0.07
P-value	0.00	0.00	0.00	0.73	0.44	0.00	0.00	0.00	0.99	0.92
Adjusted R^2	0.91					0.83				
Factor for 56 days	20.93	19.95	10.61	0.44	-2.43	4.58	4.39	4.10	0.22	0.42
P-value	0.00	0.00	0.00	0.81	0.20	0.00	0.00	0.00	0.75	0.56
Adjusted R^2	0.91					0.83				

Meanwhile, fly ash made much less contribution compared to GGBFS. But the efficient factors of K_{FA} were also positive and they still increased along with curing. On the other hand, the efficiency factors for CKD (K_{CKD} and K_{CKD}') were insignificant and sometimes negative. Such results indicated that the CKD used in this research could not provide obvious strength contribution in addition to cement. The reason was due to the high content of loss on ignition (LOI) in CKD. The high LOI content (31.4% in this research) could result in lower percentage of free lime, thus bringing reduced level of hydration (Adaska and Taubert 2008).

The adjusted R^2 values were high for Eq. 4-10 and Eq. 4-11, indicating a well prediction in overall. Furthermore, plots in Fig. 21 and Fig. 22 showed well correlations between experimental and predicted strength values for both compressive and flexural strength. However, one can still observe from Table 3 that, the significance factors (P-value) for some efficiency factors were higher than normal criteria (0.05). These efficiency factors were K_{FA}, K_{FA}', K_{CKD}, *and* K_{CKD}'. The high P-values indicated that the statistical significances of such terms were unstable. On the other hand, GU, GUL, and GGBFS had a clear and significant contribution to the strength establishment. In addition, their efficiency factors had very low P-values.

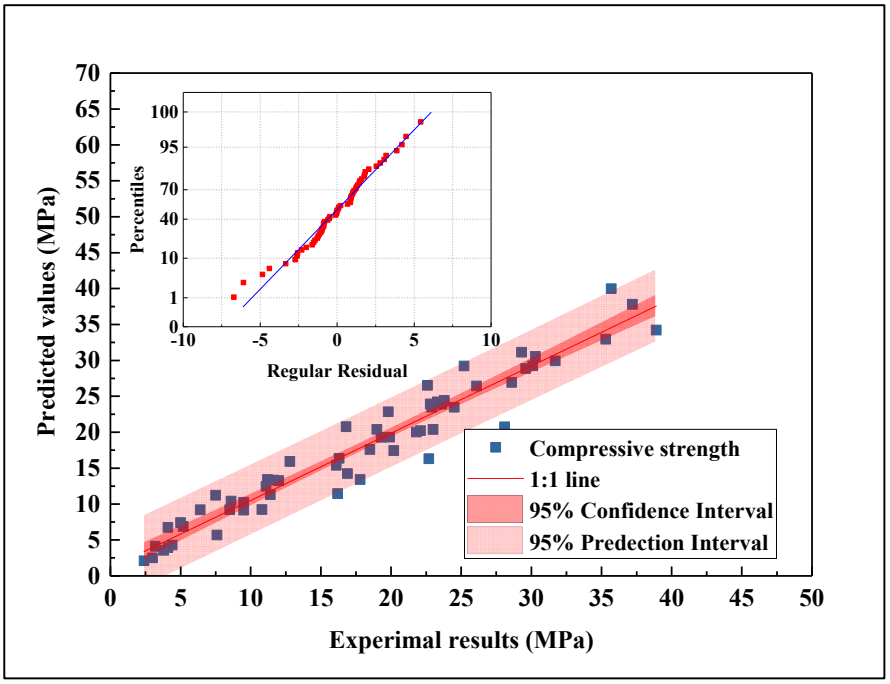

Figure 4-31 Validation of regression for compressive strength prediction

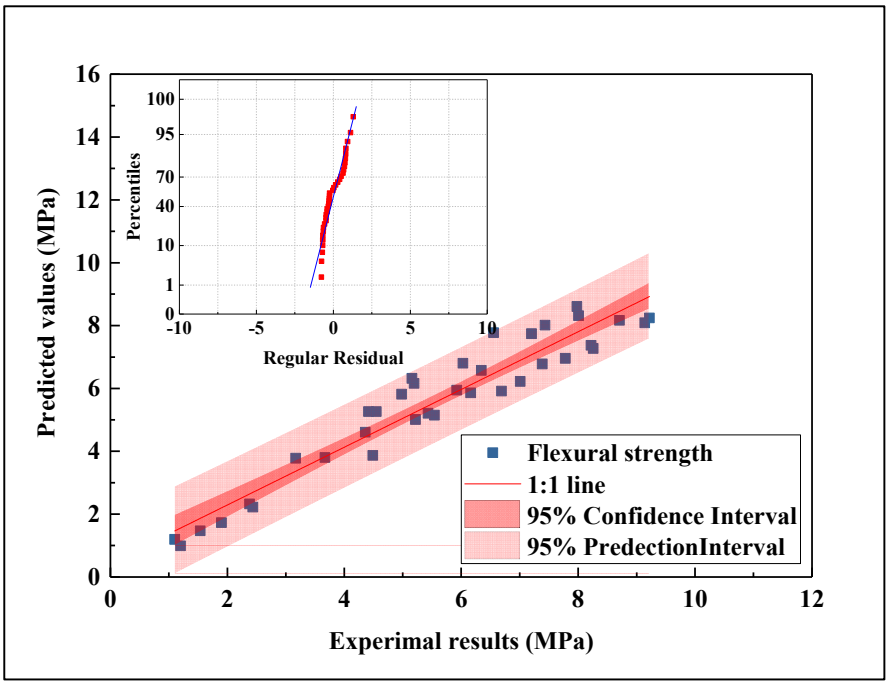

Figure 4-32 Validation of regression for flexural strength prediction

In general, strength modeling for cement and HRBs could be achieved. The compressive and flexural strength of HRBs highly correlated with w/b ratio in the mix and also to the content of main strength contributors (GU, GUL, and GGBFS in this study). The results of the model provide a reference for future study for blended cementitious systems.

4.2.5 Image Processing for Specimens after Flexural Test

The purpose of the image processing was to characterize the voids in hydrated mortar. Voids were visible in cement and HRB mortars (in Figure 4-33). The majority of voids were occupied by water during mixing. With the process of hydration and pozzolanic reactions, a substantial amount of water was consumed and absorbed. Voids were then left in hydraulically bound mixtures. The image processing was performed on the mortar beams after flexural test. Each specimen after flexural test was broken into two pieces during the test. The image processing was conducted on both sides of one specimen. Specimens with flat surfaces were chosen for image processing, see Figure 4-33.

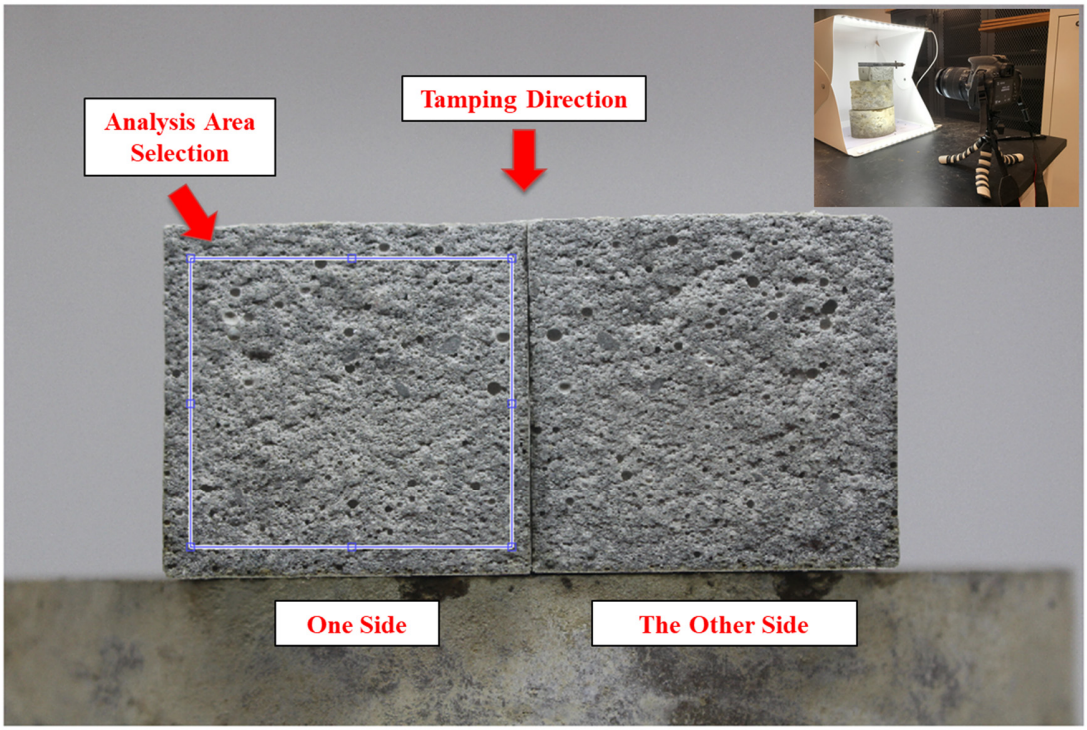

Figure 4-33 Voids detection by image processing

During the test, the specimens were placed in such a way that their tamping surface was on the top. The specimens were also placed in a light box with white light shining from all

directions in order to prevented incorrect void detection caused by shadow. For each test, the pictures were taken from a camera at the same height as the specimen. The images were later labeled, saved and processed using MATLAB software. Figure 4-34 presents the image input and analysis process in MATLAB.

The image process technology for void characterization included image filtering, segmentation, threshold determination, and voids characterization. Results were then summarized and expressed as surface porosity, and angle distribution of voids. Detailed procedure is illustrated as follows:

1) **Image filtering.** Images were first input into the system and changed into grayscale images. Based on the resolution, the grayscale images sometimes contained "salt and pepper" noises. Wavelet Filtering is used in the test to reduce the noises, smooth the void boundary without compromising the resolution.

2) **Image segmentation and edge detections.** The image segmentation and edges detections were conducted by converting a grayscale image to a binary image with a threshold. After the segmentation, all pixels which had luminance greater than threshold will be replaced with signal 1 (white), and the rest pixels were replaced by signal 0 (black). As it is seen in Figure 4-34, the white area of the image represented the voids while the black area represented the solid particles.

3) **Threshold determination.** The threshold introduced in the previous paragraph was determined by the same method that the author used in the previous research (Wang *et al.,* 2016). Otsu's algorithm was used to determine the preliminary threshold.

   As it is indicated in Figure 4-34, the change of threshold significantly affected the voids detection. Since then, a manual judgment of the threshold was conducted by author to better reflect the void condition. The threshold used in the test ranged between 63 and 68 at a mean of 65 in most cases to ensure the test consistency.

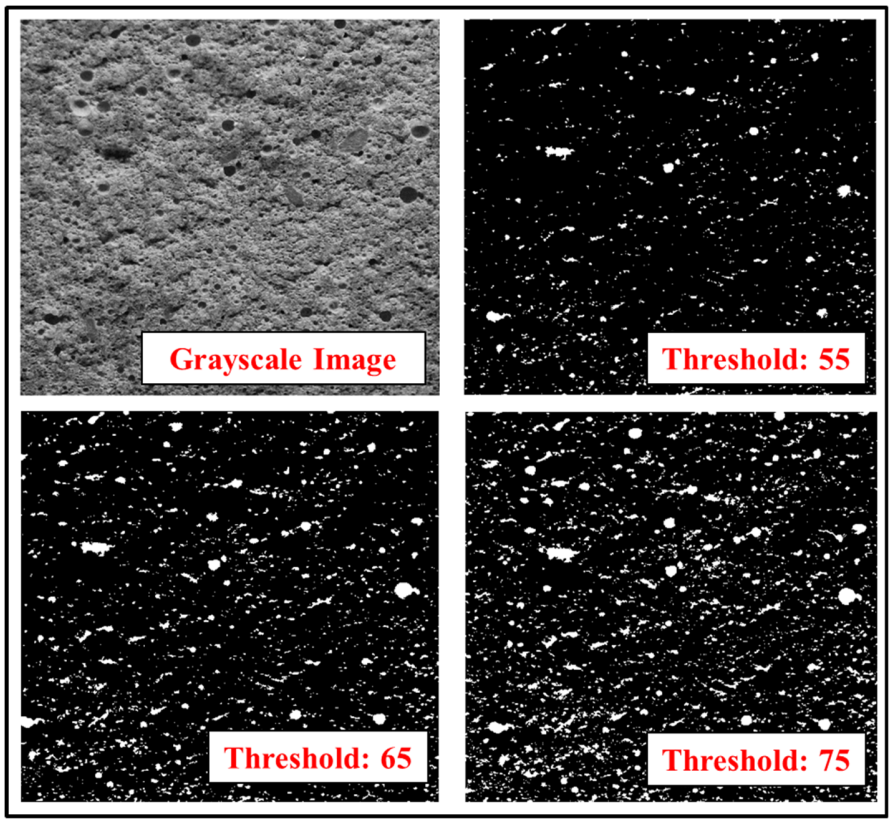

Figure 4-34 Image segmentation for processing

After the voids had been collected, they were further characterized. Surface porosity *n* was used here to indicate the ratio between the area of voids and the total surface area. Such ratio is expressed as a percentage (Wang *et al.,* 2016):

Equation 4-12

$$n = \frac{A_v}{A} \times 100\%$$

Where, A_v= total area of the voids (μm^2);

A= observation area of the specimen (μm^2).

Results of surface porosity of different HRB mortars are presented in Figure 4-35 and 4-36. As it is shown from the figures, GU and GUL specimens had surface porosity of 6.46% and 6.3% respectively at 7 days. Afterwards, the porosity reduced significantly to around 2.8% to 3.2% at 28 days, and further decreased to around 2.5% at 56 days. The reduction of porosity was due to the hydration production. The hydration products formed by water and binders continuously filled the voids and reduced the porosity with time.

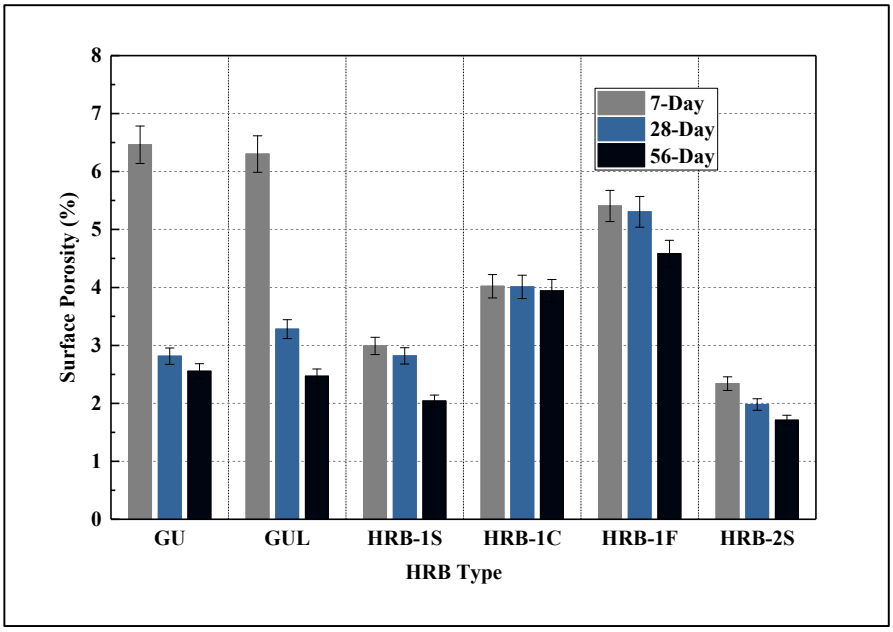

Figure 4-35 Surface porosity of cement and HRB mortars

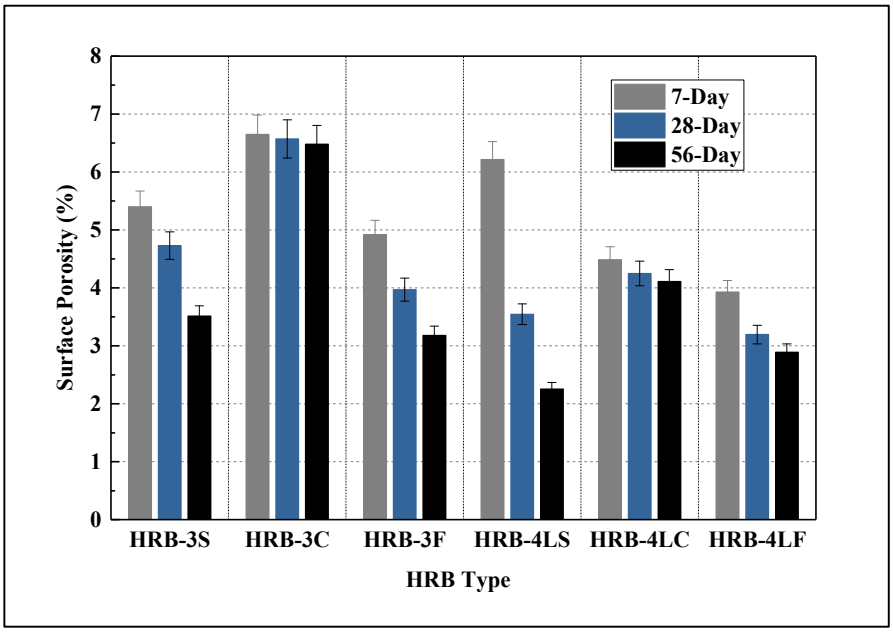

Figure 4-36 Surface porosity of HRB mortars

The phenomenon of porosity reduction was also observed in HRB mortars. The adding of SCMs especially GGBFS improved the general particle size distribution of the binder, resulting in the reduction of porosity. The observed surface porosity of HRB-1S and HRB-2S

had the overall least surface porosity among all the HRB types. On the other hand, the HRB-1F had higher porosity than HRB-1S, although the fly ash particles were found to be finer than GGBFS. The reason was that the fly ash has less water-holding capacity than GGBFS and CKD, so there was more free water in the mortar. Another reason could be due to the lower content of hydration products between fine aggregates. In addition, HRBs containing CKD had surface porosity values between those containing fly ash and GGBFS.

Moreover, angle distribution of each void was also calculated. The calculation was based on the assumption that all the voids are approximately ellipse-shaped. The angle of the void was defined between the major axis of the ellipse and the horizontal axis, shown in Figure 4-37.

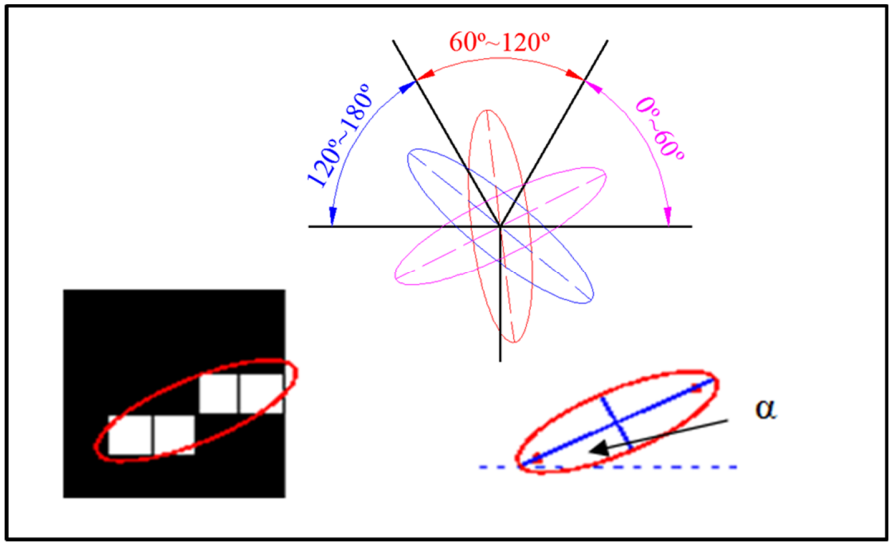

Figure 4-37 Angle explanation of each void

The value was expressed in degrees, ranging from 0° to 180°. The angles were classified in three groups: 0° to 60°, 60° to 120°, and 120° to 180°. The 0° to 60° and 120° to 180° grouped voids were the voids in a more horizontal position, whereas the 60° to 120° voids represented the voids in a more vertical position. The research calculated the percentage of voids falling in each angle group.

The result of void angle distribution was summarized in Figure 4-38 to 4-40. As it is shown, the angles of the voids were evenly distributed at all directions. The percentage of voids facing the vertical (60° to 120°) direction was larger than those facing the left (0° to 60°) or right side (120° to 180°). However, since the voids facing left or right side were highly random due to the homogeneous mixing, they can be further classified as “side” while the

voids facing top can be classified as “vertical”. The numbers of overall voids facing side are much more than the voids facing vertical. Such phenomenon could also be seen from the binary image shown in 4-34. According to the author’s point of view, the reason of the voids facing side is due to the effects of tamping.

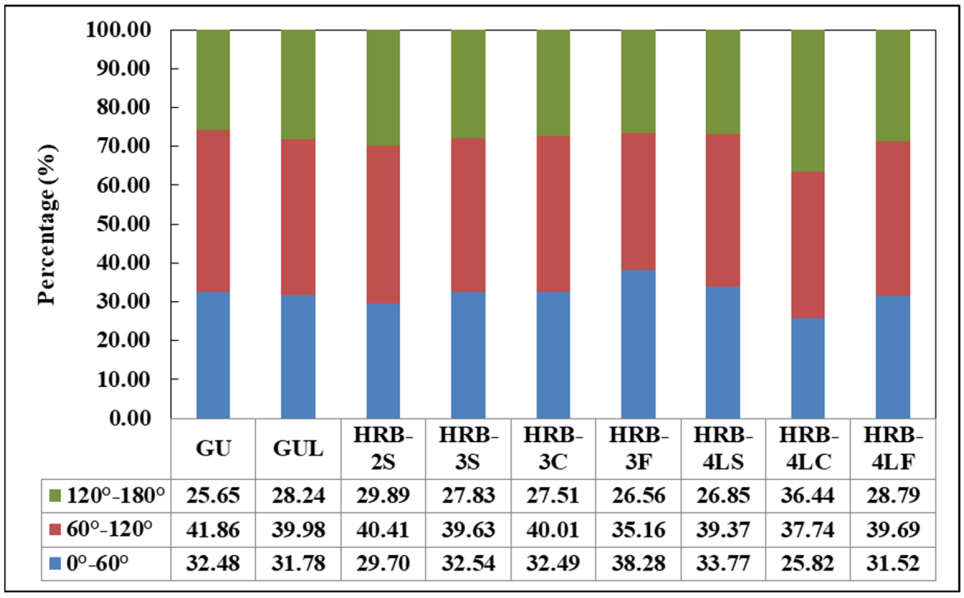

	GU	GUL	HRB-2S	HRB-3S	HRB-3C	HRB-3F	HRB-4LS	HRB-4LC	HRB-4LF
120°-180°	25.65	28.24	29.89	27.83	27.51	26.56	26.85	36.44	28.79
60°-120°	41.86	39.98	40.41	39.63	40.01	35.16	39.37	37.74	39.69
0°-60°	32.48	31.78	29.70	32.54	32.49	38.28	33.77	25.82	31.52

Figure 4-38 Void angles of mortars after 7 days

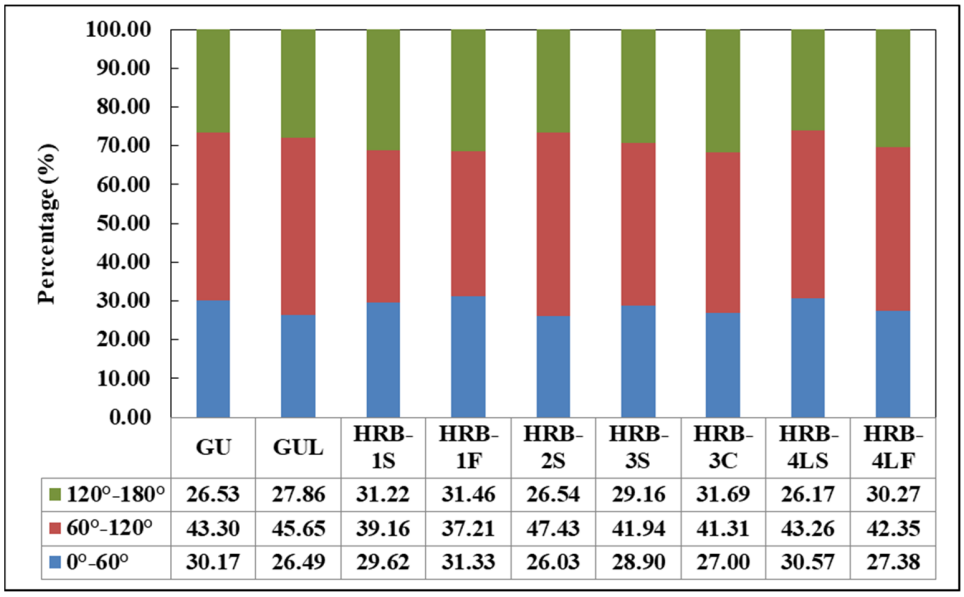

	GU	GUL	HRB-1S	HRB-1F	HRB-2S	HRB-3S	HRB-3C	HRB-4LS	HRB-4LF
120°-180°	26.53	27.86	31.22	31.46	26.54	29.16	31.69	26.17	30.27
60°-120°	43.30	45.65	39.16	37.21	47.43	41.94	41.31	43.26	42.35
0°-60°	30.17	26.49	29.62	31.33	26.03	28.90	27.00	30.57	27.38

Figure 4-39 Void angles of mortars after 28 days

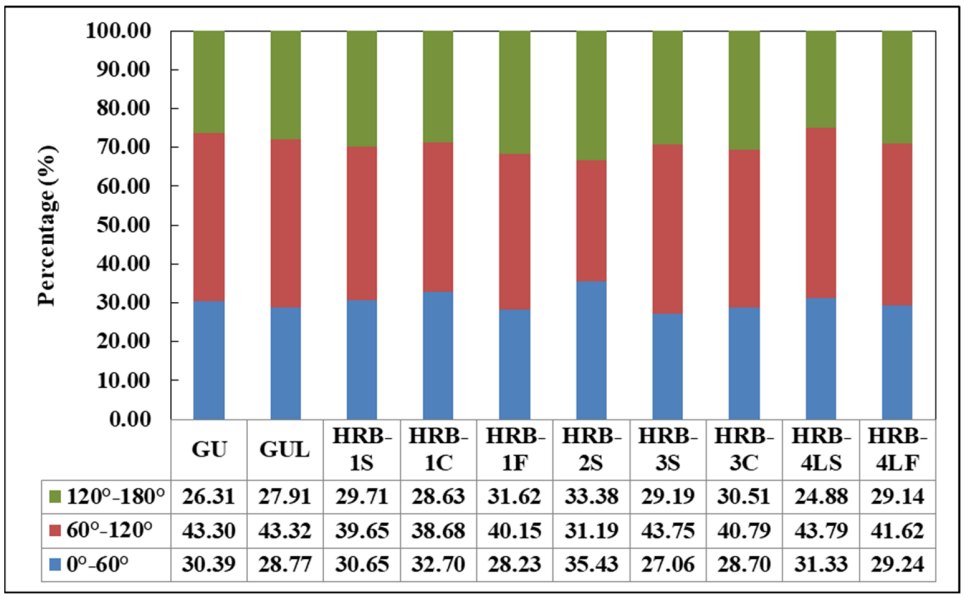

	GU	GUL	HRB-1S	HRB-1C	HRB-1F	HRB-2S	HRB-3S	HRB-3C	HRB-4LS	HRB-4LF
120°-180°	26.31	27.91	29.71	28.63	31.62	33.38	29.19	30.51	24.88	29.14
60°-120°	43.30	43.32	39.65	38.68	40.15	31.19	43.75	40.79	43.79	41.62
0°-60°	30.39	28.77	30.65	32.70	28.23	35.43	27.06	28.70	31.33	29.24

Figure 4-40 Void angles of mortars after 56 days

The differences of curing ages did not play an important role on the void angle distribution, as the specimens had hardened at the age of 7 days and the shape of voids did not change significantly. In general, voids were visible and obvious from the mortar surface. Void characterization using image processing methods was a useful tool for investigating cement and HRB mortars.

In addition, Figure 4-41 presents the relationships between the specimen's flexural strength and the surface porosity. It is evident that the increase of porosity could lead to a significant reduction of flexural strength. However, a correlation is difficult to observe from the two parameters.

Overall, the results in this section showed a potential of using image processing for voids characterization in cement-based systems. Based on the current results, it will be of great importance to compare the results of surface porosity and void size distributions with other methods, for example, Mercury Intrusion Porosimetry (MIP) test and 3D scanning test (Dolado and Van Breugel, 2011). Furthermore, numerical modeling could be conducted in the future to understand particle packing, hydration process, and particle gradations in cement-based systems.

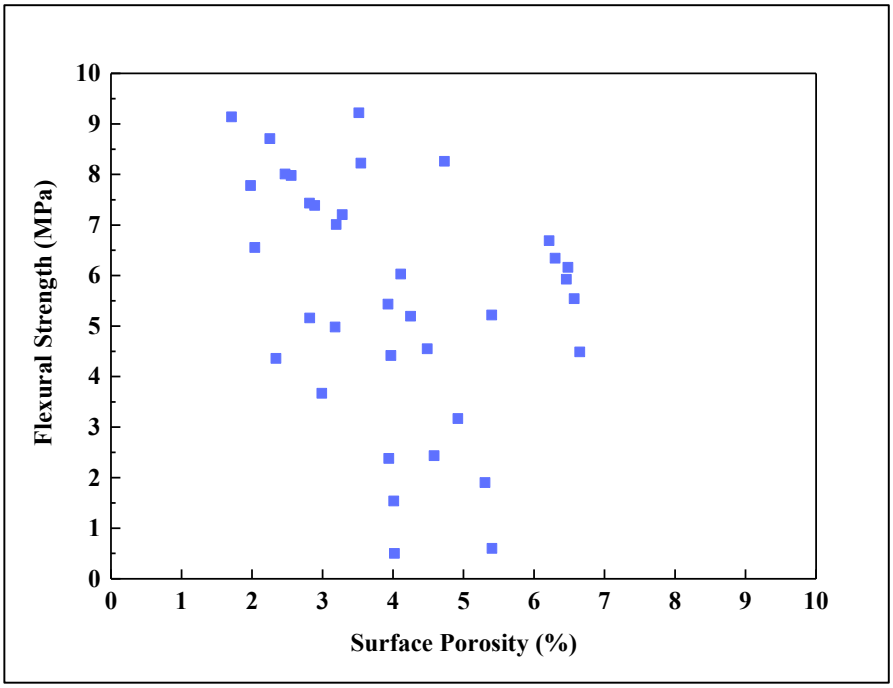

Figure 4-41 Relationships between flexural strength and its surface porosity

4.2.6 Microscopic Observation for Hydrated Mortar

The scanning electron microscope (SEM) has been widely used in chemistry, physical, and material science, it is able to present a direct observation of microstructure for cement hydration. To start the test, the electron gun at the top of equipment produces a beam of high-energy electrons, which hit the surface of sample and generates X-rays, backscattered electrons, and secondary electrons. Those ejected electrons are then collected and converted to signals, and further transformed into microscopy images. SEM images reveal information of the morphology, hydrate bonding, and texture of the observed surface. Generally, conventional SEM has observation area ranges from approximately 1 cm to 5 microns in width, with its magnification ranging between 20 and 30000. The **E**nvironmental **S**canning **E**lectron **M**icroscope (**ESEM**) is an enhanced SEM test which allows the specimens to be scanned without drying and coating. Such technology provides convenience in observation and also mitigates the effect of sample preparation on specimen's surface. The equipment used for ESEM testing is presented in Figure 4-42. The left side of the figure shows the navigator system and the image capture system while the right side shows the ESEM chamber. The ESEM images were presented from Figure 4-43 to 4-49.

Figure 4-42 Navigator and image acquiring system (left), ESEM chamber (right)

As it is shown in Figure 4-43, when the observation was conducted on the images at 1000 times magnification or less, the domain of standard sand could be clearly seen. Relatively large quartz particles were covered by both multi-sized hydration products and small mineral particles in different shapes. Moreover, when the magnifications increased to over 2000, the needle-like hydration products such as ettringite were observed substantially between particles. In addition, the C-S-H gels were also seen in various shapes with soft edges. Figure 4-47 presented the typical hydration products in GU, with magnifications at 7000.

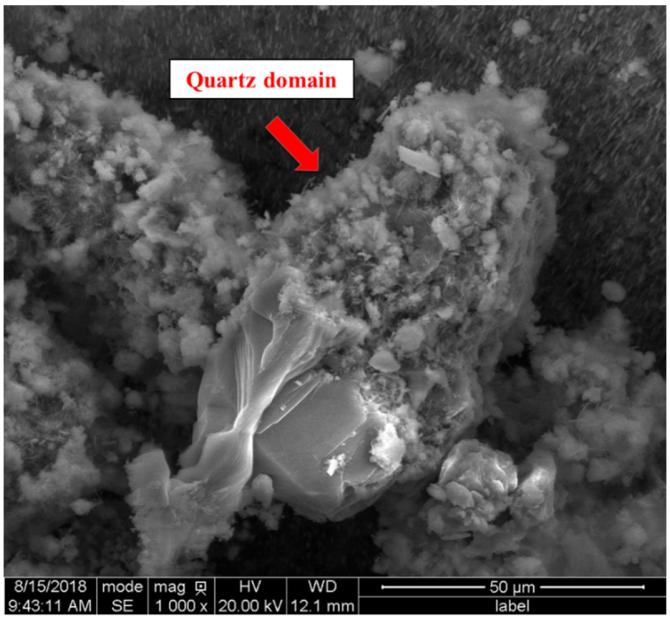

Figure 4-43 Overall microscopy of hydrated mortar (GU, 1000×)

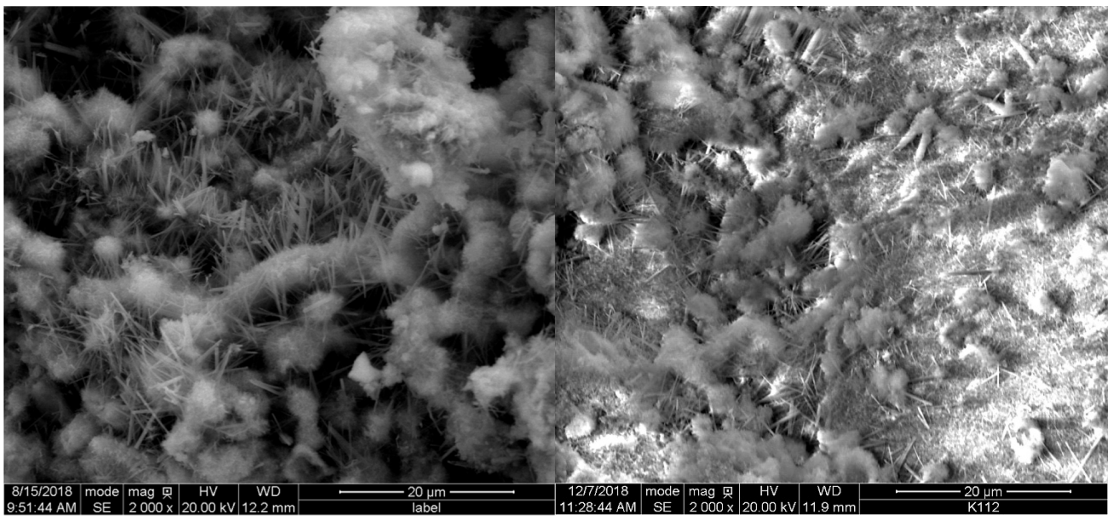

Figure 4-44 ESEM image of GU (left) and HRB-2S (right) (2000×)

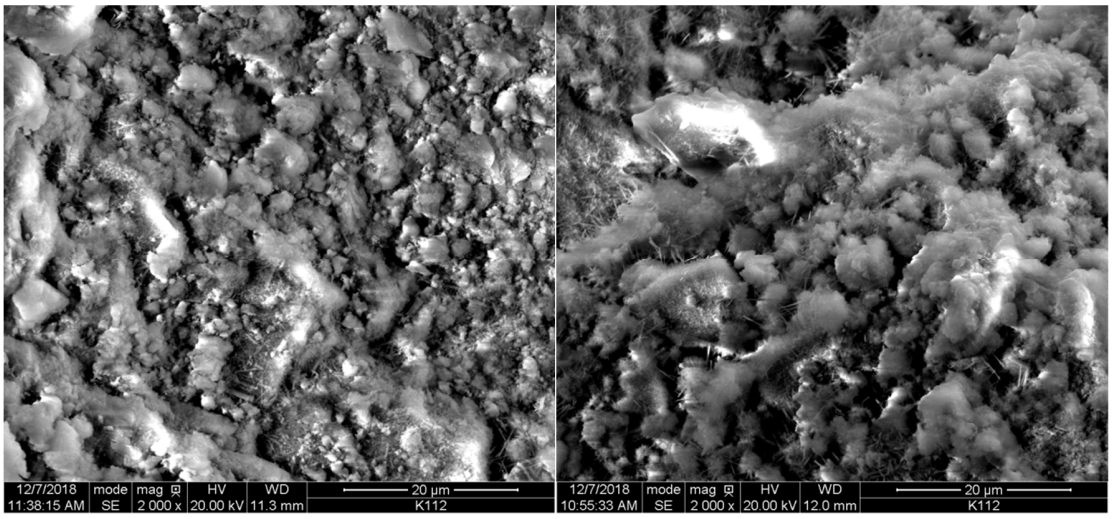

Figure 4-45 ESEM image of HRB-3S (left) and HRB-3C (right) (2000×)

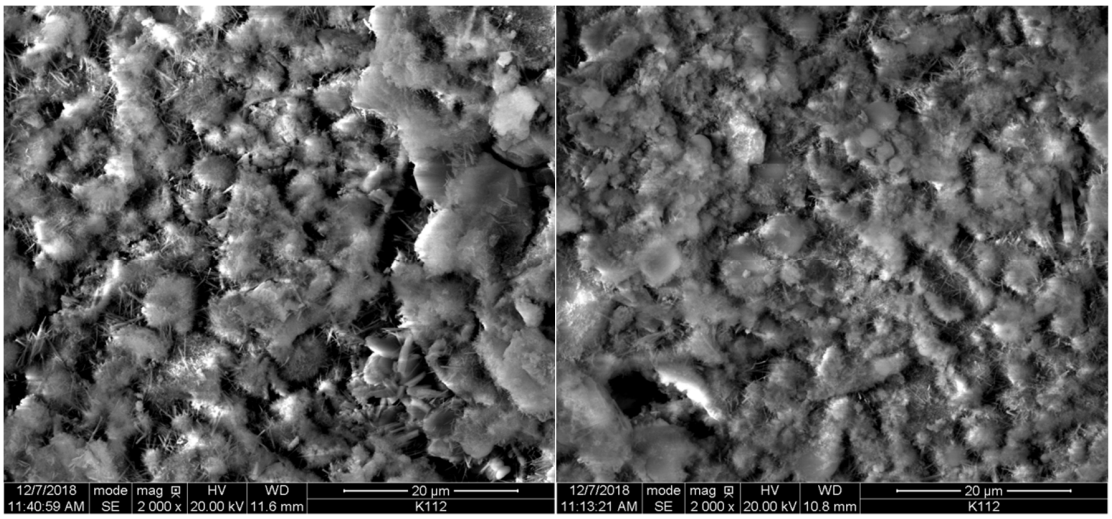

Figure 4-46 ESEM image of HRB-4LS (left) and HRB-4LF (right) (2000×)

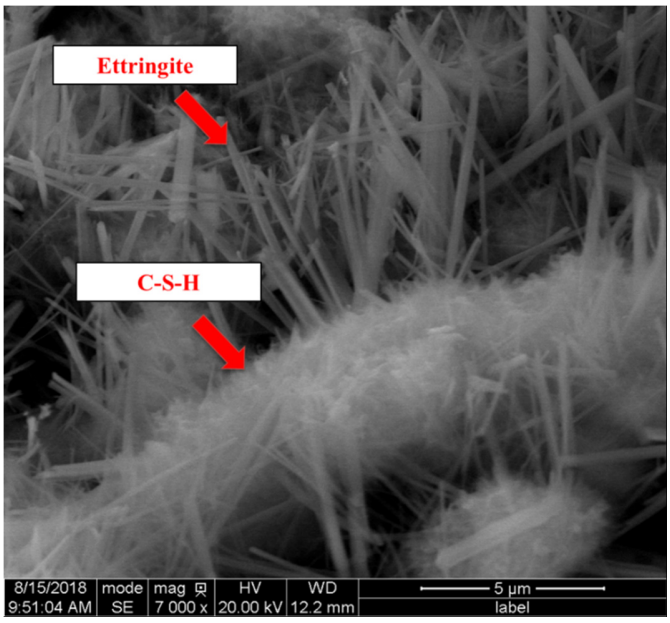

Figure 4-47 Hydration detail in GU (7000×)

One can also observe that the spread of hydration products in the mortar is homogeneous, with the help of proper mixing and curing. However, it was difficult to quantify the hydration products between different HRB types. Nevertheless, based on the overall appearance from Figure 4-45 to 4-49, it indicated that the amount of ettringite in GU mortar was more than those in HRBs. The reduction of ettringite in Portland cement was one of the important objectives in cement blending since it will reduce the potential of expansion and sulfate – induced cracks. The slight reduction of ettringite content in HRBs were also indicated from

XRD test in Figure 4-9 and 4-10.

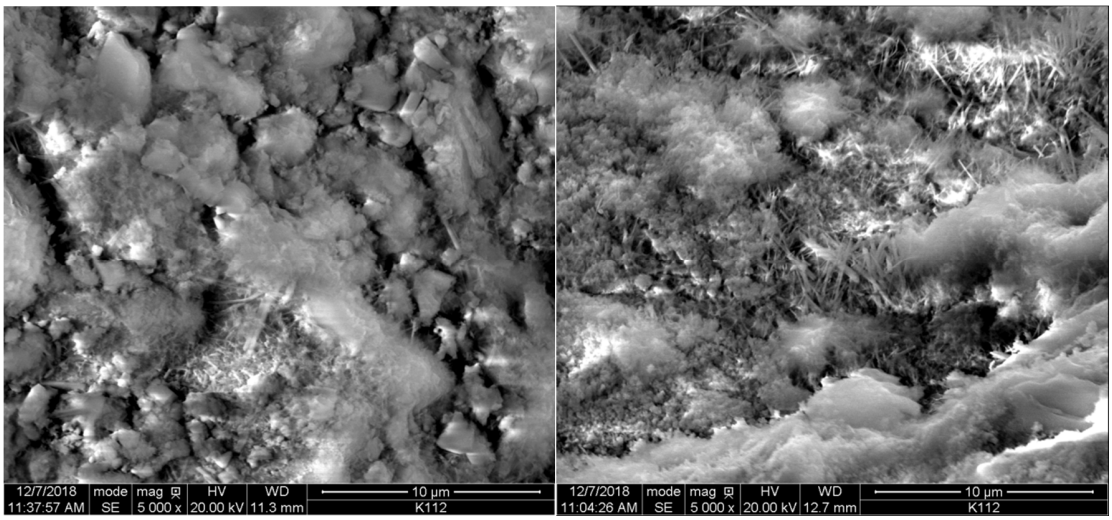

Figure 4-48 ESEM image of HRB-3S (left) and HRB-3C (right) (5000×)

Furthermore, Figure 4-48 and 4-49 further showed the microscopy of mortars in 5000 magnifications. The quartz particles were not distinct in this scale since they are too large and were hidden in the backgrounds. However, with the help of such magnifications, the formation of hydration products was more distinct. On the other hand, the HRBs containing fly ash was recognizable by the presence of ion spheres, shown in right side of Figure 4-49. The appearance of iron-rich spheres are typical features in microscopic images of fly ash and fly ash blended cements (Kutchko and Kim, 2006).

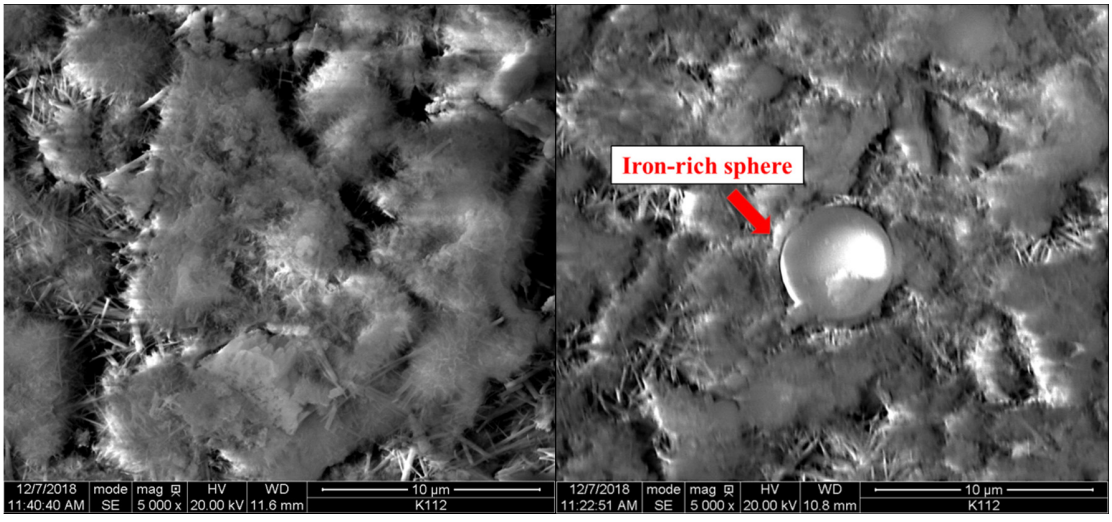

Figure 4-49 ESEM image of HRB-4LS (left) and HRB-4LF (right) (5000×)

In general, hydration products of cement and HRBs were substantially observed from microscopic images. The spread of hydration products was homogeneous throughout the image scope. HRBs were able to produce substantial amount of hydration products like GU with less needle-like ettringite. In addition, the iron-rich spheres were only observed in HRBs containing fly ash.

4.3 Summary for Chapter 4

This chapter introduced the physical and chemical analysis of different formulated HRBs in comparison with GU and GUL cement. Investigation was conducted on both paste and mortars. Based on the results, the following findings and conclusions can be drawn:

- The GU and GUL cements had the similar initial setting time of around 90 minutes. On the other hand, all HRBs had longer setting times. Among them, HRB-1S which contains 80% by mass of GGBFS had initial setting time of 232 minutes. In addition, HRB-4LS containing 80% of GUL had initial setting time of 173 minutes.
- There were obvious differences between GU, GUL, and HRBs in the hydration temperatures. Generally, HRB pastes had the reduced hydration temperature and less accumulated temperature than Portland cement during early hydration. Between them, the CKD-blended HRBs had the lowest heat release, followed by fly ash and GGBFS.
- Hydrated GU and HRB pastes had similar hydration products with different proportions. Portlandite, calcite, ettringite, and quartz were classified in hydrated pastes. The relative percentage of portlandite in hydrated GU cement was larger than those in hydrated HRBs. The EDS test proposed a high potential of forming calcium silicate hydrates and portlandite. Hydrated HRBs contained less ettringite and slightly more silica and potentially lower Ca/Si based calcium silicate hydrates compared to GU cement. In addition, hydration lead to the increase of the amount of oxygen in all binders.
- GU and HRB mortar beams shrank more substantially in the first 18 days. After 32 days of drying, the growth of shrinkage became insignificant. Among all the binder types, HRB mortars shrank less and slower than GU and GUL mortars.

- Cement content was still the main factor that influenced the strength. However, after 28 days of curing, HRBs containing not less than 50% of GGBFS had similar and, in some cases, higher strength values compared to GU and GUL. On the other hand, fly ash and CKD used in this study did not provide significant contribution to strength. Moreover, a linear correlation was found to well describe the relationships between mortar's compressive strength and flexural strength in all curing ages.
- Statistical analysis for GU and HRB strength revealed that: first, cement and SCM contents played significant roles in strength development of HRB mortars. Second, mortar strength had statistical correlations with the content of each chemical component at a given curing age. In particular, the correlations were more distinct with the binder content of GU, GUL, and GGBFS.
- Image processing of mortar specimens after flexural testing revealed a reduction of surface porosity of mortars along with curing time. However, the porosity of mortars did not correlate well with their strength. On the other hand, the angles of voids were in a more "horizontal" direction due to the effects of tamping. Overall, the results showed a potential of using image processing for voids characterization in cement-based systems. Based on the image processing technology, some other testing and modeling could be conducted in the future to understand particle packing, hydration process, and particle gradations in cement-based systems.
- Hydration products of cement and HRBs were substantially observed from microscopic images. The spread of hydration products was homogeneous. HRBs were able to produce a substantial amount of hydration products like Portland cement and with less amount of ettringite presented.

CHAPTER 5 INVESTIGATION OF SUBGRADE SOIL AND HYDRAULIC ROAD BINDER-TREATED SUBGRADE SOIL

In this chapter, the chemical and physical analysis was performed to investigate the cement and HRB improved subgrade soils. Several HRB types investigated in Chapter 4 were chosen for stabilization. As it was introduced in Chapter 4, the use of GGBFS significantly improved the strength development in HRBs mortars; therefore, HRB-1S, HRB-2S, HRB-3S, and HRB-4LS with different slag contents were selected for soil treatment. In addition, HRB-3C and HRB-4LF were also selected for soil treatment since they have slightly lower strength than slag-based HRBs but with reduced shrinkage potentials and less hydration temperatures. Researches were conducted to investigate the effect of GGBFS, fly ash, and CKD on soil treatment.

On the other hand, the target soils used were Dresden, Blenheim, and Niagara. Those soils are typical weak subgrade soils which was used in real construction projects. Soil sampling process, and soil sampling preparation had been previously introduced in Chapter 3. This chapter started with subgrade soil characterization tests, followed by the characterization and analysis for hydraulically bound mixtures. General use cement was used as the control binder as it has been used extensively for the pavement materials stabilization in the local area.

5.1 Subgrade Soil Characterization

In this section, the information about soil's natural moisture content, organic matters, Atterberg limits, CBR values are introduced.

The natural moisture contents and organic contents of soils were measured according to ASTM D2216 and D2974. The equipment for the tests is shown in Figure 5-1. Soils were heated to a temperature of 110℃ and until their weight became constant. The percentage of weight loss divided by dry mass of soil is considered as moisture content (%). See the equation 5-1. This method of moisture content measurement was substantially used in proctor test and specimen preparations in the later part of the thesis.

Figure 5-1 Oven for soil drying (left), furnace for organic matter ignition (right)

Equation 5-1

$$w(\%) = \frac{\text{mass of water}}{\text{mass of dry soil}} \times 100\%$$

On the other hand, natural organic content of soil was measured by igniting the dry soil to the temperature of 440°C and until the weight became constant. The calculation of the soil's organic content (%) is shown in Eq. 5-2.

Equation 5-2

$$\text{SOM}(\%) = \frac{\text{mass of dry soil} - \text{mass of ash}}{\text{mass of dry soil}} \times 100\%$$

Table 5-1 summarizes the natural moisture content and organic content of the three subgrade soils.

Table 5-1 Natural moisture and organic content of subgrade soils

Soil ID	Natural moisture content (%)	Organic content (%)
Dresden	19.44	4.54
Blenheim	27.47	4.90
Niagara	37.57	7.86

All the three soils contained a considerable amount of natural moisture content and organic material. In particular, natural Niagara soil had the largest amount of moisture (37.57%) compared to Dresden and Blenheim. The source of moisture content in the natural subgrade is due to precipitation, pavement drainage, and capillary rising.

On the other hand, Dresden and Blenheim soils contain approximately 4.54% to 4.90% of soil

organic matters based on ignition test. On the other hand, Niagara soil has the highest organic matter of 7.86%. High moisture content and organic matter concentrations lead to a dark color of soils.

Soil classifications and engineering properties were evaluated by particle size distribution, Atterberg limits, soil compaction proctor test, and California Bearing Ratio (CBR).

5.1.1 Particle Size Distribution

Subgrade soil's particle size distribution were conducted by a combination of sieving and hydrometer analysis (ASTM D6913 and D422, or MTO LS 702), respectively. Specifically, coarse fractions which retained on No. 4 sieve with grain size larger than 4.25 mm were analyzed by sieving. On the other hand, a proportion of fine fractions were measured by hydrometer analysis for their particle size and distribution. Figure 5-2 shows the equipment used for sieving and hydrometer. Figure 5-3 summarizes the detailed particle size distributions of the three types of subgrade soils. In addition, Table 5-2 summarizes the percentage of sand-sized, silt-sized, and clay-sized soils particle observed from analysis.

Figure 5-2 Sieves for sieving analysis (left), and sedimentation of hydrometer analysis (right)

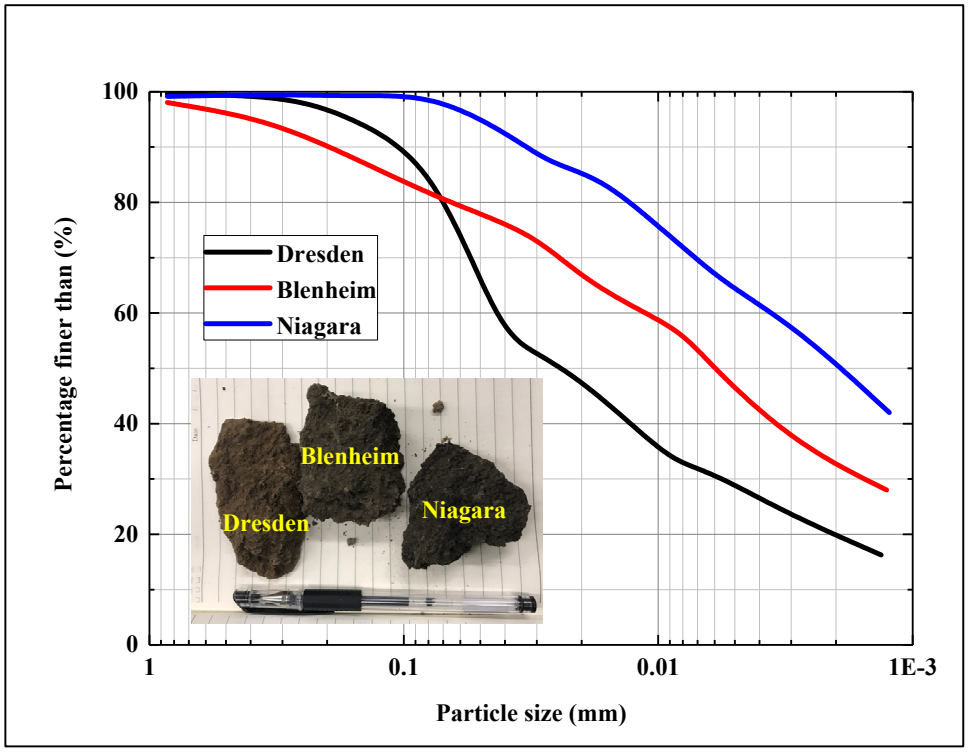

Figure 5-3 Particle size distribution of the soils

All the three types of soil are fine-grained soils and had particle size less than 1 mm. Among them, Niagara soil has the highest percentage of clay-sized particles (<0.002 mm) accounting for 57.01% by weight, the rest of soil is composed of silt-sized particles. On the other hand, Dresden soil contains 66.02% of silt-sized particles, but also has more than 20% of clay-sized particles. In general, all the three soils have high percentage of fine-grained soil particles which could cause the soil becoming plastic, soft, and susceptible to freezing and thawing.

Table 5-2 Gradation parameters and evaluations of subgrade soils

Particle size Distribution	Dresden	Blenheim	Niagara
Sand fraction (4.75~0.075mm) (%)	13.48	19.02	<1
Silt fraction (0.075~0.002mm) (%)	66.02	44.91	42.44
Clay fraction (<0.002mm) (%)	20.50	36.07	57.01

5.1.2 Moisture-Density Relationship

The moisture-density relationship test, or known as proctor compaction test, is a geotechnical test used to determine the maximum dry density γ_d and its corresponding optimal moisture content w for a compacted soil mass. There are two types of proctor test: standard proctor test and modified proctor test. The main difference between the two is the compaction effort which is 2,700 kN-m/m^3 in modified proctor and 600 kN-m/m^3 in standard proctor. Modified proctor test is commonly used to simulate heavy roller compacted surface and base layers. However, the compaction effort in modified proctor test is usually difficult to achieve at an in-field subgrade construction. Therefore, standard proctor test becomes more practical for soil classifications and specimen manufacturing. The procedure for the standard proctor test followed ASTM D698.

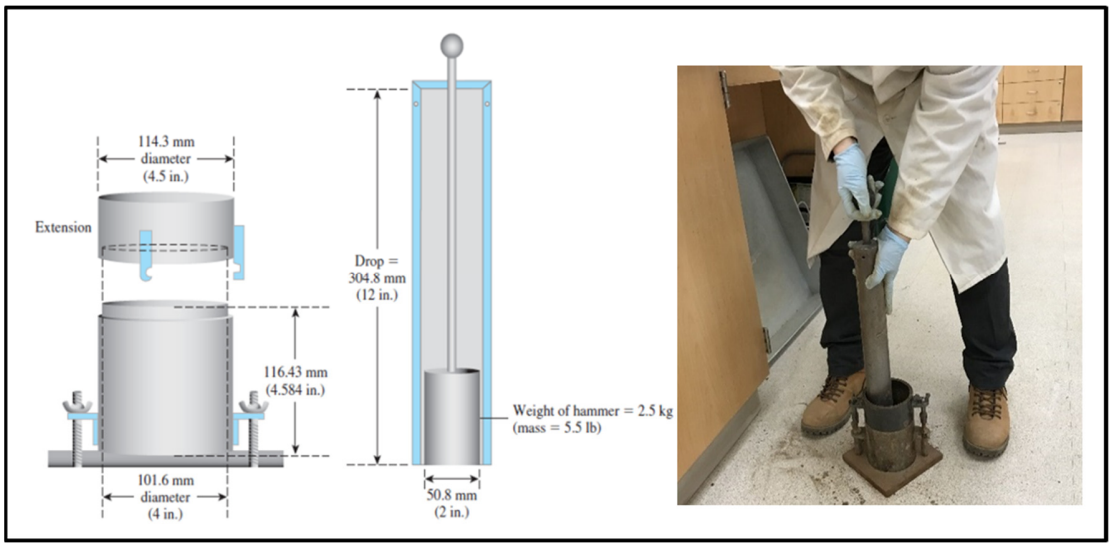

Figure 5-4 Mold used for proctor compaction (left) (Das 2015); test conducting (right)

For this study, a soil was compacted in a specific mold according to standard compaction energy. After the compaction, density of the soil and its moisture content were recorded. The procedure was repeated 4 to 6 times along with moisture content rising until a peak density has been found. A trend line of moisture-density relationship were plotted based on the data, and to find the value of maximum dry density (MDD) γ_d with its corresponding optimal moisture content (OMC) w. Theoretically, the situation of the OMC happens when the compaction degree reaches 100%, that is, all the air voids are filled with water and no excessive water exists in soil mass.

The unit weight γ of compacted soil mass can be calculated as (Das, 2015):

Equation 5-3

$$\gamma = \frac{W}{V_m}$$

where, W = soil weight (g) in the compaction mold;

V_m = inner volume (cm^3) of compaction mold.

Then, the dry unit weight γ_d can also be calculated based on the moisture content and unit weight γ (Das 2015):

Equation 5-4

$$\gamma_d = \frac{\gamma}{1 + \frac{w}{100}}$$

where, w = moisture content (%).

The moisture-density relationships of the 3 soils were plotted in Figure 5-5 and Table 5-3. The OMC for Dresden was 15.9%, Blenheim and Niagara samples had higher OMC accounting for 18.33% and 24.21%, respectively. Meanwhile, the corresponding dry density of each sample site was 1.73 g/cm^3, 1.67 g/cm^3, and 1.60 g/cm^3, respectively. Niagara soil was tested to have the highest moisture requirement and the lowest dry density.

The author also conducted multiple proctor tests for soils stabilized with 6% to 12% HRBs. Results indicated that stabilizers increase the need of moisture content in soils. It was found that the average OMC in 6% HRB-treated soils were 1.5% higher than the soil's origin OMC. Increase of stabilizer content from 6% to 12%, the OMC of treated soils further increased approximately 1.0%. Therefore, in order to prepare treated soil specimens for strength and modulus testing, an average of 2.0% moisture was added in addition to the untreated soil's OMC. Figure 5-5 presents an example of proctor test results of Dresden soil mixed with 6% of HRB-4LS.

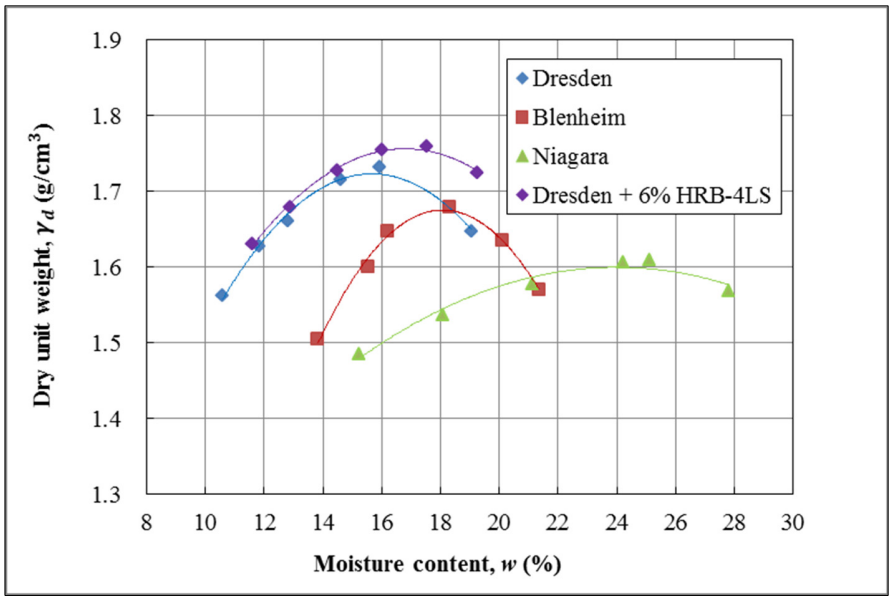

Figure 5-5 Moisture-density relationship of the soils

Table 5-3 Maximum dry density and their moisture content of 3 soils

Soil ID	Dry unit weight, γ_d (g/cm^3)	Moisture content, w (%)
Dresden	1.73	15.91
Blenheim	1.67	18.33
Niagara	1.60	24.21

5.1.3 Atterberg Limits

Atterberg limits tests were performed for soils before and after stabilization. Among them, Dresden soil behaved least plastic while the Niagara soils had highest plasticity index. By adding cement and HRBs, the plastic limit of soils had been significantly increased while their liquid limits were decreased. Such change lead to the shrinkage between liquid limit and plastic limit, thus reducing the plasticity index of soils especially in Blenheim and Niagara. An increase of stabilizer content could lead to further increase of plastic limit and resulted in a reduction of plasticity index. From the results of Table 5-4 one can observe that over 6% of GU or HRB could have the ability to reduce the soil's plasticity index less than 10.

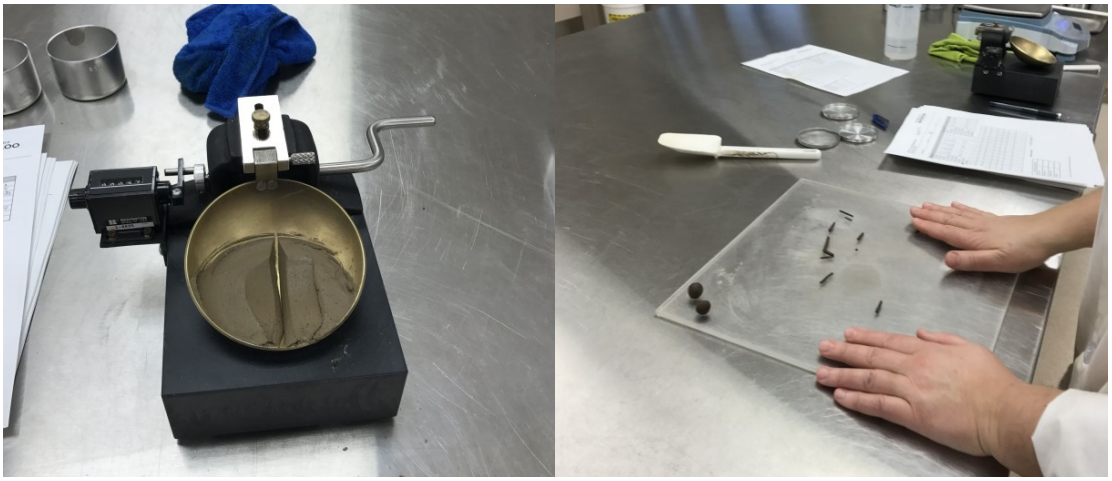

Figure 5-6 Liquid limit (left) and plastic limit (right) tests

Table 5-4 Atterberg limits of soils

Sample ID	Liquid limit (%)	Plastic limit (%)	Plasticity index
Dresden	29	19	10
Dresden + 4% HRB-2S	26	21	5
Dresden + 6% HRB-2S	26	22	4
Blenheim	39	23	16
Blenheim + 6% HRB-3C	39	30	9
Blenheim + 6% HRB-4LS	38	32	6
Blenheim + 8% HRB-4LS	38	34	4
Niagara	52	26	26
Niagara + 6% GU	53	41	12
Niagara + 6% HRB-4LF	52	42	10
Niagara + 6% HRB-4LS	52	42	10
Niagara + 8% HRB-4LS	51	43	8

5.1.4 California Bearing Ratio

The California Bearing Ratio (CBR) is a penetration test to evaluate the subgrade soil resistance and hardiness compared to a well-graded crushed stone (Pavement Interactive, 2019). Since it is a simple, quick, and cost-effective test, it has been widely used since 1930s by numerous states and provinces in North America. Currently in Canada, British Columbia, Saskatchewan, Ontario, Prince Edward Island and Nova Scotia are using soaked CBR value as the solely or one of the evaluation values for subgrade soil characterization (TAC, 2014). In this research, soaked CBR was used mainly to evaluate the bearing capacity of remolded

subgrade soil without treatment. Resilient modulus (M_r) testing, on the other hand, as a more currently adopted and advanced method, was used more frequent in the thesis in combination with unconfined compressive strength (UCS) test to investigate the soil's treatment by hydraulic binders.

In order to prepare the CBR specimen, soils were compacted according to their OMC and MDD in a 150 mm diameter mold. Then the CBR sample was soaked in tap water for 4 days for the monitor of soaking swelling under a surcharge of 4.54 kg. Test procedure of CBR followed the ASTM D1883 standard. Additionally, the soils were mixed with GU, HRB-2S, and HRB-4LF respectively to validate the effect of treatment in terms of soaking swelling. Samples were cured for 7 days before conducting soaked CBR test. Results of re-compacted subgrade soils and chemically stabilized subgrade soils are summarized in Table 5-5.

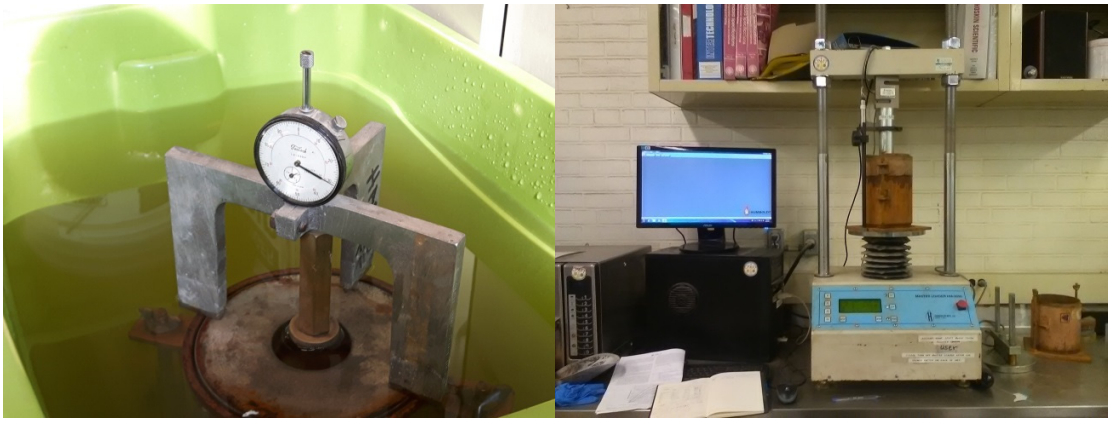

Figure 5-7 CBR soaking (left), and penetration test (right)

Table 5-5 Soil classification and evaluation

Soil ID	Soaked CBR value	Soaking Swelling
Dresden	8	1.5%
Dresden + 6% GU@7days	41	<1%
Dresden + 6% HRB-2S@7days	39	<1%
Blenheim	4	2.7%
Blenheim + 6% HRB-3C@7days	32	1.3%
Blenheim + 6% HRB-4LF@7days	38	<1%
Niagara	2	5.6%
Niagara + 6% GU@7days	10	2.3%
Niagara + 8% GU@7days	12	1.9%
Niagara + 8% HRB-4LS@7days	14	1.2%

As it is shown in tables, soaked subgrade soil samples had a very low CBR value compared to well-graded crushed stone. High percentage of fine-grained particles, and the organic matters could be the reasons which lead to the low bearing capacity. Among the three, Niagara soil had the lowest CBR value (approximately 2) with the highest potential of soaking swelling (5.6% in volume). In addition, the Blenheim and Niagara soils also lost substantial soils during soaking. The particles suspended in the water and made the water turbid.

The 7-days cured specimens had significantly increased CBR values which equal to 5 to 7 times of the values in remolded soil specimens. Besides, soaking swelling of specimens was significantly reduced due to the bonding between soil particles. Moreover, the soaking water was still clear after 4 days of curing. With the increase of stabilizer content, the CBR values had further increase while the swelling is decreased.

5.1.5 Soil Classifications

In summary of the previous lab results, the subgrade soils were then be classified based on the two soil classification systems: **U**nified **S**oil **C**lassification **S**ystem (USCS), and AASHTO soil group.

Based on the classification, Dresden soil was classified as clayey silt with low plasticity (CL). On the other hand, Blenheim and Niagara were classified as organic clayey soil (OL) and organic clay (OH), respectively. In addition, the Dresden, Blenheim, and Niagara were classified as A-5, A-6, and A-7-6 respectively based on AASHTO soil classifications. In general, all the three types of subgrade soils are fine-grained soils with substantial organic soils, making them difficult to be treated in field.

Table 5-6 Soil classification and evaluation

Soil ID	USCS system	AASHTO soil group	AASHTO suggested cement ratio by weight
Dresden	CL	A-5	8%~13%
Blenheim	OL	A-6	9%~15%
Niagara	OH	A-7-6	10%~16%

5.2 Chemical Analysis for Subgrade Soil and Treated Subgrade Soils

Soil's chemical environment plays a significant role in the strength, modulus and bearing capacity. In this thesis, chemical analysis of subgrade soil before and after stabilization include pH values testing and ion chromatography test. In order to measure the alkaline environment of stabilized soils with different HRB contents, pH value tests were conducted using a modified method of ASTM D6276, *"Standard Test Method for Using pH to Estimate the Soil-Lime Proportion Requirement for Soil Stabilization"*. The pH value was measured by a pH value detector from the soil-water-stabilizer mixture. Such mixture is formed by mixing 25 g of dried soil, certain amount of stabilizer, and 100 ml of deionized (DI) water together. The difference of pH values on duplicate specimens was controlled within ± 0.2 compared to the first trial. The left side of Figure 5-8 shows the equipment for pH value testing of subgrade soils and improved soils.

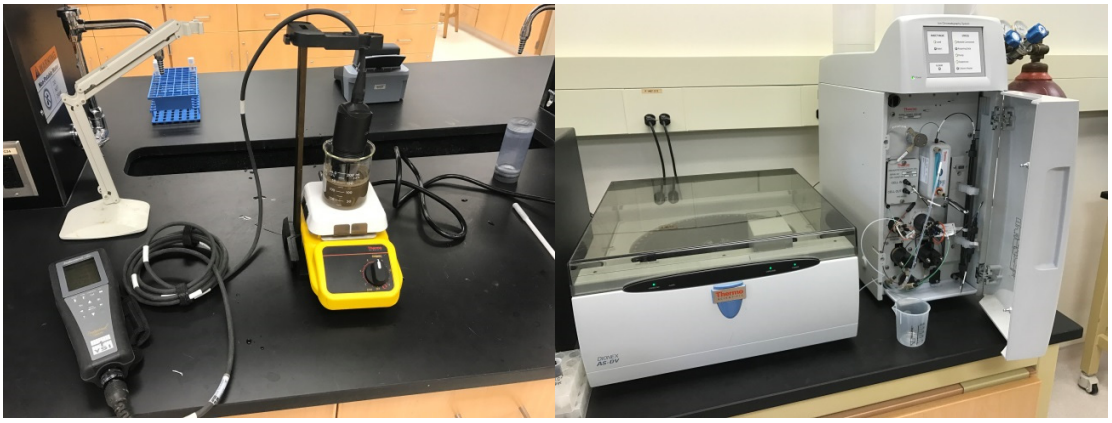

Figure 5-8 pH value test equipment (left), soluble salt test equipment (right)

The organic matter in the soil samples creates a slight and moderate acidic environment. The pH values of Dresden, Blenheim, and Niagara accounted for 6.9, 6.5, and 5.8 respectively. Among the three, Dresden soil had the nearly neutral environment. On the other hand, Niagara soil with the most organic content (7.86%) had the lowest pH value. Once cement and HRBs were added into the mixture, the soil's environment changed from acidic to alkaline with the pH ranging between 11.1 and 12.3. The alkaline environment prevented the reaction and reproduction of organic materials, and it is beneficial for HRB-soil pozzolanic reactions. It is also observed that increase of stabilizer content could lead to a further increase of pH values. However, the changes were not substantial.

Table 5-7 Average pH values of specimens with different HRB contents

Soil type	Additive type	Additive ratio					
		0%	4%	6%	8%	10%	12%
Dresden	GU cement	6.9	11.6	11.7	11.9	12.1	12.1
	HRB-1S				11.1	11.6	11.7
	HRB-3S				11.4	11.6	11.8
	HRB-3C				11.4	11.6	11.7
	HRB-4LS				11.3	11.6	11.8
	HRB-4LF				11.3	11.6	11.7
Blenheim	GU cement	6.5	11.6	11.8	11.9	12.1	12.2
	HRB-1S				11.5	11.6	11.6
	HRB-3C				11.3	11.4	11.5
	HRB-4LS				11.3	11.6	11.7
Niagara	GU cement	5.8	11.3	11.7	11.9	12.0	12.1
	HRB-1S				11.1	11.2	11.3
	HRB-3C				11.3	11.4	11.5
	HRB-4LS				11.2	11.4	11.7

Ion chromatography (IC) technology is well established for determination of ionic analysis for natural water and soil. The integrated system Thermo Scientific™ Dionex™ ICS-2100 was employed to determine the sulfate and chloride contents in the test specimens. This system includes a pump, degasser, eluent generator, and conductivity detector (Thermo Scientific Manual). The sample preparation started with mixing 6.0 g of air-dried soil with 18 ml DI water, followed by centrifuging, top liquid decanting, acidifying and filtering. Prior to test, calibration was conducted and that the system error was checked to be below 2%. Test results of ion content of soluble sulfate (SO_4^{2-}), chloride (Cl^-), and nitrate (NO_3^-) for soils and stabilized soils are shown in the Figures 5-9 to 5-12.

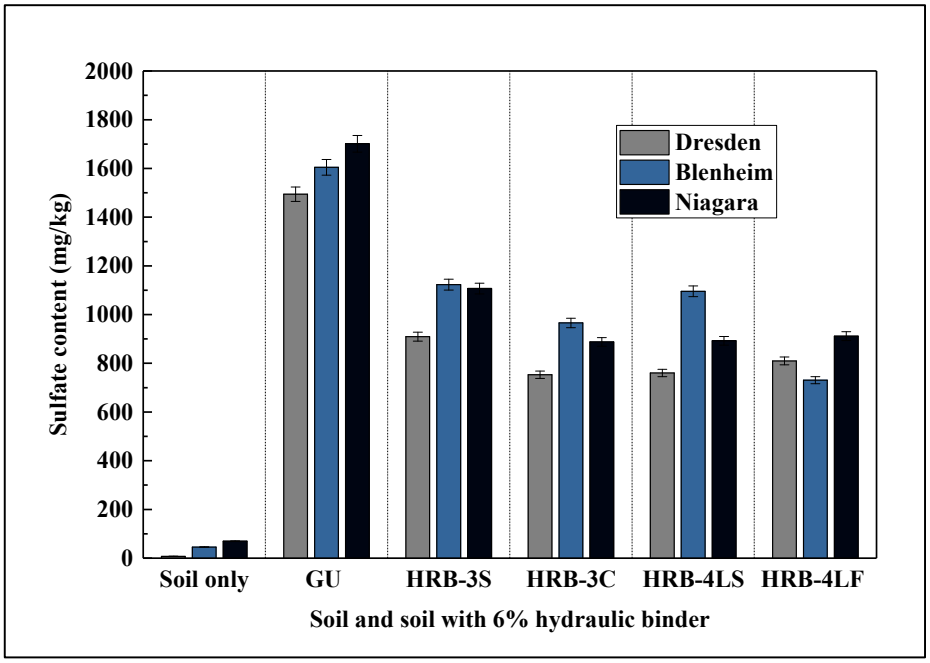

Figure 5-9 Soluble sulfate content in soils and stabilized soils with 6% of hydraulic binder

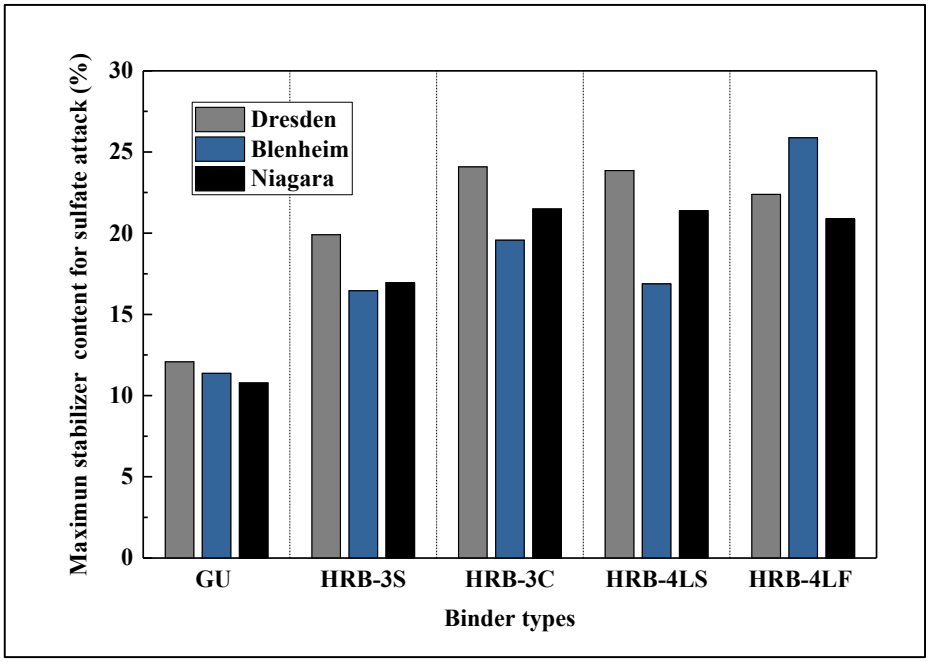

Figure 5-10 Maximum cement and HRB content (%) when sulfate reaching 3000 mg/kg

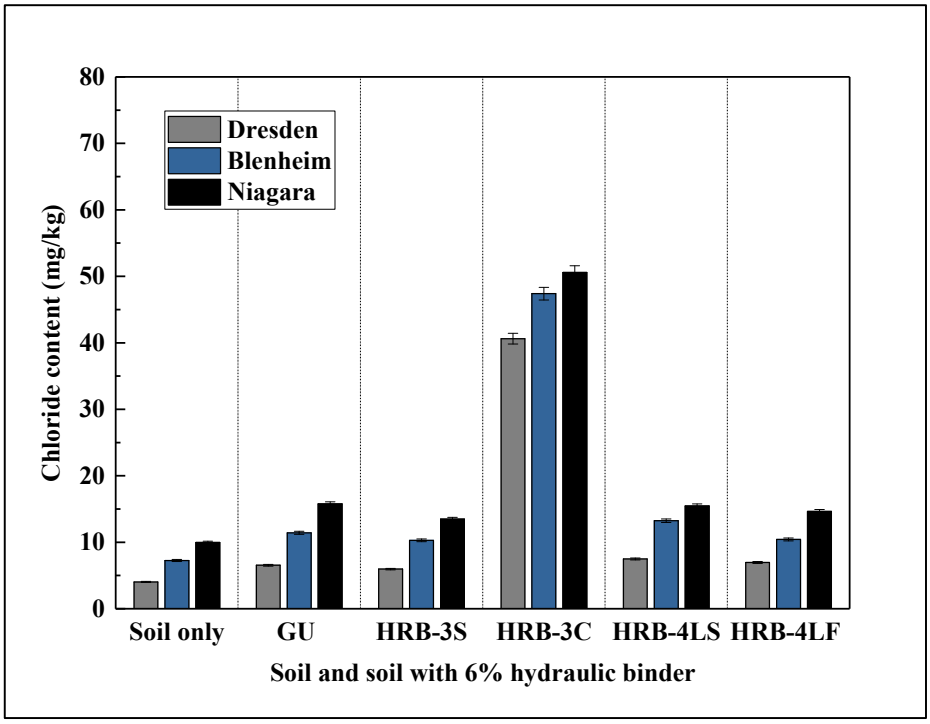

Figure 5-11 Soluble chloride content in soils and stabilized soils with 6% of hydraulic binder

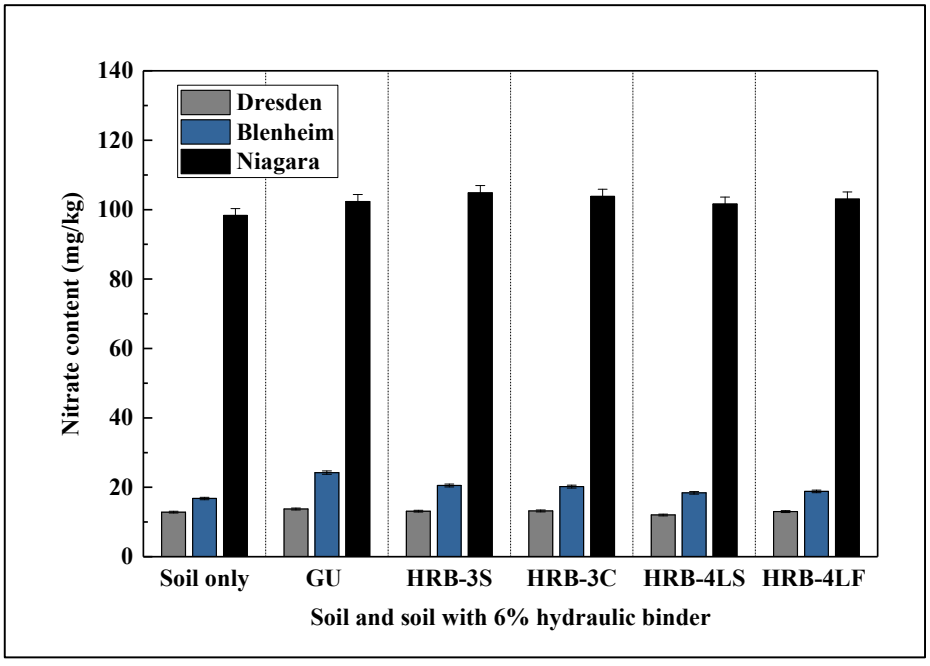

Figure 5-12 Soluble nitrate content in soils and stabilized soils with 6% of hydraulic binder

The concentration of soluble sulfate (SO_4^{2-}) could cause formation of ettringite ($Ca_6Al_2(SO_4)_3(OH)_{12}\cdot 26H_2O$) and thaumasite ($Ca_3(SO_4)(CO_3)[Si(OH)_6]\cdot 12H_2O$). The above chemical compounds can attract large amounts of water leading to volumetric swelling of clay (Saussaye *et al.,* 2013). A sulfate concentration of soils under 3000 mg/kg is generally indicated to have a low risk of sulfate induced swelling for calcium-based stabilizers (Petry and Little, 2012). According to current knowledge, the major concern is the secondary ettringite formation and swelling which occurs after the cement matrix has been formed (Little and Nair, 2009). Although in cement mortars, ettringite is generated rapidly during initial cement hydration. Nevertheless, in cement stabilized soils, the agglomerated soil particles have reduced surface area which may lead to delayed ettringite hydration after one or two days of cement hydration. Therefore, cases of sulfate-induced heave had also been reported when soils were treated with Portland cement (Rollings *et al.,* 1999).

Figure 5-9 shows that all the Dresden, Blenheim, and Niagara soils have relatively lower concentrations of soluble sulfate (7.5 mg/kg, 45.8 mg/kg, and 69.8 mg/kg, respectively). Cement and HRB increased the sulfate content in stabilized soils. By adding 6% GU cement, the sulfate content had been significantly increased to a range of 1494.1 mg/kg and 1701.2 mg/kg. On the other hand, HRB-treated soils had considerably lower sulfate concentrations. For example, the HRB-3S samples yielded a sulfate concentration between 753.1 mg/kg and 965.7 mg/kg. A reduction of total sulfate content in the treated soil and the delay of hardening could lower the risk of sulfate-induced problems. Such advantage of HRB may be more beneficial for soils containing high sulfate content. As it is shown in Figure 5-10, to mitigate the risk of sulfate attack, GU cement should be controlled to be lower than 12% for Dresden, 11% for Blenheim, and 10% for Niagara. Meanwhile, HRBs could be added in a higher content range by up to around 16% to 25% by weight of soil. The results of sulfate concentration indicated that with the same binder content, HRB improved subgrade soils have lower sulfate concentrations than cement treated ones.

On the other hand, Xing *et al.* (2009) indicated that an increase of chloride concentration may reduce the generation of calcium silicate hydrate (C-S-H) and delay the development of calcium aluminate hydrate (C-A-H). Such hydration products are crucial for strength development for cementitious materials. Besides, excessive chloride in stabilized soil was also indicated to slightly increase the potential of volumetric swelling (Saussaye *et al.,* 2013).

According to results from Figure 5-11, the chloride concentrations of the unstabilized soils are under 10 mg/kg. Most stabilizers affect slightly on the soil's chloride content, whereas HRB-3C which contained CKD increased chloride concentration to a range of 40 to 50 mg/kg with an addition of 6% CKD. However, chloride concentrations were still significantly lower than the values presented in literature (7000 mg/kg and higher) which would lead to swelling and inhibition of long-term strength development (Xing *et al.,* 2009; Saussaye *et al.,* 2013).

The discussions of effect of nitrate concentration in soil stabilizations are limited. Nevertheless, nitrogen (N) was indicated to be one of the major elements which form the soil organic matter (Terzaghi *et al.,* 1996). Nitrate is the most common ion of nitrogen which exists in organic soils. As it is shown in Figure 5-12, Niagara soil, with the most organic content, contains a higher nitrate concentration (98.3 mg/kg) compared to Dresden (12.8 mg/kg) and Bleinheim (16.7 mg/kg). Meanwhile, GU cement and HRBs contains small concentrations of nitrates and did not change the overall concentrations in soils.

5.3 Unconfined Compressive Strength

The test procedure followed the standard, ASTM D1633, *"Standard Test Methods for Compressive Strength of Molded Soil-Cement Cylinders"*. The specimens were compacted based on their optimum moisture content and their maximum dry density obtained from standard proctor tests. Cylindrical testing specimens for UCS testing were prepared to have approximately the same diameter and height (diameter = 100 mm and height = 116 mm). Prior to the UCS test, stabilized soil specimens were moved out of a humidity chamber and were submerged in water for a soaking period of 4 hours. The test used a MTS C64 system for the loading. During the test, the loading rate applied on the soil sample was set to be 0.05 in. (1.3 mm) per minute. The tolerance in strength on duplicate specimens was controlled within 5.0%.

When it is necessary, specimens were capped by gypsum at top and bottom to enable evenly load distribution. The Figure 5-13 shows the test set up and the specimen during testing. Figure 5-14 presents the conditions of UCS specimen after testing. The untreated Blenheim soil deformed significantly in the vertical direction before yielded to failure. The soil also had distinct lateral deformation. The deformation of weak soils due to loading created severe engineering disadvantages such as uneven settlement, creep, and rutting. The hydraulically treated soils, on the other hand, behave more rigid. The stress transferred within the whole

specimen, and the soil specimen did not have significant deformation in the vertical and horizontal direction. Such phenomenon is also distinct from Figure 5-15 which shows an example of stress-stain relationship during compression. The Blenheim soil without chemical treatment had prolonged deformation during the compression. When the specimen yields to failure, the strain accounted for approximately 11% to 12%. On the other hand, with 4% cement treatment, the stress in specimen increased sharply while testing and the specimen breaks quickly. Figures 5-16 to 5-21 summarize all the results of soaked UCS of three soils after 7 days and 28 days of curing, respectively.

Figure 5-13 UCS test set up (left), UCS specimen during testing (right)

Figure 5-14 Specimens after testing: untreated Blenheim (left), treated Blenheim (right)

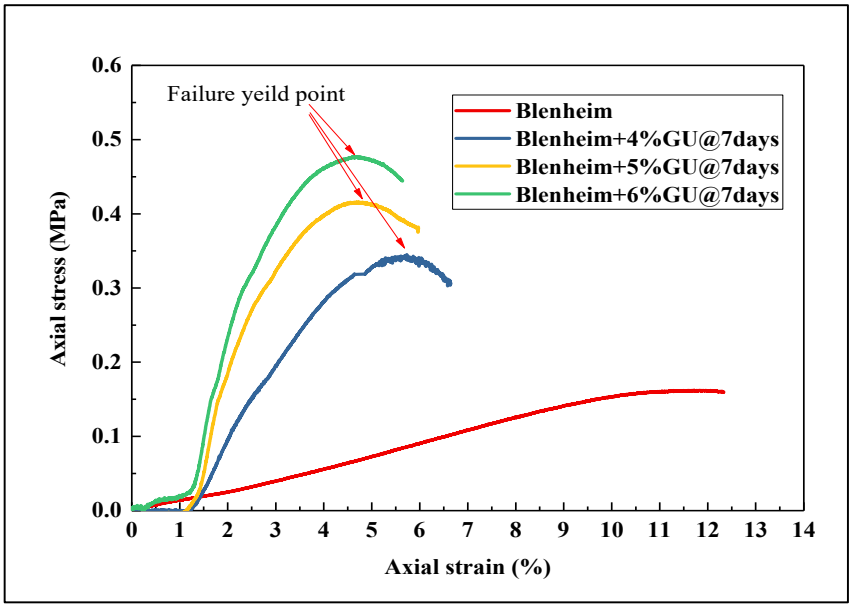

Figure 5-15 Horizontal strain versus applied pressure during UCS test

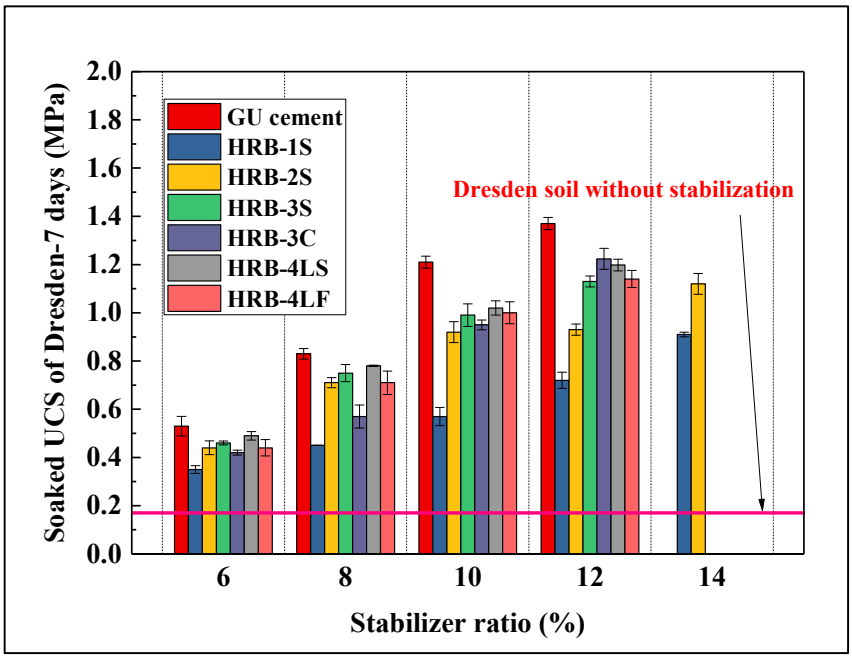

Figure 5-16 Soaked UCS of stabilized Dresden soil after 7 days curing

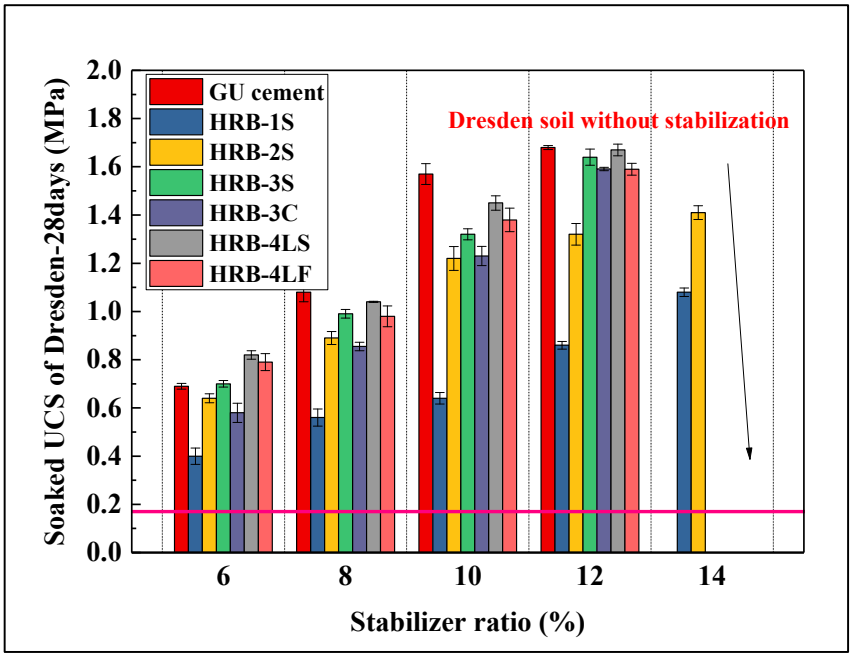

Figure 5-17 Soaked UCS of stabilized Dresden soil after 28 days curing

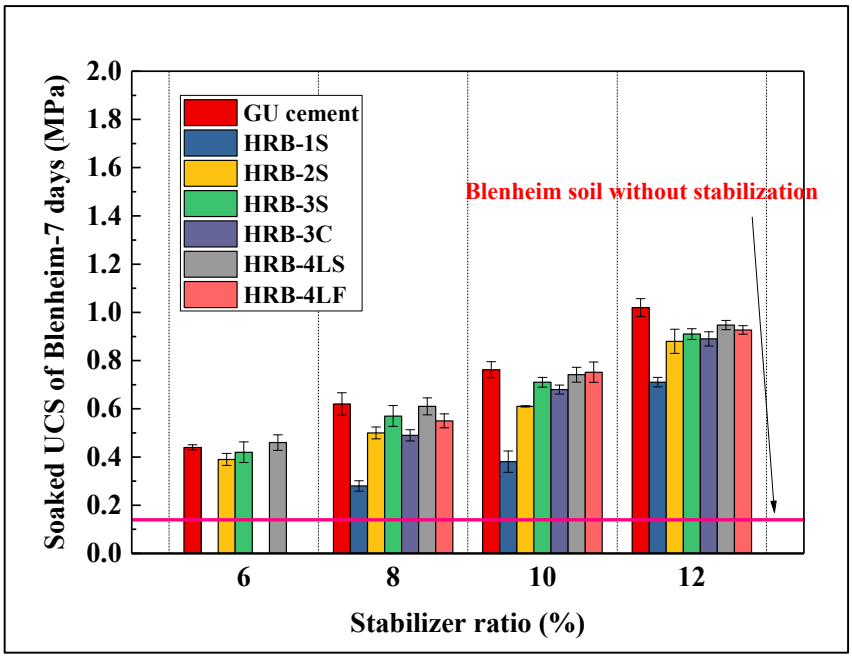

Figure 5-18 Soaked UCS of stabilized Blenheim soil after 7 days curing

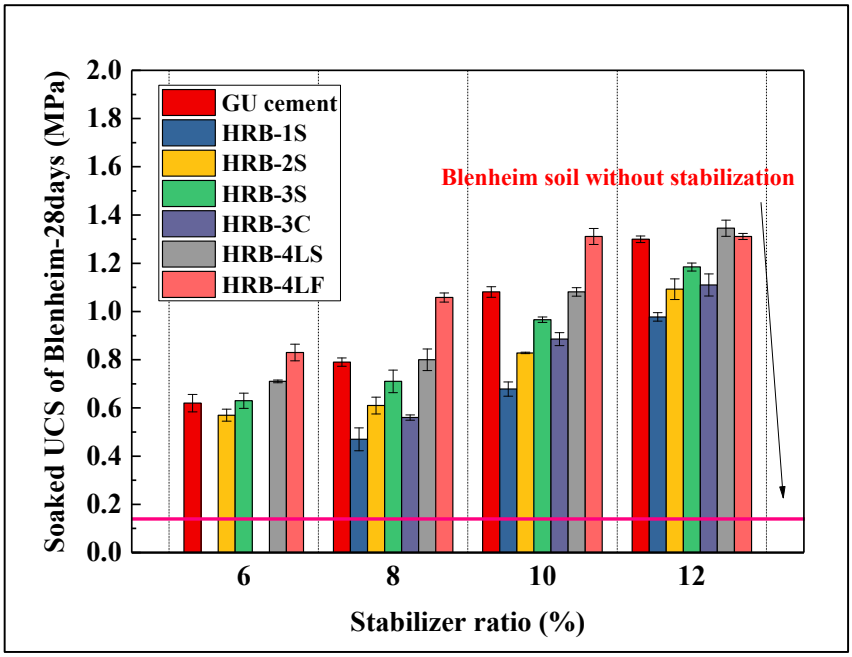

Figure 5-19 Soaked UCS of stabilized Blenheim soil after 28 days curing

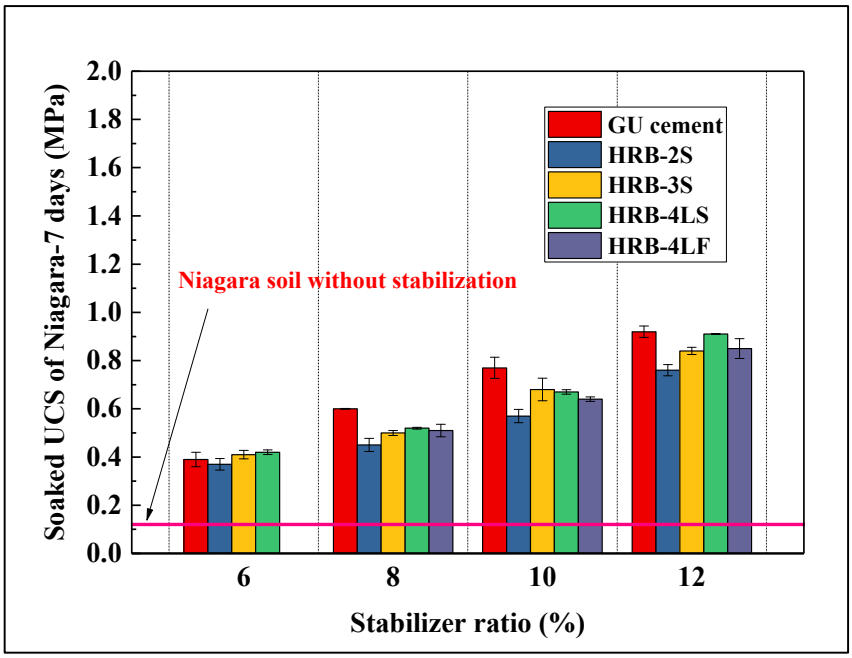

Figure 5-20 Soaked UCS of stabilized Niagara soil after 7 days curing

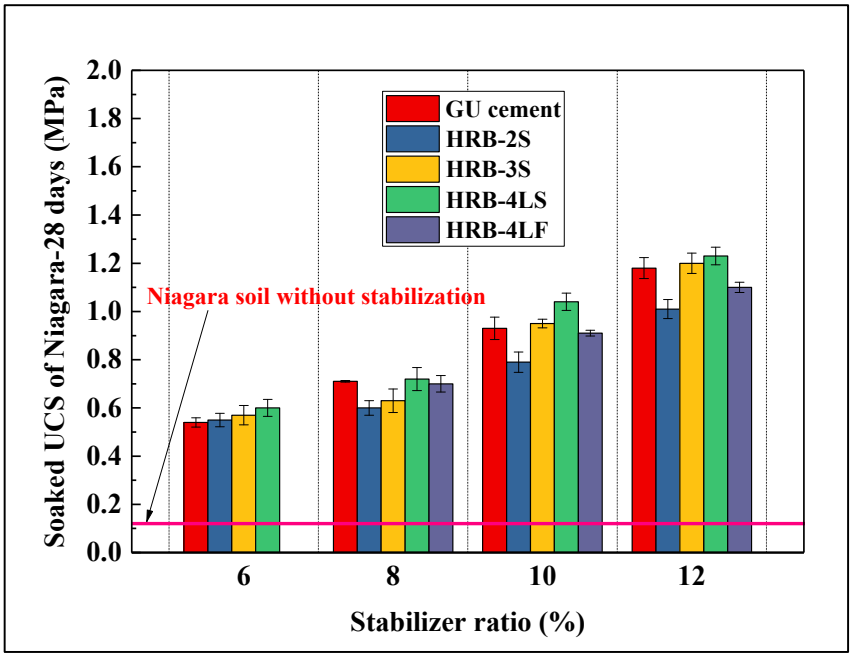

Figure 5-21 Soaked UCS of stabilized Niagara soil after 28 days curing

The unsoaked UCS values for remolded Dresden, Blenheim, Niagara soils accounted for 0.17 MPa, 0.14 MPa, and 0.12 MPa respectively. Their strength were very low indicating a weak subgrade performance. Hydraulic binders significantly improved the strength of soils upon the time they were mixed in. For instance, soaked UCS value of improved Dresden soil sample which contained 6% GU cement by weight of soil was increased to 0.53 MPa at the age of 7 days, and to 0.71 MPa at the age of 28 days. The UCS value became higher with the increase of cement content from 8% to 12%.

HRBs made a considerable contribution to the soil's UCS values. The UCS values of HRB-treated soils increased considerably with curing, they approached or even exceeded the values of cement stabilized soils at 28 days. Various HRB types lead to different levels of the soil's strength. Figure 5-22 summarizes the mean UCS values of the three soils under different treatment at the same curing age. Generally, GU, HRB-3S, HRB-3C, HRB-4LS, and HRB-4LF had similar effects for soil stabilization. For instance, at the same binder content, HRB-3S stabilized soils made up an average UCS value of 95% to 109% compared to cement stabilized ones. In contrast, HRB-1S which had lower clinker content than other HRB types had a limited improvement effect for soils. The average UCS values of HRB-1S stabilized soils accounted for 53% to 67% of GU-treated soils at the same binder content. Consequently, the low strength

graded HRBs could not be efficient compared to GU cement for local subgrade soil treatment.

Since some HRB type had similar effects on improving soil's strength. A cost-effective and environmentally friendly solution could be achieved when using HRB as an alternative to cement. The selection of the HRB type for mix design and construction also depended significantly on the availability of the materials and the manufacturing cost. For instance, the production of fly ash is not significant in east Canada. Consequently, the requirement of material manufacturing and transport will be high for HRBs containing fly ash.

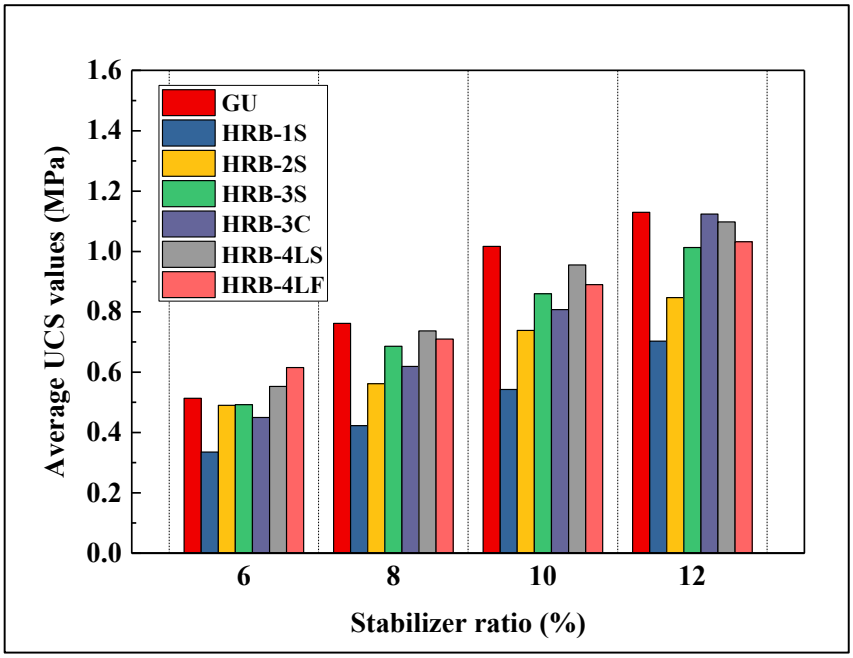

Figure 5-22 Average UCS values (7-days and 28-days) of the three soils with increase of binder content

Soil type played a significant role on the stabilization effect. Stabilized Blenheim soils which contain more clay-sized particles had mean UCS values making up approximately 81% of those of Dresden soils. Furthermore, Niagara soils containing high organic contents had even lower strength. It was indicated from the results that, fine-grained soils with high organic content have weak particle bonding and higher water attraction. The inhibition of hydration process and long-term strength development were distinct in Blenheim and Niagara soils; nevertheless, compared to untreated soils, the UCS were still significantly improved by cement and HRB stabilization. Among the stabilizers, HRB-3S and HRB-4LS again provided similar stabilization effects as the cement stabilized Blenheim and Niagara with the added benefit of

reduced cement clinker content. Meanwhile, values of HRB-2S, HRB-3C, and HRB-4LF treated Niagara soils were slightly lower.

It should be noted that according to Table 2-3, a soil-cement should have 1.38 MPa of UCS for 7 days specimen, and 1.72 MPa of UCS for 28 days specimen. Based on the results, all the three types of subgrade soils could not be improved to such a strength level by up to 12% of hydraulic binders. Therefore, in a highway construction, it could be more economic to treat such subgrade soils as an additional layer between pavement structure and weak natural subgrade soil.

In a low-volume road construction, however, the strength requirement of road base layer could be reduced according to road purpose and traffic condition. Recently in a field project, an adding of 6% cement by weight of dry soil was adopted to improve the subgrade made of Dresden. Based on lab testing and one-year field observations, the stiffness and strength of subgrade soil were significantly improved and maintained (Wang *et al.,* 2018). Detailed information can be seen in Chapter 6. In addition, as it is shown in Figure 5-17, 6% of HRB-3S, HRB4LS, and HRB-4LF stabilized Dresden could have higher strength compared the 6% cement treated soils after 28 days. However, the actual cement clinker content in the HRB-soil mixture ranges between 3.8% and 5.2%, and are lower than 6%.

5.4 Analysis of Soaked UCS Strength

As it was presented in last section 5.3, the UCS values of subgrade soil and stabilized subgrade soils are highly impacted by soil's type, stabilizer type, and stabilizer content. Moreover, UCS modelling may be of great importance to investigate the role of each factor on the strength development, strength development properties. Based on such understanding, a variety of modeling have been addressed for prediction of soil's strength. One of the empirical models which has been mentioned in several literature is expressed below:

Equation 5-5

$$q_u = \frac{A}{(w/c)^B}$$

Where, q_u = soaked UCS value (MPa) at a given curing age;

w = moisture content of soil (%);

c = cement content (%) by weight of soil;

A, B = regression coefficients.

In particular, literature indicated that the variation of A is significant while parameter B is approximately constant for the same type of soil (Horpibulsuk *et al.,* 2006; Cong *et al.,* 2014). Figures 5-23 to 5-28 below illustrate the relationships between stabilized soil's UCS and their moisture content/binder ratio (***w/HRB***). Furthermore, Table 5-8 presents the regression results subtracted from Figures 5-23 to 5-28, using the Eq. 5-5.

Results from Table 5 shows that with the change of moisture and stabilizer content, the relationship between soil's soaked UCS and moisture content/binder ratio (*w/HRB*) followed the power-formed relationship. Such phenomenon matched the hypothesis from the literature, showing that the Model Eq. 5-5 can also been used in for the modeling of HRB-treated soils.

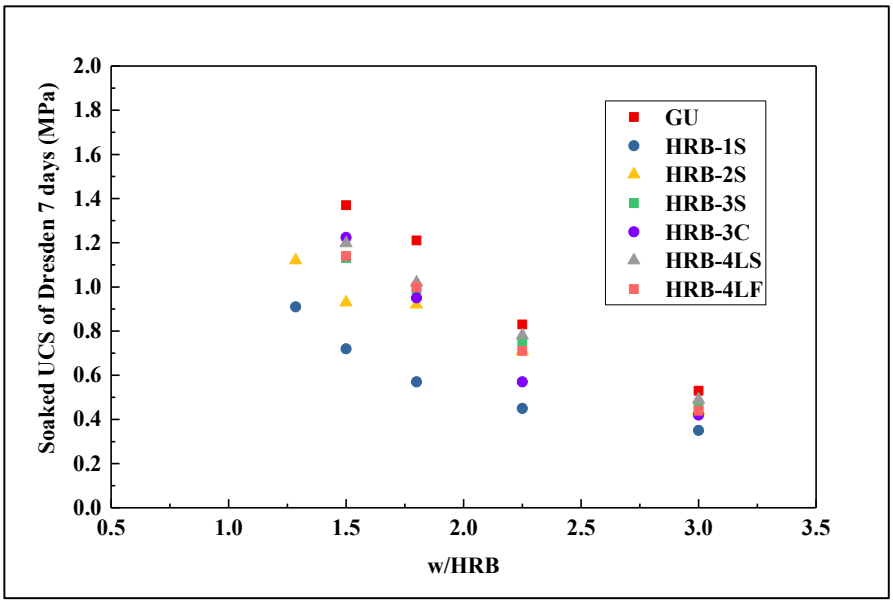

Figure 5-23 Soaked UCS vs. *w/HRB* -Dresden at 7 days

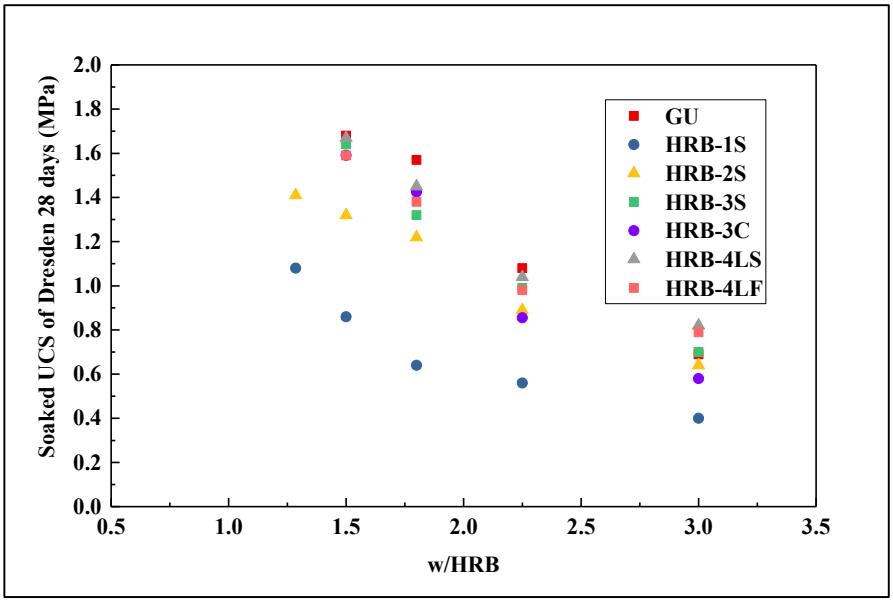

Figure 5-24 Soaked UCS vs. *w/HRB* -Dresden at 28 days

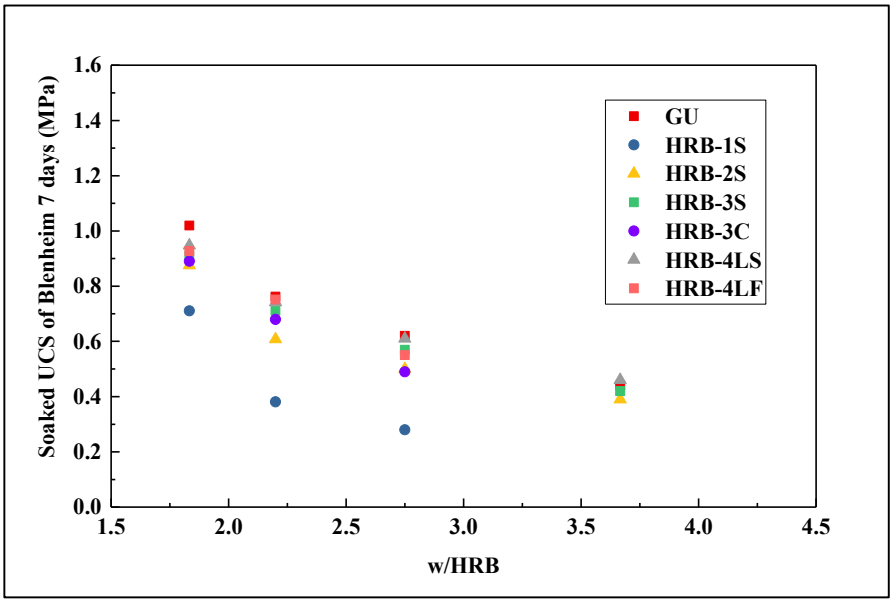

Figure 5-25 Soaked UCS vs. *w/HRB* -Blenheim at 7 days

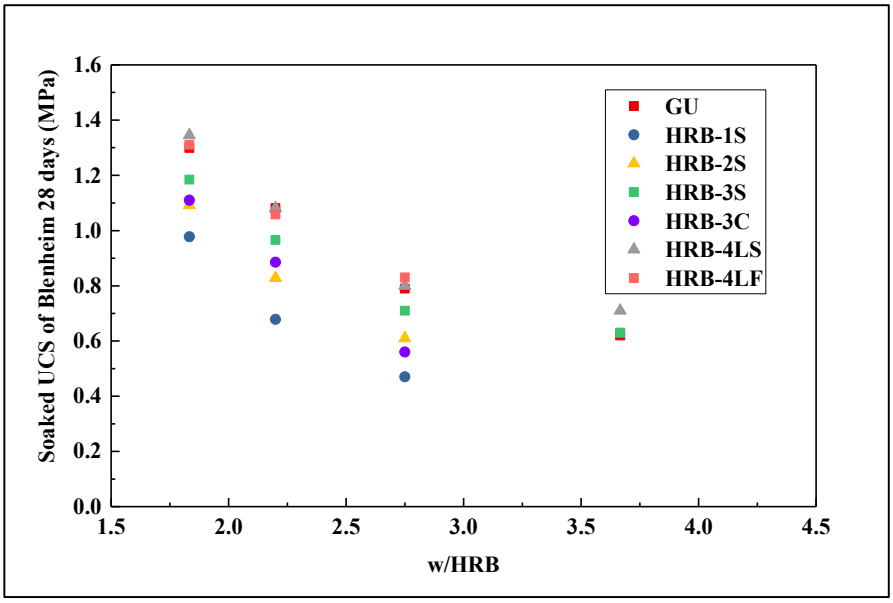

Figure 5-26 Soaked UCS vs. *w/HRB* -Blenheim at 28 days

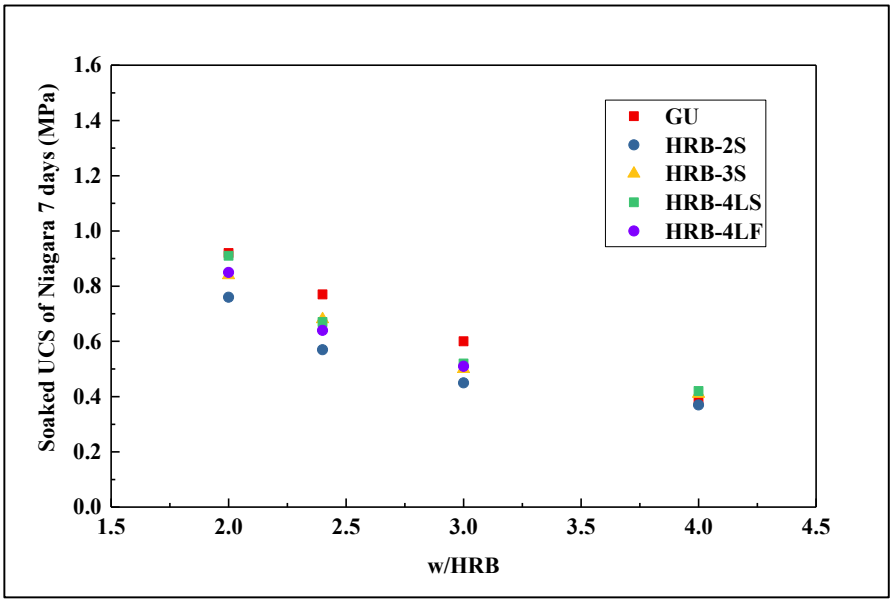

Figure 5-27 Soaked UCS vs. *w/HRB* -Niagara at 7 days

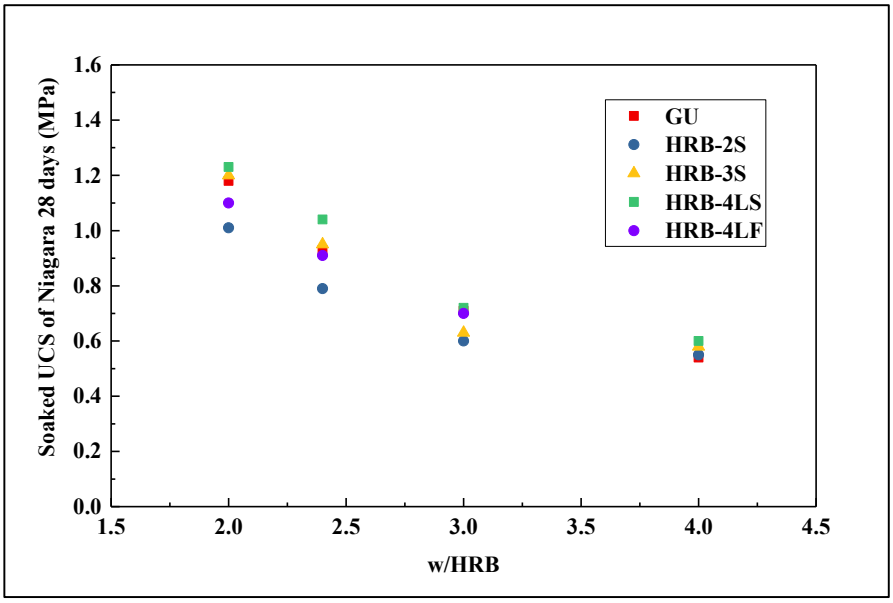

Figure 5-28 Soaked UCS vs. *w/HRB* -Niagara at 28 days

Although the model presents a very well correlation. However, one can also observe a large variability of coefficient *A*. Meanwhile, the *B* values are almost consistent for cement and HRB-treated soils for each type of soil. Therefore, the variability of *A* is influenced by stabilizer content and strength, whereas *B* is a result from soil's type. Regression model was then proposed but replaced *A* and *B* with coefficients which affecting the stabilization. The detailed process in order to derive the correlation includes several steps: first, conducted trial linear or unlinear regression models between significant factors and UCS to find the appropriate format for the characteristic. Second, added the terms including important characteristics into the model and investigate the best function. Third, randomly picked 70% of data for model training in order to come up with coefficient values. Forth, tested the model with the rest 30% data for validation.

Table 5-8 Regression results for UCS modeling using Eq. 5-5

Soil type	Curing days	HRB types	*A*	*B*	R^2
Dresden	7 days	GU	2.585	1.260	0.982
		HRB-1S	1.148	1.246	0.988
		HRB-2S	1.520	1.245	0.934
		HRB-3S	2.044	1.218	0.975
		HRB-3C	2.322	1.179	0.977
		HRB-4LS	2.120	1.205	0.984
		HRB-4LF	2.146	1.235	0.980
	28 days	GU	3.141	1.236	0.965
		HRB-1S	1.369	1.210	0.980
		HRB-2S	1.932	1.210	0.956
		HRB-3S	2.710	1.226	0.999
		HRB-3C	3.161	1.235	0.971
		HRB-4LS	2.602	1.196	0.984
		HRB-4LF	2.454	1.187	0.978
Blenheim	7 days	GU	2.022	1.249	0.992
		HRB-1S	2.600	1.186	0.938
		HRB-2S	1.596	1.169	0.955
		HRB-3S	1.734	1.208	0.996
		HRB-3C	2.171	1.180	0.999
		HRB-4LS	1.714	1.222	0.993
		HRB-4LF	2.047	1.217	0.997
	28 days	GU	2.509	1.272	0.989
		HRB-1S	2.872	1.190	0.997
		HRB-2S	2.592	1.186	0.999
		HRB-3S	2.014	1.214	0.946
		HRB-3C	3.207	1.180	0.982
		HRB-4LS	2.282	1.230	0.944
		HRB-4LF	2.585	1.213	0.999
Niagara	7 days	GU	2.239	1.115	0.990
		HRB-2S	1.457	1.112	0.965
		HRB-3S	1.703	1.052	0.979
		HRB-4LS	1.836	1.068	0.967
		HRB-4LF	1.983	1.084	0.985
	28 days	GU	2.524	1.125	0.995
		HRB-2S	1.756	1.072	0.917
		HRB-3S	2.441	1.067	0.909

Table 5-8 Continued

Niagara	28 days	HRB-4LS	2.584	1.047	0.996
		HRB-4LF	2.398	1.056	0.999

Based on the analysis, the most significant factors which affect soil's UCS values were: the compressive strength of stabilizer, curing age, pH value, soil's organic matter content, and soil's Atterberg limits. The relationships between soaked UCS values and the parameters are presented in the Figures 5-29 to 5-31. Positive relationships are found between soaked UCS and binder strength, curing time, and pH values. On the other hand, negative relationships are revealed between soaked UCS and soil's plasticity, organic matters.

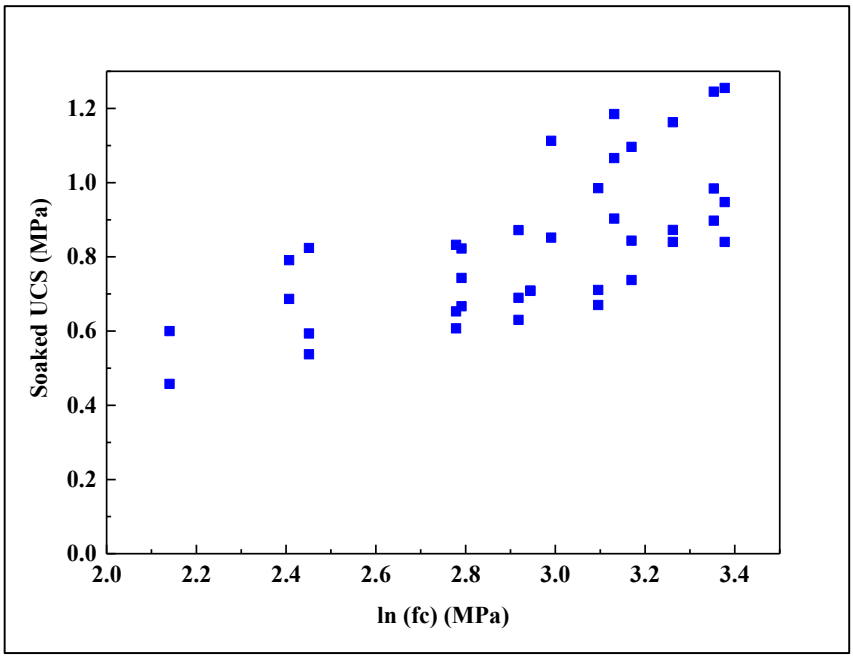

Figure 5-29 Relationships between soaked UCS and the binder's compressive strength f_c (MPa)

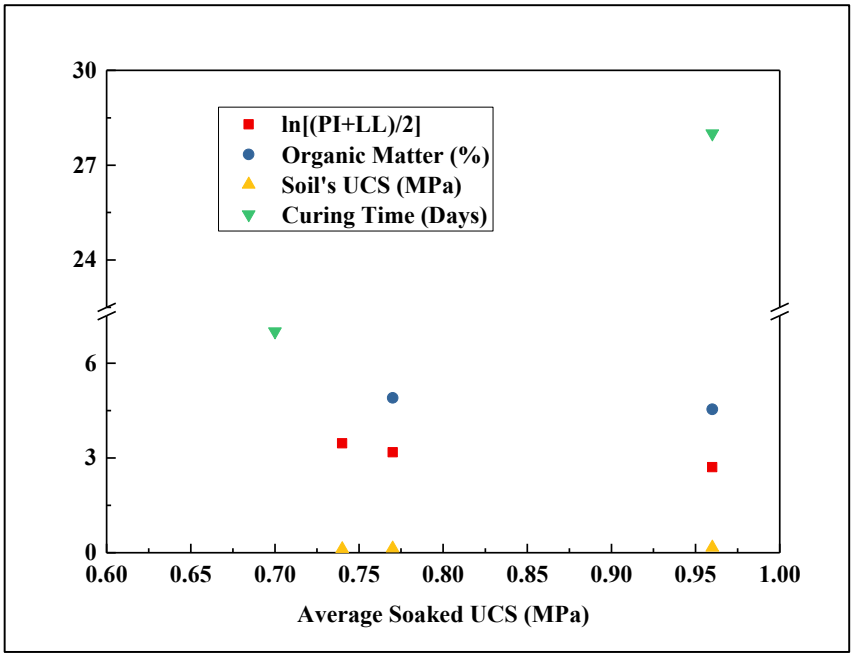

Figure 5-30 Relationships between soaked UCS and some other factors

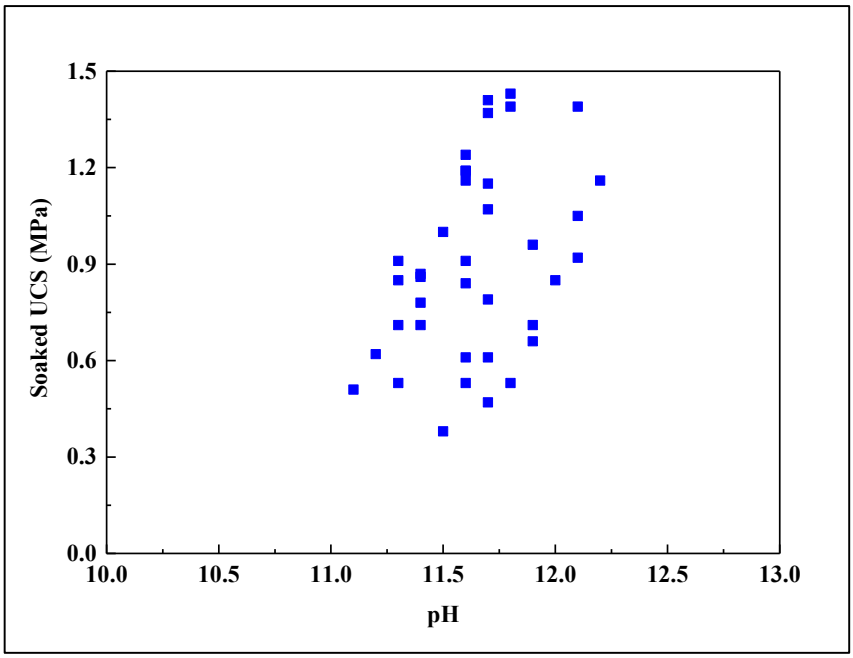

Figure 5-31 Relationships between soaked UCS and pH

Lastly, proposed strength models for soaked UCS was expressed as follows in Eq. 5-6. The proposed model had the least P-values for each term with the highest coefficient of determination (R^2) values compared to other proposed models.

Equation 5-6

$$q_u = \frac{K_s\,[(ln\,f_c)] + K_{cure}\,ln(curing\ age)}{(w/HRB)^{K_{pH}(-pH)+K_{OC}(OC)+K_{AL}ln[(PI+LL)/2]}}$$

Where, f_c (MPa) = compressive strength of HRB at a giving curing age;

pH = pH value in HRB stabilized soil;

OC = soil's organic content (%);

PI and LL = plasticity index and liquid limit of treated soil, respectively.

For instance, if the q_u indicated the 7 days UCS of HRB-1S, then f_c should equal to the compressive strength of HRB-1S at 7 days. Afterwards, 70% of experimental data was randomly chosen for regression analysis. Results are presented in Table 5-9. It is indicated that the overall prediction of the model is well. Among all the considered factors, the content of binder, its strength, curing ages, and pH values were the most important factors which will affect the soil's strength.

Table 5-9 Regression results for Eq. 5-6

	K_s	K_{cure}	K_{pH}	K_{OC}	K_{AL}
Results of coefficients	2.502	0.404	0.079	-1.671	-0.634
P-value	0.000	0.000	0.000	0.271	0.387
Adjusted R^2	0.82				

Since there were only three types of soils used in the research, it was difficult to include all the soil's geotechnical information into the complete model. Therefore, the author deleted several variables and simplified the model as follows:

Equation 5-7

$$q_u = \frac{K_s\,[(ln\,f_c)] + K_{cure}\,ln(curing\ age)}{(w/HRB)^{K_{pH}(pH)+K_{soil}(f_q)]}}$$

Where, f_q (MPa) equals to the remolded soil's UCS value without chemical treatment. Hence, the regression results changed to as follows:

Table 5-10 Regression results for Eq. 5-7

	K_s	K_{cure}	K_{soil}	K_{pH}
Results of coefficients	0.550	0.222	2.273	0.073
P-value	0.000	0.000	0.000	0.000
Adjusted R^2	0.94			

It is indicated that the overall prediction of Eq. 5-7 is better than Eq. 5-6. Then, the author used regressed coefficients to predict the rest 30% soaked UCS values and compared with the experimental values. A plot is drawn in Figure 5-32. As it can be seen from the figure, the predicted values of soaked UCS were similar to experimental values, with the scatter points adjacent to 1:1 line.

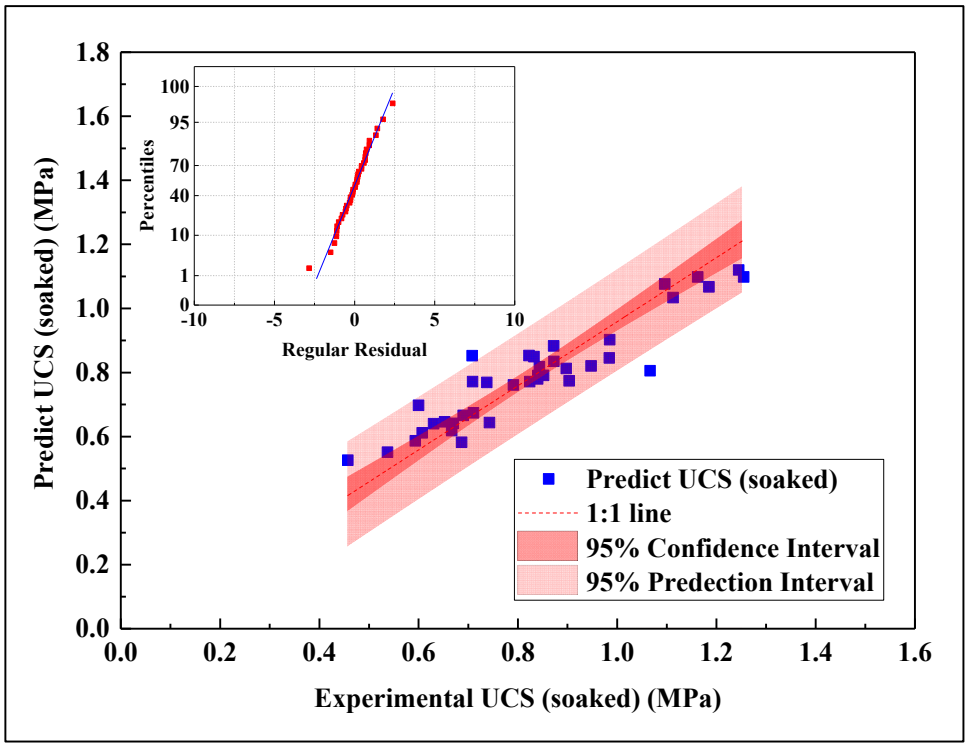

Figure 5-32 Test data vs. Predicted data

Furthermore, Figure 5-33 presents the standard residual of the predicted values from Figure 5-30 with their distribution. Overall, their residuals were falling within ±2 which is a general criterion. And the majority of standard residuals are within the range of ±1. Based on the previously results, the strength model Eq. 5-7 was valid to predict the soaked UCS values for cement and HRB improved weak soils.

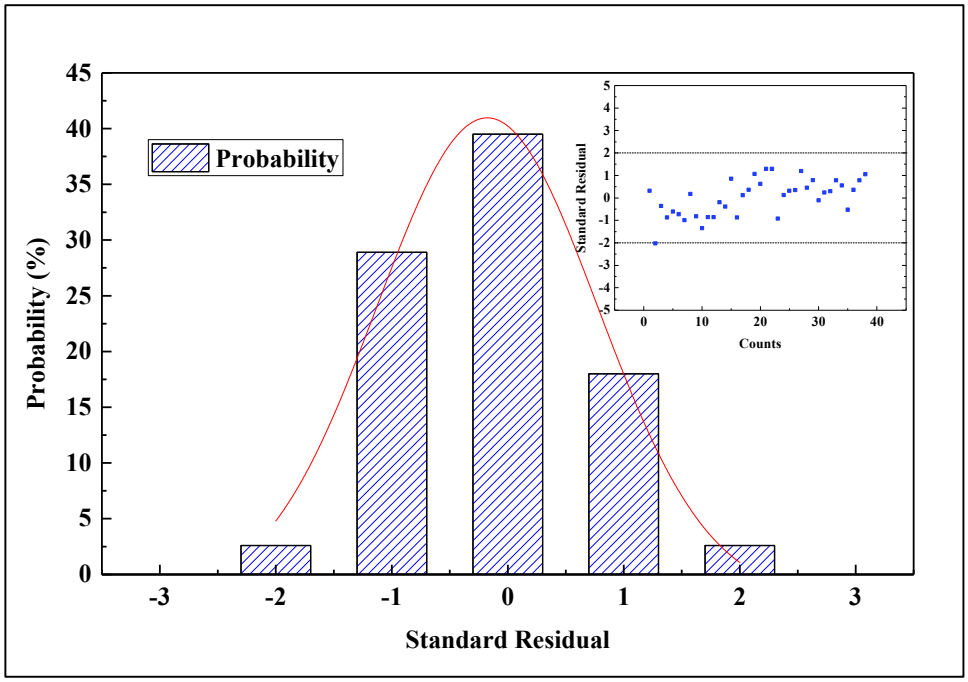

Figure 5-33 Standard residuals for UCS prediction

Overall, the summary of strength modeling for soaked UCS values can be drawn as follows:

1. There was a power-formed relationship between soil's soaked UCS and the specimen's moisture content/HRB content (*w/HRB*). Such relationship was validated in both GU and HRB improved subgrade soils.

2. Among all the considered factors, the content of binder, its strength, curing ages, and untreated soil's strength were the most important factors which affected the treatment. The soil's organic content, its plasticity index and liquid limit are other factors which could be further taken into account. A strength model was thus generated and validated to predict the experimental UCS data.

5.5 Durability

Durability tests for cement and HRB-treated soils included freezing and thawing cycles and wetting and drying cycles. The tests investigated the durability of specimens under the effects of repeated freeze-thaw and wet-dry cycles. Southern Ontario has the environment of seasonal freezing and high precipitations, making it crucial for the conducting thermal and moisture related durability testing. The durability tests used the same sized specimens as

those used in UCS tests. Additionally, both tests were conducted on specimens at the age of 7 days curing.

The freezing and thawing test follows the standard of ASTM D560, *"Standard Test Methods for Freezing and Thawing Compacted Soil-Cement Mixtures"*, whereas the wetting and drying test follows the standard of ASTM D560, *"Standard Test Methods for Wetting and Drying Compacted Soil-Cement Mixtures"*.

The freezing and thawing test started with 24 hours freezing in a fridge at a constant temperature of −24°C, followed by 24 hours of thawing in a humidity (100%) and temperature (20°C) controlled chamber, see Figure 5-34. After each cycle, the specimens were given 18 to 20 firm vertical brush strokes around the surrounding surface (see Figure 5-35). The test consists of 12 cycles, at the end of the last thawing, specimens were oven-dried (110°C) until constant mass. The final weight loss of soil specimen was then calculated as follows (ASTM D560):

Equation 5-8

$$\text{Dry loss of specimen, \%} = \frac{mass_{initial} - \frac{mass_{final}}{1+a}}{mass_{initial}} \times 100\%$$

Where, $mass_{final}$ = Final dry mass of specimen (g);

$mass_{initial}$ = Calculated initial dry mass of specimen (g);

a = Percentage of water retained in the soil by hydration (%).

a is calculated from a control specimen undertaking the same freezing and thawing cycles (or wetting and drying cycles) as other specimens, but without brushing strokes. ASTM indicated a value of 2% for hydration retention. In this study, the average a (%) value calculated ranged between 3.15% to 4.25%.

Figure 5-34 Testing of freezing and thawing cycles. Freezing in the fridge (left), and thawing in the humidity chamber (right)

On the other hand, wetting and drying cycles started with 5 hours soaking in fresh tap water, followed by 42 hours of oven drying at a temperature 71°C, see Figure 5-35. The brushing and final weight loss calculation followed the same procedure as that in freezing and thawing test.

Figure 5-35 Testing of wetting and drying cycles. Soaking (left), and drying in oven (right)

Figure 5-36 Brushing strokes at specimen's surface (left), specimens after brushing (right)

Figure 5-37 Blenheim after 12 freezing and thawing cycles

Figure 5-38 Dresden before cycles (left), specimens after 12 wetting and drying cycles

Table 5-11 Final weight loss percentage of specimens after durability test

Soil ID	Stabilizer	Weight loss of freezing and thawing (%)	Weight loss of wetting and drying (%)
Dresden	None	Sample collapsed at 1st cycle	Sample collapsed at 1st cycle
	4% GU	9.50	--
	5% GU	4.41	--
	6% GU	3.49	3.33
	10% HRB-1S	10.56	--
	12% HRB-1S	6.36	--
	6% HRB-2S	5.01	--
	8% HRB-2S	4.07	4.24
	10% HRB-2S	2.01	--
	6% HRB-3S	6.19	5.94
	8% HRB-3S	4.19	3.84
	6% HRB-4LS	4.14	3.86
	8% HRB-4LF	4.60	--
Blenheim	8% GU	9.89	6.52
	10% HRB-2S	12.77	10.04
	12% HRB-2S	10.84	7.94
	8% HRB-3S	11.54	--
	10% HRB-3S	8.98	6.24
	10% HRB-3C	9.56	8.00
	8% HRB-4LS	9.59	--
	10% HRB-4LS	6.95	6.02
	10% HRB-4LF	8.58	--
Niagara	6% GU	15.98	14.14
	8% GU	9.81	6.48
	10% HRB-2S	11.61	--
	10% HRB-3S	10.03	6.98
	10% HRB-3C	11.78	--
	10% HRB-4LS	9.39	5.94
	10% HRB-4LF	10.14	6.76

Note: "--" means the test was not conducted.

UCS results indicated that HRB-2S, HRB-3S, HRB-4LS, and HRB-4LF had good performance in improving the strength. Consequently, the test was conducted on specimens treated with GU and the mentioned HRB types. Figures 5-37 and 5-38 present the sample conditions of specimens during durability tests. Additionally, final weight loss after durability

tests are presented in Table 5-11. It should be noted that the table only presents the trials with durability loss less than 15%. Durability test results indicated that Blenheim and Niagara soils with stabilizer dosage less than 8% may either having significant weight loss during durability test (15%) or collapse during the test.

The untreated soil specimens could not go through either the first freeze-thaw or wet-dry cycle. On the other hand, all the chemically treated specimens listed previously were able to withstand the 12 durability cycles. During the brush stroke process, loose soil particles were peeled off from the specimen surface, and the size of the specimen had been reduced. Brushing of the specimens also left distinct marks on some specimens, as it is shown in Figure 5-36. The weak specimens had significant particle lose on the surface.

In general, freezing and thawing test lead to higher amount of weight loss than wetting and drying test. The reason may be due to the fact that in freezing and thawing test, the specimens were always in moist conditions. Freezing and thawing of pore moisture could also lead to change of void size. Consequently, freezing and thawing test presented the worse-case scenario. As a consequence, more freezing and thawing tests were conducted than wetting and drying tests.

Portland Cement Association (1992) recommended a weight loss requirement of less than 7% to 10% for fine-grained soils. As it is seen from the tables, Dresden soil required more than 6% of GU to achieve durability requirement. On the other hand, the requirement of HRBs highly depended on their types. Among them, 6% to 8% of HRB-3S and HRB-4LS were needed for the durability. Soil types played an important role on the weight loss values, the Niagara and Blenheim soils lose more soil particles during the testing.

Overall, the weight loss of HRBs were generally higher than GU at the same binder content. Two HRB types: HRB-4LS and HRB-4LF improved specimens were found to have similar durability property with cement treated ones at the same binder content. Therefore, it is proposed that in order to ensure the early age durability of hydraulically bound mixture, the binder content of HRB should be 1% to 2% higher than GU. It should also be noted that the test was performed on 7 days specimen. And it has been illustrated from previously chapters that the HRB-treated soils have a substantial increase of strength from 7 days to 28 days. Therefore, a better durability performance could also be expected for HRB-treated subgrade

soils under the condition of abundant curing.

5.6 Resilient Modulus

The resilient modulus (M_r) of subgrade is a critical parameter used in flexible pavement design. British Columbia, Alberta, Manitoba, Ontario, Québec, Nova Scotia, and Yukon use laboratory tested M_r or field-tested M_r for subgrade soil characterization (TAC 2014). It is also an important input for flexible pavement design.

The M_r represents the modulus of the soil mixture due to recoverable deformation. It simulates the cyclic traffic by applying very short loading period. After multiple loading, the subgrade soil will have plastic strain or permanent strain, in addition to recoverable strain or resilience strain (see Figure 5-39).

The M_r test follows the standard AASHTO T307, *"Standard Method of Test for Determining the Resilient Modulus of Soils and Aggregate Materials"*. Each cylindrical specimen was prepared to be approximately 100 mm in diameter and 200 mm in height. The height of M_r specimen is 1.73 times as the height of soaked UCS specimen but at the same cross-sectional area. In order to simulate the same compaction energy per unit volume (1 cm^3) as the one specified in the standard proctor compaction method; specimens were compacted by a standard proctor hammer in 6 layers with 25 blows for each. It was found that the dry density of "tall" specimens (height-to-diameter ratio =2) were all within 98% to 102% of that of "short" specimens (height-to-diameter ratio =1.16). Such compaction method had also been used in the past literatures (Solanki *et al.,* 2009; Tastan *et al.,* 2011).

During the test, each specimen was subjected to tri-axial loading, where σ_1 was the normal stress in vertical direction, and $\sigma_2 = \sigma_3$ was the confining stress. The value M_r was then calculated by dividing the axial deviator stress ($\sigma_d = \sigma_1 - \sigma_3$) by axial recoverable strain ε, see equation below.

Equation 5-9

$$M_r = \frac{\sigma_1 - \sigma_3}{\varepsilon} = \frac{\sigma_d}{\varepsilon}$$

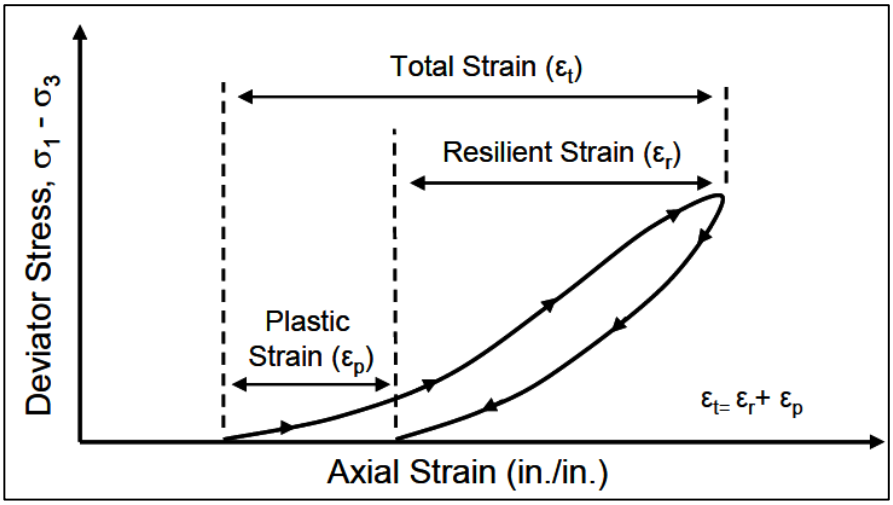

Figure 5-39 Principle of soil's resilient modulus (Buchanan, 2007)

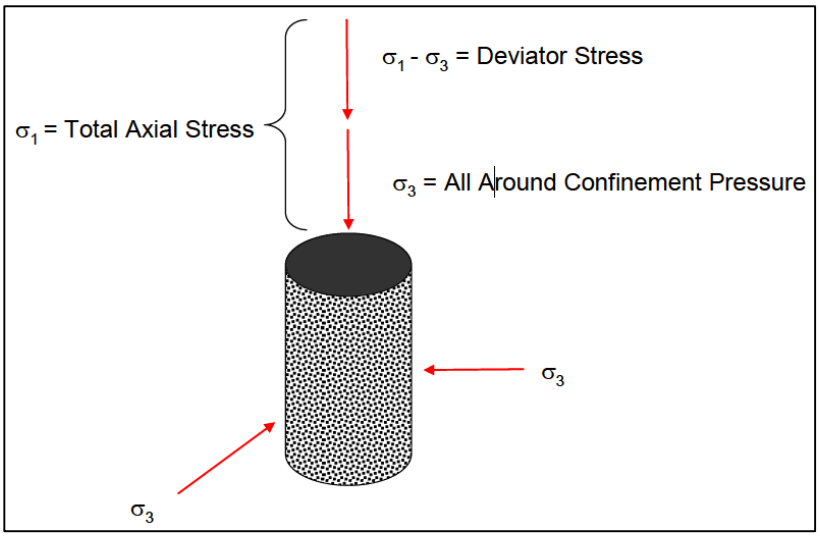

Figure 5-40 Resilient modulus stress configuration (Buchanan, 2007)

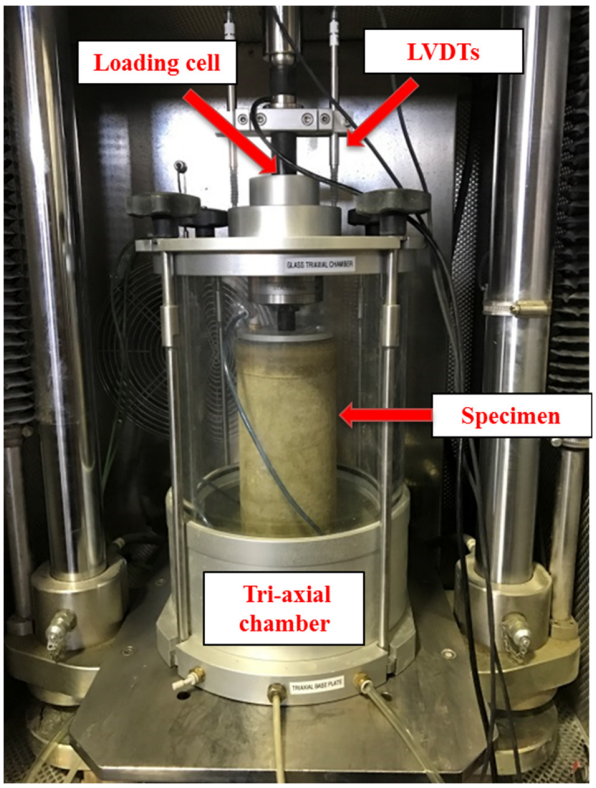

Figure 5-41 Chamber and equipment for resilient modulus

Loading of the specimen started with a conditioning period with 500 repetitions of a load equivalent to a maximum axial stress of 27.6 kPa and the mean cyclic stress of 24.8 kPa (AASHTO T307) (Solanki *et al.,* 2009). Afterwards, 15 sequences of loading each containing 100 cycles were applied on the specimens. Every cycle consisted of 0.1 second of loading and a 0.9 second of rest period. In addition, two linear variable differential transformers (LVDTs) were arranged on both sides of the specimen to measure the deformation due to cyclic loading (Figure 5-41). Every 5 sequences formed 1 step during which the confining pressure remained the same while the cyclic stress (or axial deviator stress) increased by each sequence from 12.4 kPa to 62.0 kPa.

Table 5-12 summarizes the set loading with the average M_r values at each step for the specimens.

Table 5-12 Set loading with average M_r value (MPa) at every step for each specimen

Step No.	Confining pressure, σ_3 (kPa)	Deviator stress, σ_d (kPa)	Remolded soil	7 days				28 days			
				8% GU	8% HRB-2S	8% HRB-3S	8% HRB-4LS	8% GU	8% HRB-2S	8% HRB-3S	8% HRB-4LS
				Dresden soil							
1	41.4	12.4~62.0	32.65	311.51	256.82	296.66	352.43	371.55	332.46	330.67	421.57
2	27.6	12.4~62.0	28.07	325.03	272.23	310.75	344.16	374.88	335.44	325.87	427.19
3	13.8	12.4~62.0	25.89	346.08	272.12	344.54	345.07	400.52	358.38	323.48	386.68
				Blenheim soil							
1	41.4	12.4~62.0	24.04	289.98	311.76	365.37	317.64	338.96	397.86	422.97	413.75
2	27.6	12.4~62.0	21.03	298.66	326.11	360.62	331.97	330.69	417.20	420.57	432.33
3	13.8	12.4~62.0	18.03	309.78	320.54	341.63	359.55	331.60	423.35	421.77	455.33
				Niagara soil							
1	41.4	12.4~62.0	19.47	216.29	201.07	240.14	276.12	273.91	269.51	291.63	277.06
2	27.6	12.4~62.0	16.23	228.31	212.33	250.99	259.46	272.11	275.52	288.85	265.04
3	13.8	12.4~62.0	15.73	235.28	222.33	264.82	285.52	282.24	280.36	288.38	277.93

Figures 5-42 and 5-43 summarize the average M_r values for 8% GU and HRB stabilized soils after 7 days and 28 days curing, with the variation. Unsoaked UCS for each specimen was also tested immediately after M_r test and presented in the same figure.

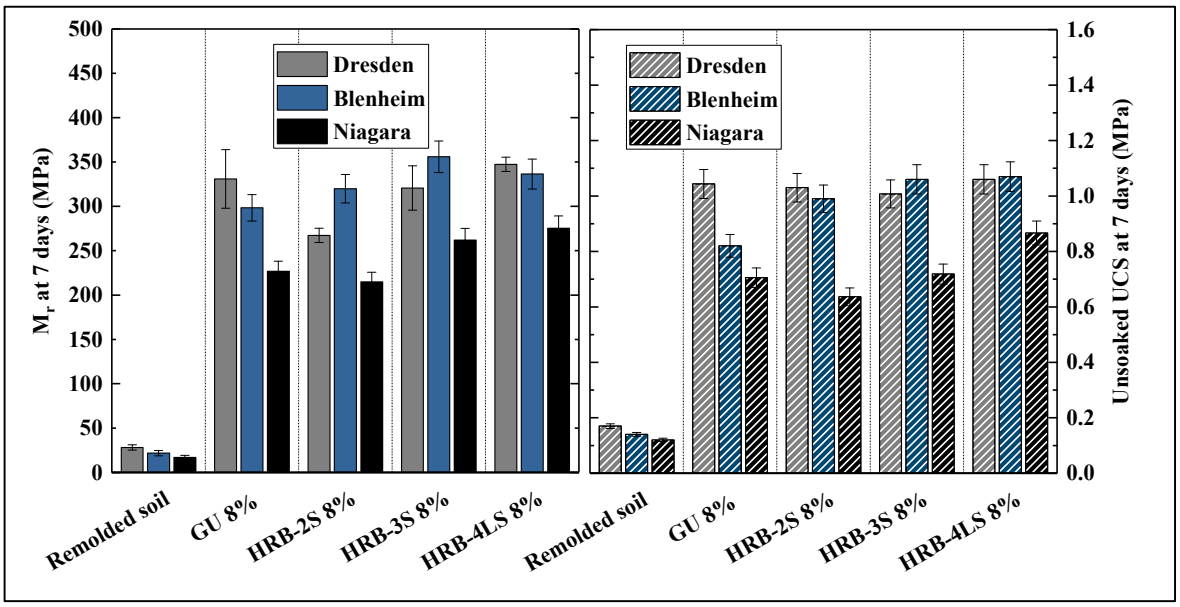

Figure 5-42 M_r with the corresponding UCS at 7 days

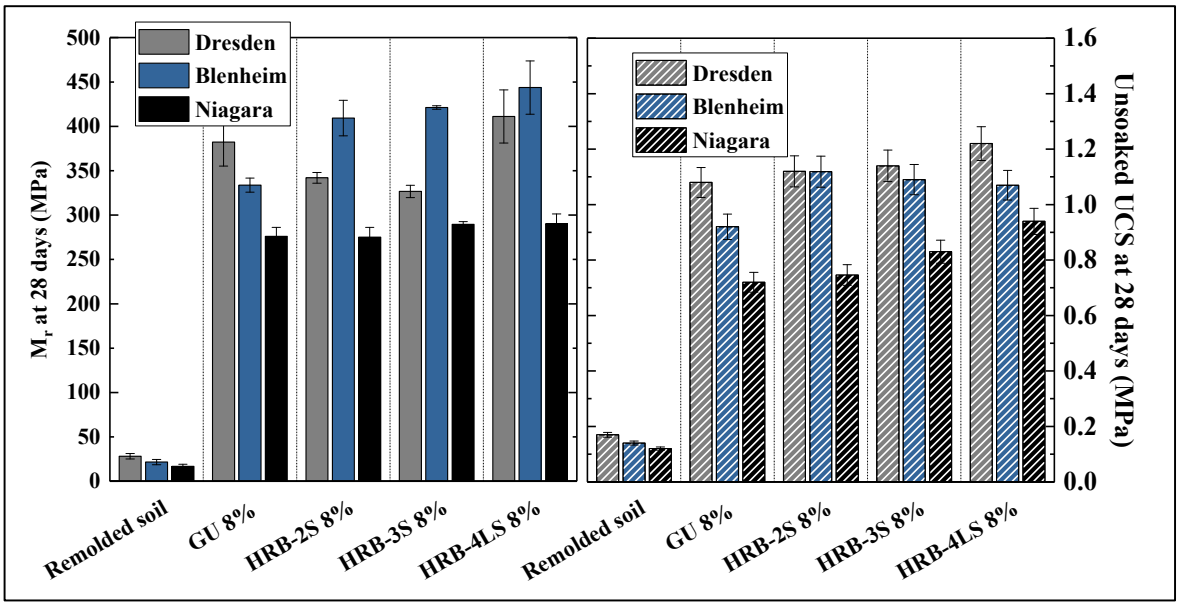

Figure 5-43 M_r with the corresponding UCS at 28 days

As it is presented from the figures, laboratory remolded Dresden, Blenheim, and Niagara soils had mean M_r values of 28.3 MPa, 21.7 MPa, and 16.8 MPa respectively. M_r values of 8% GU-treated soils had been increased by over 10 times compared to remolded soil, making up 330.8 MPa, 298.3 MPa, and 226.7 MPa respectively at the age of 7 days. HRB-2S stabilized soils showed slightly lower M_r values at early age, but HRB-3S and HRB-4LS with more cement clinker exhibited a comparative or higher effect compared to GU in soil's M_r values. Between them, 8% HRB-4LS stabilized Dresden and Blenheim had the higher M_r values, making up 347.3 MPa and 336.4 MPa at 7 days, as well as 411.1 MPa and 443.7 MPa at 28 days respectively.

It should be noted that Blenheim soil, with a substantial content of clay particles and moderate plasticity index value of 16, had a vast development of M_r with stabilization of HRBs, especially at the time of 28 days. Treated Blenheim even had resilient modulus than Dresden with HRB binders. The reason which caused this phenomenon needed to be further studied. However, it should also be noted that their soaked UCS values were significantly lower than Dresden, as it had been introduced before. This is because fine-grained soils are more sensitive to moisture change. Furthermore, Niagara soil with highest clay content and organic content had the lowest M_r values among the three types of soil. 8% Cement and HRB-treated Niagara had similar M_r values of 220 to 275 MPa at 7 days and 275 MPa to 300 MPa at 28 days. In overall, it can be seen from the figure that with the same binder content, GU and HRB-treated subgrade soils had the equivalent M_r values at the age of 7 days. However, at the age of 28 days, GU and HRB-4LS had better treatment of M_r compared to other types of HRBs.

The specimen's unsoaked UCS values were tested using the finished M_r specimens. It should be noted that there is a converting factor for UCS value between "short" (sample height to diameter ratio approximately 1.16) and "tall" (sample height to diameter ratio approximately 2) specimens. ASTM C1633 indicated the results of "tall" specimens should multiply by 1.1 to match the results of "short" specimens. In addition, the application of M_r testing would also increase the structural integrity of specimen, which may increase the strength. For such reasons, several GU-treated Dresden specimens were made in the shape of 200 mm in height and 100 mm of diameter respectively to calculate the converting factor. The calculated converting factor was 1.02 in average.

As it can be seen from Figure 5-44, the specimen's unsoaked UCS values after M_r testing were higher than those soaked values introduced previously. At the age of 7 days, hydraulic binder stabilized Dresden soil lost a mean of 31% of UCS when soaked, and Blenheim soil lost 46%, whereas Niagara soil lost 40%. After 28 days curing, stabilized soils specimens had improved resistance towards soaking, with the UCS reduction accounting for 20%, 30%, and 32% respectively. Figure 5-44 presents the relationships between soaked UCS values and unsoaked UCS values after M_r testing. As it is shown, the scatters are all below the "1:1 line". This means for each kind of soil; soaking period decreases the UCS values. However, a numerical relationship is not easy to observe from the scatters because the decrease ratio due to soaking varies significantly by soil type, stabilizer type and binder content.

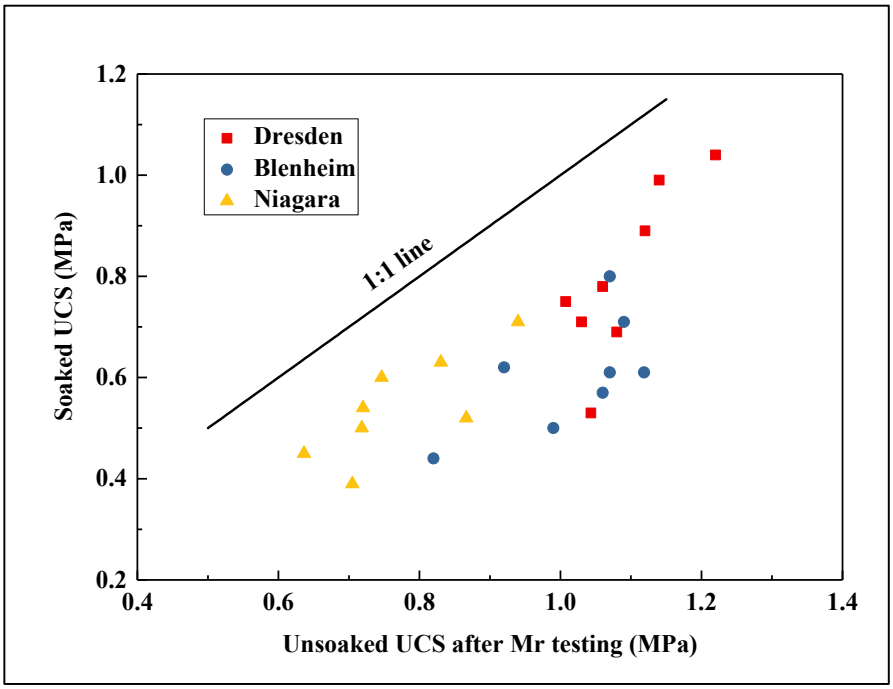

Figure 5-44 Relationships between soaked and unsoaked UCS

There is limited research addressing the possible correlations between soil's UCS values and M_r values, especially for stabilized soils. Figure 5-45 displays a plot representing the specimen's M_r with its corresponding unsoaked UCS, as well as, the corresponding soaked UCS value. It is observed that there is a well positive linear correlation between M_r value and unsoaked UCS value. The adjusted R^2 for the correlation accounted for 0.85. Such positive correlation may be due to the fact that both tests were performed on the same specimen that experienced the same compaction and preparation process. On the other hand, since the

soaking period considerably decreased the strength of soil, and different HRB stabilized soils had various deterioration rates due to soaking, a linear correlation between M_r value and soaked UCS value was not that accurate. However, one still observes a positive trend between soil's unsoaked M_r with soaked UCS.

Since the soaking procedure would significantly affect soil's strength, so it could be reasonably assumed that their resilient modulus will also be affected. However, the current standard AASHTO T307 for resilient modulus testing does not include soaking procedure. Therefore, it could be a possible research interest in the future to analyze the soaked M_r values of bound mixtures and find its correlations with their soaked UCS values which is a common mix-design factor of cement-treated pavement materials.

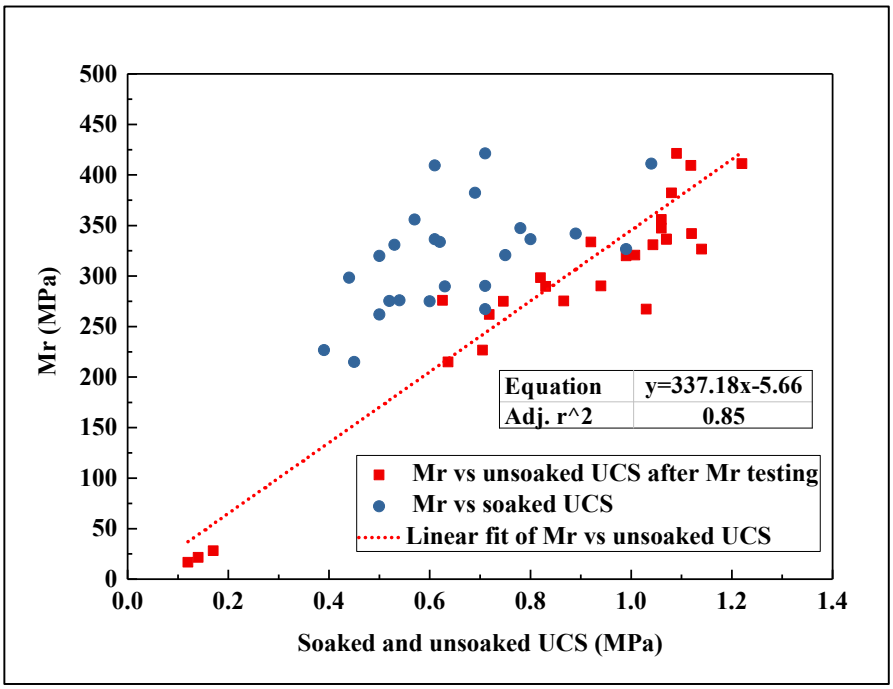

Figure 5-45 Relationships between UCS and M_r

5.7 Indirect Tensile Strength and Poisson's Ratio

The **Ind**irect **T**ensile Strength (**IDT**) test is frequently used in asphalt mixtures to detect the tensile strength due to bending conditions. IDT test is a quick and easy test. IDT tests are usually not performed on unbound materials for example gravels and untreated subgrade

soils. However, since the chemical treated subgrade soils are permanently bound and have the ability of load distribution. It also has the ability of undertaking pressure from pavement layers and distributing the loading to untreated subgrade. Therefore, when the stabilized layer undertakes the vertical load and is force to bend, tensile cracks will occur at the bottom of the layer and propagate upwards.

The study aimed to evaluate the IDT strength of HRB-treated soils at 28 days and 56 days of curing. The IDT test conducted in this research generally followed the procedure of ASTM D6931, *"Standard Test Method for Indirect Tensile (IDT) Strength of Asphalt Mixtures"*. The test used a cylindrical specimen with the diameter of approximately 150 mm, and the height of 85 mm. A gyratory compactor which located in CPATT lab was used for sample compaction and demolding. After compaction, specimens were cealed and stored in humidity chamber before testing. On the other hand, a modification of test procedure was made so that the loading ratio was controlled to be 1.3 mm per minute to avoid noisy results due to rapid loading. Such procedure was also recommended in the literature (Yeo, 2008; Melese *et al.,* 2019).

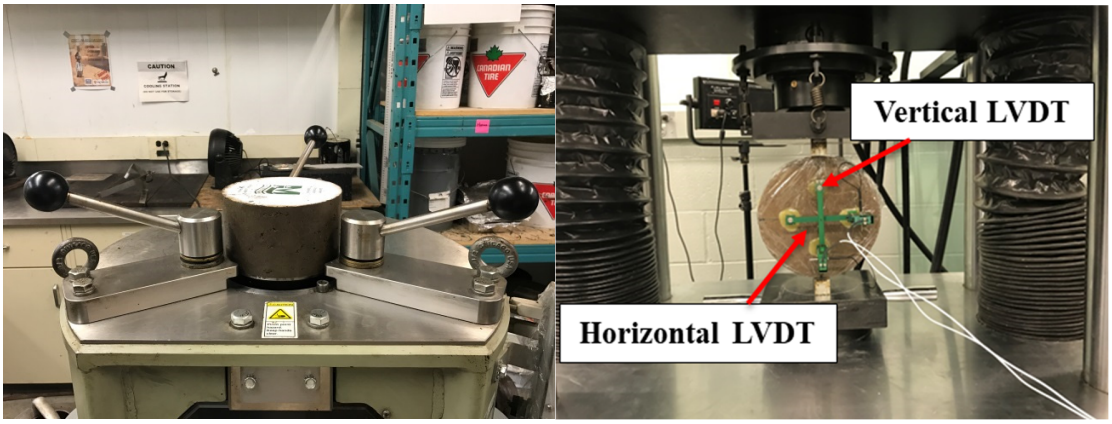

Figure 5-46 IDT sample compaction and demolding (left); test sample under loading (right)

During the test, the vertical loading was applied on the top of the specimen until the specimen yeild to failure. One horizontal and one verticle LVDT were used to record the deformation in each dirction. After the testing, the maximum load was calculated and transferred into tensile strength using the equation below.

Equation 5-10

$$\text{IDT (kPa)} = \frac{2000 \times P}{\pi \times h_{ave} \times d}$$

Where, P = maximum applied load (N);

h_{ave} = average height of the sample, here equals to 85 mm;

d = diameter of the cylinder, here is 150 mm.

Figure 5-47 draws the typical tensile cracking of IDT specimens after testing. The crack generated from the top and quickly propagated thorough the whole specimen. Such tensile crack was in a vertical direction. For this study, all the soil specimens followed such kind of failure type while yield to failure.

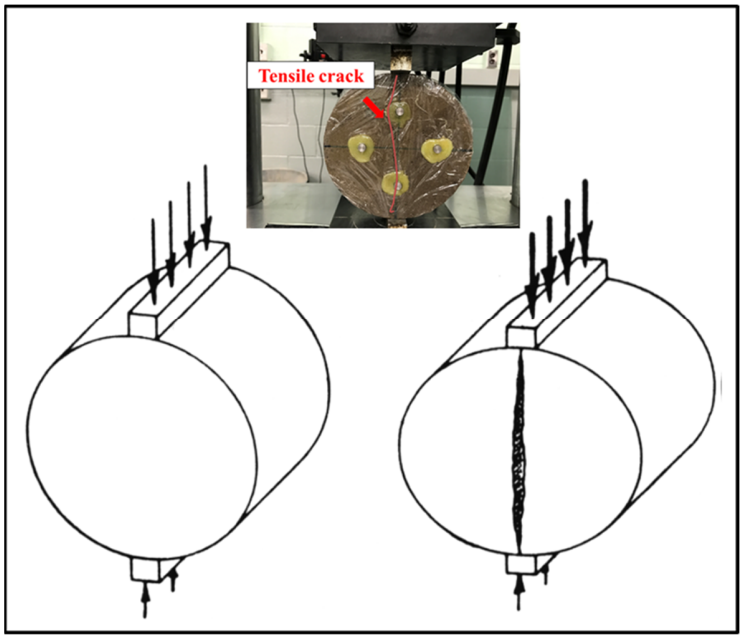

Figure 5-47 Failure type of IDT specimen, after Baaj (2002)

The results of IDT test for cement and HRB-treated soils are presented as follows in Figure 5-48 to 5-50:

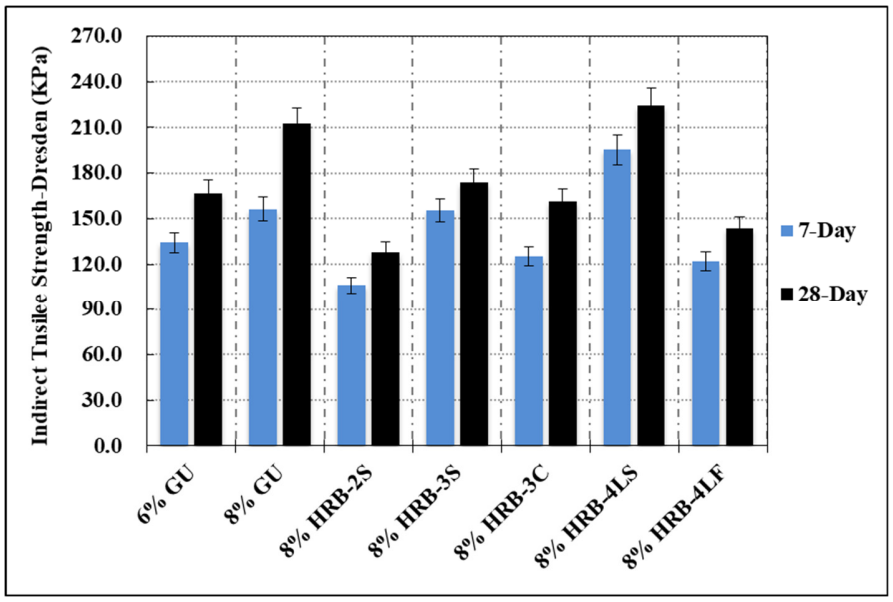

Figure 5-48 IDT strength of improved Dresden

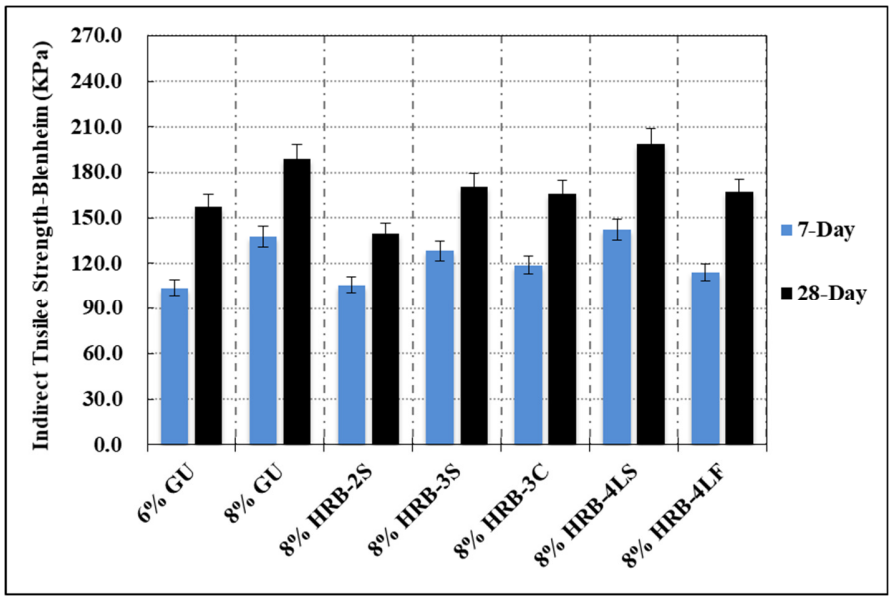

Figure 5-49 IDT strength of improved Blenheim

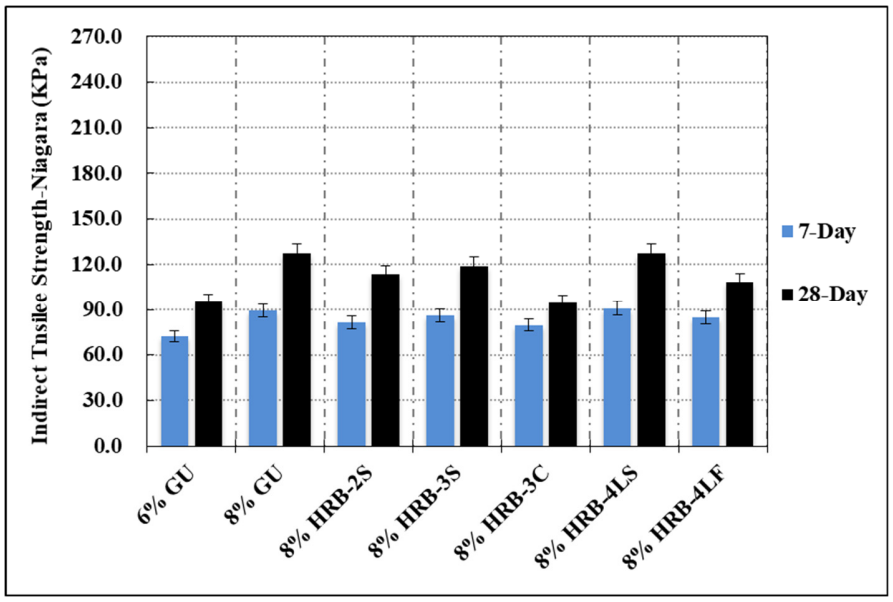

Figure 5-50 IDT strength of improved Niagara

As it is shown from the figures, at the same binder content, HRB-4LS treated subgrade soils had the highest IDT, followed by GU cement and HRB-3S. On the other hand, 8% HRB-2S, and HRB-4LF treated subgrade soils had equivalent IDT strength as 6% GU. However, the actual cement clinker content in the HRB-treated mix were both lower than GU-treated mix. Increase of GU content from 6% to 8% considerably increase the IDT values. In addition, curing from 7 days to 28 days caused a significant increase of strength. Like what had been shown in UCS and M_r test, the HRB-treated Dresden soil had higher IDT values than Blenheim and Niagara at the same binder content and curing age.

In addition, Poisson's ratio μ was determined by the followed method: the specimen was loaded at the same loading rate (1.3 mm/min) as IDT test until it reached 40% of their previous failure pressure. Then, the load was reduced to 10% of failure pressure and rose up again. The cyclic loading was performed 5 times and the LVDT recorded the recoverable displacement in both horizontal and vertical directions. Accordingly, the Poisson's ratio μ was thus determined for each specimen by dividing the recoverable horizontal deformation with vertical deformation, see Eq. 5-11 for details.

Equation 5-11

$$\mu = \frac{\varepsilon_h}{\varepsilon_v}$$

Results of Poisson's ratio for improved subgrade soils w summarized in Table 5-13. An increase of μ was observed from specimen in 7 days to specimens in 28 days. Overall, the Poisson's ratio of the improved soils ranged from 0.32 to 0.38 at 7 days and 0.30 to 0.34 at 28 days. A slight reduction was observed with the curing. However, and their change was not significant between different HRB-treated soils. Moreover, different treated soils have the same average value of accounting for 0.36 at 7 days and 0.32 at 28 days.

Table 5-13 Poisson's ratio obtained from IDT test

Soil type	Binder type	Binder content (%)	Poisson's ratio μ	
			7 days	28 days
Dresden	GU	6	0.34	0.32
	HRB-2S	8	0.32	0.30
	HRB-3S	8	0.36	0.34
	HRB-3C	8	0.36	0.31
	HRB-4LS	8	0.35	0.30
	HRB-4LF	8	0.36	0.32
Blenheim	GU	8	0.38	0.30
	HRB-2S	8	0.33	0.30
	HRB-3S	8	0.36	0.30
	HRB-3C	8	0.34	0.34
	HRB-4LS	8	0.34	0.32
	HRB-4LF	8	0.36	0.30
Niagara	GU	8	0.33	0.30
	HRB-2S	8	0.38	0.32
	HRB-3S	8	0.34	0.30
	HRB-3C	8	0.36	0.30
	HRB-4LS	8	0.37	0.30
	HRB-4LF	8	0.36	0.31

5.8 Environmental Scanning Electron Microscope (ESEM)

In this research, ESEM tests were used to observe the microscopy of HRB-treated soils. The environmental scanning electron microscope (ESEM) equipment employed in this study was a Thermo Scientific™ Quanta™ FEG 250 the same equipment used in the previous chapter for the observation of mortars. Observations were conducted in a low vacuum mode under room temperature. Soil specimens for ESEM were collected from tested UCS and M_r specimens. The ESEM chamber allows soil specimen being scanned without pre-treatment of drying, and

metallic coating. Selected ESEM images of the three types soils before and 56 days after stabilizations are presented in Figure 5-51 to 5-53.

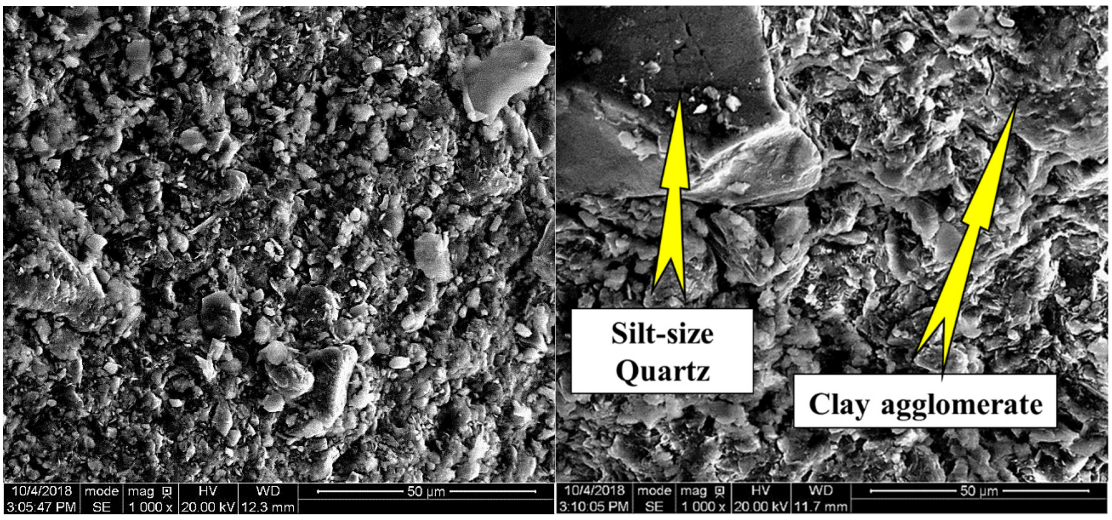

Figure 5-51 Dresden soil (left) (×1000), Dresden soil with 6% GU cement (right) (×1000)

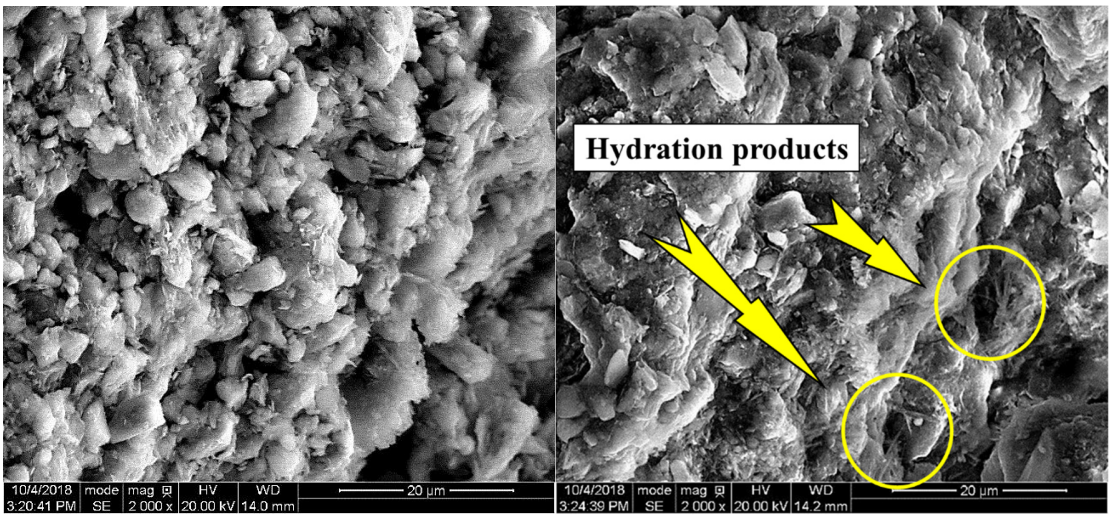

Figure 5-52 Blenheim soil (left) (×2000), Blenheim soil with 8% HRB-4L (right) (×2000)

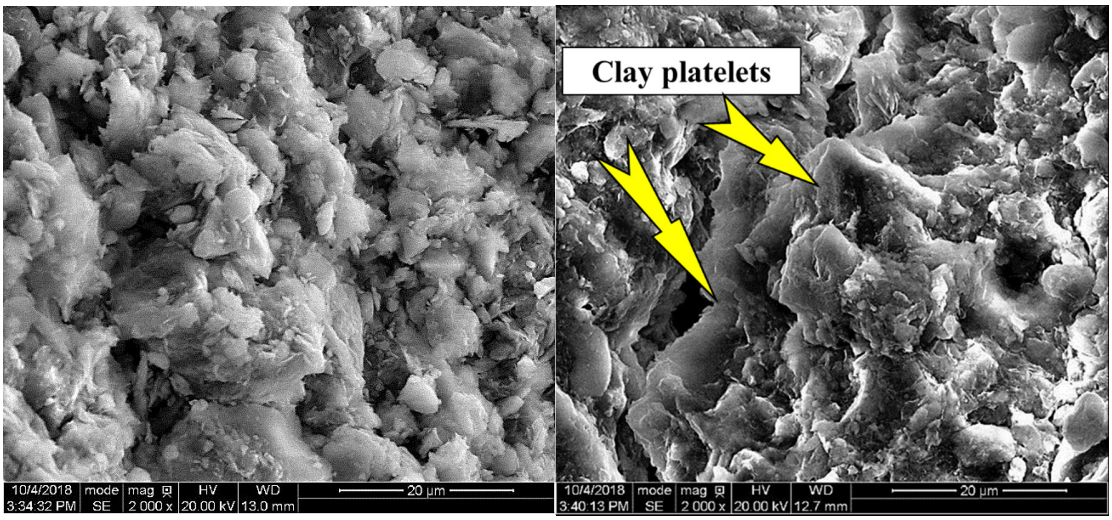

Figure 5-53 Niagara soil (left) (×2000), Niagara soil with 8% HRB-3 (right) (×2000)

As it is seen from the figures, after compaction, a dense soil structure was achieved with no large voids and or apparent cracks. Substantial clay particles and clay minerals could be clearly seen. Moreover, silt or sand-sized quartz could be occasionally observed from Dresden soil images (Figure 5-49). On the other hand, the more plastic soils showed laminar structures with dispersive, larger, and thinner clay platelets. Those platelets, as described by Lin and Cerato 2014, mostly associated in a face-to-face contact style. Such phenomenon was also observed in Blenheim and Niagara soils showing in Figure 5-52 and 5-53.

Hydraulic binders reacted with soil and water generated hydraulic as well as pozzolanic products. Cement and HRBs had the similar hydration products of calcium silicate hydrate (C-S-H), calcium aluminate hydrate (C-A-H) as well as ettringite. Those crystals can be occasionally observed from ESEM images. However, the appearance of them was not substantial because the HRB ratios were not high. As it is introduced before, hydraulic binders had the ability of restructuring and aggregating clay particles. Moreover, due to cation exchange, distances between clay particles were reduced. Consequently, tiny clay particles were agglomerated together and formed larger soil domains. The friction between soil particles could be increased, thus improving the soil's shear strength. Such phenomenon and effects could be noticed from Figure 5-51.

5.9 Recommendations for HRB-Soil Treatment

Based on the results presented in Chapter 4 and Chapter 5, a primary recommendation for HRB-soil treatment was proposed. Figure 5-54 illustrates the flow chart for HRB selection and proposed performance testing types. The decision matrix is proposed in Figure 5-55.

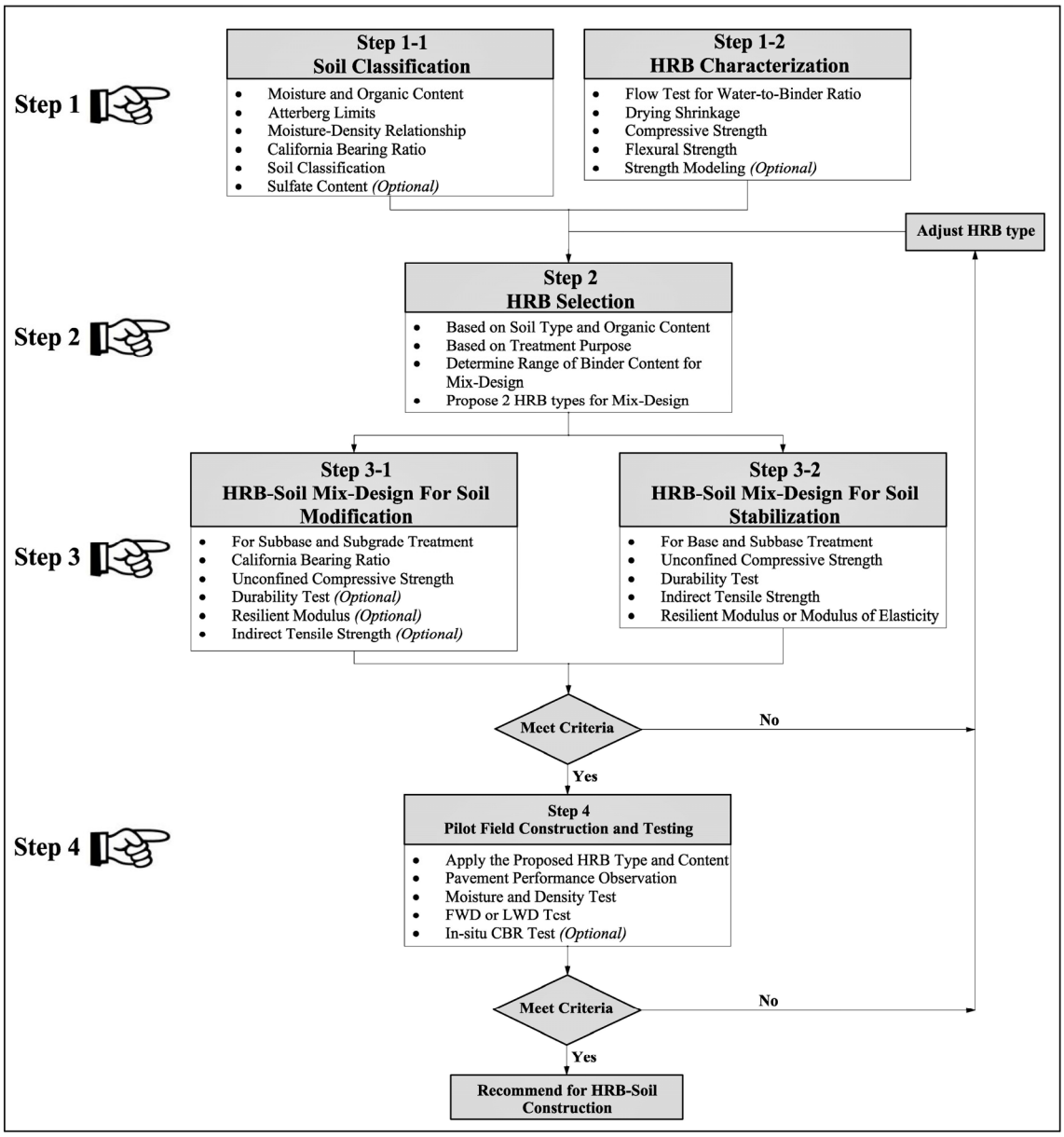

Figure 5-54 Flow chart for HRB-soil treatment

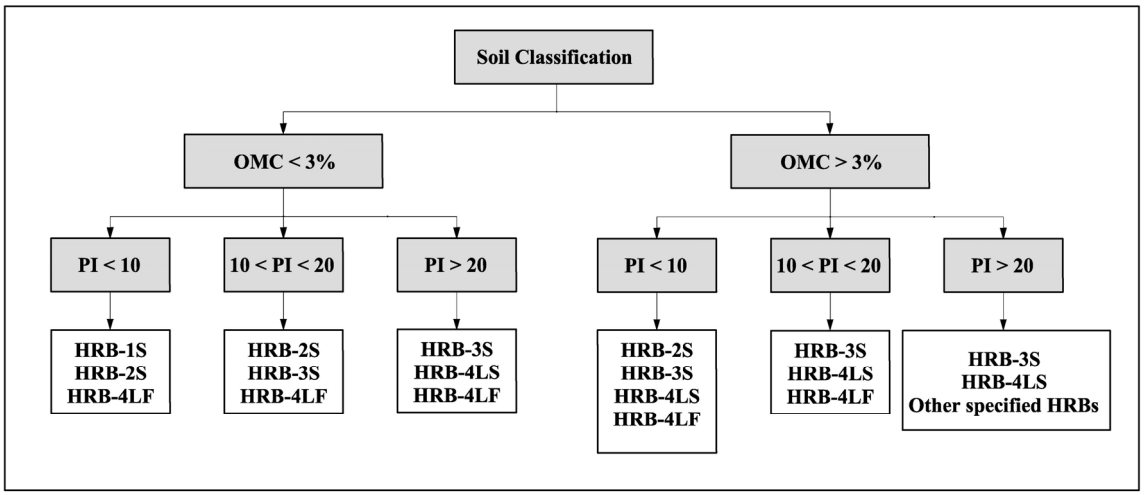

Figure 5-55 Decision tree of HRB-soil treatment

Based on the proposed design, HRB should be formulated first and evaluated to have the equivalent strength as cement. With abundant information and experiences, several commercial HRB types could be further proposed for the substantial use of HRB in pavement materials stabilization. On the other hand, for every time the target subgrade soils should be classified based on their particle size, organic matter content, Atterberg limits, and moisture-density relationship. In some areas where sulfate attack is a frequent issue, the soluble sulfate concentration of untreated soils should also be tested. Soils with higher amounts of organic matters and more plastic properties should be treated with stronger HRBs (e.g. HRB-3S and HRB-4LS in this research) and be evaluated to fulfill the strength and durability requirements. The criteria vary with the purposes of pavement design and the HRB type could be adjusted during the laboratory mix design and pilot construction for better treatment. If the condition permits, resilient modulus test and indirect tensile strength test should also be performed since they are the more important in pavement deigns. In some cases, cement could be used as the control binder to validate the adjust the use of HRB. In addition, the results will be further used to validate the HRB-soil treatment and to establish mix-design guidelines specifically for pavement constructions.

Based on the current knowledge, the recommendations of HRB types in Figure 5-55 are only suggested for fine-grained subgrade soils. It should also be noted that since only three types of

subgrade soils were studied in this research, the detailed mix-design criteria for HRB-soil treatment could not be established in this thesis. Therefore, the decision matrix referenced the current cement-soil mix design method and criteria, but take HRBs into consideration based on different binder properties.

In the future, more soil types including soils with less organic matter and clay content should be used. More mix-design experiments could contribute to the development of HRB-soil treatment guidelines and for the HRB-soil modeling.

5.10 Summary for Chapter 5

This chapter started with the classification and evaluation of soil's engineering properties. The research then investigated the cement and HRB-treated clayey and organic soils with laboratory testing of pH values, soluble salt content, unconfined compressive strength (UCS), resilient modulus (M_r), durability, indirect tensile strength, and microstructure. Based on the laboratory tests and data analysis, the following findings and conclusions can be drawn:

- All the three subgrade soils were fine-grained soils. Among them, Dresden soil had the largest proportion of silt (66.02%). On the other hand, Niagara soil had highest clay content (57.01%), highest organic content (7.86%), and lowest bearing capacity. The engineering property of Blenheim soil was between the two. The three subgrade soils were further classified as A-5, A-6, and A-7-6 respectively.
- The pH values of Dresden, Blenheim, and Niagara were between 6.9 and 5.8 (6.9, 6.5, and 5.8 respectively). This indicated a neutral to acidic environment of natural soils. Cement and HRBs were both able to change the soil's environment from acidic to alkaline with the pH ranging between 11 and 12.3. Increasing the stabilizer content could further increase pH values but the changes of the values were not substantial.
- Dresden, Blenheim, and Niagara soils had low concentrations of soluble sulfate (7.5 mg/kg, 45.8 mg/kg, and 69.8 mg/kg respectively). Adding GU and HRBs in the subgrade soils significantly increased the concentration of soluble sulfate. However, HRB-treated soils had much lower sulfate concentrations than GU-treated soils. This indicated a potential of reducing sulfate-induced problems in treated subgrade when using HRBs. In addition, both GU and most HRBs treatment did not have notable

effects on chloride and nitrate concentrations.

- Stabilized Dresden soil had higher soaked UCS values than Blenheim and Niagara which contain more clay-sized particles and organic material. Cement and HRB significantly improved the soil's soaked UCS values. GU cement increased the early strength development while HRB-treated soils had a continuous increase of strength over curing time. 6% of HRB-2S, HRB-3S, HRB-4LS, and HRB-4LF treated soils were found to have similar strength compared to the 6% cement-treated soils after 28 days. By adding 2% more HRB, 8% HRB-2 to HRB-4LF stabilized soils were found to have higher strength than 6% cement, even though the actual cement clinker content in the HRB-soil mixtures were still lower than 6%.
- There was a power-formed relationship between soil's soaked UCS and the specimen's moisture-to-cement ratio. Such relationship was highly observed in both GU- and HRB- treated subgrade soils. The content of binder, its strength, curing ages, and untreated soil's strength were the most important factors which affected the soil's treatment. A strength model was thus generated considering the above factors and was validated.
- The durability weight losses of HRBs were generally higher than GU at same adding percentages at 7 days cured specimens. On the other hand, HRB-4LS and HRB-4LF improved specimens were found to have similar durability property with cement treated ones at the same binder content.
- Remolded Dresden, Blenheim, and Niagara samples had mean M_r values of 28.3 MPa, 21.7 MPa, and 16.8 MPa respectively. Their values were increased by approximately 10 times or more by adding 8% cement or HRBs after 7 days curing. Treated Dresden soil had higher M_r values than Blenheim soil, and much higher values than Niagara soils. Unsoaked UCS values were higher than soaked ones. There was a possible linear correlation between soil's unsoaked UCS values and M_r values, especially for treated soils.
- The HRB-treated soils (especially HRB-3S and HRB-4LS) had higher IDT strength values than GU-treated ones in the same binder content. An increase of strength was

observed with the curing time. HRB-treated Dresden soil had higher IDT values than other soil types. A slight decrease of μ is observed in specimen from 7 days to 28 days. Overall, the Poisson's ratio of the improved soils ranged from 0.32 to 0.38 at 7 days and 0.30 to 0.34 at 28 days. In addition, μ did not change significantly between different HRBs.

- A dense soil structure was observed in compacted specimens. The more plastic Blenheim and Niagara showed the microstructures with dispersive, larger, and thinner clay platelets mostly associated in a face-to-face contact style. Crystals of hydration and pozzolanic products was observed from ESEM images but the presence of them is not substantial. Tiny clay particles are agglomerated together and form larger soil domains.

CHAPTER 6 IN-FIELD SUBGRADE STABILIZATION AND ITS IMPACT ON PAVEMENT STRUCTURE

6.1 Project Introduction

An in-field subgrade stabilization project was conducted in Chatham-Kent in southern Ontario, Canada. As part of the project, the constructed roads will provide access from each windfarm tower to the regional road. The location of the construction is shown in Figure 6-1.

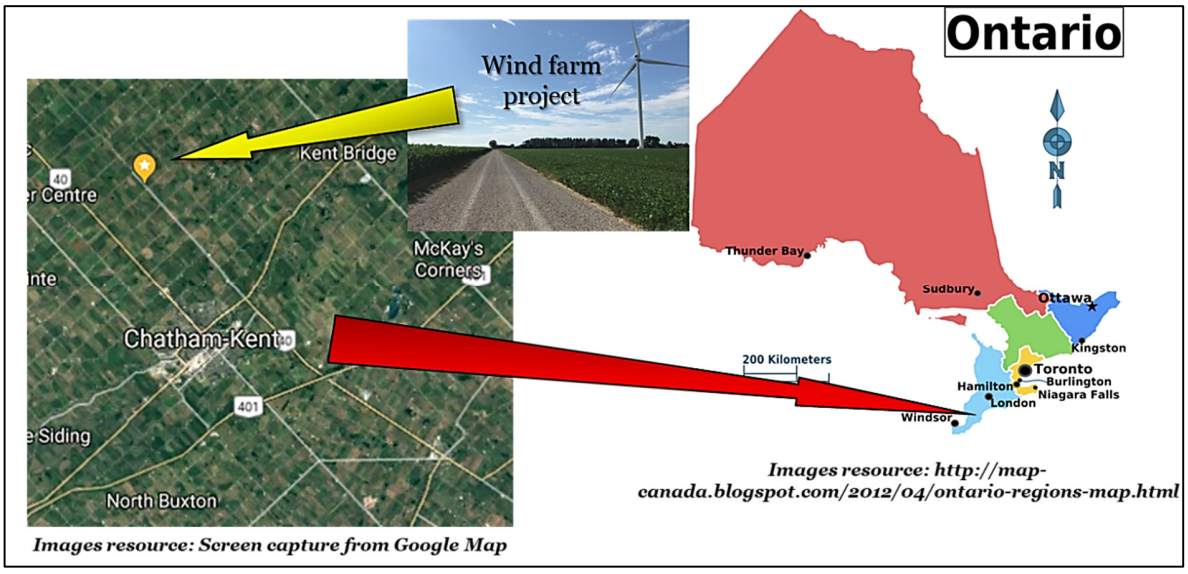

Figure 6-1 Project introduction of field test

The subgrade soils were originally used for agricultural purposes and contained substantial organic matters. The structure of the road consists of 300mm cement modified soil (CMS) on the top of the natural subgrade, and a gravel wearing course, as it is presented in Figure 6-2. The cement content was previously designed to be approximately 6% to 7% by dry weight of soil (Holt, 2010). On the top of the CMS, a 100mm thick gravel wearing coarse was placed on. It should be noted that, after 7 days of curing, the stabilized subgrade was capped with gravel cover with a granular Type A aggregate. The wearing gravels could distribute the loading, improve the drainage, prevent reflective cracking, and reduce sever rutting.

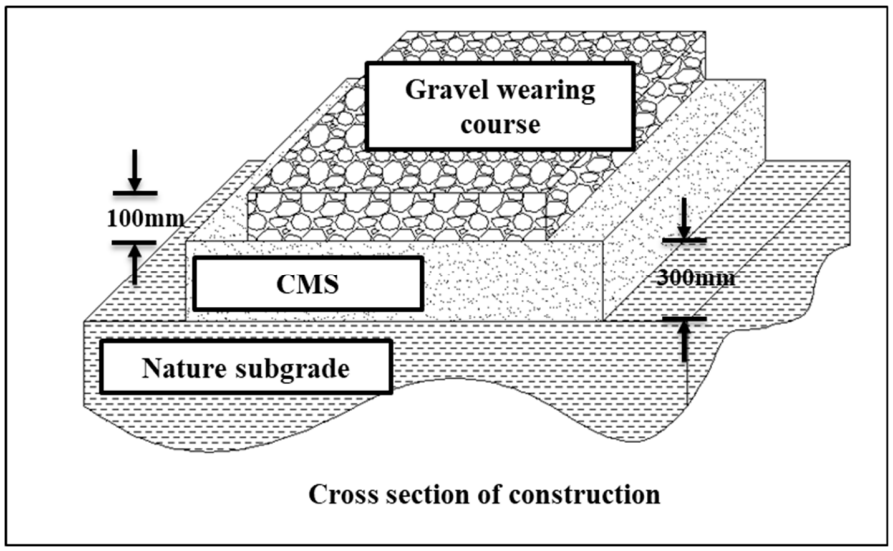

Figure 6-2 Project introduction of field test

The procedures used for subgrade soil construction project are introduced as follows:

1) **Top soil removal.** The top 10 cm of soil was abandoned to remove grass, roots and other organic matters.
2) **Soil breaking and stripping.** Soil clumps were pulverized for mixing. The treatment depth of soil was 30 cm. The moisture content of soil was checked.
3) **Water adding.** Water was added to the soil to change the moisture content. The amount of water was determined to enable the soil having a moisture content slightly above its optimum moisture content.
4) **Stabilizers spreading.** Cement and other stabilizers were spread evenly on the surface. The binder content used in this project was determined to be 6% by dry weight of soil. Water can be added after the spreading if necessary.
5) **Mixing.** Soil, stabilizer, and water are homogeneously mixed to the treatment depth.
6) **Compaction.** Use sheep foot roller for initial compaction. A vibrator is sometimes used as well to apply greater compaction energy.
7) **Grade and crown the road.** Grade and crown road with transverse degrees to allow quick drainage.
8) **Seal the road.** Use the smooth drum roller to seal the treated subgrade, additional water

can be spread in this stage if necessary.

9) **Curing and covering.** Close the traffic for 7 days before covering with gravel surface.

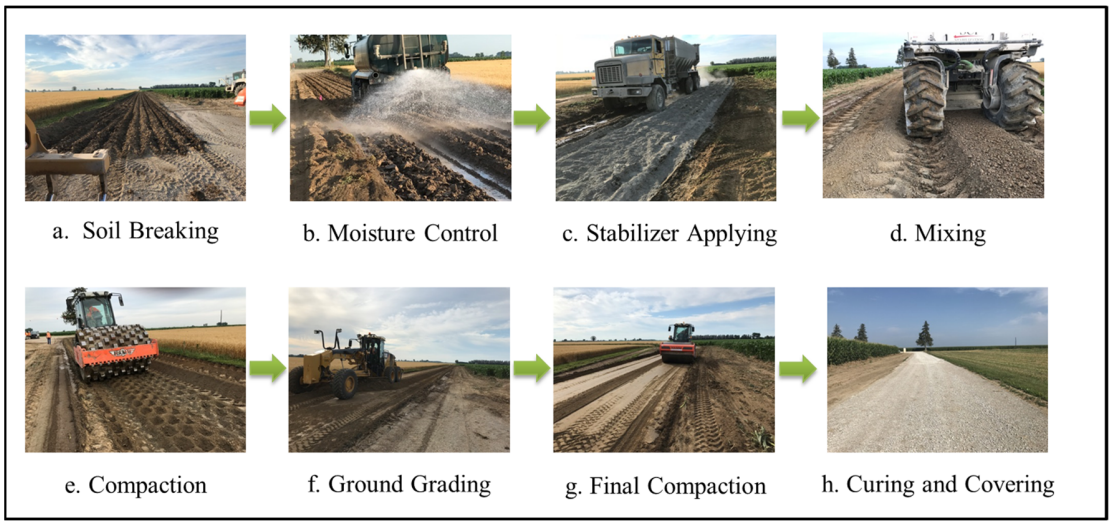

Figure 6-3 Subgrade stabilization process in field (Picture taken in Chatham-Kent, 2017)

6.2 Light Weight Deflectometer (LWD) Test on Cement Stabilized Subgrade

Light **W**eight **D**eflectometer (**LWD**) has the advantages of non-destructive, portable use, and lower cost, therefore making it suitable for measuring the stiffness for subgrade and pavement surface. The construction sections were named after each windfarm tower's name: T38, T41, T49, T15, and T32 respectively. A total of 20 test spots were conducted at the 5 test sections.

The stiffness was first measured on untreated subgrade after top soil removal. Then, the stiffness was tested 3 hours, 3 days, 7 days, 28 days, and 1 year after construction. Each of the test spots locations were identified by GPS coordinates. So, at each time, the LWD tests were conducted at approximately the same position with tolerance range within 1 m^2. Table 6-1 summarizes the locations of the construction roads and the GPS coordinates of each testing spot. The length of the 5 test sections ranged from 300m to 600m. Additionally, the distance between two adjacent test spots made up approximately 100m.

Table 6-1 LWD test points and coordinates

No.	GPS Latitude N	GPS Longitude W	Description	No.	GPS Latitude N	GPS Longitude W	Description
Section T38 @ Claymore Line				**Section T15 @ Cedar Hedge Line**			
1	42.481249	81.926073	Road end, center	1	42.494085	82.286458	
2	42.481702	82.250592	left	2	42.495390	82.288127	
3	42.482155	82.251173	right	3	42.496163	82.289007	Hill
Section T41 @ Claymore Line				4	42.496838	82.289885	
1	42.468703	82.276279		5	42.497921	82.291258	
2	42.468313	82.275773	Crown				
3	42.467833	82.275203		**Section T32 @ Country View Line**			
Section T49 @ Cedar Hedge Line				1	42.509223	82.240697	
1	42.507286	82.265538	Flat surface	2	42.509961	82.241600	
2	42.506912	82.265128		3	42.510663	82.242466	
3	42.506121	82.264126		4	42.511268	82.243196	
4	42.505357	82.263210					

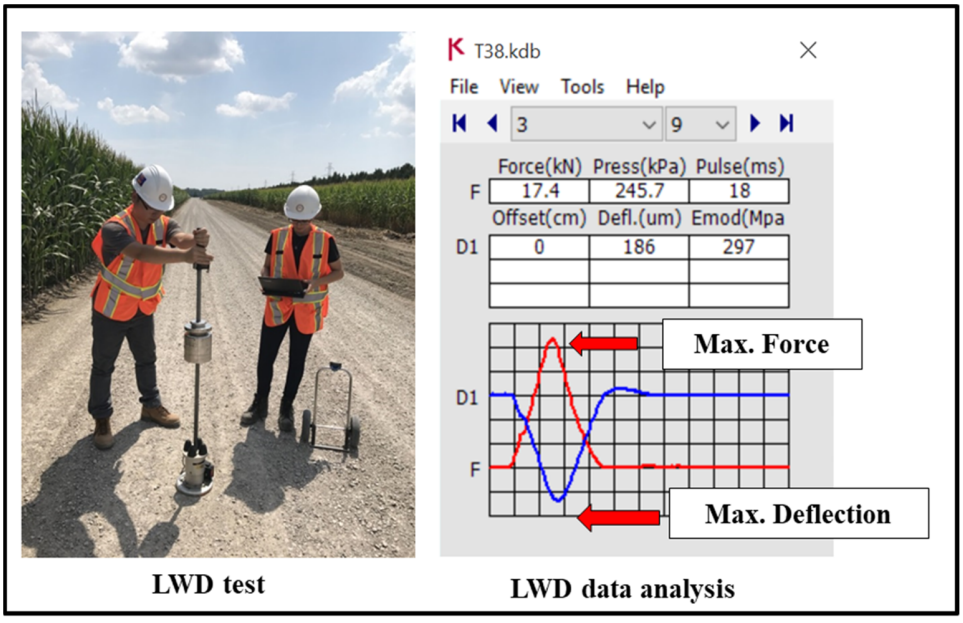

Figure 6-4 LWD field test and data analysis

Figure 6-4 illustrates the LWD stiffness monitoring process on section T38. Photo was taken at August, 2017 when the soil stabilization had been finished for 28 days. The right side of Figure 6-4 presents the data analysis window in the software that connected with LWD device. By conducting the test, a rapid loading was hit on the surface. The device then recorded the

maximum force and deflection due to the hammer dropping. The LWD stiffness was calculated based on elastic half-space (Boussinesq's Solution) theory. The calculation was conducted as follows:

Equation 6-1

$$\text{E (MPa)} = \frac{\pi \times (1 - \mu^2) \times r \times \sigma_0}{2 \times d}$$

Where, μ = soil's Poissson ratio;

r = plate radius (mm);

σ_0 = maximum force (kN);

d = the maximum deflection (μm).

At each spot, the LWD was conducted 3~5 times until the values become constant. Table 6-2 illustrated the average LWD test stiffness for each section as a result of different spots.

Table 6-2 LWD stiffness result (MPa) on natural and stabilized subgrade

Site No.		Untreated	3 hrs	3 days	7 days	28 days	1 year
T38	Average	20	62.5	216	230	312	440
	Std. Dev.	1	14	2	3	14	63
T41	Average	18	69	71	125	168	102
	Std. Dev.	1	16	11	25	44	3
T49	Average	21		136	135	253	317
	Std. Dev.	1		34	20	43	32
T15	Average	19			173	229	294
	Std. Dev.	0			15	32	56
T32	Average	19			203	250	298
	Std. Dev.	1			32	74	60

**Note: Values with yellow shade mean the section had been capped while testing. The values with grey shade mean the soil were wet during testing.*

The LWD stiffness of soil before stabilization accounted for around 20 MPa. The value remains consistent along with different test spots and sections. On the contrary, after construction, there were great discrepancies of soil's modulus between different test spots even in one test section. In-field LWD results of stabilized subgrade could be very sensitive to many variables including soil type, moisture conditions, and the spread of stabilizer. Field tests conducted on sand and clay subgrade usually have coefficient of variation (CV) accounting for

as high as more than 20% to 30% (Shivamanth, 2015). Therefore, during the data analysis, some extreme points were deleted and the average values of LWD stiffness were calculated.

As it is presented in Table 6-2, 3 hours after the construction, the stiffness of soils had increased significantly by around three times compared to the untreated ones. The immediate improvement of the subgrade soil was contributed by the pulverizing, moisture adding, compaction, and rapid hydration of cement. During the curing period, the stiffness of stabilized subgrades continued to increase. For each testing spot, a general upward trend was observed from the LWD stiffness values from 3 days to 7 days before capping. Among all the test sites, subgrade of T38 and T32 had the highest average stiffness of 230 MPa and 203 MPa respectively at 7 days. On the other hand, the subgrade of T41 had the lowest overall stiffness of merely 74 MPa after 7 days of curing. Field investigation also showed that T32 and T49 had relatively better conditions after the stabilization. Moisture content played a crucial impact on the subgrade's stuffiness. Grey shade in Table 6-1 indicates that the soil was wet.

Stabilized subgrades were capped with an approximately 100 mm thick gravel layer after 7 days curing, the material used for capping was Granular Type A aggregates. LWD test on the road surface further revealed a gaining of subgrade stiffness after capping. Due to the cementitious and pozzolanic reactions, the stiffness gaining remained continues along with 1 year of service time. The average stiffness of the 4 sections (T38, T15, T32, and T49) grew from 261 MPa at August 2017 (after capping) to 337 MPa at July 2018.

The LWD stiffness were frequently adopted as the ground resilient modulus (M_r) which is an important input for MEPDG (Mechanistic-Empirical Pavement Design Guide) pavement design methods. According to AASHTOWare pavement design guide (Tremblay, 2002), and based on the soil classifications, natural T38 soil was classified as CL, with its field modulus value (20 MPa) was judged to be "Fair" for design. Another LWD field test conducted on Highway 407, Ontario revealed a similar value of 25 MPa on a silty sand ground at a depth of 0.6m (D'Amours *et al.,* 2016).

It should be noted that T32 and T38 soils were the mainly soil source for "Dresden soil" which has been discussed previously in Chapter 5. Laboratory M_r testing was performed on GU treated soils and indicated a M_r of 28.3 MPa for untreated soil, 198.2 MPa for 6% GU-treated soil after 3 days, 205.4 MPa after 7 days, and 284.9 MPa after 28 days respectively. The

laboratory M_r values were similar to LWD modulus of T32 and T38 at the same curing ages.

6.3 Field Observation for Road Conditions

The ground conditions of road sections before and after stabilization were shown in Figure 6-5 to 6-9. As it can be seen from the figures, the natural subgrade had loose and soft surface, and the condition became worse when raining occurred. After the stabilization, the stiffness of the subgrade had been significantly improved. The stabilization dramatically changed the chemical and physical conditions of the ground and provided a uniform and robust ground surface. After 1 year of service, the road conditions of T38, T15, T32, and T49 were observed to be in fair condition with no appearance of obvious potholes, rutting, and cracks.

However, it was also observed that the condition of T41 was not successful. The ground surface become soft and a great amount of wearing courses were missing (Figure 6-9). From the results of LWD test, the stiffness of subgrade was reduced at 3 days. The reason was due to a heavy and prolonged raining happened at the same day immediately after the subgrade was stabilized. Therefore, inadequate curing could lead to the weakness of stabilized subgrade. Such failure could be avoided by proper curing and better construction plan.

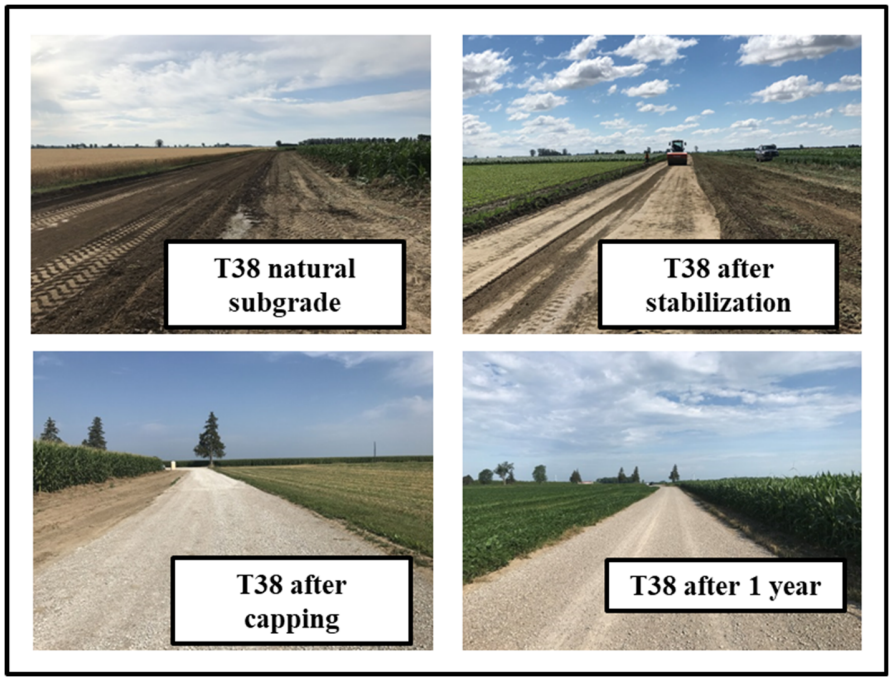

Figure 6-5 Road conditions: T38

Figure 6-6 Road conditions: T15

Figure 6-7 Road conditions: T32

Figure 6-8 Road conditions: T49

Figure 6-9 Road conditions: T41

The data collected in the field is not sufficient to produce a correlation with the laboratory results. However, it could still be concluded that cement stabilization can efficiently improve the stiffness of subgrade. With the curing time continued, a consistent gaining of LWD stiffness was observed from the field. Capping of the subgrade was found to have further improvement of the surface stiffness.

It should also be introduced that, after 1 month of road construction. Heavy construction vehicles were traveled on the road for the construction of windfarm. Afterwards, only light traffic with service vehicles were applied on the constructed road. Before the 1-year observation, all the windfarm constructions had been finished. Such design and construction could be a positive example for local low-volume road constructions.

6.4 Long-Term Pavement Performance Prediction Using AASHTOWare

A 20-years Long-Term Pavement Performance (LTPP) prediction was conducted using Mechanistic-Empirical Design (MEPDG) model and AASHTWare software. As a National Cooperative Highway Research Program (NCHRP) Project 1-37A, the method was initially developed in order to improve the design and performance of pavements. Substantial empirical models and research accomplishments were incorporated in the model for the analysis of pavement distress, including fatigue, rutting, and cracking in both flexible and rigid pavements. In addition, long-term traffic and climate data can be impute in the design for the validation and prediction of pavement design and performance.

The use of MEPDG and AASHTOWare in this research was to predict the LTPP of pavements which had a hydraulically stabilized subgrade layer included. Comparisons are conducted between conventional design, design including cement stabilized subgrade, and

design including HRB stabilized subgrade. The three different types of soils-- Dresden, Blenheim, and Niagara were used for prediction. Moreover, the climate and traffic data near the sampling locations were also considered.

Among all the prediction factors, International roughness index (IRI) and rutting were considered in this study to reflect the influence of stabilized subgrade.

IRI was developed in the 1980s to define the total deflections of a traveled wheel track in the longitudinal direction of a pavement. IRI is usually measured in field using a standardized equipment. The commonly units for IRI are meters per kilometer (m/km) or millimeters per meter (mm/m) (Pavement interactive, 2019). On the other hand, rutting is described as the depression in the wheel path, usually expressed in mm. Rutting can happen in all pavement layers which have low bearing capacity and strength. AASHTOWare calculates rutting in all pavement layers. The research took the total deformation in pavement for consideration.

6.4.1 Inputs for MEPDG

The design controls traffic, climate, asphalt surface, base coarse, and subgrade soil type the same in each location. Analysis was conducted considering different subbase layers.

Traffic and climate data

The research used Dresden, Blenheim, and Niagara soils as subgrade soils for pavement design. Traffic and climate stations were selected near to the soil sampling locations. In particular, Ontario Highway 40 in Chatham-Kent was selected to represent the traffic conditions for Dresden and Blenheim soils. On the other hand, traffic volume in Ontario Highway 58 was used for study of Niagara soil. Traffic data was downloaded from Ministry of Transportation Ontario ICorridor Backup Site. Meanwhile, climate data for the recent 30 years was input from Federal Highway Administration website. Table 6-3 and 6-4 below summarize the traffic and climate input data, respectively.

Table 6-3 Input data for traffic

		Project-Dresden	Project-Blenheim	Project-Niagara
Design period (years)		20	20	20
Traffic volume reference		ON Hwy 40	ON Hwy 40	ON Hwy 58
Initial two-way Annual Average Daily Truck Traffic (AADTT)		420	420	494
Number of lanes in design direction		1	1	1
Growth factor (%)		2.06	2.06	2.23
Operational speed (km/h)		70	70	70
Vehicle class (%)	Class 4	1.5	1.5	1.13
	Class 5	27.84	27.84	9.16
	Class 6	5.13	5.13	6.87
	Class 7	1.83	1.83	3.05
	Class 8	3.66	3.66	1.53
	Class 9	36.23	36.23	30.93

Table 6-3 Continued

Vehicle class (%)	Class 10	19.78	19.78	45.8
	Class 11	0	0	0
	Class 12	0	0	0
	Class 13	4.03	4.03	1.53

Table 6-4 Climate Input data

	Project-Dresden	Project-Blenheim	Project-Niagara
Climate Station Location (Lat. Lon. Elevation)	42.50000; -82.50000; 175	42.50000; -82.50000; 175	42.50000; -82.50000; 175
Mean annual air temperature (ºC)	9.19	9.19	9.19
Mean annual precipitation (mm)	993.14	993.14	993.14
Average annual number of freeze/thaw cycles	76.24	76.24	76.24
Water table depth (m)	10	10	10

Pavement design

For the same subgrade soil, 5 different designs were proposed. The design of surface, base course, subbase followed the typical Ontario pavement design experiences and criteria. Table 6-5 presents the structures of the pavement design for each soil type.

Table 6-5 Pavement structure of the design for each soil type

	Control design	**200mm GU stabilized**	**200mm HRB-2S stabilized**	**200mm HRB-3S stabilized**	**200mm HRB-4LS stabilized**
Hot mix asphalt concrete 1	40 mm SP 12.5 FC1	40 mm SP 12.5 FC1	40 mm SP 12.5 FC1	40 mm SP 12.5 FC1	40 mm SP 12.5 FC1
Hot mix asphalt concrete 2	100 mm SP 19	100 mm SP 19	100 mm SP 19	100 mm SP 19	100 mm SP 19
Base	150 mm Granular A	150 mm Granular A	150 mm Granular A	150 mm Granular A	150 mm Granular A
Subbase	450 mm Granular B-II	200 mm Granular B-II	200 mm Granular B-II	200 mm Granular B-II	200 mm Granular B-II
		200 mm GU stabilized subgrade	200 mm HRB-2S stabilized subgrade	200 mm HRB-3S stabilized subgrade	200 mm HRB-4LF stabilized subgrade

Among them, the Superpave grading and aggregate gradation for the hot mix asphalt layers were input according to the parameters in Table 6-6.

Table 6-6 Input parameters for asphalt concrete (MTO interim report 2019)

		SP 12.5	**SP 19**
Unit Weight (kg/m^3)		2390	2460
Effective Binder Content - by Volume (%)		11.8	11.2
Air Voids (%)		7.0	7.0
Poisson's Ratio		0.35	0.35
Dynamic Modulus		Input level: 3	
Aggregate gradation	% Passing 19 mm	100	96.9
	% Passing 9.5 mm	83.2	72.5
	% Passing 4.75 mm	54	528
	% Passing 75 μm	4	3.9
Asphalt Binder		PG 64-28	PG 58-28

The gradations of Granular A and Granular B were input according to Table 6-7. Information for Table 6-6 and Table 6-7 was captured from interim report 2019: *"Ontario's Default Parameters for AASHTOWare Pavement ME Design"*. On the other hand, the gradation and parameters of subgrade soils were obtained from results in Chapter 5. 7 days resilient Parts was used in this design. They are summarized in Table 6-8.

Table 6-7 Input parameters for Granular A and B (MTO interim report 2019)

		Granular A	Granular B-II
Coefficient of Lateral Pressure (k_o)		0.5	0.5
Poisson's Ratio		0.35	0.35
Resilient Modulus (MPa)		250	200
Aggregate gradation	% Passing 75 μm	5	5
	% Passing 0.3 mm	13.5	13.5
	% Passing 1.18 mm	27.5	25
	% Passing 4.75 mm	45	37.5
	% Passing 9.5 mm	61.5	--
	% Passing 13.2 mm	77.5	--
	% Passing 19.0 mm	92.5	--
	% Passing 25.0 mm	100	75
Liquid Limit		6	11
Plasticity Index		0	0

Table 6-8 Input parameters for subgrade soils

		Dresden	Blenheim	Niagara
AASHTO soil group		A-5	A-6	A-7-6
Poisson's Ratio		0.2	0.2	0.2
Poisson's Ratio in improved soil		0.36	0.36	0.36
Resilient Modulus of soil (MPa)		20	20	20
Resilient Modulus in improved soil (MPa)		267.0~347.2	298.3~355.9	215.2~276.4
Chemical stabilizer content (%)		6	8	8
Aggregate gradation	% Passing 2 μm	20.5	36.0	87.0
	% Passing 75 μm	85.5	81.0	99.0
	% Passing 0.18 mm			
	% Passing 0.425 mm		95.7	
	% Passing 2.00 mm	99.0	99.0	
	% Passing 4.75 mm			
	% Passing 9.5 mm			
	% Passing 12.5 mm			
	% Passing 19.0 mm			
	% Passing 25.0 mm			
Liquid Limit		30	39	52
Plasticity Index		10	16	26

The binder content of stabilizers were kept the same (8%) in order to compare the effect of different binder types. The resilient modulus values of each treated subgrade layer was adopted from results in section 5.6.

6.4.2 Results from MEPDG

This section introduces the predicted values related to pavement distresses, after 20 years of service. The overall results are summarized in Table 6-9 to 6-11.

Table 6-9 Predicted long-term pavement performance for Project-Dresden

	Target	Control design	200mm GU stabilized	200mm HRB-2S stabilized	200mm HRB-3S stabilized	200mm HRB-4LS stabilized
Terminal IRI (m/km)	2.70	2.27	2.23	2.35	2.23	2.23
AC bottom-up fatigue cracking (percent)	20.00	0.96	0.95	0.95	0.95	0.95
Permanent deformation - total pavement (mm)	19.00	14.13	13.48	13.74	13.56	13.48
Permanent deformation - AC only (mm)	6.00	3.55	2.99	2.96	2.98	2.99

Table 6-10 Predicted long-term pavement performance for Project-Blenheim

	Target	Control design	200mm GU stabilized	200mm HRB-2S stabilized	200mm HRB-3S stabilized	200mm HRB-4LS stabilized
Terminal IRI (m/km)	2.70	2.38	2.24	2.24	2.33	2.23
AC bottom-up fatigue cracking (percent)	20.00	0.96	0.96	0.96	0.96	0.96
Permanent deformation - total pavement (mm)	19.00	13.62	13.38	13.31	13.03	13.01
Permanent deformation - AC only (mm)	6.00	3.58	3.53	3.54	3.55	3.56

Table 6-11 Predicted long-term pavement performance for Project-Niagara

	Target	Control design	200mm GU stabilized	200mm HRB-2S stabilized	200mm HRB-3S stabilized	200mm HRB-4LS stabilized
Terminal IRI (m/km)	2.70	2.26	2.11	2.11	2.11	2.11
AC bottom-up fatigue cracking (percent)	20.00	0.96	0.9	0.96	0.96	0.96
Permanent deformation - total pavement (mm)	19.00	12.73	8.11	8.12	8.07	8.06
Permanent deformation - AC only (mm)	6.00	3.93	3.92	3.92	3.93	3.94

All the designed sections passed the target criteria of IRI, deformation, and asphalt bottom-up cracking. The stabilized subgrade reduced 200 mm of subbase layer, making the total pavement thickness thinner than the control design. The replacement of subbase layer to stabilized soils had minor effect on the property of Asphalt Concrete (AC) fatigue cracking and deformation. However, the change of design had significant effect on the IRI and total deformation of pavement.

The IRI of control designs varies from 2.26 to 2.38 m/km. On the other hand, when the subbase was partially replaced by HRB stabilized soils, the IRI values decreased slightly to the range within 2.11 to 2.35. The GU stabilized subgrade had similar support compared to HRB stabilized subgrade soils. Among the three types of HRBs, HRB-4LS had slightly better treatment performance than the other two.

Figure 6-10 to 6-12 below draw the prediction curve of total pavement deformation in the 20 years period. It is evident from the figures that all the designed pavements had their predicted deformations far below the threshold value which is 19 mm. Deformations in pavements constructed on Dresden and Blenheim subgrade accounted for similar values as they had the same traffic and climate inputs. The HRB-treated subgrade solutions were found to have almost the same impact on pavement deformation compared to control design, making up approximately 13 mm to 14 mm at the end of 20 years.

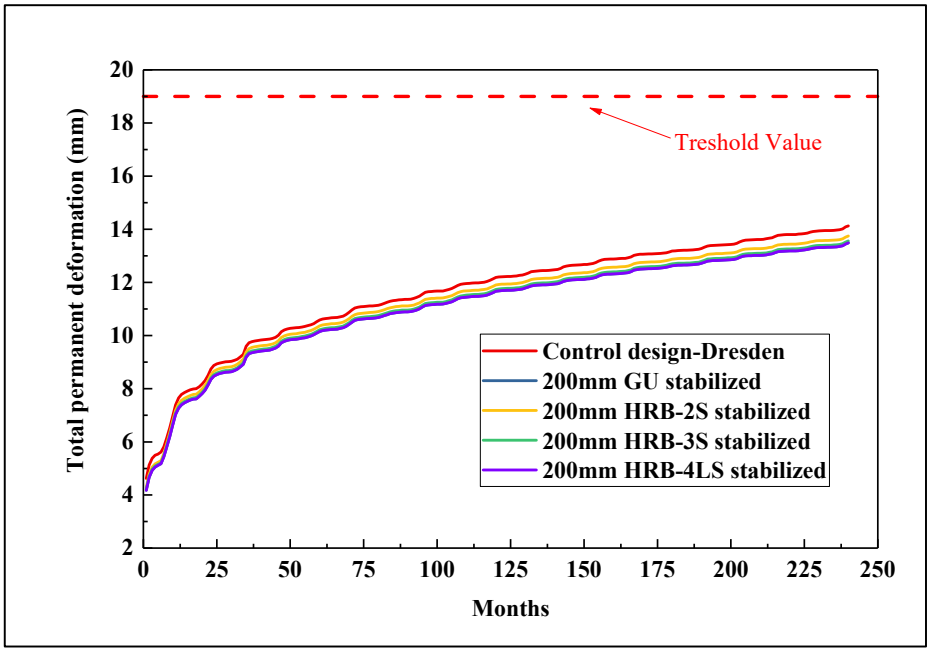

Figure 6-10 Total permanent deformation in projects designed on Dresden soil subgrade

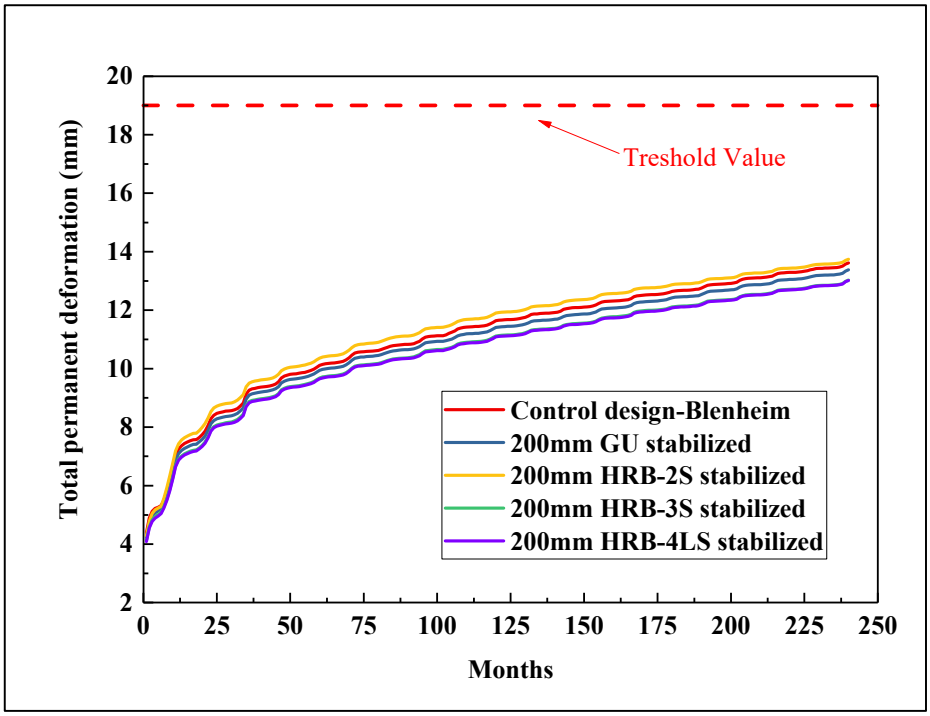

Figure 6-11 Total permanent deformation in projects designed on Blenheim soil subgrade

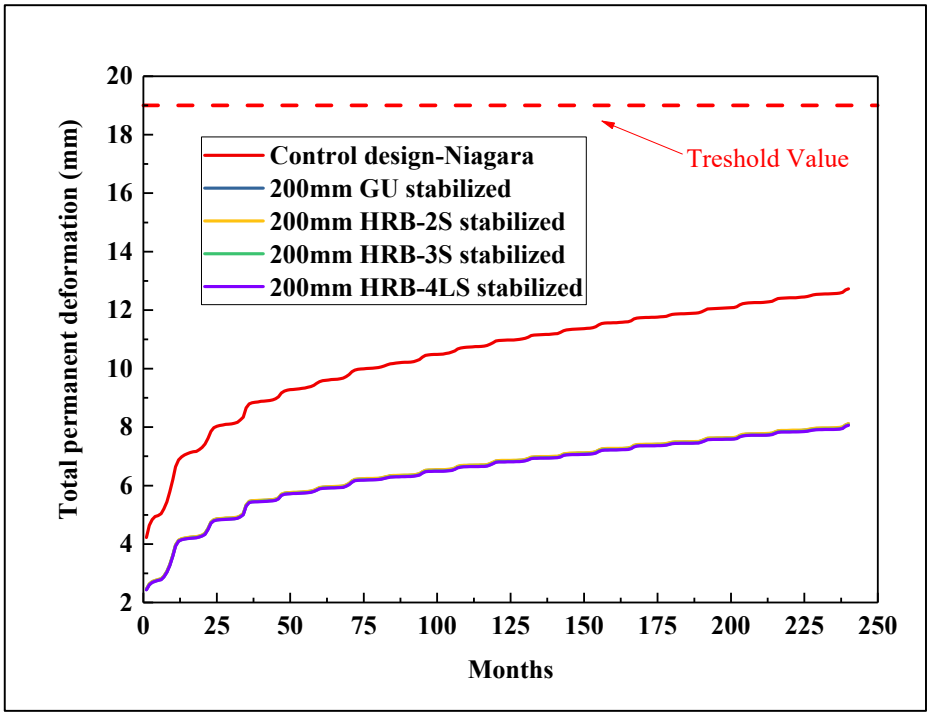

Figure 6-12 Total permanent deformation in projects designed on Niagara soil subgrade

On the other hand, a distinct optimization of deformation was observed in Niagara project. The hydraulically stabilized Niagara subgrade had much lower permanent deformation than conventional design. Such prediction may be a result from the significant improve of soil's stiffness by hydraulically mixing. Nevertheless, the difference between cement and HRB types was not obvious. The curves of their solutions were overlapped.

Overall, the LTPP prediction by MEPDG method revealed a potential feasibility of using cement and HRB stabilized subgrade reduce the granular B subbase layer. All the designs passed the required criteria. Moreover, the pavements with stabilized subgrade included could have better performances in terms of IRI and permanent deformation compared to control pavements. Furthermore, HRBs had equivalent performance in improving the subgrade according to the cement. Therefore, use of HRBs in the subgrade stabilization could be a potential solution in pavement construction which will provide both environmental and cost-effective advantages.

6.5 Summary for Chapter 6

This chapter introduced a field subgrade stabilization project in soil sampling area. The stiffness of stabilized subgrade was monitored with curing. Long-term predictions of pavement performance were also conducted for pavements containing hydraulically stabilized subgrades. Based on the results, some conclusions can be drawn as follows:

- The workability and conditions of subgrade were significantly improved by chemical treatment and compaction. LWD modulus of untreated subgrade accounted for around 20 MPa for all the 5 test sections. Immediately after construction, the modulus of subgrade had a dramatic increase. The increase was found to continue along with curing until the surface was covered with gravel. After one year of service, the road condition was satisfied in most test sections.
- Long-term pavement performance prediction proposed a feasibility of using cement and HRB stabilized subgrade in a highway pavement. All the designs passed the required criteria. Moreover, the pavements with stabilized subgrade included had better performances regarding IRI and permanent deformation compared to control pavements. Furthermore, HRBs had the same or slightly better performance in improving the subgrade according to the cement. Therefore, use of HRBs in the subgrade stabilization could be a potentially solution in pavement construction which provide engineering advantages.

CHAPTER 7 CONCLUSIONS AND RECOMMENDATIONS

7.1 Overall Conclusions

This thesis presented a comprehensive study on hydraulic road binder and its use for subgrade material treatment in the environment of Ontario, Canada. An investigation of HRB and GU was conducted and presented in Chapter 4. Furthermore, a comprehensive investigation of subgrade soil classification and treatment was further performed and is presented in Chapter 5. Lastly, Chapter 6 described a field subgrade stabilization project based on one of the laboratory tested soils. Afterwards, long-term pavement performance prediction was conducted using AASHTOWare to analyze the effect of stabilized subgrade in pavement design. The following paragraphs describe the major findings and summary of Chapters 4 to 6.

- **Chapter 4**: Compared to GU and GUL cement, HRBs had longer setting times. A reduction of hydration temperature was also found in HRB pastes compared to GU and GUL. In particular, the CKD and fly ash blended HRBs had lower hydration temperature. XRD analysis showed that hydrated HRBs had the relatively lower percentages of Portlandite and ettringite than hydrated GU and GUL, but higher ratio of quartz. These findings explain the difference in heat of hydration and setting times between GU and the tested HRBs.

  In addition, a reduction of drying shrinkage was observed in HRB mortars especially in fly ash blended HRBs. Regarding the compressive strength, HRBs had lower strength in 7 days, but a substantial strength development was observed later on. The HRBs with high compressive strength after 56 days were HRB-2S, HRB-2LS, HRB-3S, HRB-4LS, and HRB-4LF. Similar trends were found in flexural strength of mortars. In addition, a distinct linear correlation was found between the two types of strength. Models were further generated for the mortar strength prediction. Afterwards, image processing of mortar specimens after flexural testing revealed a reduction of surface porosity of mortars along with curing time.

  Moreover, hydration products of cement and HRBs were substantially present in microscopic images using ESEM. HRBs were able to produce substantial amount of

hydration products but less needle-like ettringite than GU cement. Based on literature, this would lead to a better durability of HRBs and lower the risk of alkali silica reactions. On the other hand, the iron-rich spheres were only observed in HRBs containing fly ash which is a typical sign for fly ash.

- **Chapter 5:** All the three subgrade soils named Dresden, Blenheim, and Niagara are fine-grained soils with substantial silt and clay particles and organic matters. They were classified as A-5, A-6, and A-7-6 respectively. Cement and HRBs significantly improved soil's engineering properties. The improvement included the change of the soil's chemical environment and the long-term improvement strength, durability, and resilient modulus. Among all the tested materials with HRB, the subgrade soils treated with the HRB composed GUL and slag (HRB-4LS) had the highest UCS values, followed by the soil treated with the HRB composed of GUL and fly ash (HRB-4LF).

  There was a power-formed relationship between soil's soaked UCS and the specimen's moisture-to-cement ratio. Such a relationship was repeatedly observed in both GU- and HRB- treated subgrade soils. The content of binder, its strength, curing ages, and untreated soil's strength were the most important factors which affected the soil's treatment. A strength model was thus generated considering these factors and was validated experimentally.

  It should be noted as well that the soil types played an important role in the treatment. Soils with high plasticity and high organic contents had lower strength and modulus than less plastic and organic soils. It was also found that GU- and HRB- treated Blenheim and Niagara, at the studied binder contents, were unable to fully meet the strength and durability requirements for soil-cement. However, the treatment appears to be a good solution to improve the mechanical properties of the weak subgrade that would behave as an additional layer in the pavement structure and would help to reduce the overall thickness of the pavement.

- **Chapter 6:** Field tests indicated that the workability and conditions of subgrade were significantly improved by stabilization. LWD modulus of untreated subgrade was significantly increased immediately after construction. Moreover, the modulus of subgrade further increased along with curing. After one year of service, the road

condition was satisfactory in most test sections.

Long-term pavement performance prediction revealed a potential feasibility of using cement- and HRB- treated subgrade soils to reduce the thickness of granular B subbase. All the designs passed the required criteria. Moreover, the pavements with stabilized subgrade had better performance in terms of pavement roughness and permanent deformation in comparison to control pavements. Furthermore, HRBs stabilized subgrades had equivalent performance to GU-treated one.

To summarize, this study focused on evaluating the used of hydraulic road binders formulated in Canada for pavement subgrade stabilization. The research showed that HRB mortars had similar or slightly better strength compared to Portland cement alone under the condition of sufficient curing. Moreover, The HRB improved subgrade soils were shown to perform adequately using several HRB types. In addition, the use of HRB-stabilized subgrade in pavement structure would improve the LTPP of pavement. Therefore, the use of HRB in the subgrade stabilization could be a promising solution in pavement construction due to its equivalent performance and with the potential environmental and cost advantages.

7.2 Future Research Opportunities

This research work was successful in evaluating several HRB formulations in different conditions and demonstrated the strong potential of using HRB in pavement engineering projects. The work has also put the framework for soil stabilization formulation studies and proposed different formulations that could be used with different subgrade soils. However, there are some research gaps that still need to be addressed in the future. Some of these gaps are summarized in the following bullet points:

- **Chapter 4:** Based on the results of strength test and strength modeling, the fly ash and CKD used in the research provided less contribution compared to GGBFS. In the future, other types of SCMs from different sources could be included to understand the role and impact of each stabilizer type.
- **Chapter 5:** More types of subgrade soils across Canada should be investigated for the research of stabilization. This would be beneficial for the binder selection and formulation study, as well as for the development of soil's strength model. A stabilization guideline using HRBs could thus be generated.
- **Chapter 6:** Field construction of subgrade stabilization using HRBs should be conducted in the future for the validation of laboratory mix design. Moreover, a long-term pavement performance evaluation in field should be conducted for better understanding of the stabilized layer.

REFERENCES

AASHTO. (1993). Guide for Design of Pavement Structures 1993. Washington, DC: American Association of State Highway and Transportation Officials (AASHTO).

AASHTO. (2008). Standard recommended practice for stabilization of subgrade soils and base materials. Washington, DC: American Association of State Highway and Transportation Officials (AASHTO).

Abdo, J., Serfass, J. P., & Pellevoisin, P. (2013). Pavement cold in-place recycling with hydraulic binders: The state of the art in France. *Road Materials and Pavement Design*, *14*(3), 638-665. Doi: https://doi.org/10.1080/14680629.2013.817350

Adaska, W. S., & Luhr, D. R. (2004, May). Control of reflective cracking in cement stabilized pavements. In *Proceedings of 5th International RILEM Conference on Cracking in Pavements* (pp. 309-316). Available at: https://www.researchgate.net/publication/240632158_Control_of_reflective_cracking_in_cement-stabilized_pavements

Adaska, W. S., & Taubert, D. H. (2008, May). Beneficial uses of cement kiln dust. In *2008 IEEE Cement Industry Technical Conference Record* (pp. 210-228). IEEE. Doi: 10.1109/CITCON.2008.24

Akagawa, S., & Fukuda, M. (1991). Frost heave mechanism in welded tuff. *Permafrost and Periglacial Processes*, *2*(4), 301-309. Doi: https://doi.org/10.1002/ppp.3430020405

Al-Rawas, A. A., Hago, A. W., & Al-Sarmi, H. (2005). Effect of lime, cement and Sarooj (artificial pozzolan) on the swelling potential of an expansive soil from Oman. *Building and Environment*, *40*(5), 681-687. Doi: https://doi.org/10.1016/j.buildenv.2004.08.028

Andrew, R. M. (2018). Global CO_2 emissions from cement production, 1928–2017. *Earth System Science Data*, *10*(4), 2213-2239. Available at: https://www.earth-syst-sci-data.net/10/2213/2018/essd-10-2213-2018.pdf

Arora, S., & Aydilek, A. H. (2005). Class F fly-ash-amended soils as highway base materials. *Journal of Materials in Civil Engineering*, *17*(6), 640-649. Doi: https://doi.org/10.1061/(ASCE)0899-1561(2005)17:6(640)

Baaj, H. (2002). *Comportement à la fatigue des matériaux granulaires traités aux liens hydrocarbones* (Doctoral dissertation, Lyon, INSA).

Bahar, R., Benazzoug, M., & Kenai, S. (2004). Performance of compacted cement-stabilised soil. *Cement and concrete composites*, *26*(7), 811-820. Doi: https://doi.org/10.1016/j.cemconcomp.2004.01.003

Bergold, S. T., Goetz-Neunhoeffer, F., & Neubauer, J. (2013). Quantitative analysis of C–S–H in hydrating alite pastes by in-situ XRD. *Cement and Concrete Research*, *53*, 119-126.

Brady, N. C., & Weil, R. R. (1996). The nature and properties of soils (No. Ed. 11). Prentice-Hall Inc.

Buchanan, S. (2007). Resilient modulus, what, why, and how? Available at: https://www.vulcaninnovations.com/public/pdf/2-Resilient-Modulus-Buchanan.pdf

Buczyński, P., & Lech, M. (2015). The impact of one-, two-and three-component hydraulic road binder on the properties of the hydraulically bound mixture. *Procedia Engineering*, *108*, 116-123. Doi: https://doi.org/10.1016/j.proeng.2015.06.126

Canadian Council of Motor Transport Administrators (CCMTA). (2016). Canada's Safety Strategy 2025. Available at: https://roadsafetystrategy.ca/files/RSS-2025-Report-January-2016-with%20cover.pdf

Canadian Technical Asphalt Association (CTAA) (2018). Hot mix asphalt (1st Edition). ISBN: 978-0-9869141-8-8.

Celauro, B., Bevilacqua, A., Bosco, D. L., & Celauro, C. (2012). Design procedures for soil-lime stabilization for road and railway embankments. Part 1-review of design methods. *Procedia-Social and Behavioral Sciences*, *53*, 754-763. Doi: https://doi.org/10.1016/j.sbspro.2012.09.925

Cement Association of Canada (CAC). (2016). Environmental Product Declaration (EPD)-General use (GU) and Portland-limestone (GUL) cements. Cement Association of Canada. Available at: www.stmaryscement.com/Documents/Canada/CAC%20EPD%20(GU,%20GUL).pdf

Chen, H., & Wang, Q. (2006). The behaviour of organic matter in the process of soft soil

stabilization using cement. *Bulletin of Engineering Geology and the Environment*, *65*(4), 445-448. Doi: 10.1007/s10064-005-0030-1

Chen, J. J., Sorelli, L., Vandamme, M., Ulm, F. J., & Chanvillard, G. (2010). A Coupled nanoindentation/SEM-EDS study on low water/cement ratio Portland cement paste: evidence for C–S–H/Ca (OH) 2 nanocomposites. *Journal of the American Ceramic Society*, *93*(5), 1484-1493. Doi: 10.1111/j.1551-2916.2009.03599.x

Chen, L., & Lin, D. F. (2009). Stabilization treatment of soft subgrade soil by sewage sludge ash and cement. *Journal of Hazardous Materials*, *162*(1), 321-327. Doi: https://doi.org/10.1016/j.jhazmat.2008.05.060

Cheng, T., & Yan, K. Q. (2011). Mechanics properties of the lime-steel slag stabilized soil for pavement structures. In *Advanced Materials Research* (Vol. 168, pp. 931-935). Trans Tech Publications.

Clare, K. E., & Sherwood, P. T. (1954). The effect of organic matter on the setting of soil-cement mixtures. *Journal of Applied Chemistry*, *4*(11), 625-630. Doi: https://doi.org/10.1002/jctb.5010041107

Cong, M., Longzhu, C., & Bing, C. (2014). Analysis of strength development in soft clay stabilized with cement-based stabilizer. *Construction and Building Materials*, *71*, 354-362. Doi: https://doi.org/10.1016/j.conbuildmat.2014.08.087

Cook, R. D., & Weisberg, S. (1982). *Residuals and influence in regression*. New York: Chapman and Hall.

D'Amours, L., Eng, P., Contant, A. and Ng, J., 2016. Assessment of Subgrade Soils for Pavement Design for Highway 407, East Extension Pickering to Oshawa, Ontario. In *TAC 2016: Efficient Transportation-Managing the Demand-2016 Conference and Exhibition of the Transportation Association of Canada*. Available at: http://www.tac-atc.ca/sites/tac-atc.ca/files/conf_papers/damours_0.pdf

Das, B. M. (2015). Fundamentals of Geotechnical Engineering. 5th Ed. Cengage Learning, USA.

Dempsey, B. J., and Thompson, M. R. (1973). Vacuum saturation method for predicting freeze-thaw durability of stabilized materials. *In* 52nd Annual Meeting of the Highway

Research Board, Washington, D. C., 22-26 January 1973. Transportation Research Board, New York, Vol. 442, pp. 44-57.

Department of the Army, the Navy, and the Air Force. (1994). Soil-cement stabilization for pavements. Report Number: Army TM 5-822-14/ Air Force AFJMAN 32-1019. Available at: https://www.wbdg.org/FFC/ARMYCOE/COETM/ARCHIVES/tm_5_822_14.pdf

Dolado, J. S., & Van Breugel, K. (2011). Recent advances in modeling for cementitious materials. *Cement and concrete research*, *41*(7), 711-726. Doi: https://doi.org/10.1016/j.cemconres.2011.03.014

EN 13282-1:2013 Hydraulic road binders. Rapid hardening hydraulic road binders. Composition, specifications and conformity criteria.

EN 13282-2:2015 Hydraulic road binders. Normal hardening hydraulic road binders. Composition, specifications and conformity criteria.

George, K. P. (1968). Shrinkage characteristics of soil-cement mixtures. *Highway Research Record*, *255*, 42-58. Available at: http://onlinepubs.trb.org/Onlinepubs/hrr/1968/255/255-004.pdf

Gnanendran, C. T., Valsangkar, A., and Roew, R. K. (2015). Canadian case histories of embankments on soft soils and stabilization with geosynthetics. *In* Ground Improvement Case Histories: Compaction, Grouting and Geosynthetics. *Edited by* B. Indraratna, J. Chu, and C. Rujikiatkamjorn. Butterworth-Heinemann. pp. 507–536.

Goldstein, J. I., Newbury, D. E., Michael, J. R., Ritchie, N. W., Scott, J. H. J., & Joy, D. C. (2017). *Scanning electron microscopy and X-ray microanalysis*. Springer.

Government of Canada (Website). Annual Survey of Cement, production and exports. Available at: https://www150.statcan.gc.ca/t1/tbl1/en/tv.action?pid=1610000901

Government of Canada (Website). Soil Survey Reports for Ontario. Available at: http://sis.agr.gc.ca/cansis/publications/surveys/on/index.html

Halsted, G. E. (2011). Cement-Modified Soil for Long Lasting Pavements. In *Annual Conference of the Transportation Association of Canada, Edmonton, Alberta*. Available at: http://conf.tac-atc.ca/english/annualconference/tac2011/docs/sm2/halsted.pdf

Halsted, G. E., Adaska, W. S., & McConnell, W. T. (2008). Guide to cement-modified soil (CMS). Available at: http://secement.org/wp-content/uploads/2017/04/EB242.pdf

Hampton, M. B., & Edil, T. B. (1998). Strength gain of organic ground with cement-type binders. In *Soil improvement for big digs* (pp. 135-148). ASCE. Doi:

Harris, P., Harvey, O., Puppala, A. J., Sebesta, S., Chikyala, S. R., & Saride, S. (2009). *Mitigating the Effects of Organics in Stabilized Soils: Technical Report* (No. FHWA/TX-09/0-5540-1). Texas. Dept. of Transportation. Available at: https://rosap.ntl.bts.gov/view/dot/38672

Hebib, S., and Farrell, E. R. (1999). Some experience of stabilising Irish organic soils. *In* Dry Mix Methods for Deep Soil Stabilization. *Edited by* Bredenberg, Holm, and Broms. Rotterdam; Balkema. pp. 81–84.

Hejazi, S. M., Sheikhzadeh, M., Abtahi, S. M., & Zadhoush, A. (2012). A simple review of soil reinforcement by using natural and synthetic fibers. *Construction and building materials*, *30*, 100-116. Doi: https://doi.org/10.1016/j.conbuildmat.2011.11.045

Holt, C. (2010). Chemical Stabilization of Inherently Weak Subgrade Soils for Road Construction–Applicability in Canada. In *Annual Conference of the Transportation Association of Canada Halifax, Nova Scotia*. Available: http://conf.tac-atc.ca/english/resourcecentre/readingroom/conference/conf2010/docs/d1/holt-2.pdf

Horpibulsuk, S., Katkan, W., Sirilerdwattana, & W., Rachan, R. (2006). Strength development in cement stabilized low plasticity and coarse grained soils: laboratory and field study. *Soils and foundations, 46(3),* 351-366. Doi: https://doi.org/10.3208/sandf.46.351

Iwański, M., Buczyński, P., & Mazurek, G. (2016). Optimization of the road binder used in the base layer in the road construction. *Construction and Building Materials*, *125*, 1044-1054. Doi: https://doi.org/10.1016/j.conbuildmat.2016.08.112

Jefferson, I., Rogers, C., Evststiev, D., and Karastanev, D. (2015). Improvement of collapsible loess in Eastern Europe. *In* Ground Improvement Case Histories: Compaction, Grouting and Geosynthetics. *Edited by* B. Indraratna, J. Chu, and C. Rujikiatkamjorn.

Butterworth-Heinemann. pp. 215–262.

Jones, D., Rahim, A., Saadeh, S., & Harvey, J.T. (2010). *Guidelines for the stabilization of subgrade soils in California*. University of California Pavement Research Center. Guideline: UCPRC-GL-2010-01. Available at: http://www.ucprc.ucdavis.edu/PDF/UCPRC-GL-2010-01.pdf

Juenger, M. C., & Siddique, R. (2015). Recent advances in understanding the role of supplementary cementitious materials in concrete. *Cement and Concrete Research*, *78*, 71-80. Doi: https://doi.org/10.1016/j.cemconres.2015.03.018

Kolias, S., Kasselouri-Rigopoulou, V., & Karahalios, A. (2005). Stabilisation of clayey soils with high calcium fly ash and cement. *Cement and Concrete Composites*, *27* (2), 301-313. Doi: https://doi.org/10.1016/j.cemconcomp.2004.02.019

Kowalski, T. E., & Starry Jr, D. W. (2007). Modern soil stabilization techniques. In *A nnual Conference of the Transportation Association of Canada, Saskatoon, Saskatch ewan*. Available at: http://conf.tac-atc.ca/english/resourcecentre/readingroom/conference/conf2007/docs/s8/starry.pdf

Kutchko, B. G., & Kim, A. G. (2006). Fly ash characterization by SEM–EDS. *Fuel*, *85*(17-18), 2537-2544. Doi: https://doi.org/10.1016/j.fuel.2006.05.016

Lin, B., & Cerato, A. B. (2014). Applications of SEM and ESEM in microstructural investigation of shale-weathered expansive soils along swelling-shrinkage cycles. *Engineering geology*, *177*, 66-74. Doi: https://doi.org/10.1016/j.enggeo.2014.05.006

Little, D. N. and Nair, S. (2009). Recommended Practice for Stabilization of Subgrade Soils and Base Materials. Contractor's Final Task Report for NCHRP Project 20-07. Texas Transportation Institute, Texas A&M University, College Station, Texas. Doi: https://doi.org/10.17226/22999

Lothenbach, B., Scrivener, K., & Hooton, R. D. (2011). Supplementary cementitious materials. *Cement and concrete research*, *41*(12), 1244-1256. Doi: https://doi.org/10.1016/j.cemconres.2010.12.001

Louw, S., & Jones, D. (2015). *Pavement Recycling: Literature Review on Shrinkage Crack*

Mitigation in Cement-Stabilized Pavement. Technical Memorandum: UCPRC-TM-2015-02, Department of Transportation, California. Available at: http://www.ucprc.ucdavis.edu/PDF/UCPRC-TM-2015-02.pdf

Louw, S., Jones, D., & Hammack, J. (2016). Pavement Recycling: Shrinkage Crack Mitigation in Cement-Treated Pavement Layers–Phase 1 Laboratory Testing. Research Report – UCD-ITS-RR-16-40. Available at: https://escholarship.org/uc/item/6pc4478z

Lv, Q. F., Wang, S. L., Zhao, Y. X. (2013). Permeability characteristics of modified loess under freeze-thaw cycles. Advances in Earth and Environmental Sciences, 2013, 189, 537-542.

Manso, J. M., Ortega-López, V., Polanco, J. A., & Setién, J. (2013). The use of ladle furnace slag in soil stabilization. *Construction and Building Materials*, *40*, 126-134. Doi: https://doi.org/10.1016/j.conbuildmat.2012.09.079

Melese, E., Baaj, H., Tighe, S., Zupko, S., & Smith, T. (2019). Characterisation of full-depth reclaimed pavement materials treated with hydraulic road binders. *Construction and Building Materials*, *226*, 778-792. Doi: https://doi.org/10.1016/j.conbuildmat.2019.07.317

Miller, G. A., & Azad, S. (2000). Influence of soil type on stabilization with cement kiln dust. *Construction and building materials*, *14*(2), 89-97. Doi: https://doi.org/10.1016/S0950-0618(00)00007-6

Ministry of Transportation Ontario. (2013). Pavement design and rehabilitation manual (Second Edition). Ontario. Available at: http://www.bv.transports.gouv.qc.ca/mono/1165561.pdf

Moseley, M. P., and Kirsch, K. (Eds.). (1994). Ground improvement. CRC Press.

Nalbantoğlu, Z. (2004). Effectiveness of class C fly ash as an expansive soil stabilizer. *Construction and Building Materials*, *18*(6), 377-381. Doi: https://doi.org/10.1016/j.conbuildmat.2004.03.011

Neville, A. M. (1995). *Properties of concrete* (4th Edition). London. ISBN-13: 978-0273755807

Otsu, N. (1979). A threshold selection method from gray-level histograms. *IEEE transactions*

on systems, man, and cybernetics, *9*(1), 62-66. Doi: 10.1109/TSMC.1979.4310076

Papadakis, V. G., & Tsimas, S. (2002). Supplementary cementing materials in concrete: Part I: efficiency and design. *Cement and concrete research*, *32*(10), 1525-1532. Doi: https://doi.org/10.1016/S0008-8846(99)00249-5

Pavement interactive (Website). "California Bearing Ratio". Available at: https://www.pavementinteractive.org/reference-desk/design/design-parameters/california-bearing-ratio/

Pavement interactive (Website). "Portland Cement". Available at: https://www.pavementinteractive.org/reference-desk/materials/portland-cement/

Pavement interactive (Website). "Roughness". Available at: https://www.pavementinteractive.org/reference-desk/pavement-management/pavement-evaluation/roughness/

Pavement interactive (Website). "Rutting". Available at: https://www.pavementinteractive.org/reference-desk/pavement-management/pavement-distresses/rutting/

Pavement interactive (Website). "Subgrade Performance". Available at: https://www.pavementinteractive.org/reference-desk/design/design-parameters/subgrade/

Peethamparan, S., Olek, J., & Lovell, J. (2008). Influence of chemical and physical characteristics of cement kiln dusts (CKDs) on their hydration behavior and potential suitability for soil stabilization. *Cement and concrete research*, *38*(6), 803-815. Doi: https://doi.org/10.1016/j.cemconres.2008.01.011

Petry, T. M., & Little, D. N. (2002). Review of stabilization of clays and expansive soils in pavements and lightly loaded structures—history, practice, and future. *Journal of Materials in Civil Engineering*, *14*(6), 447-460. doi: https://doi.org/10.1061/(ASCE)0899-1561(2002)14:6(447)

Portland Cement Association (PCA). (2016). Preparing an Environmental Product Declaration for Portland, Blended Hydraulic, Masonry, Mortar, and Plastic (Stucco) Cements. Portland Cement Association. Available at: http:// http://www.stmaryscement.com/Documents/US/PCA%20EPD%20(PORTLAND).pdf

Portland Cement Association. (1992). Soil-cement laboratory handbook. Illinois.

Prusinski, J., & Bhattacharja, S. (1999). Effectiveness of Portland cement and lime in stabilizing clay soils. *Transportation Research Record: Journal of the Transportation Research Board*, (1652), 215-227. doi: https://doi.org/10.3141/1652-28

Public Works Canada (1992). Manual of Pavement Structural Design. Report [AK-68-12]. Available at: http://www.captg.ca/docs/pdf/asg19e.pdf

Qi, J., Ma, W., & Song, C. (2008). Influence of freeze–thaw on engineering properties of a silty soil. *Cold regions science and technology*, *53*(3), 397-404. Doi: https://doi.org/10.1016/j.coldregions.2007.05.010

Ramaji, A. E. (2012). A review on the soil stabilization using low-cost methods. *Journal of Applied Sciences Research*, *8*(4), 2193-2196. Doi:

Rempel, A. W. (2007). Formation of ice lenses and frost heave. *Journal of Geophysical Research: Earth Surface*, *112*(F2). Available at: https://scholar.google.ca/scholar?hl=en&as_sdt=0%2C5&q=Formation+of+ice+lenses+and+frost+heave&btnG=

Rosenqvist, I. T. (1959). Physico-chemical properties of soils: soil-water systems. *Journal of the Soil Mechanics and Foundations Division*, *85*(2), 31-54.

Saussaye, L. (2012). Soils treatment with hydraulic binders: physicochemical and geotechnical aspects [Presentation]. Retrieved from: http://www.danskgeotekniskforening.dk/sites/default/files/pdf/ngm/Pdf-presentations/Presentations%20from%20auditorium%20Lumbye/11501210%20NGM201209052012LSaussayeESITC%20Caen.pdf

Saussaye, L., Boutouil, M., Baraud, F., Leleyter, L., & Abdo, J. (2013). Influence of chloride and sulfate ions on the geotechnical properties of soils treated with hydraulic binders. *Road Materials and Pavement Design*, *14*(3), 551-569. Doi: https://doi.org/10.1080/14680629.2013.779303

Savannah Cement. (2014). Savannah Cement, develops a special product to support ongoing roads infrastructure development; [online], Available at http://www.savannahcement.com/wp-content/uploads/2013/01/Savannah-cement-HRB-m

edia-release-30th-July-20141.pdf

Schaefer, V. R., Stevens, L., White, D., and Ceylan, H, Design Guide for Subgrades and Subbases. (2008). Tech. Transfer Summaries. Institute for Transportation, Iowa State University. Available at: https://lib.dr.iastate.edu/cgi/viewcontent.cgi?referer=https://www.google.com/&httpsredir=1&article=1056&context=intrans_techtransfer

Schöler, A., Lothenbach, B., Winnefeld, F., & Zajac, M. (2015). Hydration of quaternary Portland cement blends containing blast-furnace slag, siliceous fly ash and limestone powder. *Cement and Concrete Composites*, *55*, 374-382. Doi: https://doi.org/10.1016/j.cemconcomp.2014.10.001

Scrivener, K. L., Juilland, P., & Monteiro, P. J. (2015). Advances in understanding hydration of Portland cement. *Cement and Concrete Research*, *78*, 38-56. Doi: https://doi.org/10.1016/j.cemconres.2015.05.025

Segui, P., Aubert, J. E., Husson, B., & Measson, M. (2012). Characterization of wastepaper sludge ash for its valorization as a component of hydraulic binders. *Applied Clay Science*, *57*, 79-85. Doi: https://doi.org/10.1016/j.clay.2012.01.007

Service d'études sur les transports, les routes et leurs aménagements (SÉTRA). (2008). Treatment of soils with lime and/or hydraulic binders-Application to the construction of pavement base layers. Technical Guide published by SÉTRA and carried out by the French Road Engineering Committee (CFTR), 2007, translated in 2008.

Shafiee, M., Nassiri, S. and Bayat, A., 2013. Evaluation of Light Weight Deflectometer (LWD) for Characterization of Subgrade Soil Modulus. In *2013 CONFERENCE AND EXHIBITION OF THE TRANSPORTATION ASSOCIATION OF CANADA-TRANSPORTATION: BETTER-FASTER-SAFER*. Available at: https://trid.trb.org/view/1301777

Shivamanth, A., Kolase, P. K., Shama, P. S., Desai, M. K., & Desai, A. K. (2015). Study of the Light Weight Deflectometer and Reviews. *International Journal of Engineering Research and General Science, 3 (16,)*, 42-46. ISSN 2091-2730. Available at: http://www.pnrsolution.org/Datacenter/Vol3/Issue6/6.pdf

Slag Cement Association (Website). “What is Slag Cement”. Available at: https://www.slagcement.org/aboutslagcement/whatisslagcement.aspx

Stark, J. (2011). Recent advances in the field of cement hydration and microstructure analysis. *Cement and concrete research*, *41*(7), 666-678. Doi: https://doi.org/10.1016/j.cemconres.2011.03.028

Tastan, E. O., Edil, T. B., Benson, C. H., & Aydilek, A. H. (2011). Stabilization of organic soils with fly ash. *Journal of geotechnical and Geoenvironmental Engineering*, *137*(9), 819-833. Doi: https://doi.org/10.1061/(ASCE)GT.1943-5606.0000502

Terrel, R. L., Epps, J. A., Barenberg, E. J., Mitchell, J. K., and Thompson, M. R. (1979). Soil stabilization in pavement structures-a user's manual FHWA Research Report No. FHWA-IP-80-2, WA. Available at: https://ntrl.ntis.gov/NTRL/dashboard/searchResults/titleDetail/PB83186411.xhtml

Terzaghi, K., Peck, R. B., & Mesri, G. (1996). Soil mechanics in engineering practice. John Wiley & Sons.

Thom, N. (2003). Principles of Pavement Engineering (Second edition). ICE Publishing. ISBN 978-0-7277-5853-8.

Transport Canada. (2017). Transportation in Canada annual reports. Transport Canada. Available at: https://www.tc.gc.ca/media/documents/policy/Transportation_in_Canada_2017nwe.pdf

Transportation Association of Canada (TAC). (2014). Pavement Asset Design and Management Guide.

Tremblay, H., Duchesne, J., Locat, J., & Leroueil, S. (2002). Influence of the nature of organic compounds on fine soil stabilization with cement. *Canadian Geotechnical Journal*, *39*(3), 535-546. Doi: https://doi.org/10.1139/t02-002

Trivedi, J. S., Nair, S., & Iyyunni, C. (2013). Optimum utilization of fly ash for stabilization of sub-grade soil using genetic algorithm. *Procedia Engineering*, *51*, 250-258. Doi: https://doi.org/10.1016/j.proeng.2013.01.034

United Kingdom Quality Ash Association (UKQA). (2010). Embodied CO2 of UK cement,

additions and cementitious material. Technical data sheet 8.3, MPA; UK quality Ash association. Available at: http://cement.mineralproducts.org/documents/Factsheet_18.pdf

Viklander, P. (1998). Permeability and volume changes in till due to cyclic freeze/thaw. *Canadian Geotechnical Journal*, *35*(3), 471-477. Doi: https://doi.org/10.1139/t98-015

Wang, S. L., Baaj, H., Zupko, S, and Smith, T. (2018). Field and lab assessment for cement-stabilized subgrade in Chatham, Ontario | tac-atc.ca. Presented at the Conference of Transportation Association of Canada, Saskatoon, Saskatchewan. Available at: https://www.tac-atc.ca/en/conference/papers/field-and-lab-assessment-cement-stabilized-subgrade-chatham-ontario

Wang, S. L., Lv, Q. F., Baaj, H., Li, X. Y., & Zhao, Y. X. (2016). Volume change behaviour and microstructure of stabilized loess under cyclic freeze–thaw conditions. *Canadian Journal of Civil Engineering*, *43*(10), 865-874. Doi: https://doi.org/10.1139/cjce-2016-0052

Wang, T. L., Liu, J. K, and Tian, Y. H. (2011). Static properties of cement-and lime-modified soil subjected to freeze-thaw cycles. Rock and Soil Mechanics, 32(1), 193-198. (in Chinese).

White, T. L., & Williams, P. J. (1999). The influence of soil microstructure on hydraulic properties of hydrocarbon-contaminated freezing ground. *Polar Record*, *35*(192), 25-32. Doi: https://doi.org/10.1017/S0032247400026309

Xing, H., Yang, X., Xu, C., & Ye, G. (2009). Strength characteristics and mechanisms of salt-rich soil–cement. *Engineering Geology*, *103*(1-2), 33-38. Doi: https://doi.org/10.1016/j.enggeo.2008.07.011

Yadu, L., & Tripathi, R. K. (2013). Effects of granulated blast furnace slag in the engineering behaviour of stabilized soft soil. *Procedia Engineering*, *51*, 125-131. Doi: https://doi.org/10.1016/j.proeng.2013.01.019

Yeo, R. (2008). *The development and evaluation of protocols for the laboratory characterisation of cemented materials* (No. AP-T101/08).

Zhang L. X, and Wang J.C. (2002). Experimental study on frost heaving behaviors of lime

soil. Chinese Journal of Geotechnical Engineering, 24(3), 336-339. (in Chinese)